Studies on the assembly process of large subunit ribosomal proteins in *S.cerevisiae*

DISSERTATION ZUR ERLANGUNG DES DOKTORGRADES DER
NATURWISSENSCHAFTEN (DR. RER. NAT.)
DER FAKULTÄT FÜR BIOLOGIE UND VORKLINISCHE MEDIZIN
DER UNIVERSITÄT REGENSBURG

vorgelegt von

Uli Ohmayer

aus Regensburg

im Juni 2014

Das Promotionsgesuch wurde eingereicht am:
24.Juni 2014

Die Arbeit wurde angeleitet von:
Dr. Philipp Milkereit und Prof. Dr. Herbert Tschochner

Die vorliegende Arbeit wurde im Zeitraum von Mai 2010 bis Juni 2014 am Lehrstuhl für Biochemie III des Instituts für Biochemie, Genetik und Mikrobiologie der Universität Regensburg unter Anleitung von Dr. Philipp Milkereit und Prof. Dr. Herbert Tschochner angefertigt.

Ich erkläre hiermit, dass ich diese Arbeit selbst verfasst und keine anderen als die angegebenen Quellen und Hilfmittel verwendet habe.

Diese Arbeit war bisher noch nicht Bestandteil eines Prüfungsverfahrens.

Andere Promotionsversuche wurden nicht unternommen.

Regensburg, den 23.06.2014

Uli Ohmayer

Table of contents

1 Summary

Ribosomes are ribonucleoprotein (RNP) particles that catalyze the translation of the genetic information of messenger RNA (mRNA) into proteins. The biogenesis of eukaryotic ribosomes is a highly complex process that starts in the nucleolus where the ribosomal RNA (rRNA) is synthesized by RNA Polymerases I and III. Three of the four rRNA molecules are produced as one precursor molecule (pre-rRNA) that contains spacer sequences that are not part of mature ribosomal subunits but are removed during ribosome biogenesis. Besides these processing events, rRNA is heavily modified.

In the course of ribosome assembly, the numerous (around 80) ribosomal proteins (r-proteins) and the rRNA (precursors) join together in a highly dynamic and defined manner. Initial interactions of most of the r-proteins to preribosomes occur already in the nucleolus or in the nucleus; some seem to be incorporated in the cytoplasm where the some final maturation events happen. Most of the r-proteins are required for an efficient accumulation of functional ribosomal subunits in the cytoplasm. Interestingly, depletion of essential LSU r-proteins resulted not in one common but in several different pre-rRNA processing phenotypes indicating their requirement for specific maturation events. *In vitro* reconstitution experiments on prokaryotic ribosomal subunits (whose structures are highly similar to the ones of their eukaryotic counterparts) helped to analyze the hierarchical interrelationships between the individual r-protein assembly events. In eukaryotic cells, the production of ribosomal subunits does not occur in a “self assembly” mechanism but requires numerous transiently interacting proteins, the so called ribosome biogenesis factors, and many small nucleolar RNAs (snoRNAs). Most of our current knowledge on eukaryotic ribosome biogenesis comes from studies in the yeast *S.cerevisiae*. Highly resolved structural information of mature yeast ribosomes (which is available since a few years) contributed to a better understanding of ribosome function but also ribosome biogenesis. Although the knowledge of the binding sites of the structural components (r-proteins) in the mature ribosomal subunits might not fully reflect how these “endpoints” are established *in vivo*, the final structure is very helpful to better understand features like hierarchical interrelationship of r-protein assembly events and/or their requirement for specific maturation events.

In this work, the assembly process of the 46 r-proteins of the yeast large ribosomal subunit was aimed to be characterized in terms of several previously fragmentary or unresolved aspects. By comparing the respective amounts of the individual LSU r-proteins in differently maturated LSU precursors to each other and/or to the ones in mature LSUs, the assembly characteristics of each of the 46 LSU r-proteins was addressed applying a combination of affinity purification (*ex vivo*) and quantitative mass spectrometry. In a complementary approach, the interaction of a number of essential LSU r-proteins with the nascent particles was investigated in a comparative way by affinity purification of epitope tagged LSU r-proteins and quantitative analysis of the co-purified (pre-) rRNA species. In order to better understand the requirement of individual LSU r-proteins for certain assembly or maturation events, various LSU r-protein expression mutants were then used to investigate changes in

the composition of the mutant preribosomes. Both, changes in the association of other LSU r-proteins and LSU ribosome biogenesis factors were analyzed. The results were then compared to previously published data from *in vivo* and *in vitro* experiments.

The comparative analyses on the composition of differently maturated LSU precursors indicated that most LSU r-proteins seem to already start interacting with preribosomes of early maturation stages. In average, the affinity of these initial interactions seems to be rather low, though. The binding strength of most LSU r-proteins is then stabilized in the course of ribosome maturation. Therefore, the stable incorporation of most LSU r-proteins seems to be a multistep, rather than a one step event. Some LSU r-proteins however showed a specific assembly behavior which was characterized by an underrepresentation in early (or early and intermediately) maturated LSU precursors. Their (stable) incorporation seems to occur at later stages; for one group of LSU r-proteins in the cytoplasm.

Clear evidences for hierarchical interrelationships among LSU r-protein assembly events *in vivo* could be deduced from the analyses of the *RPL* mutants. They can be categorized into two kinds of effects. One effect observed after depletion of most LSU r-proteins was characterized by a partial destabilization of the mutant preribosomes in the direct neighborhood of the depleted LSU r-protein or in the same secondary structure domain. Second, more general effects which can be related to the depletion phenotype of the respective r-protein were observed in most cases. A comparison to the results of previously published *in vitro* reconstitution experiments of prokaryotic LSUs revealed clear differences between the observed hierarchical interrelationships *in vivo* (in yeast) and *in vitro* (in *E.coli*), which are discussed. In addition, specific changes in the association of several ribosome biogenesis factors to the mutant preribosomes were observed. While in some cases the recruitment of several biogenesis factors to the preribosomes was disturbed, evidences for an inhibited release of others were provided. Altogether these results can contribute to a better understanding of the interplay between r-protein assembly events and the transient association of ribosome biogenesis factors. In addition, information of the molecular prerequisites for several maturation events, which are disturbed in the individual mutants (as pre-rRNA processing or nuclear export), can be deduced from these results.

Zusammenfassung

Ribosomen sind Ribonucleoprotein (RNP) Partikel, die für die Translation der in mRNA enthaltenen genetischen Information in Proteine verantwortlich sind, indem sie die Verknüpfung der einzelnen Aminosäuren zu Proteinen katalysieren. Ihre Biogenese ist in eukaryotischen Organismen ein sehr komplexer Vorgang welcher im Nucleolus beginnt und im Zytoplasma endet. Ribosomale RNA (rRNA) wird in der Bäckerhefe im Nucleolus von den beiden RNA Polymerasen I und III hergestellt. Drei der vier rRNA Moleküle werden nicht einzeln, sondern als zusammenhängendes Vorläufermolekül produziert, das so genannte „Spacer“ Bereiche enthält, die im Laufe der Ribosomenbiogenese entfernt werden.

Die zahlreichen (in Eukaryoten etwa 80) strukturellen Proteinkomponenten (r-Proteine) werden im Zuge der Ribosomenbiogenese in das entstehende Vorläuferribosom eingebaut. Die meisten dieser Interaktionen zwischen (Vorläufer-) rRNA und r-Proteinen beginnen wohl bereits sehr früh im Nucleolus (vielleicht schon während der Synthese der rRNA) und im Zellkern. Ein paar andere scheinen dagegen erst im Zytoplasma stabil eingebaut zu werden. Depletionsanalysen haben ergeben, dass die meisten r-Proteine für die Reifung von Vorläuferribosomen benötigt werden. Fehlen sie, so stoppt die Reifung an verschiedenen Stellen, indem beispielsweise bestimmte Vorläufer rRNAs nicht mehr prozessiert werden können. Zahlreiche *in vitro* Rekonstitutionsexperimente mit prokaryotischen ribosomalen Untereinheiten (deren Struktur sehr ähnlich ist) zeigten, dass einige r-Protein - Assemblierungsereignisse voneinander abhängig sind, während andere unabhängig voneinander geschehen können. Der Prozess der Ribosomenbiogenese kann in eukaryotischen Zellen nicht von selbst ablaufen, sondern benötigt zahlreiche Protein- oder RNA (snoRNA) Komponenten die im Zuge der Reifung mit den verschiedenen Vorläuferpartikeln interagieren. Sowohl der Prozess der eukaryotischen Ribosomenbiogenese als auch die Struktur reifer Ribosomen wurde am intensivsten an der Bäckerhefe (*S.cerevisiae*) untersucht. Detaillierte Strukturdaten reifer Ribosomen (in atomarer Auflösung) sind seit ein paar Jahren verfügbar. Diese tragen sowohl zum besseren Verständnis der Translation, als auch zum Prozess der Herstellung ribosomaler Untereinheiten bei.

Ein Ziel dieser Arbeit war, den Assemblieungsprozess der 46 r-Proteine der großen ribosomalen Untereinheit der Bäckerhefe bezüglich einiger bisher unverstandenen oder nur teilweise bekannten Aspekte zu analysieren. In einem Ansatz wurden dabei unterschiedlich weit gereifte Vorläuferribosomen aus Hefezellextrakten gereinigt und hinsichtlich ihrer Zusammensetzung miteinander verglichen. Durch quantitative Analyse der darin enthaltenen r-Proteine sollte so ermittelt werden, welche r-Proteine zu welchem Zeitpunkt der Reifung (stabil) eingebaut werden. Um die hierarchischen Beziehungen zwischen der Assemblierung einzelner r-Proteine in den Zellen zu erforschen, wurden r-Protein Expressionsmutanten verwendet, in denen einzelne r-Proteine depletiert werden können. Die Änderung in der Zusammensetzung der daraus gereinigten Vorläuferribosomen sollte Aufschluss darüber geben, welche anderen r-Proteine und/oder Biogenesefaktoren von der Assemblierung des

depletierten r-Proteins abhängen. Die daraus gewonnenen Daten über hierarchische Beziehungen sollten mit bisher bekannten Daten aus *in vivo* und *in vitro* Experimenten verglichen werden. Außerdem konnten (mit Hilfe der ribosomalen Kristallstruktur) die identifizierten hierarchischen Abhängigkeiten mit den Positionen der jeweiligen r-Proteine im reifen Ribosom in Zusammenhang gebracht werden.

Die vergleichenden Studien an unterschiedlich gereiften Vorläuferpartikeln zeigten, dass die meisten r-Proteine der großen Untereinheit bereits mit sehr frühen Vorläufern interagieren können. Diese ersten Interaktionen scheinen aber eher schwach zu sein und erst im Laufe der weiteren Reifung stabilisiert zu werden. Deshalb kann der Einbau der meisten r-Proteine der großen Untereinheit als mehrstufiger Prozess betrachtet werden und weniger als ein einzelnes Ereignis. Einige r-Proteine zeigten allerdings ein deutlich anderes Assemblierungsverhalten. Sie scheinen erst mit etwas weiter gereiften (bzw. schon sehr weit gereiften, zytoplasmatischen) Vorläufern stabil zu interagieren, da sie in früheren Vorläufern nur in sehr geringem Maß vorhanden waren.

Die Analysen der mutierten Vorläuferribosomen, die aus Zellen gereinigt wurden in denen jeweils ein bestimmtes r-Protein depletiert wurde, deuteten auf klare hierarchische Beziehungen zwischen einzelnen Assemblierungsereignissen von r-Proteinen in der Zelle hin. Diese Beziehungen können zwei Kategorien zugeordnet werden. Nach Depletion der meisten r-Proteine tendierte spezifisch die Bindung jener r-Proteine geschwächt zu sein, die in der Nähe des depletierten r-Proteins binden bzw. mit derselben rRNA Sekundärstrukturdomäne interagieren. Neben diesen spezifischen „lokalen“ Effekten wurden Effekte beobachtet, die eher mit dem jeweiligen Depletionsphänotyp in Zusammenhang gebracht werden können. Betroffen waren in diesen Fällen vor allem jene r-Proteine, die normalerweise erst nach dem unterbrochenen Reifeschritt (z.B. Prozessierung von Vorläufer rRNA) stabil eingebaut werden. Verglichen mit den bisher bekannten hierarchischen Beziehungen einzelner r-Proteine, die vor allem aus *in vitro* Experimenten prokaryotischer r-Proteine stammen, ergaben sich klare Unterschiede, deren Ursache diskutiert wird.

Neben den r-Proteinen wurde in diesen Mutanten auch die veränderte Wechselwirkung von Ribosomenbiogenesefaktoren analysiert. Oft schien die Rekrutierung bestimmter Faktoren gestört zu sein, während in anderen Fällen die Freisetzung nicht mehr effizient funktionierte. Durch diese zusätzlichen Informationen können in vielen Fällen Assemblierung von r-Proteinen und Interaktion von Faktoren mit dem jeweiligen Reifungsereignis (z.B. Prozessierung der Vorläufer rRNA) in Zusammenhang gebracht werden, um die molekularen Voraussetzungen für dieses Ereignis besser verstehen zu können.

2 Introduction

2.1 The Ribosome – Function and Structure

2.1.1 Function of the Ribosome

Ribosomes are ribonucleoprotein (RNP) particles that (in all growing cells in all domains of life) catalyze the translation of the genetic information of messenger RNA (mRNA) into proteins. Their name derives from the terms “ribonucleic acid” and “soma” (Greek, meaning “body”) and was first introduced in 1958 by Richard B. Roberts. All ribosomes are composed of a large and a small subunit (LSU and SSU, respectively) that consist of two types of macromolecules: ribosomal proteins (r-proteins) and ribosomal RNAs (rRNAs). They catalyze the synthesis of proteins by promoting the formation of peptide bonds between the different amino acids. The individual amino acids are provided by aminoacyl-tRNAs whose anticodons base pair with the respective codons on the mRNA template. The establishment of the peptide bonds occurs in “N to C” direction starting with a methionine residue. Both ribosomal subunits are required for translation. The SSU contains the decoding centre and is required for binding of the mRNA whereas the LSU is catalyzing the formation of the peptide bond in its so called peptidyle transferase center (PTC). Three tRNA binding sites, designated A, P, and E sites have been described. The aminoacyl tRNA which contains the amino acid to be attached to the C terminus of the nascent peptide/protein is bound at the A site while the P site binds the so called peptidyl-tRNA (the “previous” tRNA which is still bound to the nascent peptide/protein). The E-site binds the free tRNA before it is released from the ribosome.

Initial structural data revealed that the PTC is almost completely devoid of ribosomal protein residues why the catalytic activity of the ribosome was attributed to the RNA components, leading to classification of the ribosome as a “ribozyme”. The detailed mechanism of the peptide bond formation in the PTC is not yet fully understood and was for long times under debate. Some higher resolved structural data emerging at the beginning of this century (see 2.1.3) and the high degree of conservation of some rRNA residues at the active center brought up the idea that an adenine residue (A2451 in *E.coli*) adopts a direct chemical role, perhaps in a general acid/base catalysis (Nissen et al., 2000). However, this and other potentially crucial rRNA residues could be mutated without drastically reducing the reaction rate arguing against a direct involvement of rRNA residues in the actual catalytic mechanism (Thompson et al., 2001). Instead, as described a few years later, a part of one of the substrates, namely the site 3’ residue of the P-site tRNA (A76) seems to be directly involved in the actual reaction with its 2’OH group (Weinger et al., 2004; Zaher et al., 2011). As mentioned before, the detailed mechanism of this “substrate-assisted” catalysis of the peptide bond formation is not yet entirely understood but it seems clear that the function of the ribosome itself is rather to correctly position the substrates in regard to each other. Therefore, the role of the ribosome in peptide bond formation (which is enhanced by a factor of around 10^7 by the ribosome) is likely not primarily to reduce the enthalpy of activation by

stabilizing the transition state(s) of the reaction (which is normally the case for “classical” enzymes). Instead, the increase of the reaction rate by the ribosome was characterized to be largely of entropic origin why the ribosome was described to function as “entropic trap” (Sievers et al., 2004).

Ribosomal proteins, which were initially described to be completely absent from the active center within a range of about 20Å and therefore thought to be not involved in the actual catalytic reaction, are also crucial for the function of the ribosome, directly or indirectly. The publication of a highly resolved crystal structure of a prokaryotic ribosome loaded with A- and P-site tRNAs proved that two ribosomal proteins of the large subunit (L16 and L27) are directly interacting with the tRNA substrates in the PTC and therefore involved in the peptidyl transfer (Voorhees et al., 2009). In addition, r-proteins, most of which are essential for growth, often have different roles. Most of them are mainly required to enable the formation and the maintenance of a stable structure or to mediate binding of translation factors. The so called “exit tunnel”, through which the nascent peptide leaves the LSU, contains several LSU r-proteins which might contribute to the development of an appropriate folding environment for the nascent protein (for a review see for example Fedyukina and Cavagnero, 2011). Furthermore, a few r-proteins have been described to be involved in codon – anticodon recognition (Brodersen and Nissen, 2005; Ogle et al., 2001). In addition, most essential r-proteins are required for the cytoplasmic accumulation of mature ribosomal subunits by being involved (directly or indirectly) in several maturation events of pre-mature ribosomes (see e.g. Ferreira-Cerca et al., 2005; Pöll et al., 2009, citations therein and more detailed in sections 2.2 and 2.3). Selected reviews describing the current knowledge about the translation process and its regulation can be found in (Benelli and Londei, 2009; Hinnebusch, 2014; Moore and Steitz, 2011; Rodnina, 2013; Rodnina and Wintermeyer, 2009; Sonenberg and Hinnebusch, 2009; Steitz, 2008; Voorhees and Ramakrishnan, 2013; Wilson and Doudna Cate, 2012).

2.1.2 Components of the Ribosome

The terminology of ribosomes of the different domains of life as well as those of their subunits refers to one of their physical features, namely the sedimentation coefficient (s) that is given in Svedberg units (S). Prokaryotic 70S ribosomes consist of a large 50S and a small 30S subunit. The 50S LSU consists of two rRNA molecules, the 23S and the 5S rRNAs, respectively (3042 nucleotides in *E.coli*), and more than 30 r-proteins. The 30S SSU contains the 16S rRNA (1542 nucleotides in *E.coli*) and more than 20 r-proteins. All these components add up to a total mass of more than 2.5 MDa and to a size of about 20 to 25 nm.

The eukaryotic 80S ribosome is composed of a large 60S subunit and a small 40S subunit. The 60S LSU consists of three rRNAs and at least 46 r-proteins. The 40S SSU consists of one rRNA molecule and 33 r-proteins. The length of the rRNAs varies remarkably in different eukaryotic organisms. In *S.cerevisiae* for instance, the 5.8S, 25S, and 5S rRNAs that constitute the LSU add up to a total length of 3675 nucleotides. The 18S rRNAs which is part

of the SSU contains 1800 nucleotides. The rRNA species of metazoans are in general longer: in comparison to *S.cerevisiae*, the total number of rRNA nucleotides in *D.melanogaster* and *H.sapiens* is increased by 13% and 31%, respectively. The number of eukaryotic r-proteins is more conserved and varies by only one additional LSU r-protein that is not found in *S.cerevisiae.* However, the total r-protein mass in these two metazoans is remarkably increased by 8% (*D.melanogaster*) and 6% (*H.sapiens*) (Anger et al., 2013). Due to the increased number of nucleotides and amino acids, both, the mass and the size of eukaryotic ribosomes are higher than the one of its prokaryotic counterparts. Most of the additional rRNA and protein stretches specifically found in eukaryotes are located on the surface (see sections 2.1.4 and 2.1.5).

2.1.3 Structural information has constantly improved

To better understand the mode of action of complex RNPs like the ribosome, detailed structural information is extremely helpful. During the last four decades a lot of effort has therefore been made in dissolving its structure. The first reports of the overall ribosomal structure and its features like shape or orientation of the subunits to each other come from studies mainly performed in the 1970ies and 1980ies using electron microscopy (EM) (Lake, 1976; Stöffler and Stöffler-Meilicke, 1984). The first structures of ribosomal subunits in atomic resolution were solved in the year 2000 by several groups using X-ray crystallography. The publication of the atomic structure of the LSU of the archaeon *Haloarcula marismortui* at a resolution of 2.4Å (Ban et al., 2000) was followed by the structures of the SSU of the prokaryote *Thermus thermophilus* at resolutions of 3.3Å and 3.0Å, respectively (Schluenzen et al., 2000; Wimberly et al., 2000). The first crystal structure of an entire 70S ribosome with a resolution of 5.5Å from *Thermus thermophilus* was published in 2001 (Yusupov et al., 2001). A few years later, the resolution increased with the *E.coli* 70S ribosome crystal structure (Schuwirth et al., 2005). Structural information on eukaryotic ribosomal subunits or entire 80S ribosomes were for a long time limited to cryo-EM data with a resolution of not more than about 15Å (Spahn et al., 2001). Recent milestones in the field were the crystallization and determination of high resolution X-ray structures of eukaryotic LSUs or 80S ribosomes isolated from *Tetrahymena thermophila* and *S.cerevisae,* respectively (Klinge et al., 2011; Ben-Shem et al., 2011). Crystal structures of higher eukaryotes are still lacking. However, high resolution cryo-EM structures of human and *D.melanogaster* ribosomes with resolutions of up to around 5Å are available since 2013 (Anger et al., 2013). Finally it should be mentioned that structural information on premature ribosomes is, for several reasons, highly limited to a few cryo-EM structures of late pre-LSUs or pre-SSUs (Bradatsch et al., 2012; Campbell and Karbstein, 2011; Leidig et al., 2014).

2.1.4 General structural features of pro- and eukaryotic ribosomes and their components

Despite the above (2.1.2) mentioned variations in number and length of both, r-proteins and rRNAs in the different domains of life, all ribosomes share substantial morphological similarities. Prominent “landmarks” found in all ribosomes are the central protuberance, acidic- (or phospho-), and L1-stalk or the exit tunnel for the LSU and “body”, “platform” or “head” domains for the SSU (see Figure 1).

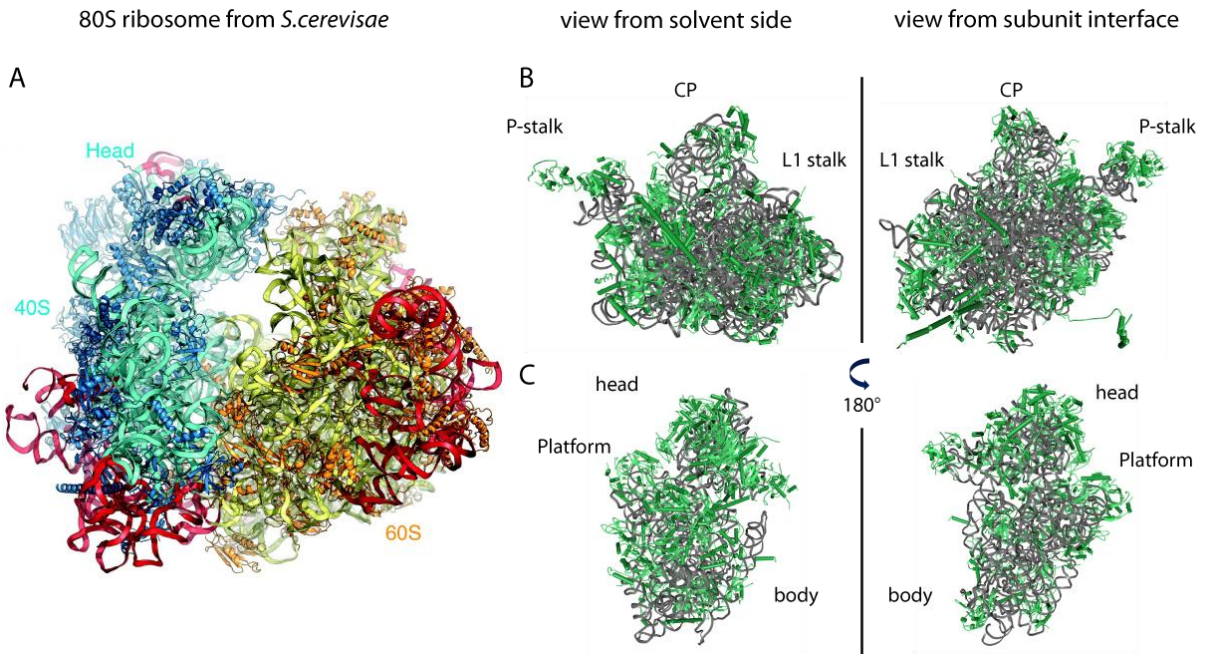

Figure 1 - Crystal structure of the entire yeast 80S ribosome and its subunits

A) shows the yeast 80S ribosome viewed from the A-site (entry side / aminoacyl tRNA binding site). rRNA and r-proteins from the SSU are colored in cyan and blue, respectively. Those of the LSU are colored in yellow and orange, respectively. Yeast specific expansion segments of the rRNA (in comparison to prokaryotic ribosomes) of both subunits are colored in red. Adapted from Jenner et al., 2012. Both subunits are depicted isolated from each other in **B)** and **C)** viewed from the subunit interface and the opposite “solvent” side, respectively. R-proteins are colored in green and rRNA in dark gray. **B)** shows the LSU with prominent features as the central protuberance (CP), acidic- or phospho-stalk (P-stalk) and the position where the L1 stalk is located (note that rpL1 is missing in this X-ray structure. **C)** shows the SSU with its structural features head, platform and body based on PDB files 3U5F, 3U5G, 3U5H, and 3U5I from Ben-Shem et al., 2011.

Looking at the morphology of the single components, one can observe that many r-proteins consist of a globular domain that is often bound at the surface and extensions or loops protruding into rRNA areas, often connecting different helices (Ben-Shem et al., 2011). Due to the high affinity to rRNA many of them have higher-than-average pI values.

Most rRNA regions fold into helical elements that are connected by loops; they are called stem-loop structures. Many rRNA stretches are parts of RNA double helices, which can even be made of rRNA stretches from different rRNA molecules. In addition, RNA pseudoknot structures are found in all ribosomes. Secondary structure elements of SSU and LSU rRNAs were predicted long before the first detailed structures came up (Fox and Woese, 1975;

Noller et al., 1981; Woese et al., 1980). The secondary structures for SSU and LSU rRNAs were subdivided into three and six major domains, respectively (Figure 2A). Once 3D information on ribosomal subunits was available, the organization of the secondary structures domains of both subunits could be compared to their positioning in space what gave different results for both subunits. Concerning the SSU, each of the three major rRNA domains forms an individual morphological region: the 5' domain forms shoulder and foot, the central domain forms the platform and the 3' domain (which can be subdivided into a 3' major and a 3' minor domain) mainly forms the head. The ensemble of shoulder, foot, and platform has been given the term "body". In contrast to that, the segregation of the LSU rRNA into distinct domains in 3D is not as apparent as for the SSU. The six rRNA domains are much more intertwined and give the LSU a rather "one-domain" – like appearance (Figure 2B).

2.1.5 Differences in ribosome composition and structure between the different domains of life

Even if the ribosomal core (which mainly consists of rRNA) is well conserved in ribosomes of all domains of life, eukaryotic ribosomes contain additional, variable regions (VR) which are mainly located on the surface. These so called expansion segments (ESs) can reach substantial lengths and were first described in comparative analyses on the rDNA of different species of different domains of life performed in the 1980s (Clark et al., 1984; Gerbi, 1986). The length of ES7L for instance is around 200 nucleotides in *S.cerevisiae* and more than 850 nucleotides in *H.sapiens* (Figure 2C). A total of 58 VRs or ESs have been described (Figure 2A and Anger et al., 2013). Notably, the 5.8S rRNA which is not found as a separated rRNA molecule in prokaryotes is actually highly homologue to parts of the LSU 23S rRNA domain I and is therefore only partially specific for eukaryotes.

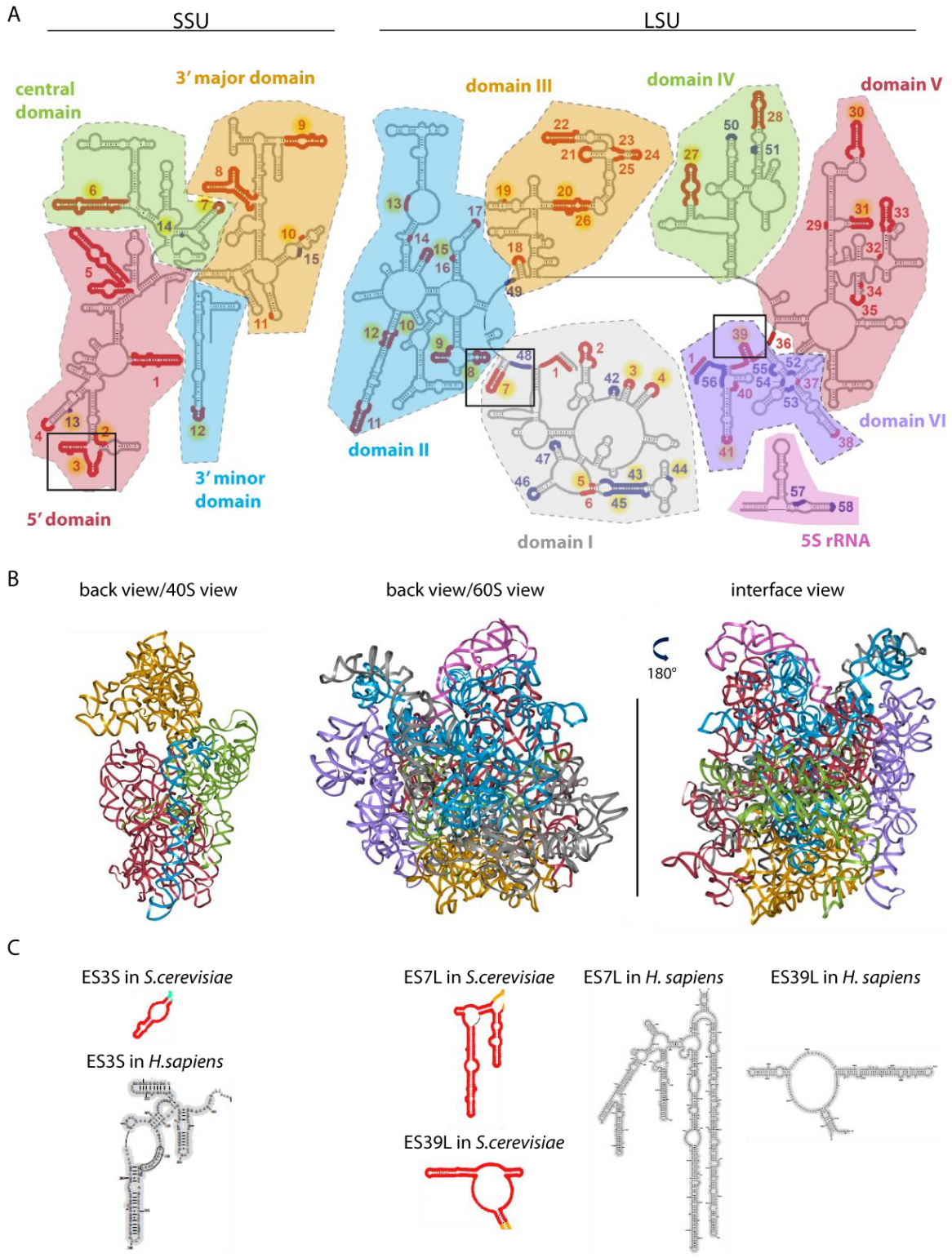

Figure 2 - Comparison of the secondary rRNA structure domains of both subunits to their tertiary organisation in space

A) Scheme of the secondary structure domains of prokaryotic rRNA (16S, 23S, 5S rRNAs) of both subunits. Eukaryote specific variable regions (VR) and expansions segments (ES) are highlighted and numbered in blue and red, respectively, as introduced in Anger et al., 2013. The secondary structure domains are highlighted in different colors. Examples of three ES are marked with black boxes, their strucutre in yeast and human are shown in C). **B)** shows the 3D organisation of the rRNA domains of both eukaryotic (yeast) ribosomal subunits using the same colors as in the 2D scheme of A). The structure derived from PDB files 3U5F-3U5I published by Ben-Shem et al., 2011. **C)** shows three ES and their 2D structure in yeast and human ribosomes as adapted from Jenner et al., 2012 and Anger et al., 2013, respectively.

The above described nature of rRNA core conservation can be expanded to the whole 3D structure including its r-proteins. About half of the ~80 eukaryotic r-proteins are conserved in prokaryotes (Lecompte et al., 2002, see also table 1). Some eukaryote specific r-proteins have been described to interact with other protein (complexes) and likely fulfill additional cellular functions (see e.g. Rachfall et al., 2013 and citations therein). The recently published high resolution crystal structure of a eukaryotic (*S.cerevisiae*) 80S ribosome revealed that the additional, eukaryote-specific r-proteins often contact eukaryote-specific ESs and form an addional RNA-protein layer located on the surface (Ben-Shem et al., 2011). The structures of metazoan ribosomes show that the in part massively prolonged ESs build additional RNA-RNA and/or RNA-protein interaction networks that are located on "top" of the first RNA-protein layer. The term "layered evolution" has therefore recently been introduced to describe these observations (Anger et al., 2013 and Figure 3). In cryo-EM reconstructions of mammalian ribosomes, many of the in part massively prolonged mammalian specific ESs contributed only verly little to the electron densitiy suggesting that they might be highly flexible (Anger et al., 2013; Chandramouli et al., 2008; Dube et al., 1998; Morgan et al., 2000). Deletion of ES27L of *tetrahymena* was shown to be lethal indicating a possible functional relevance (Sweeney et al., 1994). Another example for the requirement of a variable rRNA region was described for helix 6 of the SSU rRNA from *S.cerevisae,* whose mutation resulted in severe effects in the maturation of the SSU (van Nues et al., 1997). The increased complexity of eukaryotic translation regulation might also explain their presence (see reviewed in Sonenberg and Hinnebusch, 2009; Wilson and Doudna Cate, 2012). In summary, the detailed roles of most of them remain unclear, though.

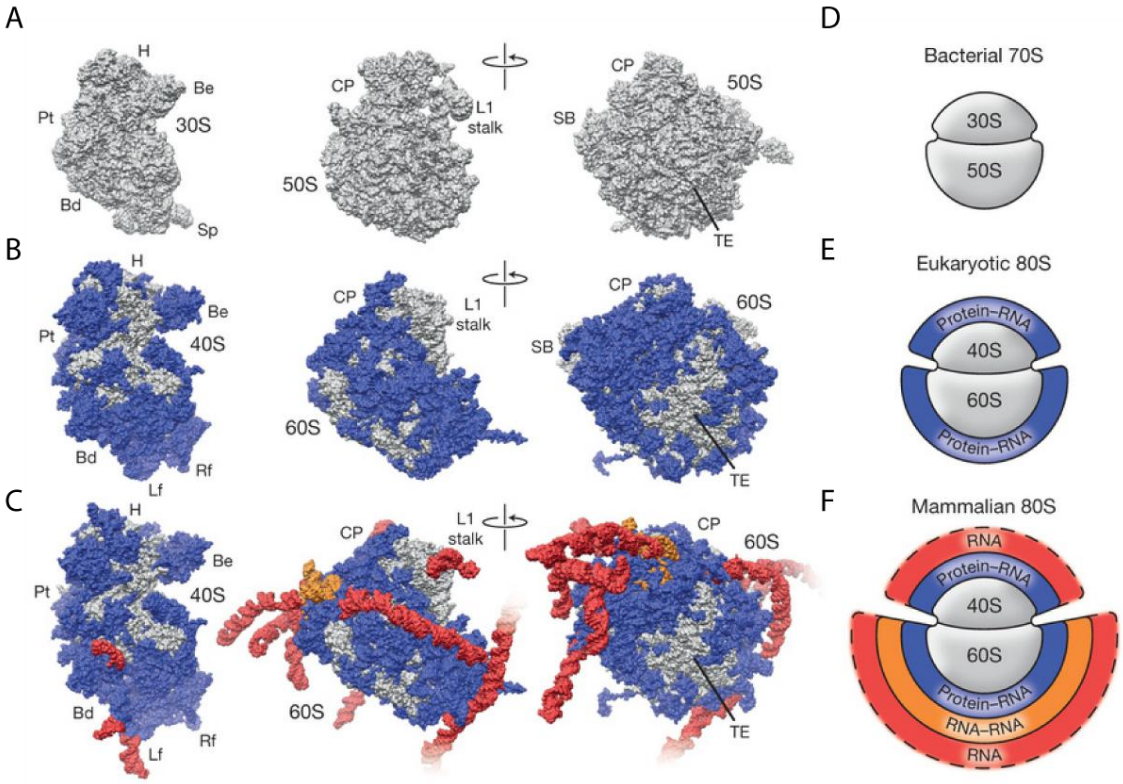

Figure 3 (previous page) - Evolution of ribosomes from prokaryotes to higher eukaryotes by highlighting main structural differences

A) The structure of both ribosomal subunits of prokaryotic (*T.thermophilus*) 70S ribosomes. The LSU is depicted from two perspectives. Abbreviations: H=head; Be=beak; Pt=platform; Bd=body; Sp=spur; CP=central protuberance; SB= P-stalk base; TE= tunnel exit **B)** shows the structures of yeast ribosomal subunits using the same scale. Eukaryote specific rRNA and r-protein regions are highlighted in blue ("eukaryote specific first RNA – protein layer"). **C)** Illustrates *H.sapiens* ribosomal subunits highlighting the additional human specific "layers" ("RNA-RNA" layer in orange and a "RNA only" layer in red. **D-F)** highlight the different layers the authors defined in their description of the "layered evolution". Adapted and modified from Anger et al., 2013.

2.2 Eukaryotic Ribosome Biogenesis

2.2.1 Overview

The process of eukaryotic ribosome biogenesis is enormously complex and energy demanding. As example, a single cell of the yeast *S.cerevisiae* contains nearly 200 000 ribosomes, that hold 80% of the total RNA pool. Considering a generation time of around 100 minutes, the growing yeast cell has to produce in average 2000 ribosomes per minute (Warner, 1999). All three RNA Polymerases are involved in this process. RNA Polymerase I and III transcribe the genes coding for the rRNAs whereas RNA Polymerase II transcribes the genes coding for the r-proteins. The nucleolus, a non-membrane-bound sub-compartment of the nucleus is the place where RNA Polymerase I starts ribosome biogenesis by synthesizing most of the rRNA (see 2.2.2). The latest maturation steps are done in the cytoplasm where the mature subunits finally enter the cycle of translation. On the way from rRNA synthesis to functional ribosomal subunits many crucial processes occur. These include extensive modification, processing and folding of the rRNA (2.2.3), stable association of the r-proteins (2.3), and transport of the premature ribosomal subunits to the cytoplasm (2.2.5 and 2.2.6). In addition to that, the action of more than 70 small nucleolar RNAs (snoRNAs) and around 200 trans-acting proteins, the so called ribosome biogenesis factors, were described, many of which are essential to enable the production of functional subunits (2.2.4, 2.2.5, and 2.2.6). Recent reviews with focus on different aspects of ribosome biogenesis can be found for example in Henras et al., 2008; Kressler et al., 2010; Strunk and Karbstein, 2009; Thomson et al., 2013; Woolford and Baserga, 2013. The whole process was for several reasons most extensively studied in *S.cerevisiae.* Therefore, if not otherwise declared, all following statements in this work refer to the situation in *S.cerevisae* which will be termed "yeast".

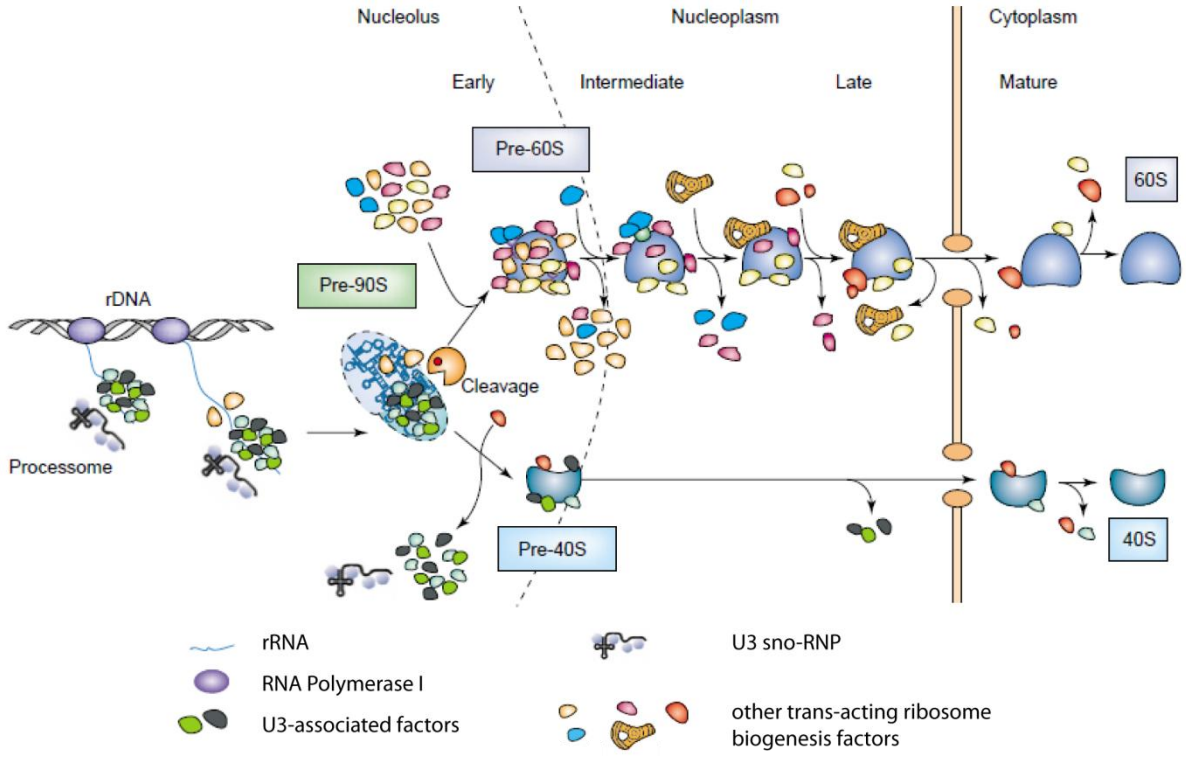

Figure 4 - Simplified scheme of eukaryotic ribosome biogenesis

The processes of eukaryotic ribosome biogenesis is illustrated very simplified in this textbook scheme adapted from Tschochner and Hurt, 2003, starting with rDNA transcription of RNA Polymerase I in the nucleolus. See text for further explanation and note that r-proteins and their incorporation are not illustrated in this scheme.

2.2.2 Transcription of the genes encoding the ribosomal RNAs in the Nucleolus

The nucleolus, which is defined by the ongoing transcription of the rDNA (the genes coding for rRNA (Thiry and Lafontaine, 2005)) by RNA Polymerase I, is visible by light microscopy as a darker region in the nucleus. More detailed electron micrographs show that (in yeast) it often adopts a semi lunar shape (see for example Léger-Silvestre et al., 1999). In yeast, under normal conditions, each nucleus contains only one nucleolus which is formed around the rDNA loci. The rDNA loci are organized in the so called “rDNA repeats” that are all located on Chromosome XII (Long and Dawid, 1980; Petes, 1979). In total, the ~150 copies make up around 10% of the whole yeast genome. In each repeat, the sequences coding for three of the four rRNAs are organized in one 6.6kb long operon-like gene that encodes the 35S rRNA, a precursor rRNA (pre-rRNA) that contains the sequences of the 18S, 5.8S and 25S rRNAs (Figure 5A). This precursor is synthesized by RNA Polymerase I; the three comprising rRNA sequences are separated by spacer sequences which are not part of mature ribosomes and consequently have to be removed (see 2.2.3). The forth rRNA, the 5S rRNA, whose gene is separated by the 35S rRNA gene by a non coding intergenic spacer (IGS), is transcribed by RNA Polymerase III (Philippsen et al., 1978). To initiate transcription of the 35S rRNA gene by RNA Polymerase I several factors are required, (described for example in Blattner et al., 2011; Moss et al., 2007). Once transcription is initiated, RNA Polymerase I maintains an average elongation rate of 40-60 nucleotides per second to

achieve the required massive production of rRNA (French et al., 2003; Kos and Tollervey, 2010). The mechanism of the termination of Polymerase I transcription is not known in detail but it depends on several RNA cis-elements that are located downstream of the 3' end of the 35S pre-rRNA as well as on trans-acting factors that interact with these elements. An RNA endonuclease was described to release the 35S rRNA likely during transcription, albeit alternative, unknown termination mechanism(s) cannot be excluded (see e.g. Németh et al., 2013). The yeast RNA Polymerase I is a large holoenzyme consisting of 14 subunits, many of which are shared with the other two RNA Polymerases. Recently published crystal structures of this huge machinery allow some deeper insights on how the transcription process occurs and how it might be regulated (Engel et al., 2013; Fernández-Tornero et al., 2013). Both, the requirement to fulfill the high demand of rRNAs and their equimolar production might explain the high number of the rRNA genes and their operon like composition, which is conserved in all eukaryotes. The physical adjacency of the 5S rRNA gene to the 35S rRNA gene as it is found in *S.cerevisiae* is often different in other eukaryotes, whose 5S rRNA gene repeats are separated from the nucleolar repeats, though (Drouin and de Sá, 1995; Haeusler and Engelke, 2006). One way to investigate and quantify ongoing RNA Polymerase I transcription is the direct visualization of chromatin spreads by electron microscopy (EM). Since this technique was established by Oscar Miller in the late 1960s the resulting EM images are called "miller spreads" (Miller and Beatty, 1969). The numerous RNA Polymerase I complexes that "sit" on single rDNA repeats having transcribed the 35S rRNA gene to different degrees, and the nascent rRNA give the miller spreads a "Christmas tree" like appearance (Figure 5B). Interestingly, not only the process of transcription but also the first steps in ribosome biogenesis can be visualized and investigated with this method, as the first steps occur co-transcriptionally (see 2.2.3 and Figure 7).

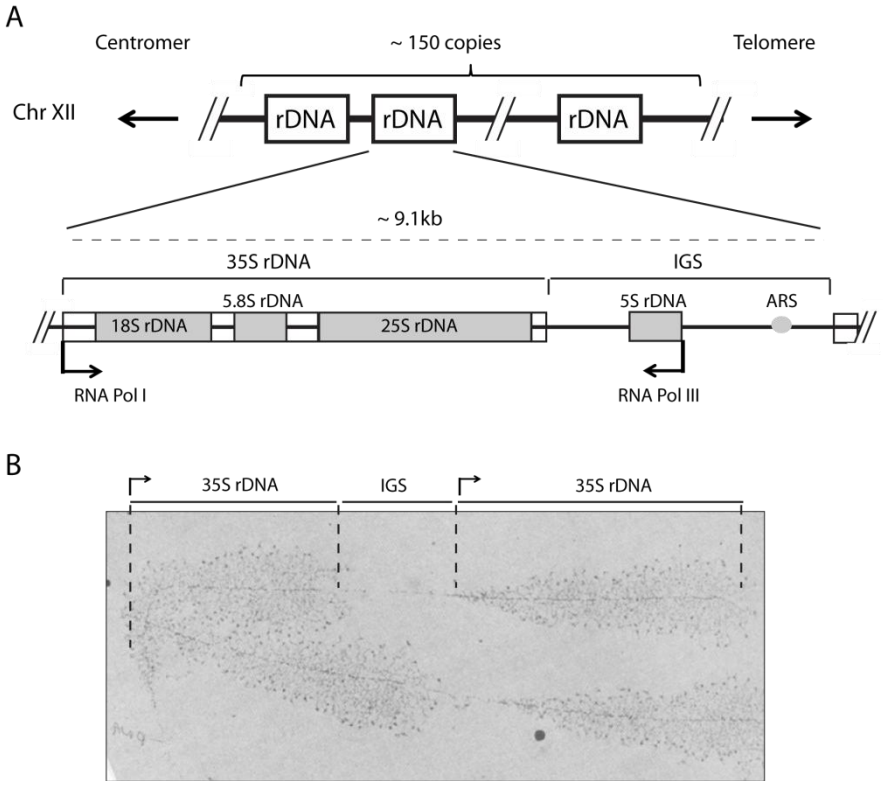

Figure 5 - Organization of rDNA loci in yeast and visualization of nascent rRNA ("Miller spreads")
A) shows the organization of the ~ 150 copies of the rDNA in yeast which are located on chromosome XII. The composition of one rDNA repeat which has a length of about 9.1 kbp is illustrated in more detail. The 35S rDNA which is coding for the 35S pre-rRNA (containing the sequences of the mature 18S, 5.8S, and 25S rRNAs and some spacer sequences in between) is transcribed by RNA Polymerase I, while the 5S rRNA coding gene is transcribed by RNA Polymerase III in the opposite direction. The region separating the 35S rDNA sequences of neighboring rDNA repeats is called intergenic spacer (IGS). Each repeat contains one autonomous replication sequence (ARS). **B)** shows an electron micrograph of several nascently transcribed rDNA loci from *Triturus viridescens* (newt) oocytes. The nascent rRNA molecules ("branches" of the "tree") contain terminal knobs ("Christmas ornaments") at their ends which correspond to the nascently formed precursor RNP. The rDNA represents the "trunk" of the "Christmas tree". Adapted from Miller and Beatty, 1969.

2.2.3 Processing and modification of ribosomal RNAs

As already mentioned above, the initial 35S pre-rRNA contains, beside the sequences of the 18S, 5.8S, and 25S rRNAs, spacer sequences which are not present in mature subunits and therefore have to be removed by processing events. The 5' or 3' external transcribed spacers (termed 5'ETS and 3'ETS, respectively) "frame" the sequences of the three rRNAs which are separated by the two internal transcribed spacer regions 1 and 2 (ITS1 and ITS2, respectively) (see Figure 6). These four spacers are removed in a successive way by both, endo- and exonucleolytic processing reactions (Venema and Tollervey, 1995). The sites where the cleavages occur determine the size of the different pre-rRNA intermediates which are termed according to their sedimentation coefficient and (sometimes) the cleavage site at their end (see processing scheme in Figure 6). In eukaryotes, these processes were initially thought to occur exclusively after transcription. In this situation, the 3' end of the 35S pre-rRNA is created by an endonucleolytic cleavage event which is in yeast performed by Rnt1, a homologue of the bacterial endonuclease RNase III. For fast growing and quickly dividing eukaryotes like yeast grown under laboratory conditions, this concept of post-transcriptional

cleavage was challenged about 10 years ago, though. Thoroughly performed investigation of the sizes of the "ornaments" at the end of the branches of the "Christmas trees" visualized in the miller spreads which represent the nascent RNPs, lead to the conclusion, that 40-80% of the nascent transcripts are co-transcriptionally cleaved in the ITS1 (Osheim et al., 2004). This observation was more recently confirmed by a different approach using rapidly harvested metabolically labeled yeast cultures. The resulting kinetic data were then mathematically modeled with the outcome, that 70% of the nascent transcripts are indeed co-transcriptionally cleaved (Kos and Tollervey, 2010). In the "normal" case of a post-transcriptional cleavage (which is likely the case for higher eukaryotes), where the first processing substrate is the 35S pre-rRNA (in yeast), the next cleavage events normally happen in the 5' ETS at sites A0 and A1 resulting in the production of the 33S and 32S pre-rRNAs (see processing scheme in Figure 6). The first cleavage of the 35S pre-rRNA can, however also occur in the ITS1 at site A2 normally resulting in the production of the 20S and 27SA2 pre-rRNAs. Notably, site A2 is the one at which co-transcriptional cleavage was described to likely occur (Kos and Tollervey, 2010). Since the 20S pre-rRNA is precursor of the SSU 18S rRNA and the 27SA2 pre-rRNA contains both LSU 5.8S and 25S rRNAs, the processing (and assembly) pathway of both subunits is separated at this stage. Concerning the further pre-rRNA processing of the LSU, the pathway splits in two possible ways at the level of the 27SA2 pre-rRNA: In around 90% of the cases the subsequent cleavage is an MRP RNAse-catalyzed endonucleolytic reaction at site A3 (Chu et al., 1994; Lindahl et al., 1992) resulting in a short lived 27SA3 pre-rRNA whose remaining ITS1 spacer sequences are trimmed away by the 5'-3' exonucleases Rat1 and Rrp17. These exonucleolytic cleavages stop at site B1s which forms the 5' end of the 5.8S rRNA in the $27SB_s$ pre-rRNA (Henry et al., 1994; Lygerou et al., 1996; Oeffinger et al., 2009; Schmitt and Clayton, 1993). The remaining ~10% of the 27SA2 pre-rRNA are endonucleolytically cleaved at site $B1_l$ (by an unknown endonuclease) which is located 6nt further 5' of site $B1_s$. This cleavage results in the production of the $27SB_l$ pre-rRNA which consequently is 6nt longer than the $27SB_s$ pre-rRNA.

The following processing events are identical for both 27SB intermediates. First, the 5.8S and 25S sequences are separated by an endonucleolytic cleavage reaction in the ITS2 (by an unknown endonuclease) at site C2 resulting in the production of the $7S_{s/l}$ and 25.5S pre-rRNAs. The remaining ITS2 sequences of the 25.5S pre-rRNA are 5'-3' exonucleolytically removed by Rat1 which halts at the 5' end of the 25S rRNA (Geerlings et al., 2000).

The residual ITS2 sequences of the $7S_{s/l}$ pre-rRNA are trimmed away in several steps described in the following. The first step in the removal of the ~130 nucleotides of the ITS2 sequences 3' of the 5.8S rRNA is catalyzed by the core exosome which includes 3'-5' exonucleases (Allmang and Tollervey, 1998; Mitchell et al., 1996). The resulting "5.8S + 30" pre-rRNA is further processed by Rrp6 leading to the 6S pre-rRNA which is the 5.8SS rRNA extended by 5-8 nucleotides (Briggs et al., 1998). The 3'-5' exonucleaes Rex1 and Rex2, which are part of the RNase D family, and which were in yeast described to be involved the processing of other RNAs, continue to shorten the 6S pre-rRNA by a few nucleotides yielding

in an intermediate whose 5.8S rRNA precursor is only extended by around 5 nucleotides (van Hoof et al., 2000). The 3' end of the 5.8S rRNA is finally created by Ngl2 which is encoded by a nonessential gene (Faber et al., 2002). The finding that the "5.8S + 5" intermediate accumulates in the cytoplasm after Ngl2 depletion lead to the conclusion that this very last processing event occurs in the cytoplasm (Thomson and Tollervey, 2010). The fact that Ngl2 is nonessential under normal laboratory conditions opens up the question whether there exists an alternative processing way or the removal of the few remaining nucleotides is nonessential for the LSU function in translation. The presence of parts of the "5.8S + 30" pre-rRNA in polysomes described after Rrp6 depletion argues for the latter possibility (Briggs et al., 1998). Remarkably, both mature 5.8S rRNA species ($5.8S_s$ and $5.8S_l$ rRNAs), whose presence is conserved among eukaryotes exist in mature LSUs and seem to be functional as they were identified in polysomes (Woolford and Baserga, 2013).

The 20S pre-rRNA of SSU precursors, which contains parts of the ITS1 sequences is processed by an endonucleolytic cleavage at site D in the cytoplasm which is catalyzed by Nob1 (Fatica et al., 2003a; Lamanna and Karbstein, 2009, 2011; Udem and Warner, 1973).

Defects in the preribosomal maturation pathway can lead to the appearance of aberrant pre-rRNA species and/or to some accumulation or reduction of the level of one or the other pre-rRNA intermediate. In general, defective preribosomal particles are efficiently degraded since their massive accumulation could lead to the sequestration of components (ribosome biogenesis factors or snorRNAs) that are essential for ribosome biogenesis what would eventually lead to a complete block of ribosome maturation (Houseley and Tollervey, 2009). The major pathway for the turnover of the pre-rRNA content of defective pre-ribosomes occurs in the nucleus and involves the action of the exosome and the TRAMP complex (Allmang et al., 2000; Fang et al., 2005; LaCava et al., 2005; Vanácová et al., 2005). Interestingly, the exosome is also required in the 3'→5' removal of ITS2 sequences 3' of the 5.8S rRNA precursors (see above).

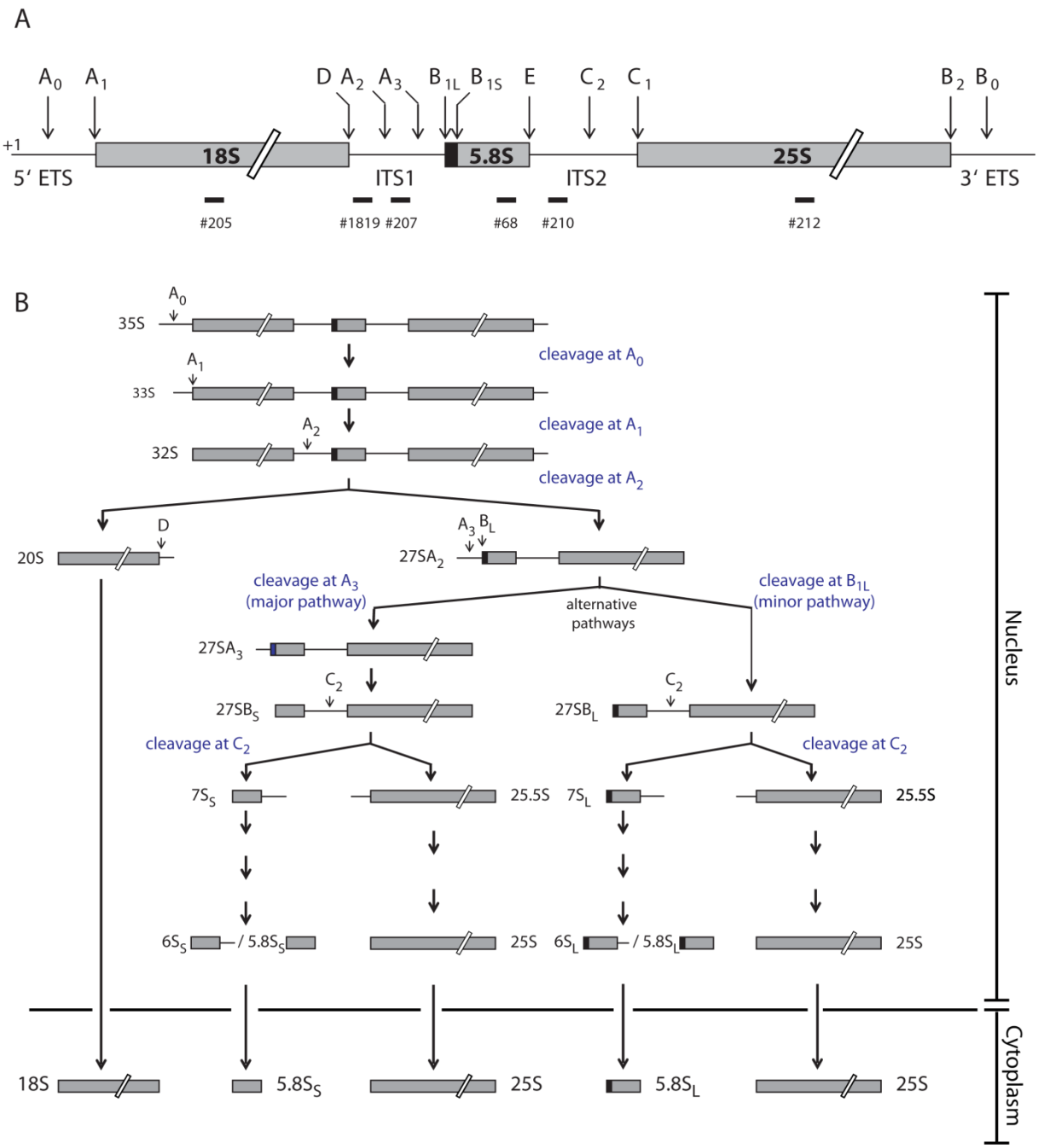

Figure 6 - Scheme of the primary RNA Polymerase I pre-rRNA transcript and its processing in yeast

A) One 35S pre-rRNA molecule is schematically depicted. The sequences corresponding to the mature 18S, 5.8S, and 25S rRNAs are separated by external and internal transcribed spacer sequences (5' ETS, ITS1, ITS2, 3' ETS). The positions of the individual processing sites which are 5' or 3' of ends of rRNA (precursors) are indicated. Note that the lengths of rRNA and spacer sequences are not in proportion to their real lengths. The transcription start site is indicated by "+1". The positions and numbers of the DNA oligo probes used for detection of the different rRNA (precursors) by Northern blotting are illustrated below. **B)** shows the main pathway of 35S pre-rRNA processing including the two alternative ways of 27SA2 pre-rRNA processing. Some important pre-rRNA processing events are described in blue letters and the resulting pre-rRNA intermediates are named in black letters. Adapted from Ohmayer et al., 2013. See text for more detailed explanation.

Pre-rRNA is not only processed but also extensively modified at specific sites. Mainly two kinds of modification are observed: methylations which can occur either at the base or at the 2' oxygen of the ribose and pseudouridylations which are generated by base rotation of uridines (Brand et al., 1977; Retèl et al., 1969). Most of the modifications are introduced by

small nucleolar ribonucleoprotein particles (snoRNPs) which consist of a snoRNA and several protein components (reviewed in Watkins and Bohnsack, 2012). The variable snoRNAs function as guide by base pairing with the specific modification site of the pre-rRNA. The protein components are in principle common and contain the enzymes that catalyze the actual modification. Two classes of snoRNPs, which have been named by their conserved snoRNA sequence motives, exist: box C/D snoRNPs catalyze the methylation of the ribose-2'oxigen at 67 sites of the rRNA while box H/ACA snoRNPs are responsible for the pseudouridylation of 44 bases. The definite function of the single modifications is mostly not clear but it seems that many of them contribute to the "optimization of ribosome structure and function" (Baxter-Roshek et al., 2007; King et al., 2003; Liang et al., 2007, 2009). The lack of individual modifications is in most cases not lethal and does not cause detectable effects on cell growth or ribosome biogenesis, though (Charette and Gray, 2000). Depletion of certain protein components of snoRNPs resulting in the depletion of many single modifications, has more severe effects and is often lethal (Gautier et al., 1997; Lafontaine and Tollervey, 1999). Finally, several (in part essential) modifications are catalyzed by individual proteins that act without requiring the guiding activity of a snoRNAs (Lafontaine et al., 1994; White et al., 2008; Wurm et al., 2010).

2.2.4 General functions of transiently interacting ribosome biogenesis factors

As described above, processing and modification of rRNA (precursors) require the action of snoRNPs and proteins that transiently interact with the premature ribosome. Beside these so called ribosome biogenesis factors, several snoRNAs are required for specific maturation events, other than base modification. Among the best characterized are U3, U14 and snR30 (see 2.2.5).

Fare more trans-acting protein biogenesis factors (in yeast around 200 or more, most of which are essential) were described to be involved in maturation events of preribosomes during their maturation pathway (see 2.2.5 and 2.2.6). Many of them have been assigned to be important for a specific maturation event since their depletion often leads to a specific phenotype; the detailed molecular function for most of them remains unclear, though. Some have predicted or proved enzymatic activity and/or high affinity to RNA or other proteins. They are speculated / described to be nucleases, RNA- or protein modifying enzymes, GTPases, ATPases, RNA helicases, Kinases, or Phosphatases. Biogenesis factors that bind to the earliest ribosomal rRNA precursors (sometimes already during transcription) might be crucial to protect the nascent rRNA from degradation and/or to enhance the establishment of proper sub-structures (see 2.2.5 and for example Hierlmeier et al., 2012). Some factors were described to likely fulfill a role in coordinating specific early assembly/maturation events to each other providing a kind of quality control checkpoint for later assembly/maturation events (see for example Jakob et al., 2012). Some factors were described to prevent the entry of not yet fully maturated ribosomal subunits into the translation cycle by "occupying" crucial interaction sites or to control the export competence of nuclear pre-ribosomal subunits. Considering the sophisticated structure of mature ribosomal subunits and the numerous

contact sites of their different rRNA domains with each other (see 2.1), it is likely that numerous structural changes have to occur during the transition of early preribosomes to mature subunits. As mentioned above, many ribosome biogenesis factors, especially those that bind to early preribosomes are assigned to be involved in these structural changes as well in the stabilization of intermediates (see 2.2.5 and 2.2.6 or Hierlmeier et al., 2012; Lebaron et al., 2013; Pérez-Fernández et al., 2007, 2011). Often, both, binding and/or release of biogenesis factors are related to certain maturation events like pre-rRNA processing, stable incorporation of r-proteins or nuclear export. In other cases, the binding or release of groups of factors is interdependent and follows strictly established hierarchical interrelationships (Jakob et al., 2012; Talkish et al., 2012).

In the last 15 years, improved or newly established methods like epitope tagging with subsequent affinity purification and analysis of the co-purified rRNA intermediates step by step deciphered the maturation state of the preribosomal population the single yeast biogenesis factors interact with. Furthermore, the highly sensitive detection of co-purified proteins by mass spectrometry contributed to the identification of additional (potential) ribosome biogenesis factors (Bassler et al., 2001; Fatica et al., 2002; Grandi et al., 2002; Harnpicharnchai et al., 2001; Saveanu et al., 2001). Some ribosome biogenesis factors have been shown to build modules that are also stable when they don't interact with preribosomes (Hierlmeier et al., 2012; Krogan et al., 2004; Merl et al., 2010; Milkereit et al., 2001). Others are (in part) homologous to r-proteins why they were initially speculated to act as "placeholder" for these r-proteins before their incorporation (Saveanu et al., 2003). A list of most of the yeast ribosome biogenesis factors (often also termed "assembly factors") and (if known) their roles in maturation of pre-SSUs or pre-LSUs can be found for example in (Woolford and Baserga, 2013).

2.2.5 Assembly and maturation of the earliest precursors and the small ribosomal subunit in yeast

The maturation state of the different subsequently generated pre-ribosomal particles is most clearly defined by the processing state of the precursor rRNA(s) they contain (see 2.2.3). In yeast, in the case of post-transcriptional cleavage, the earliest precursors contain the 35S pre-rRNA that comprises the sequences of both, SSU and LSU rRNAs. With the cleavage in the ITS1 (which also occurs co-transcriptionally) the precursors for both subunits are separated and subsequently further processed independently. This and the following chapter focus on the main events that have to occur to enable proper progress in the maturation pathways of these earliest precursors as well as the resulting pre-40S and pre-60S ribosomes. Since in this work the assembly behavior of large subunit r-proteins was investigated in detail, the maturation events of the LSU will be more elaborately introduced and discussed (2.2.6).

To achieve the separation of the SSU- and LSU precursors, hence cleavage at site A2 in the ITS1, the function of numerous components is required. Among them are around 50

ribosome biogenesis factors and three snoRNAs: U3, U14 and snR30 (Kass et al., 1990; Li et al., 1990; Morrissey and Tollervey, 1993; Savino and Gerbi, 1990). In addition, the depletion of a group of SSU r-proteins also resulted in an inhibition (or significant delay) of ITS1 cleavage (Ferreira-Cerca et al., 2005). Studies on the earliest assembly intermediates in terms of how they are formed, what they are composed of, and how they are further processed turned out to be, for several reasons, very challenging. The different approaches and their interpretation were for a long time under debate and in part still are today. Pioneering experiments in the 1970s described a preribosome that sediments at 90S and contains the 35S pre-rRNA (Trapman et al., 1975; Udem and Warner, 1972). On the other hand, images of rDNA chromatin spreads show that the nascent rRNA forms compact structures at their ends (Figure 7). Among other findings, the loss of these “terminal balls” or “terminal knobs” which was observed after depletion of U3 snoRNA strongly proposed that the formation of the earliest precursors occurs co-transcriptionally (Dragon et al., 2002). The release of these knobs observed in many, namely about 70% of the nascent transcripts was interpreted as co-transcriptional cleavage in the ITS1 releasing a 20S pre-rRNA containing RNP (Osheim et al., 2004 and Figure 7).

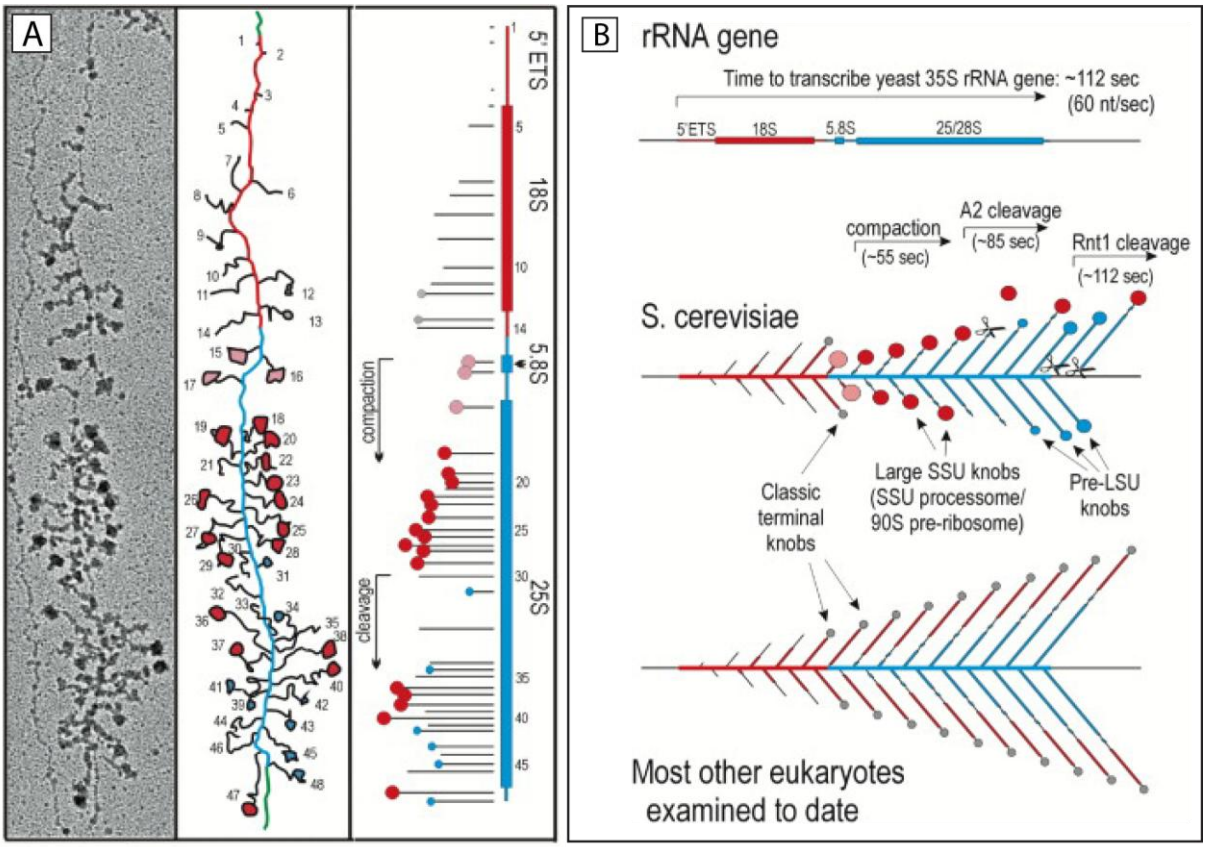

Figure 7 - In yeast, processing of rRNA precursors can already occur during transcription

A) The left panel shows an electron micrograph of an extensively transcribed rRNA gene in which transcription starts at the top and is fulfilled at the bottom. In the middle panel this micrograph is transformed into a scheme from which the information on the lengths of the transcripts, the size of the “terminal knobs” and, both combined, the occurrence of co-transcriptional cleavage events can be deduced. For a better illustration, these data are schematically shown in the right panel. Combination of the data from several of such transcribed rRNA genes as depicted in A) led to the interpretation drawn in **B):** in contrast to most other so far investigated eukaryotes some of the nascent transcripts are cleaved in the ITS1 during transcription what leads to the disappearance of the large, “SSU” knobs (corresponding to the SSU processome). The remaining, shorter transcripts form new “pre-LSU knobs”. Adapted from Osheim et al., 2004.

The obtrusive question of how these earliest precursors are formed and further processed, what they are composed of and whether or not the earliest 20S pre-rRNA containing RNPs (which had been co-transcriptionally released) or 35S pre-rRNA containing 90S pre-ribosomes (which were not cleaved co-transcriptionally) differ in their protein composition was extensively addressed mainly by affinity purifications performed by several groups early in this century. Two of the most challenging issues in these pull down experiments are (i) the question of whether or to what extent the co-transcriptionally formed and not yet released terminal knobs can be co-purified and (ii) whether single precursor populations or a mixture of several subsequently produced populations are co-purified. Pull down experiments of several epitope tagged nucleolar biogenesis factors lead to the co-purification of pre-ribosomal particles that sediment at 90S and contain a total of 35 “pre-rRNA factors” (biogenesis factors), the U3 snoRNP and 5’ ETS sequences not yet removed. (Grandi et al., 2002). Using a similar approach, the Baserga group purified a large preribosomal particle they termed, due to its composition, “SSU processome” (Dragon et al., 2002). This RNP contained, beside the U3 snoRNP and some SSU r-proteins, a set of 17 undescribed proteins that were named Utp1-17 (“U three protein”) and which turned out to affect the maturation of the small subunit. Further studies confirmed the at that time described and identified additional proteins involved in the formation and/or processing of the SSU-processome (Bernstein et al., 2004; Gallagher et al., 2004).

The assembly of the 90S/SSU processome was described to happen in a modular, coordinated and at least in part hierarchical order (Figure 8). Several protein-modules or subcomplexes could be isolated by gel filtration and/or high speed centrifugation of cell extracts. The latter leads to the depletion of large, fast sedimenting RNPs as the SSU processome while the smaller submodules remain in the supernatant (Krogan et al., 2004). A subgroup of UTPs (U three proteins) were described to form three complexes: UTP-A, UTP-B, and UTP-C contain 7, 6, and 4(6) proteins, respectively (Bernstein et al., 2004; Dosil and Bustelo, 2004; Gallagher et al., 2004; Krogan et al., 2004; Samanta and Liang, 2003). Other described SSU processome modules are the U3 snoRNP (Lukowiak et al., 2000; Venema et al., 2000), the Noc4-Nop14 complex (Kühn et al., 2009; Milkereit et al., 2003), and the Mpp10-Imp3-Imp4 complex (Granneman et al., 2003; Lee and Baserga, 1999). In addition, the large 193 kDa protein Rrp5, which can form a complex with Noc1 and Noc2, and which is required for the synthesis of both subunits, seems to have a crucial role in coordinating pre-rRNA processing and assembly (Hierlmeier et al., 2012; Lebaron et al., 2013; Venema and Tollervey, 1996).

A very upstream event in the assembly hierarchy of the SSU processome is the binding of the UTP-A complex to the nascent pre-rRNA, which seems to occur independently of other proteins, including several SSU r-proteins, whose prokaryotic homologues have been described to be primary rRNA binders in an *in vitro* reconstitution system (see 2.3.1.1 for more details) (Jakob et al., 2012; Pérez-Fernández et al., 2007). Therefore it seems plausible that in eukaryotes, the UTP-A components overtake a role as primary binders

several prokaryotic r-proteins seem to fulfill in prokaryotes (as observed in the *in vitro* reconstitution systems of prokaryotic ribosomal subunits – see 2.3.1.1).

The UTP-A complex was also described to play a role in linking RNA polymerase I transcription and pre-rRNA processing by being associated to the chromatin of the rDNA locus; in this aspect the single components were termed “transcription-UTPs” – tUTPs (Gallagher et al., 2004; Granneman and Baserga, 2005). This essential first step is followed by two independent, but not mutual exclusive assembly branches (Figure 8): in one, binding of the UTP-B and U3 snoRNP complexes is accompanied by binding of the Mpp10 complex and seven additional proteins what leads to a stabilized intermediate (Dosil and Bustelo, 2004; Pérez-Fernández et al., 2007, 2011). In the other branch, binding of Rrp5 facilitates the subsequent binding of the UTP-C complex (Pérez-Fernández et al., 2007; Vos et al., 2004).

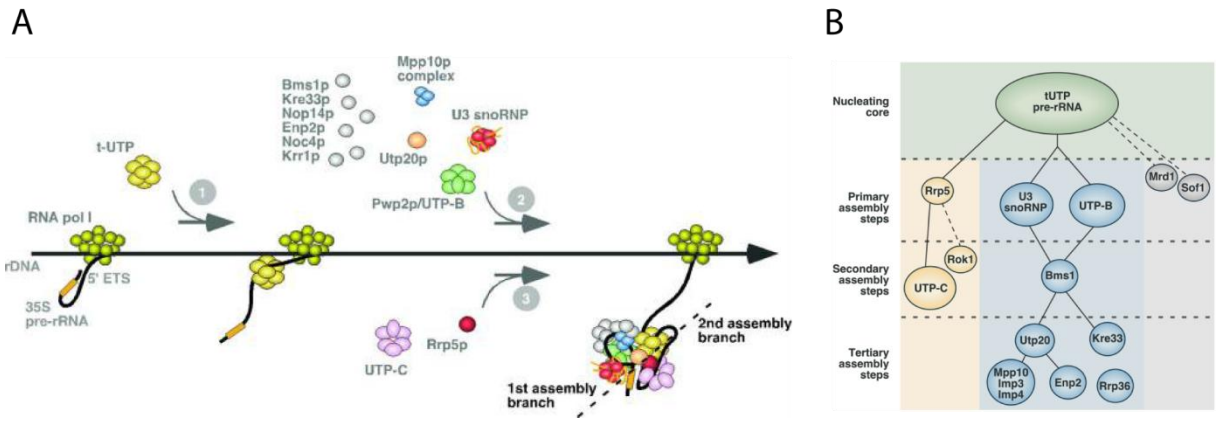

Figure 8 - Scheme of a model for the assembly of the SSU processome components on pre-rRNA

A) The t-UTP (UTP-A) complex initially binds to nascent pre-rRNA independently of other factors (1). The subsequent binding of the other SSU components (UTP-B/UTP-C/Rrp5...) occurs in a hierarchical and coordinated manner (see text), which is illustrated in **B)**. The formation of the “nucleating core” is followed by primary, secondary, and tertiary assembly steps which are partially independent or dependent of each other. Both parts are adapted from Pérez-Fernández et al., (2007, 2011).

Several SSU central domain r-proteins, whose depletion result in similar pre-rRNA processing phenotypes as depletion of SSU processome components do, are required for the association of the SSU-processome component Noc4 and other proteins including the UTP-C complex (Ferreira-Cerca et al., 2005; Jakob et al., 2012). Noc4 itself is required for the efficient incorporation of another group of SSU r-proteins (Jakob et al., 2012). Interestingly, in mature SSUs, the latter group of SSU r-proteins binds to the 3’ domain of the 18S rRNA whereas the former group (which is required for efficient Noc4 recruitment) binds in mature ribosomes to 5’ and central domains of the 18S rRNA (Ben-Shem et al., 2011). In summary, these observations point into the direction that some SSU processome components fulfill a role as transient primary pre-rRNA *in vivo* binders whereas others (as Noc4) are involved in the coordination of the proper assembly of the SSU domains (Jakob et al., 2012).

After the cut in ITS1 at site A2, the resulting nucleolar 20S pre-rRNA containing pre-40S particles undergo one last pre-rRNA processing event, namely the removal of the remaining ITS1 sequences 3' of the 18S rRNA sequences. This cleavage occurs at site D and is catalyzed by the endonuclease Nob1 in the cytoplasm (Lamanna and Karbstein, 2009). At some stage(s) on their way from the nucleolus through the nucleus to the cytoplasm the composition of these pre-40S particles is changing quite drastically. Only around ten ribosome biogenesis factors were identified to stably associate to the cytoplasmic 20S pre-rRNA containing particles and/or to be required for the cleavage at site D (Fromont-Racine et al., 2003; Henras et al., 2008; Karbstein, 2011; Schäfer et al., 2003; Strunk and Karbstein, 2009). Among them are Nob1 and Pno1/Dim2 (Senapin et al., 2003; Vanrobays et al., 2004), Dim1 (Lafontaine et al., 1994), Tsr1, Ltv1 and Rrp12 (Seiser et al., 2006) which were described function in nuclear export, and the kinases Rio1 and Rio2 (Vanrobays et al., 2003). Systematic analyses of RNA-protein interaction sites using the CRAC (Cross link and amplification of cDNA) technique identified the binding sites of six of these late SSU biogenesis factors (Granneman et al., 2010). A "conformational switch" was suggested to happen prior to the actual cleavage event (Granneman et al., 2010; Lamanna and Karbstein, 2011). Other biogenesis factors were described to bind in a way to prevent 60S joining (Dim1) or binding of translation initiation factors (Nob1, Pno1).

Beside this set of biogenesis factors, most of the essential SSU r-proteins are also required for an efficient processing of 20S pre-rRNA; their depletion leads to different maturation phenotypes (Ferreira-Cerca et al., 2005; Jakovljevic et al., 2004; Léger-Silvestre et al., 2004). In general, these and other observations were interpreted as "quality control" mechanisms of ribosome biogenesis (reviewed for example in Karbstein, 2013; Woolford and Baserga, 2013). As described above, the role of earlier biogenesis factors as Noc4 in coordinating the proper assembly state of different SSU domains to each other is another example for a quality control mechanism in ribosome biogenesis. In general, many other maturation events (of both subunits) were described to depend on a well defined assembly state of the respective precursor particle (see 2.2.6). Another, recently described quality control mechanisms is a "translation-like cycle" suggested by two groups, in which parts of the translation machinery (including eIF5b/Fun1 and a mature 60S subunit) are used to "test-drive" premature SSUs what leads to the conformational switch that enables D-site cleavage (Lebaron et al., 2012; Strunk et al., 2012). Aberrant preribosomes do not strongly accumulate in the cell but are efficiently degraded by default (see 2.2.3).

2.2.6 Maturation of the large ribosomal subunit in yeast

2.2.6.1 Formation and composition of the earliest specific pre-60S particles and general features of their maturation

In the pre-60S maturation pathway several distinct rRNA precursor intermediates are present, that define the maturation state of the respective pre-60S particle (see pre-rRNA processing pathway in 2.2.3). The pre-rRNA processing events that result in these subsequently formed intermediates occur mainly in the nucleolus or nucleoplasm (see

following sections 2.2.6.2 - 2.2.6.5); a last trimming event of remaining ITS2 sequences 3' of the 5.8S rRNA (Thomson and Tollervey, 2010) and some other processes as association and release of a few biogenesis factors (2.2.6.6) as well as the incorporation of a few r-proteins (see 2.3) are described to occur in the cytoplasm, though. Both, LSU r-proteins and LSU specific biogenesis factors were strongly underrepresented in the compositional analyses of the 90S/SSU processome (see 2.2.5). In the case of co-transcriptional cleavage in the ITS1, miller spread analyses show the formation of "new" terminal structures which were termed "pre-LSU knobs" and which most likely contain proteins (Figure 7). Whether or not these proteins are specific LSU biogenesis factors and/or LSU r-proteins is not absolutely clear, though. Beside the Rrp5/Noc1/Noc2 protein module, evidence for co-transcriptional association of only two more LSU biogenesis factors, Nop15 and Nop53, was provided (Granato et al., 2008; Hierlmeier et al., 2012; Wery et al., 2009).

The first specific pre-60S particle contains the 27SA2 pre-rRNA. As introduced in 2.2.4, the maturation state(s) of the preribosome(s) most biogenesis factors interact with is known. Analysis of the individual depletion phenotypes provided evidences for which maturation step each factor might be required. However, the detailed molecular function for many of them remains still unclear. The composition of these earliest (and also later) LSU-precursors was systematically investigated about 10 years ago by affinity purification of several epitope tagged biogenesis factors and analysis of the co-purified proteins by mass spectrometry (Dez et al., 2004; Fatica et al., 2002). More than 30 LSU biogenesis factors, many LSU r-proteins and some proteins with other functions as cell cycle progress or translation were identified in these studies. Since for their detection only qualitative mass spectrometry was applied, the determination of the binding strength of those proteins to the pre-60S particles (which would allow statements for the specificity of their binding) was hampered. Remarkably, 6 of the around 20 RNA helicases that were described to be involved in ribosome biogenesis (Rodríguez-Galán et al., 2013) were identified in these studies, what lead to the conclusion that several structural rearrangements might occur at these early stages of pre-60S maturation. A potential multi-protein subcomplex consisting of the proteins Nop8, Npa1, Npa2, Rsa3, and the helicase Dbp6, many of which exhibit multiple genetic interaction among each other and with other RNA helicases might contribute to such likely occurring structural rearrangements (de la Cruz et al., 2004; Rosado et al., 2007a).

Whether or not also compositional changes accompany or follow these structural rearrangements (or vice versa) is very difficult to investigate since most of the biogenesis factors remain bound to several of the subsequently produced intermediates. Their affinity purification therefore also leads to the co-purification of several subsequently generated pre-60S populations. After depletion of early acting LSU biogenesis factors, the steady state levels of the 27S pre-rRNA species as well as whose of all subsequently produced intermediates are strongly decreased. Pulse chase experiments show that that the 27S pre-rRNA species do not strongly accumulate but are rapidly turned over (see also 2.2.3). This is a general feature which is also observed after depletion of later acting ribosome biogenesis factors and most r-proteins (see 2.3). However, the decrease in the steady state levels of the

subsequently produced pre-rRNA species does not necessarily mean, that the processing event leading to this decreased intermediate is completely blocked. It is well possible that the respective processing step can occur but the product is strongly destabilized in the absence of the depleted protein and, due to its rapid degradation, not detectable.

2.2.6.2 Prerequisites of 27SA3 pre-rRNA containing pre-60S particles to enable the generation $27SB_s$ pre-rRNA

As shortly described in 2.2.3, the remaining ITS1 sequences of the 27SA3 pre-rRNA containing pre-60S particles are “trimmed” away by the 5’-3’ exonucleases Rat1 and Rrp17 (Henry et al., 1994; Oeffinger et al., 2009). This trimming reaction halts at site B1s, the 5’ end of the $5.8S_s$ rRNA sequence of the resulting $27SB_s$ pre-rRNA. Besides these two RNAses more than ten additional LSU biogenesis factors are required for an efficient production of this intermediate. Among these biogenesis factors which were referred to as “A3 factors” or “A3-cluster proteins” are Brx1, Cic1/Nsa3, Drs1, Ebp2, Erb1, Has1, Nop7, Nop12, Pwp1, Nop15, Rlp7, Rrp1, and Ytm1 (Figure 9A and Adams et al., 2002; Dembowski et al., 2013a; Dunbar et al., 2000; Fatica et al., 2003b, 2003b; Granneman et al., 2011; Horsey et al., 2004; Huber et al., 2000; Kaser et al., 2001; Merl et al., 2010; Miles et al., 2005; Oeffinger et al., 2002; Pestov et al., 2001; Sahasranaman et al., 2011; Shimoji et al., 2012; Talkish et al., 2014; Tsujii et al., 2000; Wu et al., 2001). Interestingly, with the exception of the DEAD box RNA helicases Drs1 and Has1, the “A3 factors” are not predicted to have any enzymatic activities. Rlp7 was suggested to act as placeholder for rpL7 since it has high sequences homology to it (Dunbar et al., 2000). Recently performed UV cross-linking (CRAC) analyses however showed that the binding site of Rlp7 in pre-60S particles is far apart from the binding site of rpL7 in mature LSUs (Dembowski et al., 2013b; Ben-Shem et al., 2011). This and the observation that rpL7 was efficiently co-purified with tagged Rlp7 contradict the “placeholder” hypothesis (Babiano et al., 2013). One easy explanation for the requirement of the “A3 factors” in 27SA3 pre-rRNA processing would be a potential function in recruiting the exonucleases Rat1 and Rrp17. This hypothesis was directly tested for Rlp7 and proved true only for Rrp17 whose binding was affected to some extent; recruitment of Rat1 (and its cytoplasmic homolog Xrn1), were not affected (Sahasranaman et al., 2011). Since the assembly of six “A3 factors”, including Rlp7 (and Erb1, Nop7, Ytm1, Nop15 and Cic1/Nsa3) was reported to be mutually interdependent and required for the subsequent assembly of two more “A3 factors” (Drs1 and Has1), it was concluded that all these A3 factors are neither required for recruitment of Rat1 (Sahasranaman et al., 2011). The binding site of several “A3 factors” was investigated by *in vivo* chemical probing using the CRAC-technique (Figure 9B). Surprisingly, the tested “A3 factors” were not cross-linked near the A3 site in the ITS1 but rather distant in ITS2 and the adjacent 5.8S rRNA 3’, and 25S rRNA 5’ regions, respectively (Granneman et al., 2011). Several evidences for physical interactions among many “A3 factors” were provided suggesting another potential subcomplex of ribosome biogenesis factors acting “together” (Merl et al., 2010; Miles et al., 2005). Secondary structure predictions and structure probing experiments of ITS1-5.8S sequences provided evidence that in pre-60S particles, which still harbor ITS1 sequences, the 5’ region of the 5.8S rRNA base pairs with 3’ areas of the ITS1 (Figure 9C and van Nues et al., 1995; Yeh et al., 1990).

In mature LSUs however, the 5' region of 5.8S rRNA (including its 5' end – the B1s site) base pairs with nucleotides of helix2 of the 25S rRNA (Ben-Shem et al., 2011). This suggests a "conformational switch" which might lead to the establishment of a stable helix whose formation might be triggered by the action of some "A3 cluster" proteins (Figure 9C and Granneman et al., 2011).

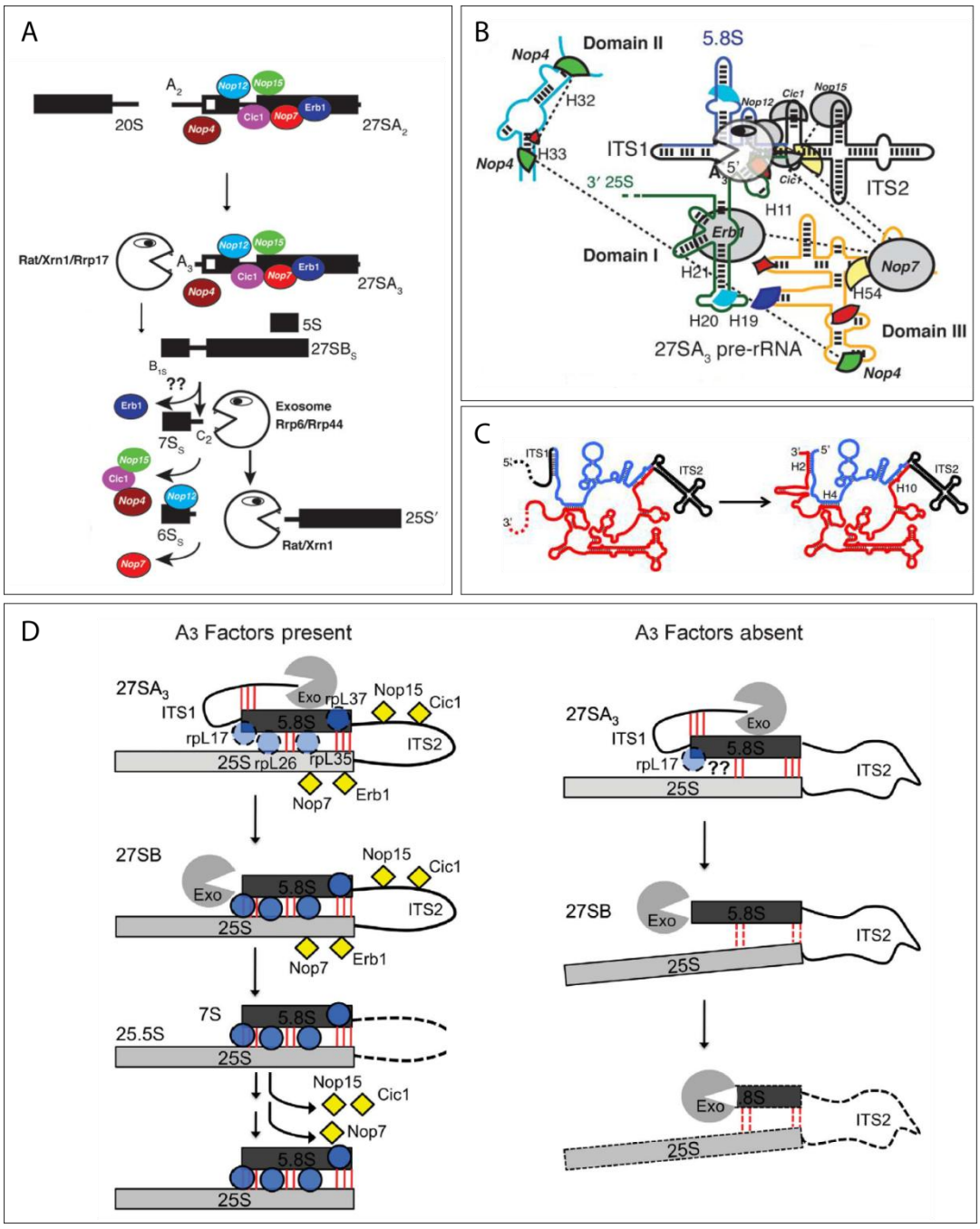

Figure 9 - Main processing pathway of 27SA2 pre-rRNAs by a series of endo- and exonucleolytic cleavage events resulting in 27SBs pre-rRNAs.

A) Schematic presentation of the main processing pathway of yeast 27SA2 pre-rRNA resulting in formation of the 5' end of the 5.8S rRNA sequence in the 27SB pre-rRNA and further processing of 27SB pre-rRNA. Some known RNA exonucleases and LSU biogenesis factors that are involved in these steps ("A3 factors") are illustrated. **B)** The secondary structure of the ITS1, 5.8S, and ITS2 sequences of 27SA3 pre-rRNA and parts of LSU domains I, II and III are illustrated. The binding sites for some "A3 cluster proteins", Rat1, and Nop4 are indicated in gray and green, respectively (see legend). Interactions between these proteins are indicated as dashed black lines.

Coloured segments represent the binding sites of LSU r-proteins rpL17, rpL25, rpL26, and rpL37. A) and B) were adapted from Granneman et al., 2011. **C)** illustrates the "conformational switch" of parts of the precursor rRNAs. In ITS1 containing pre-rRNAs (27SA), the 5' end of the 5.8S rRNA sequences base-pairs with the ITS1 while after processing of the ITS1 (in 27SB and further maturated (pre-) rRNAs) it base-pairs with the 3' end of 25S rRNA domain I (resulting in helix2). Adapted from Jakovljevic et al.,2012. **D)** Proposed degradation of mutant pre-rRNAs by the 5' to 3' exonucleolytic degradation by Rat1. While the binding of the indicated LSU r-proteins (blue) and "A3 factors" (yellow) leads to the block of Rat1 processing at site B1s (left side), in their absence (right side), the mutant LSU precursor is degraded by Rat1.Red lines indicate base pairing between 5.8S rRNA and ITS1 or 25S rRNA sequences. Adapted from Sahasranaman et al., 2011.

Interestingly, depletion of all tested "A3 factors" leads to a strong decrease in levels of $27SB_s$ pre-rRNA and the appearance of some Rat1 specific shorter fragments thereof. This and the proved presence of Rat1 in pre-60S particles depleted of "A3 factors" provided evidence for a rapid degradation of the misassembled pre-60S particles lacking the "A3 factors". According to this, not the actual 5'-3' exonucleolytic trimming of the ITS1 sequences would be inhibited but its termination at site B1s. It is well possible that the "Stop trigger signal" for the exonucleases is achieved by a "physical road-block", some kind of structural feature that inhibits a further progress of the exonucleases. Besides the "A3 factors", a group of LSU r-proteins is required for this maturation event since their depletion resulted in the same or a similar pre-rRNA processing phenotype (Gamalinda et al., 2014; Li et al., 2009; Pöll et al., 2009). Among them are rpL7, rpL8 and about six others. Remarkably, with the exception of rpL3 they are all mainly bound (in mature ribosomes) to LSU rRNA domain I or II, whose structural integrity seems to be affected in their absence. The establishment of the helical structures between the 5' nucleotides of the 5.8S rRNA and parts of domain I of the 25S rRNA was therefore speculated to be also inhibited (Pöll et al., 2009). The inhibited formation of this helix, which might constitute such a structural feature leading to an efficient "road block" of the exonucleolytic trimming of the ITS1 spacer sequences, might explain the observed phenotype and the rapid turnover of pre-ribosomes (Pöll et al., 2009). Alternatively, the observation that several LSU r-proteins that bind (in mature LSUs) in even closer proximity to the 5' end of the 5.8S rRNA, among them rpL17, were underrepresented in pre-60S particles after depletion of "A3 factors", brought up the idea that their partial disassembly (or reduced ability to assemble) might constitute (or at least be part of) the missing "road-block" (Figure 9D and Sahasranaman et al., 2011). However, after depletion of rpL17 significant amounts of 27SB pre-rRNA and even subsequently produced intermediates could be detected, what argues against the hypothesis that rpL17 might be the main "road-block" (Pöll et al., 2009).

In this work, most of those LSU r-proteins that exhibit this "early" pre-rRNA processing were systematically depleted and the composition of the resulting mutant preribosomes was investigated aiming to finally better understand the molecular cause of the observed phenotype (see section 3.3.2).

2.2.6.3 Structural and compositional prerequisites for the processing of $27SB_{s/l}$ pre-rRNAs by cleavage in the ITS2

The removing of the ITS2 of 27SB pre-rRNAs which separates the 5.8S and 25S rRNA sequences, occurs in several steps (see 2.2.3), first of which is an endonucleolytic cleavage at site C2 in the nucleus. More than 10 LSU biogenesis factors, whose individual depletion causes a strong decrease in steady state levels of the 7S pre-rRNA, have been described to be required for this first step. Interestingly, this group of biogenesis factors (containing Nop2, Nip7, Rpf2, Rrs1, Spb1, Spb4, Mak11, Rlp24, Tif6, Nog1, Nug1, Dbp10, and Nsa2 – see also Figure 10), which are sometimes referred to as “B-factors”, contains no known or predicted nuclease. Several of these biogenesis factors have been described to be part of several subcomplexes, which can be isolated from cell extracts. For instance, Rpf2 and Rrs1 form a subcomplex containing two LSU r-proteins (rpL5 and rpL11) and the 5S rRNA (Morita et al., 2002; Zhang et al., 2007). Other examples are Nip7 and Nop2, that form a heterodimer (Talkish et al., 2012) or Nog1 and Rlp24 (and possibly Mak11) physically interacting with each other (Saveanu et al., 2003, 2007). Many “B factors” were described to already interact with early pre-60S particles, for example purified by Npa1 (Nip7 and Nop2 - (Dez et al., 2004)) or even 35S pre-rRNA containing 90S pre-ribosomes (the 5S RNP of Rpf2, Rrs1, rpL5, rpL11 and the 5S rRNA - (Zhang et al., 2007)). The recruiting of these factors to pre-60S particles was recently described to occur (comparable to the “A3 factors”) in a sequential and hierarchical way via two independent assembly trees that converge on Nog2 (Talkish et al., 2012, see also Figure 10A). According to these studies, Nog2 assembly, which was described to happen “just before” the C2 cut, was suggested to act as a check point - a “LSU maturation quality control mechanism” that prevents the irreversible cleavage of not yet properly assembled pre-60S particles. After depletion of Nog2, however, substantial amounts of 7S pre-rRNA are still produced and even accumulate arguing against a strict requirement of Nog2 in 27SB pre-rRNA processing (Saveanu et al., 2001). A recent study revealed the binding site of Nog2, which is located (in the mature LSU) on the subunit interface and largely overlaps with the binding site of the putative export adaptor Nmd3 (Figure 10B, see also 2.2.6.6). Due to this and other functional studies the authors concluded that Nog2 acts rather as a “regulatory GTPase” that “monitors” pre-60S maturation, with release from its “Nmd3 placeholder site” linked to recruitment of the nuclear export machinery” (Matsuo et al., 2013 – see also Figure 11B). The accumulation of 27SB pre-rRNA observed after its depletion could therefore be a secondary effect which might for example be explained by the disturbed release of one or the other LSU biogenesis factor required for earlier steps as observed in a former study after depletion of Nsa2, or Ebp2 (Lebreton et al., 2008). In analogy to this, the depletion of Rsa4, another LSU biogenesis factors that was not described to be involved in 27SB processing, results in a highly similar pre-rRNA processing phenotype, namely the increase of steady state levels of both, 27S and 7S pre-rRNAs (de la Cruz et al., 2005).

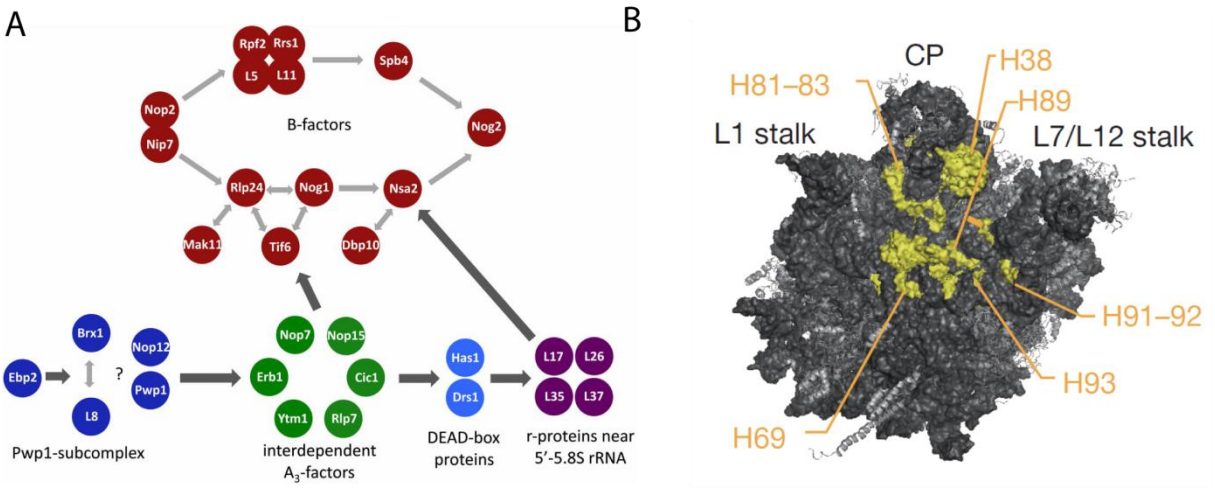

Figure 10 - Model of a described hierarchical recruitment of LSU biogenesis factors and some r-proteins involved in early and intermediate processing events and the rRNA contacts of the GTPase Nog2 in late yeast LSU precursors illustrated on the mature yeast LSU.

A) A hierarchical pathway for the stable association of some LSU biogenesis factors and r-proteins to LSU precursors is illustrated. According to this model, the assembly of the "B factors" depends on previous binding of other biogenesis factors, including the "A3 factors" and some LSU r-proteins. Two in parts interdependent "assembly trees" converge in the recruitment of Nog2, whose strict requirement for 27S pre-rRNA processing is not clear, though (see text). Adapted from Woolford and Baserga, 2014. **B)** The binding sites (cross linking sites) of Nog2 to late LSU precursors is illustrated using the structure of the mature LSU. The rRNA sequences that cross linked to Nog2 are highlighted in yellow. The number of the corresponding rRNA helices are given. CP = central protuberance, "L7/L12 stalk" represents the acidic- / phospho-stalk. Adapted from Matsuo et al., 2013.

With the exception of Nog2, whose strict requirement for 27SB pre-rRNA processing is under debate (see above), detailed information of the binding sites of all "B-factors" as determined by chemical structure probing are still lacking. Recent cryo-EM structures revealed the location of several "B factors" including Tif6, Rlp24, and Nog1 (Figure 12B and Leidig et al., 2014). Even if the position and the fold of the ITS2 spacer (whose processing is inhibited) is not known, none of these B factors seems to be positioned in very close proximity to its boundary (which is the 3' end of the 5.8S rRNA and the 5' end of the 25S rRNA). Rlp24 and Tif6, for instance seem to bind rather distal of the LSU precursor near rpL23 (which is also required for this processing event). Therefore it seems plausible that, in analogy to the "A3 factors", that seem to bind not in proximity to the "A3 site" (see 2.2.6.2), at least some "B factors" also bind distal of the C2 site-harboring ITS2 and therefore might overtake a rather indirect role in the actual cleavage event. Interestingly, several (but not all, as rpL23 – see above) members of the group of LSU r-proteins that are also required for 27SB processing at site C2 (Pöll et al., 2009) do bind near this "ITS2 area" (Ben-Shem et al., 2011, see also Figure 23). Among them are the 25S rRNA domain III binders rpL19, rpL27, and rpL34. Depletion of rpL25, rpL35, or rpL37 which connect 5.8S rRNA/25S rRNA domain I to each other or to domain III also results in the same pre-rRNA processing phenotype.

The roles of those LSU r-proteins in the assembly state of LSU domains in pre-60S particles (including assembly or release of LSU biogenesis factors) were also systematically studied in this work what will be described and discussed in section 3.3.3.

2.2.6.4 The removal of some LSU biogenesis factors required the action of NTPases

Concomitant with the ITS2 cleavage at site C2 (or shortly before or after it) a number of early acting LSU biogenesis factors are released from the nuclear pre-60S particles whereas a set of others are described to bind (Nissan et al., 2002, 2004). Several studies investigated in more detail the mechanism of how the removal of some of these biogenesis factors is mediated by using cryo-EM techniques and a number of *in vitro* assays on purified nuclear pre-60S particles. According to these studies, the release of Rsa4, Ytm1, and Nsa1 was described to be catalyzed by the AAA ATPases Rea1 and Rix1, respectively (Bassler et al., 2010; Kressler et al., 2008; Nissan et al., 2004; Ulbrich et al., 2009). These energy dependent processes, which were described to trigger some striking conformational changes resulting in a “mechochemical stripping” of the biogenesis factors, were also described for the removal of some LSU biogenesis factors in the cytoplasm (Figure 11A, see also section 2.2.6.6 and Pertschy et al., 2007 or recently reviewed in Kressler et al., 2012a). More recently, the GTPase activity of Nog2 was described be coupled to the above described ATPase activities of Rea1 resulting in Rsa4 release and Nmd3 recruitment what can be seen as a “checkpoint” for export competence of nuclear LSU precursors (Figure 11B and Matsuo et al., 2013). Whether or not some of the numerous remaining LSU biogenesis factors are “stripped” off the nascent pre-60S particles in a comparable way or even by the same NTPases, is still unclear.

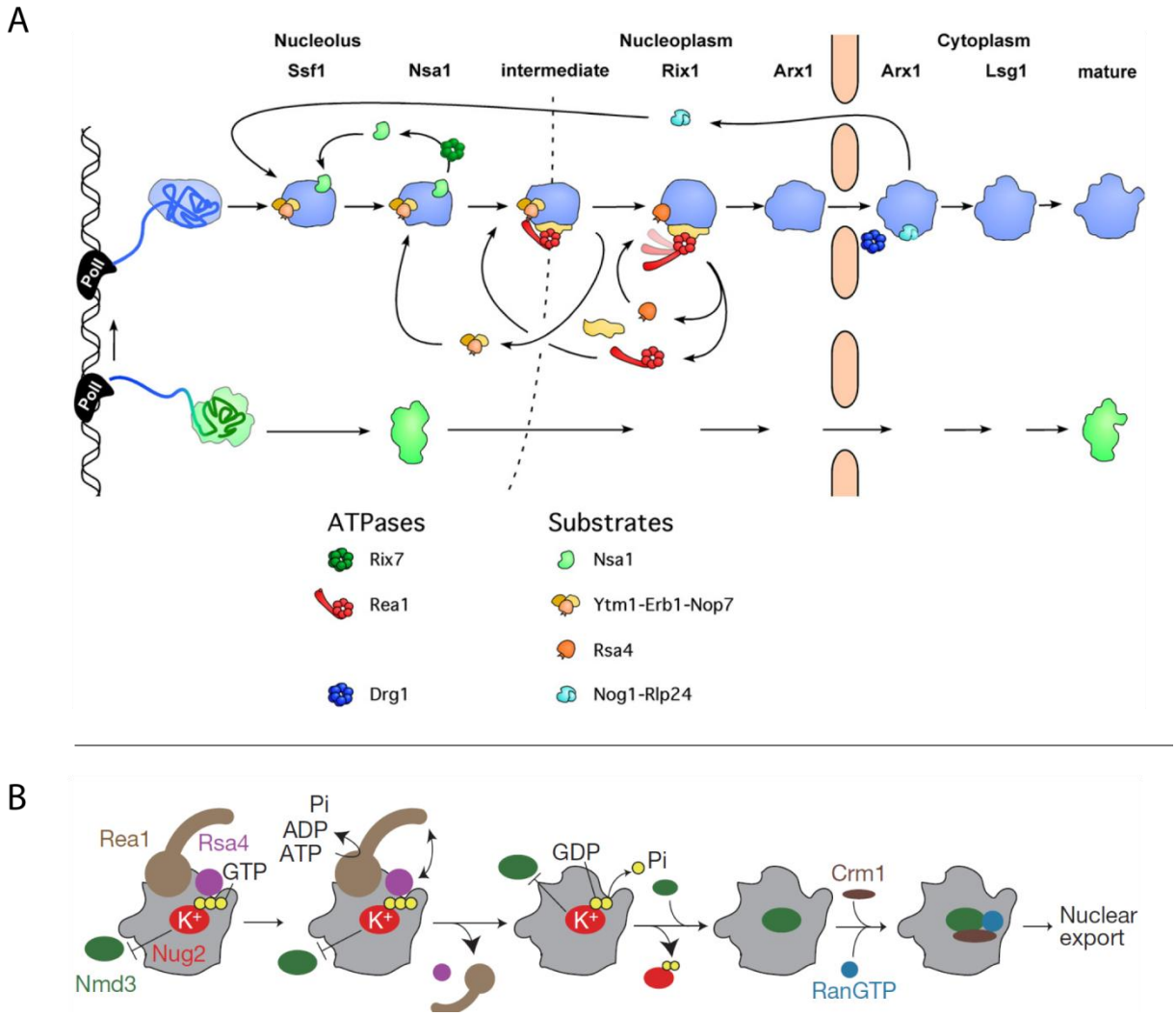

Figure 11 - Illustrations of the potential "mechanochemical" removal of several biogenesis factors from nascent LSU precursors

A) Illustration of some energy dependent release events of LSU biogenesis factors from LSU precursors adapted from Kressler et al., 2012. The current ideas of the energy dependent action of the ATPases Rix7, Rea1, and Drg1 which result in the release of their substrates are illustrated. **B)** The above described "checkpoint for pre-60S export" involving the GTPase Nog2 and the ATPase Rea1 is illustrated. GTP-bound Nog2 first leads to the Rea1 dependent release of Rsa4. After hydrolysis of the γ-phosphate of the GTP, GDP binding Nog2 can be released from nuclear LSU precursors what enables the binding of the export adapter Nmd3. Adapted from Matsuo et al., 2013.

2.2.6.5 Several LSU r-proteins and biogenesis factors are required for the removal of ITS2 sequences yielding the mature 5.8S and 25S rRNAs

The remaining ITS2 sequences forming the 3' and 5' regions and of the 7S and 25.5S pre-rRNAs, respectively (see processing scheme in 2.2.3), are subsequently removed in several steps, last of which might occur in the cytoplasm. Several r-proteins (including rpL2, rpL43, rpL21, rpL28 rpL10 and some more) and ribosome biogenesis factors (as Nog2, Rsa4 or the Rix1/Ipi1/Ipi3 complex) are required for some of these events (de la Cruz et al., 2005; Galani et al., 2004; Pöll et al., 2009; Saveanu et al., 2001). Interestingly, neither most of the LSU r-proteins (Ben-Shem et al., 2011) nor the biogenesis factors Rsa4 or Nog2 seem to bind in close proximity to the ITS2 regions whose processing is disturbed in their absence (Leidig et

al., 2014; Matsuo et al., 2013). Therefore it remains unclear why they are still required for these processing events and how they contribute to the processing of these late 5.8S rRNA precursors.

In this work, the effects of the lack of several of the above mentioned LSU r-proteins on the assembly state of pre-60S particles was analyzed aiming to better understand the molecular cause for their requirement (3.3.4).

2.2.6.6 Nuclear export of pre-60S particles and their final maturation in the cytoplasm

Passage of all substrates that cannot diffuse through the double membrane surrounding the nucleus occurs through the nuclear pore complex (NPC), a large multi protein complex which is embedded in the nuclear envelope. Although ions, single proteins or molecules with a size of up to around 60kDa can diffuse through the NPC, the export of larger RNPs as preribosomal subunits has to be actively mediated by specific energy demanding mechanisms (Pemberton and Paschal, 2005; Wang and Brattain, 2007). Several specific export receptors bind the export target and interact with components of the NPC, the so called nucleoporins, whose hydrophobic phenylalanine/glycine repeats (FG-repeats) form a "three-dimensional meshwork with hydrogel-like properties" (Frey et al., 2006). One of these export receptors that was described to be required for the export of ribosomal subunits is Crm1 (also known as exportin1 – Xpo1) which interacts with "cargo" proteins containing a nuclear export signal (NES) in a RanGTP depend way (Stage-Zimmermann et al., 2000; Thomas and Kutay, 2003) . Regarding pre-60S (or pre-40S) export, this interaction could be directly between Crm1 and NES-containing r-proteins or adapter proteins that contain an NES and function in bridging pre-ribosomes and export receptors. Considering the hydrophobic "mesh" of the NPC and the rather hydrophilic surface of ribosomal subunits it is not surprising that not only one but several export factors were described to be involved in pre-60S export. Among them are Arx1, Nmd3, Mex67/Mtr2, Ecm1, and Bud20 that were described to function together and bind to different regions of the nuclear pre-60S particle (see below) (Altvater et al., 2012; Baßler et al., 2012; Bradatsch et al., 2007; Gadal et al., 2001; Ho and Johnson, 1999; Ho et al., 2000; Hung et al., 2008; Yao et al., 2007, 2008, 2010). Nmd3, whose binding site was recently dissolved by *in vivo* chemical probing, was described to function as an export adapter interacting with pre-60S particles near the binding site of rpL10 in parts of 25S rRNA domains II and V and bridging them to the export receptor Crm1 (Ho et al., 2000; Matsuo et al., 2013; Sengupta et al., 2010).

In addition, depletion of many r-proteins results in nuclear export defects (Pöll et al., 2009 and citations therein). These defects might be either caused by direct effects as disturbed recruitment of export adaptors or effects as inhibition of previous pre-rRNA maturation events or inhibited release of biogenesis factors. The release of several LSU biogenesis factors seems to be also crucial to ensure nuclear export competence; their association to nuclear LSU precursors might therefore constitute a retention signal preventing an untimely export. The release of factors as Rsa4 or Nog2, the position of last of which was described to "clash"

with the position of Nmd3 at the subunit interface are examples for such retention signals. Due to the (partial) overlap of their binding sites, Nog2 and the export adapter Nmd3 seem to be not present on the same particle (Matsuo et al., 2013). The premature recruitment of Nmd3, which was described to occur after depletion of Nog2, is however not sufficient for export, further arguing for the existence of other retention signals which might be crucial for the nuclear export competence.

A direct structural visualization of late pre-60S particles with reasonable resolution which can be easily compared to the mature LSU structure allowing to monitor some major late structural changes and/or the location of late associating biogenesis factors was recently published. Epitope tagged Arx1 was used to purify late nuclear and cytoplasmic pre-60S particles whose structure was reconstructed by cryo-EM to a resolution of about 12Å (Figure 12A, Bradatsch et al., 2012), very recently even around 8 Å (Figure 12B, Leidig et al., 2014). In general, the structure of this “Arx1-particle” (population) is comparable to the one of the mature LSU. Some structural features as the central protuberance or the acidic stalk seem to be not fully established yet, though. Additional densities can be interpreted as late biogenesis factors (and/or ITS2 sequences); the location of some of them is in agreement with the ones previously described or suggested. Some biogenesis factors, for which structural information is available, were fitted to the “additional” densities of the cryo-EM structure. Among them are Tif6 and Arx1. Others, as the export adapters Mex67/Mtr2 and Nmd3, or the LSU biogenesis factors Nog1, Rsa4, Mrt4, or Rlp24 were assigned to other additional densities based on different publications (Figure 12B, Bradatsch et al., 2012; Leidig et al., 2014). Another cryo-EM study confirmed the binding site of Arx1 near the exit tunnel by adding the recombinant proteins Arx1, and Jjj1 plus Rei1, both of which have been implicated in Arx1 recycling, to mature LSUs (Greber et al., 2012). The structural data provided in this publication indicate that the nucleoporin binding pocket of Arx1 faces the ribosomal exit tunnel why the nucleoporin access might be (partially) restricted. Therefore, Arx1 was suggested to be (in addition to its putative function in pre-60S nuclear export) involved in conformationally locking the pre-60S particles to inhibit the “premature association of nascent chain-processing factors to the polypeptide tunnel exit” (Greber et al., 2012). Furthermore, Arx1 and several other LSU biogenesis factors including Tif6, Nmd3, Lsg1, Alb1, Rei1 or JJJ1 seem to be also able to interact with mature LSUs, as observed after inhibition of rRNA transcription (Merl et al., 2010). If this observed affinity to mature LSUs is of any functional relevance, other than inhibiting association with SSUs, remains unclear. The orientation of the nucleoporin binding pocket of Arx1 towards the ribosomal exit tunnel was speculated to be “optimal for interaction with nascent chains emerging from the exit tunnel”, opening up the possibility of a direct role of Arx1 in translation (Greber et al., 2012).

Many LSU export adapters seem to be located at rather different sites of the nuclear pre-60S particle what might reflect the requirement to establish contacts with the FG repeat containing nucleoporins at several distributed sites on the surface of the pre-60S particles. The lack of individual contacts might be dispensable, though, since Arx1 for instance is not

essential. The determination of higher resolved structural data of these late precursors (which would allow better conclusions) remains challenging.

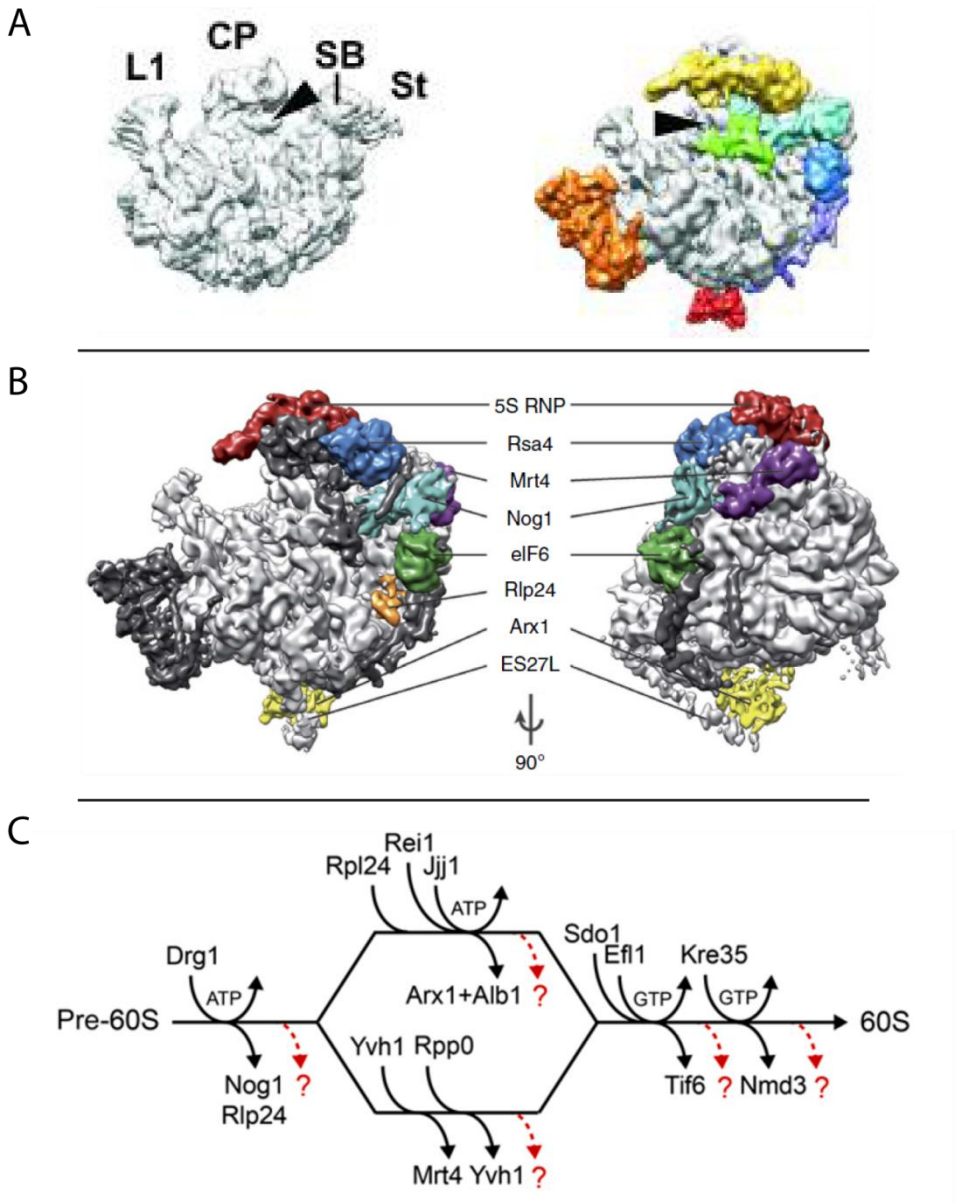

Figure 12 - Structures of late yeast LSU precursors with proposed associated biogenesis factors and illustration of cytoplasmic maturation steps

A) The cryo-EM structure of a late (Alb1-TAP affinity purified) yeast LSU precursor at a 11.9 Å resolution (right) is compared to the structure of a mature LSU (left). Additional densities are highlighted in colors: near the exit tunnel (red – corresponds to Arx1); "below" the L1 stalk (orange); around the central protuberance (yellow); in the "center" of the subunit interface (green – could correspond to Nmd3); "next" to the stalk base (cyan and blue); in the P site (cyan) and between the area below the stalk base and the exit-tunnel region (purple). Abbreviations: CP = central protuberance; L1 = rpL1-stalk; St = acidic- / phospho stalk; SB = base of the phospho stalk. Adapted from Bradatsch et al., 2012. **B)** shows a better resolved (8.7 Å) yeast Arx1 particle highlighting additional densities and assigning these to associated biogenesis factors (see colors). eIF6 and ES27L correspond to Tif6 and expansion segment 27 of the LSU rRNA, respectively. Regions in dark gray correspond to additional, non-assigned densities. Adapted from Leidig et al., 2014. **C)** illustrates the proposed cytoplasmic maturation events of the LSU precursors (including the binding of late LSU r-proteins and the release of late biogenesis factors) as described in Altvater et al, 2012 and citations therein.

After export to the cytoplasm several last maturation events occur to enable the production of translation competent LSUs. These include the release of the exported biogenesis factors (for some of which the action of additional factors is required), presumably some last ITS2 trimming events (see 2.2.6.5), and the stable incorporation of a few r-proteins (see also 2.3). The removal of the exported LSU biogenesis factors was described to occur in a coordinated way involving the action of several ATPases and GTPases (Lebreton et al., 2006a; Pertschy et al., 2007). Initially, the AAA-ATPase Afg2/Drg1 was described to be recruited to cytoplasmic pre-60S particles by Rlp24 which also stimulates its ATPase activity (Kappel et al., 2012; Pertschy et al., 2007). Since in these studies the release of only Rlp24 was triggered by ATP hydrolysis *in vitro*, the release of the shuttling LSU biogenesis factors Nog1, Tif6, and Arx1 which was also described to be dependent on the action of Afg2/Drg1 (Pertschy et al., 2007), might occur (at least the release of some of them) further downstream (Lo et al., 2010). The levels of rpL24 (which shows significant sequence identity with Rlp24) on pre-60S particles, were significantly reduced after Drg1 inactivation, why it was suggested to by recruited to pre-60S particles after Rlp24 had left (Pertschy et al., 2007). The release of Arx1 and the associated Alb1 was described to be mediated by the action of Rei1 and its interaction partner Jjj1 whose recruitment to pre-60S particles is stimulated by binding of rpL24 (Demoinet et al., 2007; Lebreton et al., 2006a; Meyer et al., 2007, 2010). In parallel, the binding of the phosphatase Yvh1 triggers the release of Mrt4, a protein with high sequence identity to rpP0 (Kemmler et al., 2009; Lo et al., 2009; Rodríguez-Mateos et al., 2009a, 2009b). Finally, the releases of Nmd3 and Tif6 are mediated by the GTPases Lsg1/Kre35 and Elf1, respectively (Hedges et al., 2005; Kallstrom et al., 2003; Lo et al., 2010). Remarkably, the latter resembles the elongation factor 2 (Elf1 – elongation factor 2 like protein) and was described to be recruited after proper formation of the phospho-stalk. In a way, its binding triggers a step that mimics aspects of translocation, a part of the translation cycle, and was therefore described to "provide a mechanism to functionally check the nascent subunit" (Lo et al., 2010). This would depict a kind of quality mechanism in part analogous to the "translation like" cycle described to trigger the final SSU maturation (see 2.2.5).

To conclude it should be mentioned that several aspects of cytoplasmic LSU maturation are still poorly understood and sometimes (at least in parts) highly speculative. Improved methodologies in the field of structural biology making use of systematic analysis of a large number (>100 000) of cryo-EM pictures of certain inhomogeneous specimen (as purified pre-ribosomes certainly are) to finally "sort" them according to the population they belong to, might contribute to a better understanding of several of these incomprehensive aspects.

2.2.7 Mammalian ribosome biogenesis and related diseases

Studies with human cell lines and the systematic investigation of the evolution of ribosome assembly lead to the conclusion that the general process of ribosome biogenesis, including the action of many ubiquitous ribosome biogenesis factors, seems to be well conserved in eukaryotes (Ebersberger et al., 2013). Some additional, human specific factors or differences

in one or the other maturation event seem to have evolved, though (e.g. Sloan et al., 2013; Tafforeau et al., 2013).

A class of human genetic diseases that affect ribosome biogenesis, the so called “ribosomopathies” has been described (reviewed for example in Freed et al., 2010 or Sondalle and Baserga, 2014). Among them are Diamond–Blackfan anemia (DBA) and Shwachman–(Bodian) Diamond syndrome (S(B)DS). DBA is a very rare chronic anemia that is characterized by a decreased number of erythrocytes (and their precursor cells). The disease is in most cases caused by mutations in one of several ribosomal protein genes (often RPS19), resulting in a haploinsufficiency and an imbalance between rRNA synthesis and ribosomal proteins during ribosome biogenesis (Ball, 2011; Draptchinskaia et al., 1999; Horos and von Lindern, 2012; Léger-Silvestre et al., 2005). A key component in the pathophysiology is the activation of the p53 pathway finally leading to apotosis. Studies in yeast contributet to a better understanding of the consequences of mutations or deletions of r-protein genes as RPS19 (Gregory et al., 2007; Léger-Silvestre et al., 2005; Moore et al., 2010 and citations therein). S(B)DS is also a rare genetic disease (around 1:10000 – 1:20000 live birds) that is characterized by exocrine pancreatic insufficiency, impaired hematopoiesis, and leukemia predisposition (reviewed in Burroughs et al., 2009; Vinokurova et al., 2014). It is caused by mutations in the Shwachman - Bodian - Diamond syndrome gene (SBDS). Deletion of its yeast homolgue, SDO1, resulted in a severe growth defect (Menne et al., 2007). Further studies on Sdo1 in yeast revealed that its mutation or depletion resulted in a disturbed release of Tif6 from late cytoplasmic 60S presursors what leads to an abnormal translational activation (Finch et al., 2011).

In addition, numerous publications indicate the existence of direct links between errors in ribosome biogenesis (or ribosomal components) and the development of cancer, which seem to be highly complex and hence only poorly understood, though. Deregulation of ribosome biogenesis was described to lead to alterations in cell cycle, cell proliferation and increased susceptibility to cancer (Freed et al., 2010; Montanaro et al., 2008; Ruggero and Pandolfi, 2003). Many defects in ribosome biogenesis lead to the loss of the integrity of the nucleolar structure what was designated as “nucleolar stress”. These defects are thought to cause (amongst other effects) misregulation of the tumor suppressor p53. As one consequence of “nucleolar stress”, ribosomal components (e.g. the 5S RNP (5S rRNA, RPL5, and RPL11) were described to bind and inactivate MDM2, the main E3-ligase of p53 which promotes p53 degradation by ubiquitinating it. This r-protein induced MDM2 -inactivation leads to an activation of p53 (Chakraborty et al., 2011; Sloan et al., 2013 and citations therein). Therefore, proteins that regulate the formation, localization, and integration of the 5S RNP (or other r-proteins) into the ribosome might be involved (directly or indirectly) in MDM2 regulation. Among these proteins are ribosome biogenesis factors, one of which, PICT1 (the human homologue of Nop53), was recently described as a tumor suppressor by “relocalizing” RPL11 into the nucleolus and thereby activaing p53 (Golomb and Oren, 2011; Sasaki et al., 2011; Suzuki et al., 2012). Besides the function of these r-proteins in MDM2 mediated p53 regulation, others were proposed to regulate the activity of p53 through other, yet unknown

mechanisms (Freed et al., 2010 and citations therein). Due to these links, ribosome biogenesis (which is especially for cancer cells crucial to enable their high growth and proliferation rates) might become an important therapeutic target in cancer treatment. Targeting ribosome biogenesis in cancer cells might allow the p53 mediated effects as cell cycle arrest or apoptosis.

2.3 Assembly of ribosomal proteins in Pro- and Eukaryotes

A large part of the current knowledge of how r-proteins assemble on rRNAs comes from *in vitro* studies of prokaryotic ribosomes purified from *E.coli*. Starting in the 1960s, the groups of Nierhaus and Nomura succeeded in reconstituting functional ribosomal subunits by bringing together in a defined way the purified r-proteins and rRNAs (Dohme and Nierhaus, 1976; Nierhaus and Dohme, 1974; Traub and Nomura, 1968, 1969). This finding suggested the *E.coli* ribosome to be a self-assembling RNP. However, looking at the conditions of the *in vitro* reconstitutions, which are clearly non-physiological in terms of ion concentrations and temperature (see 2.3.1.1) this idea was soon challenged. What also became evident in these pioneering and extensive following studies was that the assembly of r-proteins occurs in a hierarchical order (also see 2.3.1.1). *In vitro* reconstitution of functional eukaryotic ribosomal subunits failed, presumably due to the above described highly complex pathway of eukaryotic ribosome biogenesis (including cell compartmentalization and the requirement of numerous ribosome biogenesis factors) (see also 2.3.1.2).
In vivo, the interplay of all the processes occurring during ribosome maturation (as described in 2.2), including the action of ribosome biogenesis factors and, in eukaryotes, the presence of pre-rRNA spacer sequences and the compartmentalization of the cell clearly influence the assembly of r-proteins on the (pre-)rRNAs. The state of the art of the ideas how r-protein assembly might occur *in vivo*, which come from several studies performed in both, pro- and eukaryotes will be introduced in 2.3.2.

2.3.1 *In vitro* assembly

2.3.1.1 *In vitro* assembly of prokaryotic r-proteins

The reconstitution of both ribosomal subunits from purified r-proteins and rRNAs requires defined conditions (reviewed in Nierhaus and Wilson, 2004). The *E.coli* small 30S subunit can be reconstituted in a one step procedure by adding the 30S r-proteins to the 16S rRNA in a buffer containing 0.3 – 0.5M KCl, 10 – 30M $MgCl_2$ and a pH of 6.5-8 at a temperature of 40°C. What turned out in these studies is that the ionic strength must be well balanced since unspecific interactions would be increased if the KCl concentration would be too low whereas too high concentrations would disturb inter- and intramolecular interactions. The presence of Mg^{2+} ions is essential for the establishment of stable rRNA secondary/tertiary structures which can be crucial for an efficient binding of r-proteins and the stabilization of these interactions. The relatively high temperature of 40°C turned out to be required for a final conformational change of the SSU intermediate to make it translation competent.

Interestingly, the simple association of the SSU r-proteins to the 16S rRNA occurs also at low temperatures of 0°C.

The *in vitro* reconstitution of translational active large 50S subunit requires two steps, whose buffer compositions are in general comparable to the one used in the 30S reconstitution assays (see above). The first step, which occurs at 44°C, results in an early assembly intermediate, termed "RI_{50*} (1)" which does not contain all r-proteins yet. Remarkably, two populations of this first intermediate were identified which do not differ in their r-protein composition but drastically in their sedimentation coefficient (33S vs. 41S). The interpretation of the presence of these two initial intermediates was that during the formation of the second intermediate a conformational change happens which determines the rate-limiting step (and hence requires the high temperature of 44°C) (Nierhaus and Wilson 2004 and citations therein). The stable incorporation of the remaining LSU r-proteins occurs in a second step which requires even higher temperatures (50°C), a higher Mg^{2+} concentration (20mM vs. 4mM for the first step) and more time (90 minutes vs. 20 minutes for the first step). Also during the long incubation of this second step, which is required for the production of translational competent 50S LSUs, an intermediate, termed "RI_{50} (2)" could be identified which contains all r-proteins but is totally translation inactive. Therefore, a second conformational change, determining the rate limiting stage of this step, was described to be required to enable the development of the translation competence (Nierhaus and Wilson, 2004).

The obvious next step after the successful *in vitro* reconstitution of active ribosomal subunits was the repetition of the reconstitution experiments but omitting single r-proteins or groups of r-proteins to test (in case the assembly of the respective subunit could still occur) their requirement for translation efficiency or fidelity. In case the omission of single r-proteins results in a disturbed assembly of ribosomal subunits, their respective requirement for (a) certain assembly step(s) could be revealed. In addition, by adding the r-proteins in different combinations (and with varying orders) to the rRNA(s), the assembly dependencies and the hierarchical interrelationships among most of the r-proteins could be deciphered. Depending on whether the individual r-proteins were able to bind rRNA independently of other r-proteins or only after the previous binding of one or more than one other r-protein, they were classified as primary, secondary, or tertiary *in vitro* binders. The results of these extensive studies on both subunits were brought together in the two *in vitro* "assembly maps" (see Figure 13 and Held et al., 1974; Herold and Nierhaus, 1987; Mizushima and Nomura, 1970).

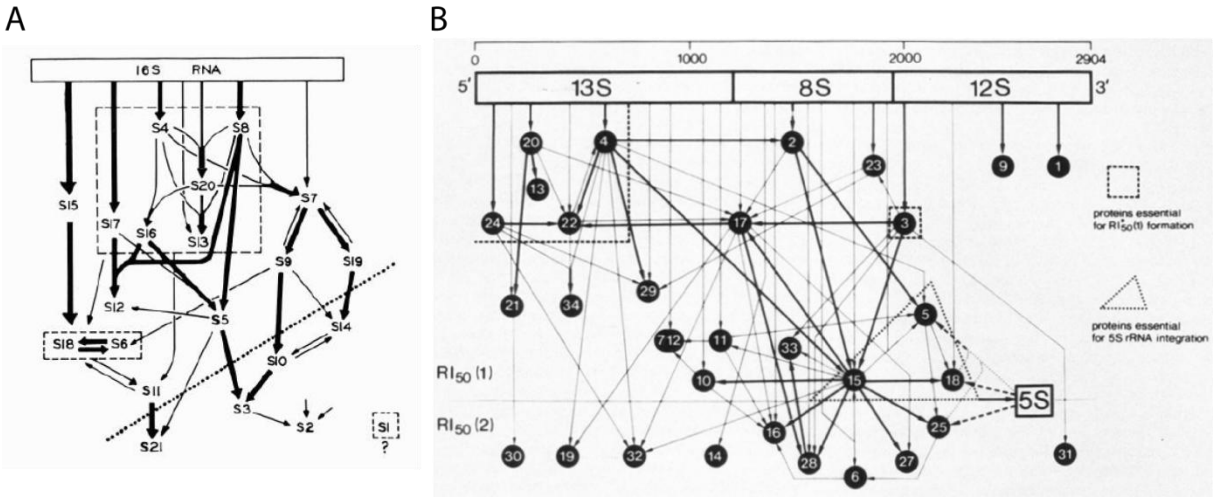

Figure 13 - Prokaryotic *in vitro* r-protein assembly maps of both ribosomal subunits

The two *in vitro* assembly maps of prokaryotic r-proteins of SSU and LSU are depicted in **A)** and **B)**, respectively. Functional prokaryotic ribosomal subunit could be reconstituted by mixing r-proteins and rRNA *in vitro* (see text for details). Some r-proteins are able to bind to rRNA *in vitro* without the previous binding of other r-proteins and were therefore assigned to as "primary *in vitro* binders". In the maps, they are directly connected to the rRNA by arrows. The interdependencies of the binding of the other, secondary and tertiary *in vitro* binders are illustrated by the network of arrows (see text for more details). The SSU and LSU *in vitro* assembly maps were adapted from Held et al. (1974) and Herold and Nierhaus (1987), respectively.

The natures of the two assembly maps differ insofar, that the LSU assembly map shows more complex binding hierarchies with much more hierarchical interconnections between single r-proteins than the SSU assembly map does. As described in section 2.1, the 3D organization of the secondary structure domains of the rRNA(s) of both subunits significantly differs. While the rRNA domains of the SSU are pretty clearly separated in space, the LSU rRNA secondary structure domains are much more intertwined resulting rather in a "one-domain-like" appearance. LSU r-proteins therefore often contact several different domains of the LSU. The more complex and interconnected assembly trees of the LSU assembly map might therefore well reflect these fundamental structural differences of both subunits. In addition, as described above, the reconstitution of the LSU only succeeded in a two step procedure applying higher temperatures and longer incubation times than the SSU reconstitution required. The sum of these findings might have been one reason why after the description of the two *in vitro* assembly maps in general more effort was put (at least more results have been published) in the more detailed decipherment of the *in vitro* assembly of the SSU. As example, with the possibility of *in vitro* transcription in the 1990s, several groups succeeded in reconstituting one of the three 16S rRNA domains independently of each other by incubating each of the 16S rRNA fragments with the respective SSU r-proteins binding to these regions according to the assembly map. Structural EM analyses showed that the general morphology of each domain resembles the one seen in the mature SSU what goes in line with the previous hypothesis that the "assembly trees" along the 16S rRNA can form independently of each other (Agalarov et al., 1998, 1999; Samaha et al., 1994; Weitzmann et al., 1993). A comparable approach for the LSU was never published, presumably because, due to its structural complexity (see above), it did not succeed. Finally it should be mentioned that the single experiments that finally contributed the determination of the hierarchical

interrelationships among the r-proteins (as summarized in the *in vitro* assembly maps) were often deduced from *in vitro* reconstitution reactions in which only a defined subset of components (rRNA and r-proteins) was present. (e.g. Röhl et al., 1982). It can therefore not be excluded that some of the described hierarchies in the assembly maps are not valid in the case of the presence of a more complete set of structural components and therefore not fully reflecting the situation *in vivo*.

The location of the individual SSU r-proteins relative to the 16S rRNA (and the effect of their binding on the rRNA structure) was determined using chemical structure probing methods in which binding of r-proteins (and the thereby induced establishment of certain rRNA structural features) protects the rRNA from cleavage what results in a “footprint” on the rRNA. This procedure is relatively straightforward for primary binders where the rRNA is only incubated with the respective r-protein. It becomes much more complicated for secondary or tertiary binders, though. The Noller group started to combine the SSU *in vitro* reconstitution (following the Nomura SSU *in vitro* assembly map) with systematic chemical probing in order to try to understand the dependencies of later assembling SSU r-proteins on earlier assembly events (Stern et al., 1989 and citations therein). The mechanisms of these dependencies were described to be (in principle) explained by two extreme models. “In one model, based purely on protein-protein interactions, protein A contains the binding site for protein B, explaining why prior assembly of protein A is obligatory for incorporation of protein B. At the other extreme is a model in which cooperativity is mediated by RNA. Binding of protein A produces a conformational change in 16S rRNA, unveiling a cryptic RNA binding site for protein B” (Stern et al., 1989). In general, a combination of parts of both of these models might be the case for the assembly of many secondary or tertiary SSU r-proteins. Too sum up, the binding of several r-proteins might act cooperatively to stabilize a conformational change in the rRNA which then enables binding of another r-protein.

More recently performed kinetic RNA structure probing experiments by the Woodson group, using hydroxyl radical foot printing, gave evidence that some interaction sites of individual r-proteins with rRNA can change during the time course of the *in vitro* reconstitution. Some of the contacts between r-proteins and rRNA, especially those in which r-proteins bridge certain “in-cis distant” rRNA regions, are established late during assembly in the *in vitro* reconstitution experiments. Based on these and the previous findings (see above), an “induced fit” mechanism for the stable assembly of certain r-proteins was suggested in which the fast occurring, initial r-protein - rRNA interactions lead to a quick (in the range of a few milliseconds) stabilization of local rRNA structure. The often more time consuming and therefore later fulfilled establishment of some final r-protein - rRNA interactions can then occur via induced fit (Adilakshmi et al., 2008; Mayerle et al., 2011).

A recent study investigated the kinetics of the *in vitro* SSU assembly process using isotope (N^{15}) labeled SSU r-proteins which were incubated with the 16S rRNA for a short time (“pulse”). This assembly reaction was then “chased” with an excess of unlabeled (N^{14}) r-proteins. The composition of the resulting intermediates was investigated using quantitative

mass spectrometry. In general, the results showed a good correlation between the assembly kinetics of SSU r-proteins and their role as primary, secondary or tertiary binders (Talkington et al., 2005). In addition, SSU r-proteins that interact with the 5' domain of the 16S rRNA were described to bind faster to rRNA than SSU r-proteins that bind to the 16S rRNA 3' domain. This is in agreement with previous kinetic studies of the Noller group (see above) in which the assembly of SSU r-proteins was followed by combining the *in vitro* reconstitutions with chemical probing methods at different time points and lower temperatures (Powers et al., 1993 and citations therein). According to their "assembly pace" the SSU r-proteins where divided into four groups, the earliest of which contains 8 SSU r-proteins. Remarkably, all of these 8 proteins bind to the 5' half of the 16S rRNA in the 5' or central domain, what lead to the conclusion of a 5' to 3' polarity in the SSU *in vitro* assembly. Interestingly, four (S4, S15, S17, S20) of the six primary *in vitro* binders identified by the assembly studies (see above) are part of this "early" 5'-half binding group. The remaining two primary *in vitro* binders (S8 and S7) bind in the central and 3' domain, respectively, though. Please note that the nomenclature of ribosomal proteins is described in more detail in section 2.3.3 (see also table 1).

This 5' to 3' polarity or "assembly gradient" observed in the *in vitro* studies became even more evident for the LSU. The above described conformational shift of the "$RI_{50*}(1)$" intermediate (which results in a drastically different sedimentation coefficient), *in vitro* only requires the presence of a few, namely five LSU r-proteins (and one more that stimulates this step). With the exception of the stimulating L3, all five of these LSU r-proteins (L4, L13, L20, L22, and L24) have binding sites located towards the 5' end of the 23S rRNA, strongly suggesting the existence of a 5' to 3' assembly gradient also for the LSU (Spillmann et al., 1977). Transferring this hypothesis to the situation *in vivo*, where the assembly presumably starts co-transcriptionally with a much shorter nascent 5' 23S rRNA-fragment, the formation of this first assembly platform could occur easier since all the downstream rRNA sequences are not yet transcribed and therefore cannot compete for the binding of the early LSU r-proteins. With the words of Knut Nierhaus, the presumably reduced number of rRNA components *in vivo* leads to an "entropic advantage" in comparison to the situation *in vitro* (reviewed in Nierhaus and Wilson, 2004). Of course this description of the putative situation *in vivo* is highly speculative since the conditions *in vivo* are very different than *in vitro*. The experimental validation of these ideas is very challenging (see section 2.3.2 describing *in vivo* assembly in more detail).

The non-physiological conditions that are required for the *in vitro* reconstitution of functional prokaryotic ribosomal subunits suggested the involvement of trans-acting factors *in vivo*. In fact, a growing number of ribosome biogenesis factors were described and further characterized *in vitro* and *in vivo*. As example, the DnaK/Hsp70 system of chaperones (DnaK, DnaJ, GrpE), which was previously shown to be involved in aspects of protein folding (reviewed in Agashe and Hartl, 2000), was reported to also be involved in 30S assembly by facilitating reconstitution of 30S subunits under otherwise permissive conditions *in vitro* (Maki et al., 2002, 2003). However, this facilitating role could not be confirmed by the Nierhaus

group and was therefore under debate (Alix and Nierhaus, 2003). A more direct role of three other putative biogenesis factors on the assembly of SSU r-proteins was more recently reported by the Williamson group (Bunner et al., 2010). The addition of either of these three proteins to the *in vitro* reconstitution experiments resulted in a modulated (faster or slower) "assembly time" of some r-proteins as read out by quantitative mass spectrometry (see above and Talkington et al., 2005). More than 20 known or potentially new prokaryotic biogenesis factors were recently identified in various pre-ribosomal particles purified *ex-vivo* from *E.coli* (Chen and Williamson, 2012).

2.3.1.2 *In vitro* assembly of eukaryotic r-proteins

In contrast to prokaryotic ribosomal subunits, the "de novo" *in vitro* reconstitution of functional LSUs or SSUs failed in eukaryotes. Now, as we know that *in vivo*, eukaryotic ribosome biogenesis requires a large number of ribosome biogenesis factors and that biogenesis starts with transcripts containing more spacer sequences that finally have to be removed, (see 2.2) this is not very surprising. In addition, the eukaryotic cell is compartmentalized (and ribosome biogenesis starts in the nucleolus and ends in the cytoplasm). How this compartmentalization is influencing biogenesis of functional subunits in detail is not certain but it is clearly not reflected in *in vitro* experiments. These facts indicate that the eukaryotic ribosome is no "self assembling" RNP and can therefore not simply be reconstituted by mixing its components.

What has been published is a partial reconstitution of functional rat 60S and 40S subunits, from which several r-proteins had been stripped off before by high salt concentrations and/or organic compounds as ethanol or dimethyl-maleic anhydride (DMMA) (Lavergne et al., 1988; Reboud et al., 1972). Functional ribosomal subunits from the amoeba *Dictyostelium discoideum* were reported to be reconstituted at room temperature *in vitro*. The adding of a nuclear RNA fraction (probably snoRNAs) purified from the same amount of cells used for the r-protein extraction turned out to be essential for this process, though. In addition, the ribosomal subunits showed higher translation rates when premature rRNA sequences were added (Mangiarotti and Chiaberge, 1997).

2.3.2 *In vivo* assembly

The *in vitro* reconstitution studies provided clear evidences for some general principles (binding hierarchies, cooperativity, "induced fit", 5'-3' assembly gradient... – see above) of how the stable binding of r-proteins into rRNA presumably occurs. The task to decipher how these principles are carried out during the complex process of ribosome biogenesis *in vivo* was and still is very challenging. The essential heat steps and the long incubation time(s) required *in vitro* point out the involvement of additional mechanisms *in vivo*. The current knowledge on pro- and eukaryotic r-protein assembly *in vivo* will be introduced in the next two sections.

2.3.2.1 Prokaryotic *in vivo* assembly of r-proteins

Whether or to what extent the actual hierarchical assembly interrelationships among the r-proteins as summarized in the *in vitro* assembly maps, can be transferred to the situation *in vivo* is still pretty unclear. The most direct approach to test the transferability of individual *in vitro* hierarchical interrelationships to the situation *in vivo* would be to deplete (shut down *in vivo* expression of) individual r-proteins and subsequently analyze the consequence of their absence on the assembly state of the respective subunit-precursor. However, this approach remains challenging since an appropriate genetic system to systematically deplete single genes is not as established in *E.coli* as it is for example in yeast. A system to create single gene knock-out mutants, the "Keio-collection", exists since a few years but it is not applicable for essential genes, many of which are coding for r-proteins. Recently however, one group succeeded in arresting the synthesis of L5 which is essential for cell growth. The analysis of the accumulating defective pre-50S particles revealed the lack (or strong underrepresentation) of most of the components of the central protuberance, including 5S rRNA, L5, L16, L18, L25, L27, L31, L33 and L35 (Korepanov et al., 2012; Schuwirth et al., 2005). In the *in vitro* assembly map however, only effects on assembly of L18 and L25 are indicated. Thus, in this case, the *in vivo* expression shut down of one LSU r-protein resulted in a more drastic effect as one would predict strictly following the *in vitro* assembly map. In another recent study, a number of *Bacillus subtilis* ribosomal protein genes were inactivated to investigate their requirement for general cellular processes. For some LSU r-protein mutants, the changes in the composition of the resulting mutant (pre-) ribosomes was analyzed in more detail allowing to deduce some *in vivo* hierarchical interrelationships between LSU r-proteins (Akanuma et al., 2012).

The composition and structure of late prokaryotic pre-50S particles (45S particles) were recently enriched and characterized by *in vivo* expression shut down of an essential ribosome biogenesis factor what leads to the massive accumulation of immature 45S particles (Jomaa et al., 2013; Li et al., 2013). Quantification of the r-protein composition of the 45S particles by mass spectrometry showed that a group of r-proteins bound at or near the central protuberance (in mature 50S subunits) were strongly underrepresented in these particles. Lacking densities at these positions in the cryo-EM structures confirmed these findings and suggested that the central protuberance and important contact sites required for interaction with the SSU are formed at very late stages in the maturation of the LSU in prokaryotes.

Remarkably, some r-proteins which fulfill a role as primary binder in the *in vitro* assembly map turned out to be not essential for cell growth (under laboratory conditions). Among them is *E.coli* S15 and the group of Gloria Culver investigated the *in vivo* assembly state of SSUs in absence of S15. They came to the conclusion that the assembly of the secondary/tertiary binders that should (according to the *in vitro* map) depend on previous binding of S15 were able to bind, what disagrees with the *in vitro* data (Bubunenko et al., 2006). This and some similar rather unexpected findings argue for the existence of important mechanistic differences *in vivo* and the requirement of further *in vivo* studies addressing the hierarchical

interrelationships in more detail. The above (2.3.1.1) described often reductionist *in vitro* experiments from which the assembly maps were deduced might also be a reason why a potential primary binder as S15 at the “beginning” of one assembly cascade is apparently not strictly required for the assembly of the “downstream” r-proteins *in vivo*. In this case, components from other assembly cascades which might have simply not been present in the respective *in vitro* experiments might also enable the downstream events. Alternatively, trans-acting ribosome biogenesis factors might contribute to their assembly *in vivo* (see above).

Combining stable *in vivo* isotope pulse labeling with quantitative mass spectrometry of different assembly intermediates, the Williamson group focused not primarily on the hierarchical interrelationships of the r-proteins during their assembly, but on the time the individual r-proteins need to be stably bound to different assembly intermediates purified *ex-vivo* from *E.coli* cell lysates. The levels of the individual r-proteins in the different (pre-) ribosomal particles, which were determined by quantitative mass spectrometry, were subjected to unbiased statistical cluster analyses creating four and six “assembly groups” for the small and large subunit, respectively (Chen and Williamson, 2012; Chen et al., 2012). The two *in vitro* assembly maps were then adapted in a way to match these kinetic data (see Figure 14). Since the hierarchical interrelationships among the r-proteins (depicted as arrows in the maps) were not addressed in this approach, the adaption of the *in vitro* maps only concerned the Y-axis (“time” axis) in which single r-proteins or whole “cascades” were positioned further up or down (see Figure 14B and D). As example, L2 (which was initially described as primary binder) was grouped in the fourth of six assembly groups arguing that its stable assembly occurs at rather intermediate or late stages in ribosome maturation. L15 on the other hand, whose assembly depends (according to the *in vitro* assembly map) on the previous binding of several r-proteins (L2, L3, L4) was put in the second of the six assembly groups indicating that its assembly occurs earlier. The positions of these two (and many other r-proteins) were therefore shifted further “down” (L2) or “up” (L15) (compare the two *in vitro* assembly maps shown in Figures13 and 14). However, potential weaker interactions of one or the other r-protein with earlier precursors might have been not detectable in these approaches since they might have been disrupted during the purification procedure (when the conditions were too harsh). In general, the adaptations in the “new”, modified assembly maps do not argue against the above described 5’ – 3’ assembly gradient, which had been suggested to occur *in vivo*.

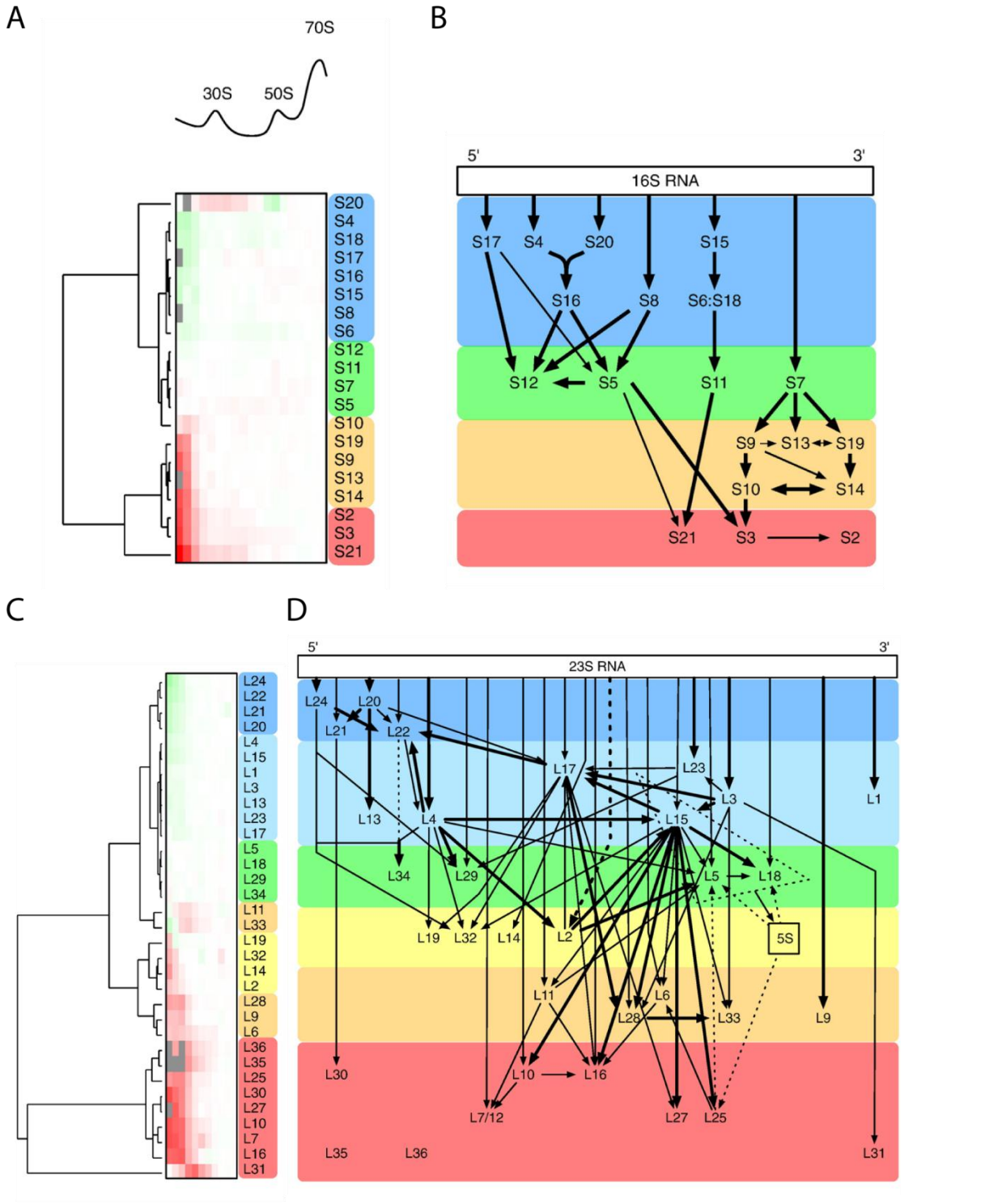

Figure 14 - modified prokaryotic *in vitro* r-protein assembly map generated by *in vivo* stable isotope pulse labeling approaches using quantitative mass spectrometry

In vivo stable isotope pulse labeling of *E.coli* cultures followed by quantitative mass spectrometry resulted in a clustering of wild type assembly intermediate r-protein levels to form modified *in vitro* ("*in vivo*") prokaryotic 30S and 50S assembly maps. **A)** Groups of r-proteins with distinct "protein-level trends" (more abundant to less abundant) across increasingly dense fractions of a sucrose gradient are marked as blue, green, orange, and red. Their linkage, as analyzed by hierarchical cluster analyses is indicated in the dendrogram on the left. **B)** shows the "new", modified assembly map of the SSU according to the data shown in A) and the previously publisehd SSU map (see text and Figure 13). **C)** Similar analyes as in A) focusing on the LSU. Six distinct groups of LSU r-proteins resulted from the results of this pulse labeling / MS approach. **D)** shows the "new", modified LSU assembly map based on these data and the previously published ones (see text Figure 13). Adapted from Chen and Williamson (2012), see text for more details.

The potential of this approach to also address *in vivo* the hierarchical interrelationships among the r-proteins (thus, to verify the correctness of the “arrows” in the *in vitro* maps) by depleting individual r-proteins is obvious.

Recent studies by the laboratory of Sarah Woodson investigated several aspects of the role of SSU r-proteins *in vivo* by applying X-ray radical footprinting, fluorescence resonance energy transfer (FRET), or also quantitative mass spectrometry approaches (Clatterbuck Soper et al., 2013; Kim et al., 2014; Mayerle and Woodson, 2013). The requirement for some prokaryotic SSU r-proteins on RNA folding and/or the assembly of other SSU r-proteins were described.

2.3.2.2 Eukaryotic *in vivo* assembly of r-proteins

Starting almost 40 years ago, the *in vivo* assembly of eukaryotic r-proteins, which are highly conserved, was investigated in several organisms by numerous different approaches. In comparison to the *in vitro* assembly studies, whose feasibility and potential turned out to be limited in eukaryotes (see above), the situation *in vivo* is even more complex. The interplay of all the processes introduced in 2.2 clearly influences the way how the stable interactions of r-proteins and rRNA found in the mature ribosomal subunits are formed. These include features as presence of pre-rRNA spacer sequences, the modifications of rRNA, requirement of numerous dynamically interacting ribosome biogenesis factors and snoRNPs, and cell compartmentalization. Since in this work the focus is set on the assembly of eukaryotic LSU r-proteins, this section mainly summarizes the current knowledge of the assembly of LSU r-proteins. Please note that several studies which will be referred to in the following analyzed the assembly behavior of both SSU and LSU r-proteins even if only details of the latter will be described.

Some studies on ribosome biogenesis factors provided clear evidences for a functional link of their action to certain r-protein assembly events (e.g. Bussiere et al., 2012; Hofer et al., 2007; Jakob et al., 2012; Kemmler et al., 2009; Lo et al., 2009; Sahasranaman et al., 2011; Schäfer et al., 2006; Zhang et al., 2007). Since biogenesis of both ribosomal subunits occurs mainly in the nucleus, the r-proteins (whose mRNA is translated in the cytoplasm) somehow have to reach the nuclear pre-ribosomal particles. Their nuclear import was described to be mediated in an energy dependent manner by nuclear import receptors, which recognize different types of nuclear localization sequences (NLSs) of the respective r-proteins (Chook and Süel, 2011; Görlich and Kutay, 1999; Rout et al., 1997). A recent study suggested that this import and the subsequent incorporation into pre-ribosomes of certain r-proteins might occur in a coordinated way by specific factors which could also enable the import of (functionally/structurally connected) r-proteins in stoichiometric amounts (Kressler et al., 2012b). However, since this specific potential import factor Syo1, which was described to mediate the import of rpL5 and rpL11, is not essential, there must be alternative pathways. Due to the small size of most r-proteins (rpL3 is the largest r-protein in yeast with a molecular

weight of 43.8 kDa – most others are significantly smaller), it cannot be excluded that one or the other r-protein simply diffuses through the nuclear pore.

Visualization of chromatin ("Miller") spreads of rDNA and the ongoing rRNA transcription by electron microscopy gave strong evidence for ribosome biogenesis already starting during transcription on the nascent transcripts (see 2.2.2 and 2.2.3 and Miller and Beatty, 1969). In addition, many SSU r-proteins were identified in the earliest pre-ribosomal particles (the SSU processome), indicating that r-proteins start to interact very early with pre-rRNA (Bernstein et al., 2004). An earlier study that combined the "Miller spreading" technique with immuno labeling of r-proteins suggested that some r-proteins co-localize with the nascent pre-rRNA transcripts providing evidence for some initial interactions of r-proteins with pre-rRNA during transcription (Chooi and Leiby, 1981). However, this often assumed model of co-transcriptional assembly of r-proteins was challenged in a recent study that analyzed the nucleolar localization of several early binding r-proteins in human cells, applying various methods (Krüger et al., 2007).

In the late 1970s, several groups started to investigate the kinetics of eukaryotic r-protein assembly *in vivo*. Ribosomes from cellular extracts, whose newly made proteins had been metabolically labeled for various times, were isolated and subsequently analyzed. R-proteins that assemble at early stages in the maturation pathway would still mainly be distributed in premature ribosomes shortly after the "metabolic pulse" and therefore be underrepresented in mature ribosomes. In contrast, r-proteins with a comparably high incorporation of the label in the mature ribosomes isolated shortly after the introduction of the pulse were interpreted as being incorporated late during ribosome biogenesis (or as being exchangeable). In addition, the composition of nuclear preribosomal particles was analyzed and compared to the one of mature ribosomes enabling the identification of r-proteins that were specifically underrepresented in the premature nuclear fraction and therefore likely incorporated late in the cytoplasm. Since the detection of r-proteins by 2D gel electrophoresis often was tricky and the different groups used distinct 2D gel systems and a different r-protein nomenclature, some of the results of these studies are ambiguous. The r-protein nomenclature used by these groups can be found in (Dick et al., 1997; Mager et al., 1997; McConkey et al., 1979 and citations therein). Usually, the numbering of r-proteins started at the top left corner of the 2D gels and ended at the bottom right side, why in general, r-proteins with are small number are normally larger than r-proteins with a high number (see Figure 15 and for example in Kruiswijk and Planta, 1974). The nomenclature of all r-proteins from yeast has been standardized in Mager et al., 1997; Planta and Mager, 1998. Concomitant with the publication of the yeast ribosome crystal structure by the Yusupov group (Ben-Shem et al., 2011) a new, unique nomenclature for r-proteins of all phyla has been proposed what facilitates the direct comparison of pro- and eukaryotic ribosomal proteins (Jenner et al., 2012, see also table 1). Since this "new" nomenclature is not yet adopted by the *Saccharomyces* Genome Database (SGD) (http://www.yeastgenome.org), which is used as reference for all annotated genes in *S.cerevisiae*, please note that the nomenclature used in

this work is the one of the SGD which was introduced by Planta and Mager in the late 1990s (Mager et al., 1997; Planta and Mager, 1998).

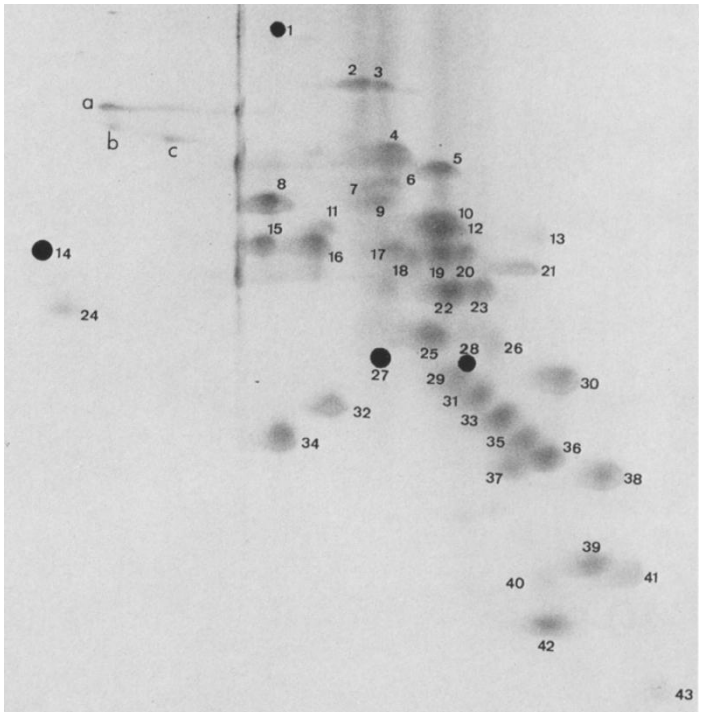

Figure 15 - Yeast LSU r-proteins separated by 2D electrophoresis and the LSU r-protein nomenclature of the Planta laboratories (1974).

The second dimension (SDS PAGE) is downwards. Indicated numbers were used for the nomenclature of the LSU r-proteins. Proteins highlighted by a black spot were only obtained in "low-salt" preparations of LSUs. Spots indicated by A, B, and C indicate to r-proteins which were only occasionally visible. Adapted and modified from Kruiswijk and Planta, 1974.

Despite these dubieties in terms of nomenclature and unambiguous identification, consistent evidences for rpL10 and rpL24 being incorporated at very late stages of eukaryotic LSU maturation were provided by several groups working with yeast, mouse, and human cells, respectively (Auger-Buendia et al., 1979; Kruiswijk et al., 1978; Lastick, 1980; Lastick and McConkey, 1976). In addition to rpL10 and rpL24, some other, less consistent candidates of late incorporated r-proteins were identified. Besides some r-proteins of unclear identity, these include rpL19 (Kruiswijk et al., 1978; Lastick, 1980), rpP2 (Kruiswijk et al., 1978), rpL29 and rpL40 (Auger-Buendia et al., 1979), last of which was recently confirmed to be incorporated late and to be required for nuclear - cytoplasmic export and final cytoplasmic LSU maturation (Fernandez-Pevida et al., 2012). The results of a former study however indicated that nuclear - cytoplasmic export is still possible after depletion of rpL40 and only affected to minor extent (Pöll et al., 2009). For some r-proteins, evidence for the ability to replace the respective copy of itself on a mature ribosome was provided. This exchangeability was suggested for mammalian (human or rat) rpL10, rpL19, rpL24, and the phospho stalk proteins rpP0, rpP1 and rpP2 (Lastick and McConkey, 1976; Rich and Steitz, 1987; Tsurugi and Ogata, 1985). In yeast, rpL10 and the three phospho proteins (rpP1, rpP2 and rpP0) were described to be exchangeable (Dick et al., 1997; Mitsui et al., 1988; Saenz-Robles et al., 1990; Zinker, 1980; Zinker and Warner, 1976). The finding that the amount of the phospho proteins rpP1 and

rpP2 present on isolated ribosomes is not constant in exponentially growing versus stationary yeast cells was interpreted as a putative regulatory role of these r-proteins in the “ribosomal activity” (translation). Consistently, their amount in polyribosomes was found to be higher than in 80S ribosomes (Ballesta and Remacha, 1996; Saenz-Robles et al., 1990).

More recently, in the studies on affinity purified yeast pre-ribosomal particles which mainly aimed to decipher the function of the numerous ribosome biogenesis factors (see 2.2), additional information on the LSU r-protein composition of the different assembly intermediates was sometimes provided (even if it was in most cases not directly addressed). However, these studies did not directly address the general assembly behavior of the entire group of LSU r-proteins. Despite this, data from several studies were in agreement with the late assembly behavior of a group of LSU r-protein suggested in the earlier studies (see above). These include rpL10, rpL24 and the phospho stalk proteins rpP0, rpP1, and rpP2 (Bradatsch et al., 2012; Kemmler et al., 2009; Kressler et al., 2008; Lo et al., 2009; Rodríguez-Mateos et al., 2009a; Saveanu et al., 2001). Another, more direct way to test the association of LSU r-proteins to the different subsequently formed pre-60S assembly intermediates is an affinity purification of the respective epitope tagged LSU r-protein and a subsequent analysis of the co-purified (pre-) rRNA content. These experiments were also not performed systematically but with individual r-proteins under different conditions and often not analyzing all (pre-) rRNA species, what complicates clear statements. Nevertheless, TAP-tagged rpL10 only co-purified 5.8S but no detectable amounts of 7S pre-rRNA, what is in line with its previously described late assembly (Saveanu et al., 2001). HA-tagged rpL40 which had been described as a candidate for being late incorporated behaved similarly (Fernandez-Pevida et al., 2012). RpL35 (Babiano and de la Cruz, 2010) and the 5S RNP components rpL5 and rpL11 (Zhang et al., 2007) were co-purifying significant amounts of early pre-rRNAs, whereas association of rpL17, rpL37 (Gamalinda et al., 2013), and rpL26 (Babiano et al., 2012) started to pre-60S particles with an intermediate (27SB pre-rRNA containing) maturation state.

Several studies applying quantitative mass spectrometry to detect changes in the protein composition of pre-60S assembly intermediates purified from wild type and/or mutant yeast strains were published within the last years (Lebreton et al., 2008; Merl et al., 2010; Sahasranaman et al., 2011). However, these studies mainly focused on the changes of the levels of ribosome biogenesis factors. Levels of r-proteins were, if at all, only given in average (of all identified SSU and LSU r-proteins, respectively). A more recent study addressing the compositional changes of pre-60S particles before and after nuclear export applied targeted proteomics of a number of biogenesis factors and 10 LSU r-proteins (Altvater et al., 2012). Several epitope tagged LSU biogenesis factors that interact with partially different populations of pre-60S particles were used to compare the respective levels of various co-purified biogenesis factors. However, the average levels of the 10 LSU r-proteins included in the targeted proteomic readout were assumed to not change and even used for normalization to enable the quantification of the LSU biogenesis factors of interest. Whether or to what extent the individual levels of the included 10 LSU r-proteins vary,

remains elusive. Putative small changes of individual r-protein levels might have been under the detection limit, especially when the “background” of contaminating mature LSUs (not shown in this study) was too high. Another study addressing the role of a group of early acting LSU ribosome biogenesis factors (the “A3 factors – see 2.2.6.2) on assembly of LSU r-proteins and other biogenesis factors succeeded in detecting and quantifying changes in the levels of a group of LSU r-proteins after depletion of one “A3 factor” (Sahasranaman et al., 2011).

2.3.3 Characteristics of LSU r-proteins of *S.cerevisiae*

By definition, r-proteins co-purify with mature ribosomes (under physiological conditions) in stoichiometric amounts (in yeast this stoichiometry is maintained also at higher salt concentrations of up to around 500 mM KCl - Warner, 1971). Under standard laboratory conditions, 64 of the in total 79 yeast r-proteins are essential (Giaever et al., 2002; Steffen et al., 2012). Mainly due to a whole genome duplication (WGD) event occurring about 100 million yeast ago in yeast, many (59) of the r-proteins are encoded by a pair of paralogous genes (Wolfe and Shields, 1997). The protein products of these genes are in most cases identical or very similar (see table 1) and most show a decelerated evolution (Kellis et al., 2004). In many cases only one of the two paralogues is required for growth although the fact that more than half of the ribosomal duplicate genes are haploinsufficient indicates that (in yeast) the dosage of the r-protein coding genes can be crucial (Deutschbauer et al., 2005; Steffen et al., 2012). Despite the high similarity among the r-protein paralogues, deletion of one can have a different phenotype than deletion of the other, what could be either simply explained by different expression levels and/or by paralogue specific functions. The reported examples of these differences (see Gilbert, 2011; Komili et al., 2007; Xue and Barna, 2012 and citations therein) suggested the existence of a “ribosome code” in which the heterogenity in ribosome constitution might result in functionally specialized ribosomes providing an additional level of translation regulation.

Since in this study the general and specific assembly characteristics of yeast LSU r-proteins were aimed to be characterized, this section shall summarize several features of LSU r-proteins, most of which are summarized in table 1. As mentioned above (2.1) most LSU r-proteins directly contact one or several LSU rRNA secondary structure domains what often results in a bridging of two domains. Systematic depletion of most essential yeast LSU r-proteins (using a conditional expression system in which expression can be shut down by a simple change in the carbon source of the medium the yeast cells are cultivated in) was done and showed the following results. While the structurally highly intertwined LSU rRNA domains (see also 2.1) could hypothesize the existence of only one common depletion phenotype, these studies showed that depletion of most LSU r-proteins results in a specific (pre-)rRNA processing phenotype (Babiano and de la Cruz, 2010; Babiano et al., 2012; Fernandez-Pevida et al., 2012; Gamalinda et al., 2013; Hofer et al., 2007; Li et al., 2009; Pöll et al., 2009; Rosado et al., 2007b; Steffen et al., 2012).

Table 1 – Summary of yeast LSU r-proteins including class of pre-rRNA processing phenotypes, *E.coli* homologue, "new" (Yusupov) name, and main contacts to LSU domains

LSU r-protein	essential for growth [1]	rRNA processing phenotype class (if published)	Allele A/B	length (AA)	systematic name (SGD)	sequence identity of the 2 alleles	*E.coli* homolgue	"new name" (Yusupov nomenclature) [5]	(main) contacts to rRNA sec. domain(s) [6]	Direct contacts to LSU r-proteins	expression mutant analyzed here?
rpL1	yes	**4**[2]	rpL1A	217	YPL220W	100%	L1	L1	V		no
			rpL1B	217	YGL135W						
rpL2	yes	**3**[2]	rpL2A	254	YFR031C-A	100%	L2	L2	II; III; IV; V		yes
			rpL2B	254	YIL018W						
rpL3	yes	**1**[2]	rpL3	387	YOR063W	-	L3	L3	VI		yes
rpL4	yes	**1**[2]	rpL4A	362	YBR031W	>99%	L4	L4	II; I		yes
			rpL4B	362	YDR012W						
rpL5	yes	**3**[2]	rpL5	297	YPL131W	-	L18	L18	V; 5S		no
rpL6	yes	**1**[2]	rpL6A	176	YML073C	94%	-	L6e	I; VI		no
			rpL6B	176	YLR448W						
rpL7	yes	**1**[2]	rpL7A	244	YGL076C	98%	L30	L30	II		yes
			rpL7B	244	YPL198W						
rpL8	yes	**1**[2]	rpL8A	256	YHL033C	97%	-	L8e	I (5.8S); V; (III)		yes
			rpL8B	256	YLL045C						
rpL9	yes	**2**[2]	rpL9A	191	YGL147C	98%	L6	L6	VI; II		yes
			rpL9B	191	YNL067W						
rpL10	yes	**3**[2]	rpL10	221	YLR075W	-	L16	L16	II; V; 5S		yes
rpL11	yes	**3**[2]	rpL11A	174	YPR102C	>99%	L5	L5	II; V; 5S		yes
			rpL11B	174	YGR085C						
rpL12	no		rpL12A	165	YEL054C	100%	L11	L11	II		no
			rpL12B	165	YDR418W						
rpL13	yes	**3**[2]	rpL13A	199	YDL082W	99%	-	L13e	I; (II; V)		yes
			rpL13B	199	YMR142C						
rpL14	yes		rpL14A	138	YKL006W	>99%	-	L14e	I; VI		no
			rpL14B	138	YHL001W						
rpL15	yes	**1**[3]	rpL15A	204	YLR029C	>99%	-	L15e	I		no
			rpL15B	204	YMR121C						
rpL16	yes	**1**[2]	rpL16A	199	YIL133C	90%	L13	L13	II; VI		yes
			rpL16B	198	YNL069C						
rpL17	yes	**3**[2]	rpL17A	184	YKL180W	>99%	L22	L22	5.8S; I; III (V)		yes
			rpL17B	184	YJL177W						
rpL18	yes	**1**[2]	rpL18A	186	YOL120C	100%	-	L18e	II		yes
			rpL18B	186	YNL301C						
rpL19	yes	**2**[2]	rpL19A	189	YBR084C-A	100%	-	L19e	III; IV		yes
			rpL19B	189	YBL027W						
rpL20	yes	**1**[2]	rpL20A	172	YMR242C	100%	-	L20e	I (ES7); II; 5S		yes
			rpL20B	172	YOR312C						
rpL21	yes	**3**[2]	rpL21A	160	YBR191W	99%	-	L21e	II; V		yes
			rpL21B	160	YPL079W						

rpL22	no		rpL22A	121	YLR061W	86%	-	L22e	III		no
			rpL22B	122	YFL034C-A						
rpL23	yes	**2**[2]	rpL23A	137	YBL087C	100%	L14	L14	IV; V; VI		yes
			rpL23B	137	YER117W						
rpL24	no		rpL24A	155	YGL031C	99%	-	L24e	VI		no
			rpL24B	155	YGR148C						
rpL25	yes	**2**[2]	rpL25	142	YOL127W	-	L23	L23	5.8S; III		yes
rpL26	no		rpL26A	127	YGR034W	99%	L24	L24	5.8S; I		no
			rpL26B	127	YLR344W						
rpL27	yes	**2**[2]	rpL27A	136	YDR471W	>99%	-	L27e	III		yes
			rpL27B	136	YHR010W						
rpL28	yes	**3**[2]	rpL28	149	YGL103W	-	L15	L15	II		yes
rpL29	no		rpL29	59	YFR032C-A	-	-	L29e	II; V		no
rpL30	yes		rpL30	105	YGL030W	-	-	L30e	III		no
rpL31	no	(**2**[4])	rpL31A	113	YDL075W	>99%	-	L31e	III; VI		no
			rpL31B	113	YLR406C						
rpL32	yes	**1**[2]	rpL32	130	YBL092W	-	-	L32e	II		yes
rpL33	yes	**1**[2]	rpL33A	107	YPL143W	>99%	-	L33e	II; VI		yes
			rpL33B	107	YOR234C						
rpL34	yes	**2**[2]	rpL34A	121	YER056C-A	98%	-	L34e	III		yes
			rpL34B	121	YIL052C						
rpL35	yes	**2**[2]	rpL35A	120	YDL191W	100%	L29	L29	5.8S; I		yes
			rpL35B	120	YDL136W						
rpL36	yes		rpL36A	100	YMR194W	98%	-	L36e	I		no
			rpL36B	100	YPL249C-A						
rpL37	yes	**2**[2]	rpL37A	88	YLR185W	93%	-	L37e	5.8S; I; II; III		no
			rpL37B	88	YDR500C						
rpL38	no		rpL38	78	YLR325C	-	-	L38e	III		no
rpL39	no		rpL39	51	YJL189W	-	-	L39e	5.8S; III		no
rpL40	yes	**4**[2]	rpL40A	128	YIL148W	100%	-	L40e	V; VI		no
			rpL40B	128	YKR094C						
rpL41	no		rpL41A	25	YDL184C	100%	-	L41e	IV		no
			rpL41B	25	YDL133C-A						
rpL42	yes		rpL42A	106	YNL162W	100%	-	L44e	V		no
			rpL42B	106	YHR141C						
rpL43	yes	**3**[2]	rpL43A	92	YPR043W	100%	-	L43e	II; III; IV; V		yes
			rpL43B	92	YJR094W-A						
rpP0	yes		rpP0	312	YLR340W	-	L10	P0	II		no
rpP1	no		rpP1A	106	YDL081C	55%	-	P1			no
			rpP1B	106	YDL130W						
rpP2	no		rpP2A	106	YOL039W	50%	-	P2			no
			rpP2B	110	YDR382W						

1 - Steffen et al., 2012
2 - Pöll et al., 2009 (and citations therein)
3 - phenotype of rpL15 not analyzed in detail (long depletion times, not compared to other LSU r-proteins (Li et al., 2009)
4 - no steady state levels of 7S pre-rRNA or 5.8S rRNA shown (Gamalinda et al., 2014), not essential under normal conditions – synthetic lethality with rpL39 (Peisker et al., 2008)
5 - "New" nomenclature as introduced by Yusupov group (Jenner et al., 2012)
6 - the main contact to the LSU rRNA domains were assigned "visually" according to the yeast crystal structure (Ben-Shem et al., 2011)

Since r-proteins are stoichiometrically incorporated in nascent ribosomes (and therefore quickly “titrated away”) the expression shut down of most LSU r-proteins lead to the establishment of the rRNA processing phenotypes already 2-8 hours after shift to the restrictive conditions. Due to the high amount of mature ribosomes (up to 200 000 per cell - Warner, 1999) the yeast cells are able to fulfill a few cell divisions after r-protein expression shut down, though. Careful analysis of steady state levels of the different subsequently produced pre-rRNA intermediates and application of metabolic pulse labeling techniques resulted in the introduction of four different phenotypic classes one of which each analyzed essential LSU r-protein was assigned to (see table1 and Pöll et al., 2009). With the exception of rpL1 and rpL40, depletion of all other tested essential LSU r-proteins resulted in a reduced ratio of 25S over 18S rRNAs indicating that LSU pre-rRNA processing is inhibited or strongly delayed after their depletion. The first, “early” phenotypic class (class 1 in table 1) is characterized by a significantly increased steady state level of 27SA2 over total 27S (27SA2, 27SA3 and $27SB_{l/s}$) pre-rRNA. The second, “intermediate” class (class 2 in table 1) consists of LSU r-proteins after whose depletion $27SB_{l/s}$ pre-rRNA can still be produced but the subsequent processing that results in production of 7S pre-rRNA species is disturbed. The third, “late” class (class 3 in table 1) is characterized by a strong delay of the last maturation events, namely the further processing of 7S/6S pre-rRNAs and/or the export of pre-60S particles to the cytoplasm. The two members of class 4 (rpL1 and rpL40) did not exhibit a significant inhibition of any LSU pre-rRNA processing step.

Note that in many cases also earlier processing events were significantly disturbed, but the classification was based on the last (pre-)rRNA species that could still be produced after expression shut down the respective LSU r-protein. Remarkably, in comparison to wild type cells, the levels of the earliest pre-rRNAs (35S and 32S) were in most cases strongly increased. Also note that the steady state levels of the respectively last produced pre-rRNA intermediate did normally not increase (as one might expect comparing the levels to the one of newly produced the SSU specific 18S rRNA which derives from the same precursor transcript). As described previously (section 2.2.6) this points towards an efficient degradation of these nascent LSUs which lack an essential r-protein, an observation also made after depletion of many essential LSU ribosome biogenesis factors (see 2.2). The systematic analyses of the depletion phenotypes of most LSU r-proteins and the thereof deduced apparent requirement for specific maturation steps (rRNA processing and/or nuclear transport), in principle suggest various molecular functions of LSU r-proteins in terms of ribosome biogenesis which can be compared to the ones of various LSU biogenesis factors. Some LSU r-proteins might have intrinsic endo- or exonucleolytic activity required for one or the other pre-rRNA processing step. Others were shown to be required (directly or indirectly) for the efficient recruitment of ribosome biogenesis factors to the nascent LSUs (see 2.3.2). Some might directly interact with components of the nuclear pore to facilitate the nuclear export. It is also possible that LSU r-proteins are required for two or more subsequently occurring maturation events, latest of which are not detectable due to the inhibition of earlier events.

2.4 Objectives of this work

The recently solved crystal structure of the yeast 80S ribosome was an outstanding milestone in the field that can help to better understand not only ribosome function but also ribosome biogenesis. With the structure, the interaction sites of the numerous r-proteins with rRNA and with each other are known. However, much less is known on how these interactions are established *in vivo*. Detailed structural information on eukaryotic preribosomes is limited to a few late pre-40S or pre-60S particles. The structure of earlier assembly intermediates remains elusive since the purification of a homogenous population among the different subsequently formed pre-mature particles is very challenging. The dynamic interaction of the numerous ribosome biogenesis factors among whom the binding sites for only a few are know (see 2.2.6) and the presence of pre-rRNA spacer sequences (2.2.3) also contribute to the complexity in investigating structures of pre-mature ribosomal subunits. Although the knowledge of the binding sites of the r-proteins in the mature subunits might not fully reflect how these “endpoints” are established in the course of ribosome biogenesis, the final structure is very helpful to understand features like hierarchical interrelationships among r-proteins or the establishment of the different pre-rRNA processing phenotypes.

The yeast *S.cerevisiae* has served as model organism to study numerous eukaryotic intracellular processes. In the field of eukaryotic ribosome biogenesis it was used to shed some light on all major occurring processes: RNA Polymerase I transcription, pre-rRNA modification and processing, transient interaction of numerous ribosome biogenesis factors, assembly of r-proteins, and intracellular transport. In addition, the best resolved structural information on eukaryotic ribosomes comes from yeast 80S ribosomes (see above). The possibility to easily introduce epitope tags to individual proteins or their conditional expression, as well as the short generation time and the easy and cheap handling are additional reasons for the frequent use of yeast as model organism. The relatively small number (and low complexity) of proteins (around 5000) facilitates the use of mass spectrometry methods; almost the entire yeast proteome is well characterized.

In this study, the assembly of the 46 r-proteins of the LSU, whose six rRNA domains are arranged in a sophisticated way with numerous interactions among each other, was aimed to be characterized in terms of several previously fragmentary or unresolved aspects. By comparing the respective amounts of the LSU r-proteins in different pre-60S intermediates to each other and/or to the ones in mature LSUs, the assembly characteristics of each of the 46 LSU r-proteins was addressed applying a combination of affinity purification and quantitative mass spectrometry. In a complementary approach, the interaction of a number of essential LSU r-proteins with the nascent particles was investigated in a comparative way by affinity purification of epitope tagged LSU r-proteins and quantitative analysis of the co-purified (pre-) rRNA species. By a careful combination of the different comparative analyses and the use of biological replicates, a large dataset was created which was subjected to statistical

analyses to monitor the establishment of (stable) interactions of the LSU r-proteins with the nascent LSU in the course of its maturation.

Various conditional r-protein expression mutants were then used to further characterize the requirement of individual LSU r-proteins for certain assembly or maturation events. Although the depletion phenotype of most essential LSU r-proteins had been characterized in terms of pre-rRNA processing (see above), the effect of expression shut down on the assembly of other LSU r-proteins and LSU biogenesis factors was largely unknown. By comparing the protein content of the various mutant pre-60S particles to the one of the respective wild type particles in a quantitative way, the *in vivo* hierarchy of eukaryotic LSU r-protein assembly events was aimed to be characterized. In addition, interrelationships between LSU r-protein assembly and the transient interaction of ribosome biogenesis factors with LSU precursors were addressed by the same means. A comparison of the generated data to previously published data deduced from *in vivo* and *in vitro* analyses (e.g. the prokaryotic *in vitro* assembly maps), will be discussed in more detail.

3 Results

3.1 Introduction to the general approach to analyze r-protein assembly and its methodology

The general workflow followed in this work to analyze and compare the composition of differently maturated (pre-) ribosomal particles starts with their purification *ex-vivo* from total yeast cell extracts. In principle, there are several ways to purify RNPs from whole cell extracts. One general way is trying to make use of specific physical properties as size, shape, density, or electronic charge. By applying established methods as density gradients, affinity columns or size exclusion columns it is possible to isolate specific RNPs. However, in the case of eukaryotic (pre-) ribosomal particles these physical differences are not sufficient to enable the purification of several different particles with a specific maturation state from wild type yeast cells; the purified (precursor) populations would overlap too much and be largely contaminated with mature ribosomal subunits and/or 80S ribosomes which are highly abundant in the cell. Therefore, in this work, the purification occurred via specific epitope tagged proteins that interact with (pre-) ribosomal particles of specific maturation state(s). These epitope tagged fusion proteins were either trans-acting LSU specific biogenesis factors or r-proteins. In the case of the former, the used epitope was Protein A whereas the (in average clearly smaller) r-proteins were fused to the smaller FLAG epitope. A one step purification was performed via IgG coupled to magnetic beads and anti-FLAG coupled sepharose beads, respectively (for details see materials and methods section 5.2.6).

To create the yeast strains expressing the epitope tagged fusion proteins, two different established techniques were applied (see also 5.2.1.4). Either the DNA sequence coding for the epitope was introduced by homologous recombination using a PCR product containing these sequences and being flanked by homologous regions or the respective wild type genes were entirely deleted and the epitope fused copy of the gene was ectopically expressed. In both cases, the epitope fused protein was the only expressed product of the respective gene (no co-expression with a wild type allele). The general criterion to make sure that the introduced epitope does not severely interfere with the function of the respective protein or other cellular processes was, that the cell growth did not (strongly) slow down. For detailed information see materials and methods and the lists of yeast strains (5.1.1), plasmids (5.1.2), and oligonucleotides (5.1.3) used in this work.

As shown in sections 3.2.1 and 3.2.2, the affinity purified RNPs were characterized and compared to each other both in terms of their protein and (pre-) rRNA content. In the following, the methodology used to study the former will be introduced in more detail.

As briefly illustrated in Figure 16, the (pre-) ribosomal particles purified *ex-vivo* from cell extracts of the respective yeast strains were further processed to enable the analysis of their

protein content by semi quantitative mass spectrometry. After an overnight tryptic digest, the proteins were cleaved into defined peptides of smaller size that are more appropriate for being analyzed by mass spectrometry. The here applied method to enable a comparison of the amounts of individual proteins from different samples is based on a covalent linkage of the tryptic peptides with an amine-reactive isobaric reagent. It is called iTRAQ (isobaric tag for relative and absolute quantitation) and was introduced ten years ago (Ross et al., 2004). The different reagents which were used to label the peptides of interest have the same mass (isobaric) and the same chemical structure, but they contain a different combination of isotopes. In general, beside the amine specific reactive leaving group (NHS) they consist of a "reporter group" and a "balance group" which have different individual masses that, in all cases, add up to the same mass (145 Da). In detail, the masses of the reporter groups used in this work are in a range between 114 and 117 Da. They are balanced by a "balance group" ranging between 31 and 28 Da always resulting in a total mass of 145 Da (Figure 16A). When two trypsin digested samples are labeled with different iTRAQ reagents and subsequently mixed with each other, the individual peptides per se cannot be distinguished any more since they carry a tag with the same mass. However, the reporter groups (that do have different masses) can be cleaved off in the tandem mass spectrometry mode (MS/MS procedure) when precursor ions are colliding with gas molecules and thereby further fragmented. By quantifying the intensity of the peaks of the released reporter ions, the individual iTRAQ ratios can be determined (illustrated in Figure 16B-E). Of course the other fragment ions of each peptide created by the collision induced fragmentation in the MS/MS mode are also required to determine sequence information and hence, the identity of each peptide. If several distinct peptides derived from the same protein were identified, their average iTRAQ ratio could be calculated.

Since the different (pre-) ribosomal particles of interest can contain up to 79 r-proteins and numerous (>100) ribosome biogenesis factors, the complexity of the purified RNPs is rather high. Therefore, the resulting tryptic iTRAQ labeled peptides have to be fractionated prior to their analysis by mass spectrometry. The separation occurred by reverse phase nano liquid chromatography (RP-HPLC). Since the mass spectrometry device used in this work was a MALDI-TOF machine (Matrix assisted laser desorption ionization – time of flight), the peptide mix eluting from the HPLC cannot be ionized "online" (as for example by electron spray ionization – ESI) but has previously to be mixed with the used matrix and crystallize on an appropriate sample plate. Using an automated system that mixes the peptides eluting from the column with the matrix and "spotting" it onto the sample plate, it is possible to separate the complex peptide mix into more than 380 fractions. Considering that the MALDI-TOF machine can select and further fragment up to ten fractions per spot, more than 3500 peptides can (in theory) be processed (what can take up to 20 hours).

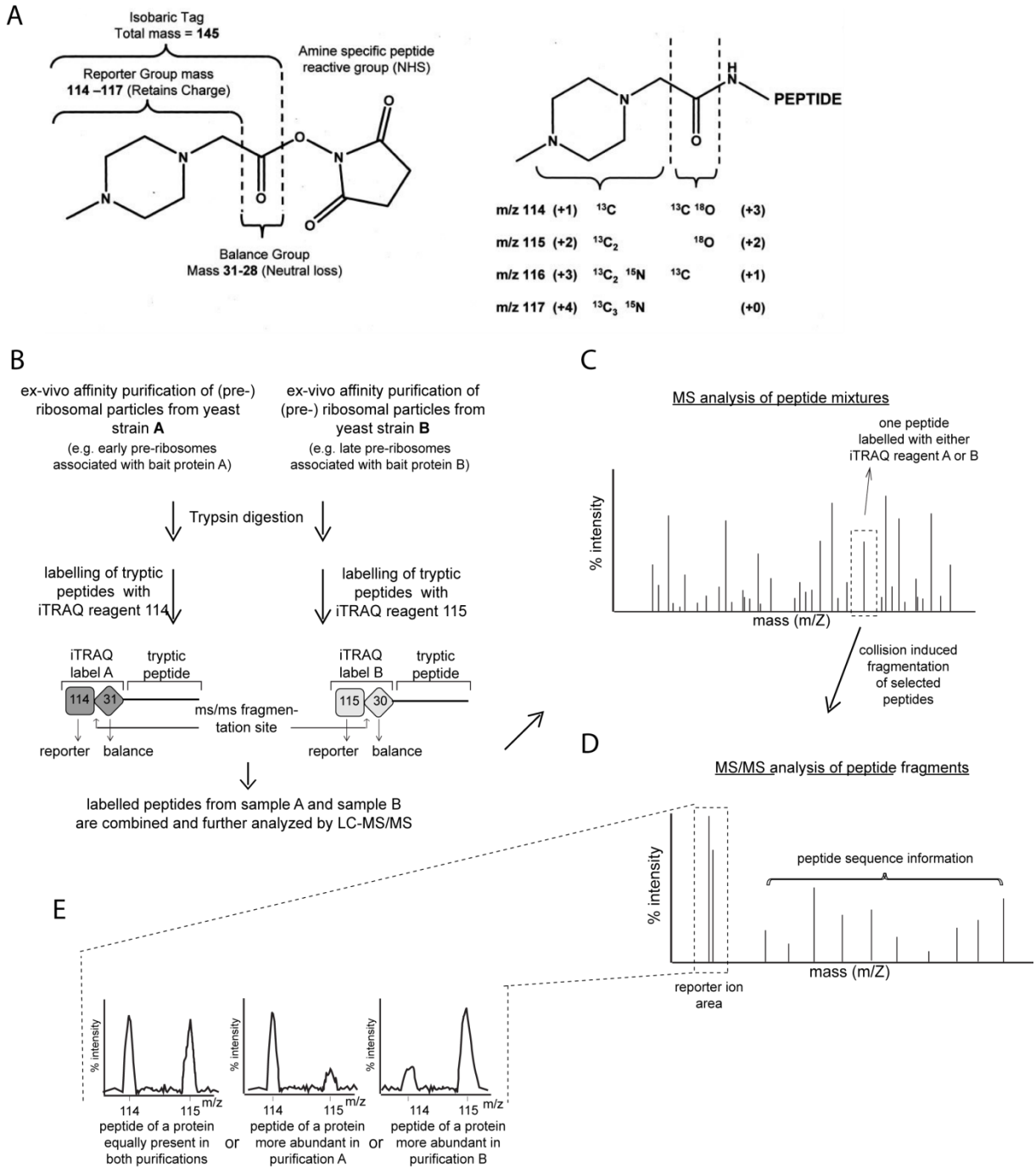

Figure 16 - Illustration of the iTRAQ reagents and the experimental work-flow applied in all analyses using semi quantitative mass spectrometry of this work.

A) The chemical structure of the iTRAQ reagent is illustrated on the left. The covalently linked iTRAQ reagent to primary amino groups of the tryptic peptides (N-termini and ε-amino groups of lysine residues) is illustrated on the right. Adapted from Ross et al (2004). **B)-E)** illustrate the experimental work flow highlighting its most important features. Parts of the Figure were adapted from Ohmayer et al. (2013). See text above and sections 5.2.6, 5.2.7, and 5.2.8 for more experimental details.

To follow and identify changes in the assembly states of LSU r-proteins, the protein content of several affinity purified LSU precursor particles of different maturation states were compared to each other and/or to mature 80S ribosomes using the semi-quantitative mass spectrometry approach described above. The stable association of both, LSU r-proteins and trans-acting ribosome biogenesis factors to the subsequently produced (pre-) ribosomal

particles in the course of their maturation should be detectable by this comparative approach. Considering an LSU r-protein that is incorporated at very late stages in the maturation pathway, it should be underrepresented in all pre-60S particles of earlier maturation stages. As described above (2.2), the exact maturation state of the respective particles purified *ex-vivo* can be determined by analyzing the processing state of the respective (pre-) rRNA species they contain. Therefore, in this work, the (pre-) rRNA content of all purified (pre-) ribosomal particles was routinely analyzed to pinpoint the respective maturation state in more detail. In addition, by also analyzing the respective co-purified amounts of RNA species that should not specifically interact with the purified particle (e.g. tRNAs or the SSU 18S rRNA), statements on the purity could be made. Contamination with mature ribosomal subunits turned out to be critical, especially when comparing the amounts of r-proteins present in differently maturated **pre-**60S particles.

The resulting data of the above described semi quantitative particle comparisons using iTRAQ reagents are ratios of the intensities of the reporter ion peaks of the respective iTRAQ reagents used to label the protein content of purification A versus B (Figure 16). Each single tryptic peptide that can be identified in this procedure yields a certain iTRAQ ratio. In case more than one peptide of a certain protein can be identified, the average iTRAQ ratio of all identified single peptides of this protein can be calculated, increasing the statistical relevance and making the approach more resistant to “outliers”. Biological reproductions of the same pair-wise comparison (e.g. affinity purified particles “A versus B”) and variations of the bait proteins and the resulting possible pair-wise comparisons (e.g. affinity purified particles “A versus C”, or “B versus C” and so on) further increased the resulting amount of raw data (which are average iTRAQ ratios).

After proper processing, normalization, and combination of the average iTRAQ ratios from all single pair wise comparisons to one meta-data set, several statistical analyses can be performed to test the reproducibility and statistical relevance of the approach. The general procedure used in this work to analyze the data with respect of their similarity and the way of their visualization are also illustrated in Figure 17. In general, the first step was always a “log2 transformation” of the average iTRAQ ratios. This was required since otherwise ratios below 1 would be underrepresented in comparison to ratios above 1. The normalization of the “log2 transformed”, average iTRAQ ratios of each pair wise comparison occurred via the median value of the group of identified proteins of interest. In case the same bait protein was used (see section 3.3), the normalization was done via the average iTRAQ ratio of the bait protein. For more details see section 5.2.9. First, the similarity of the data resulting from individual pair wise comparisons in regard to each other was computed by applying hierarchical cluster analyses. The similarity of individual “pair-wise” comparisons was visualized in a self organizing tree (dendrogram) with similar behaving comparisons grouping in the same branch. To compute the similarity in the behavior of the proteins of interest in regard to each other, hierarchical cluster analyses of a similar kind were applied. Again, similar behaving proteins were grouped in the same branch of a dendrogram. The value of

the actual data (=log2 transformed, normalized average iTRAQ ratios of the respective proteins) was visualized in a heat map (illustrated in Figure 17).

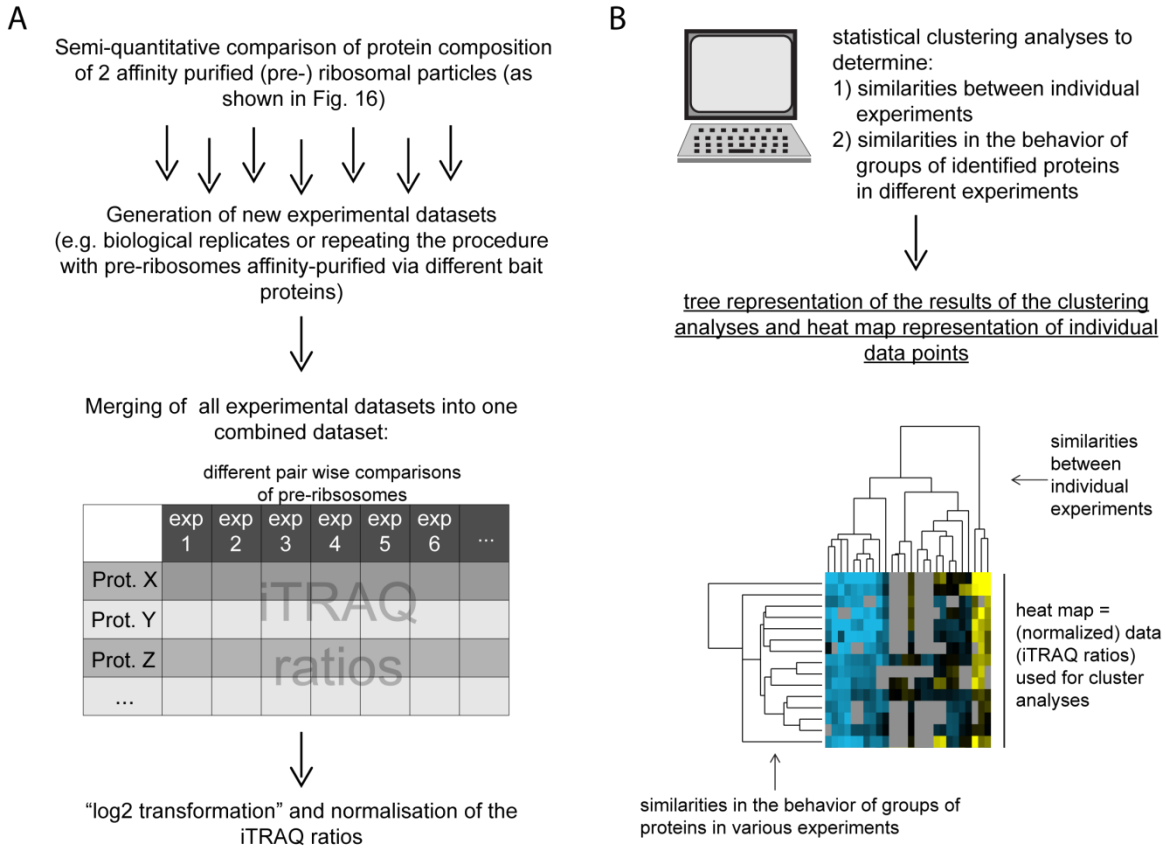

Figure 17 - Schematic presentation of the *in silico* work-flow including data collection, processing, and analyses by hierarchical cluster algorithms.

A) Starting with the results of single pair-wise comparisons, (raw data = unmodified iTRAQ ratios), the iTRAQ ratios of several of such pair-wise comparisons were combined and merged to one meta dataset which was log2 transformed and normalized (see text and section 5.2.9) for more details. **B)** illustrates the features of the hierarchical cluster analyses resulting in the dendrograms and the heat maps. Adapted and modified from Ohmayer et al. (2013).

3.2 Comparative analyses of differently maturated (pre-) 60S particles purified from “growing”, wild type-like yeast cells

3.2.1 Proteomic approach using semi-quantitative mass spectrometry

Mature 80S ribosomes were purified *ex-vivo* via the FLAG tagged SSU component rpS26 which was described to assemble very late in the maturation pathway of the SSU (Ferreira-Cerca et al., 2007; Strunk et al., 2011). Several LSU specific biogenesis factors were used as (C-terminally TAP tagged) bait proteins to purify *ex-vivo* the differently maturated LSU precursor particles. Among them were Noc2, Nog2, Nop53, Rsa4, and Arx1 which were previously described to bind to either earlier, intermediate or late precursor populations (Bassler et al., 2001; Granato et al., 2005; Hierlmeier et al., 2012; Nissan et al., 2002; Saveanu et al., 2001; Ulbrich et al., 2009). To verify the described association behavior of these bait proteins, total RNA was extracted from the cell extracts of the individual yeast strains expressing the TAP tagged LSU biogenesis factors (“Input”) and from the respective affinity purified fractions (“IP”) and analyzed by northern blotting (Figure 18). Note that the pre-rRNA processing pathway is described in section 2.2.3 and summarized in Figure 6. According to the (pre-)rRNA content that was co-purified with the respective bait protein, the purified LSU (precursor) particles could be grouped into “early”, “middle”, “late”, and “mature” classes. “Early” LSU precursor particles (containing slight amount of 35S/32S and higher amounts of 27SA2 pre-rRNAs) were co-purifying with Noc2-TAP, which, consistent with previous publications (Hierlmeier et al., 2012), also co-purified significant amounts of the 27SB pre-rRNA containing “middle” LSU precursors.

As described previously Nog2-TAP, Nop53-TAP, and Rsa4-TAP mainly co-purified LSU precursors of “middle” to “late” maturation stages as marked by 27SB pre-rRNA and large amount of 7S pre-rRNA (Granato et al., 2005; Saveanu et al., 2001). In addition, 25.5S/25S (pre-) rRNAs with levels slightly above background could be detected in these cases.

The populations co-purified via Arx1-TAP represented a late class of (pre-) 60S subunits containing only slight amounts of 27SB pre-rRNA but significant amounts of 7S, 5.8S and 25.5/25S (pre-) rRNAs. Co-purification of the fully processed 5.8S and 25S rRNAs can be either explained by the described association of Arx1 to fully processed nascent LSUs (Bradatsch et al., 2007; Hung et al., 2008; Nissan et al., 2002) or its ability to bind to free mature LSUs (Greber et al., 2012; Merl et al., 2010).

Finally, the rRNA populations co-purifying with rpS26-FLAG contained, as expected, predominantly amounts of mature rRNAs. The 18S rRNA precursors could not be detected confirming the suggested late association of rpS26 to fully processed nascent SSU precursors (Ferreira-Cerca et al., 2007; Strunk et al., 2011). Consequently, significant amounts of mature 80S ribosomes and fully processed or mature free SSUs were co-purifying with rpS26-FLAG.

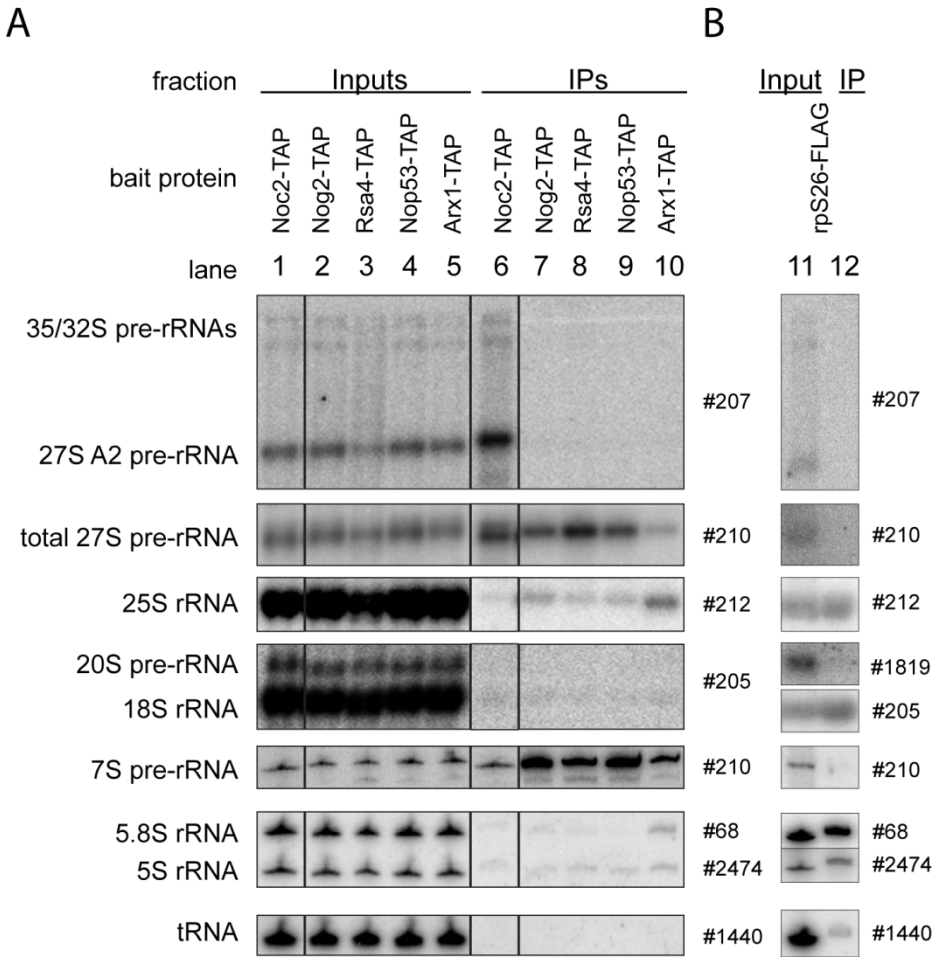

Figure 18 - Analysis of the (pre-) rRNAs contained in various affinity purified LSU (precursor) particles.

Yeast strains Y1878, Y1879, Y2398, Y2404, Y2410 and Y485 expressing the indicated TAP-tag fusion proteins **A**) or carrying a C-terminally FLAG-tagged allele of RPS26 under control of the galactose-inducible GAL1/10 promoter **B**) were cultivated to exponential growth phase in galactose-containing medium (YPG). The tagged proteins were affinity purified from total cellular extracts using rabbit IgG coupled to magnetic beads (**A**) or an anti FLAG M2 matrix **B**) as described in sections 5.2.6. (Pre-) rRNA species from total cellular extracts (Input) and affinity purified fractions (IP) were analyzed by northern blotting using oligonucleotide probes indicated on the right. Equal signal intensities of the Input and bead (IP) fractions indicate 3% **A**) or 6% **B**) co-purification efficiencies of the respective (pre-) rRNA with bait proteins, respectively. Adapted from Ohmayer et al. (2013).

Before looking at the relative amounts of each of the individual LSU r-proteins present in different (pre-) 60S particles co-purified with the above described bait proteins, the focus was set on the behavior of the LSU biogenesis factors present in these RNPs. For most known LSU biogenesis factors, the maturation state of the pre-60S particles they interact with is described in the literature. Therefore, the behavior of most of the LSU biogenesis factors in the comparative approach applied here could be compared to previously published data, what should enable a first evaluation of the specificity and statistical relevance of the approach. As introduced above (Figures 16 - 17 and in section 3.1), the results from in total 26 individual pair-wise particle comparisons were combined to one dataset that was subjected to hierarchical cluster analyses. All known LSU biogenesis factors that could be identified in at least 50% of all pair-wise comparisons were included in these analyses. First, the similarity of each of the 26 individual pair wise comparisons (which had been combined to one meta-dataset) in regard to each other was addressed by applying hierarchical cluster

analyses to this meta-dataset. The results are depicted in Figure 19A. As a general feature of these types of clustering analyses, the similarity (or difference) of the 26 individual datasets is visualized in a dendrogram where similar behaving datasets are grouped in the same branches of the self-organizing tree. Biological and technical replicates of particle comparisons of the same type (lanes 1-10: middle/late particles versus early/middle particles; lanes 11-13 middle/late particles among each other; lanes 14-19: middle/late particles versus 80S ribosomes; lanes 20-23: late versus middle/late particles, lanes 24-26: early/middle particles versus 80S ribosomes) showed highest similarity to each other and clustered in the same branches. These results indicated that most of the observed differences in particle composition were reproducible and statistically relevant.

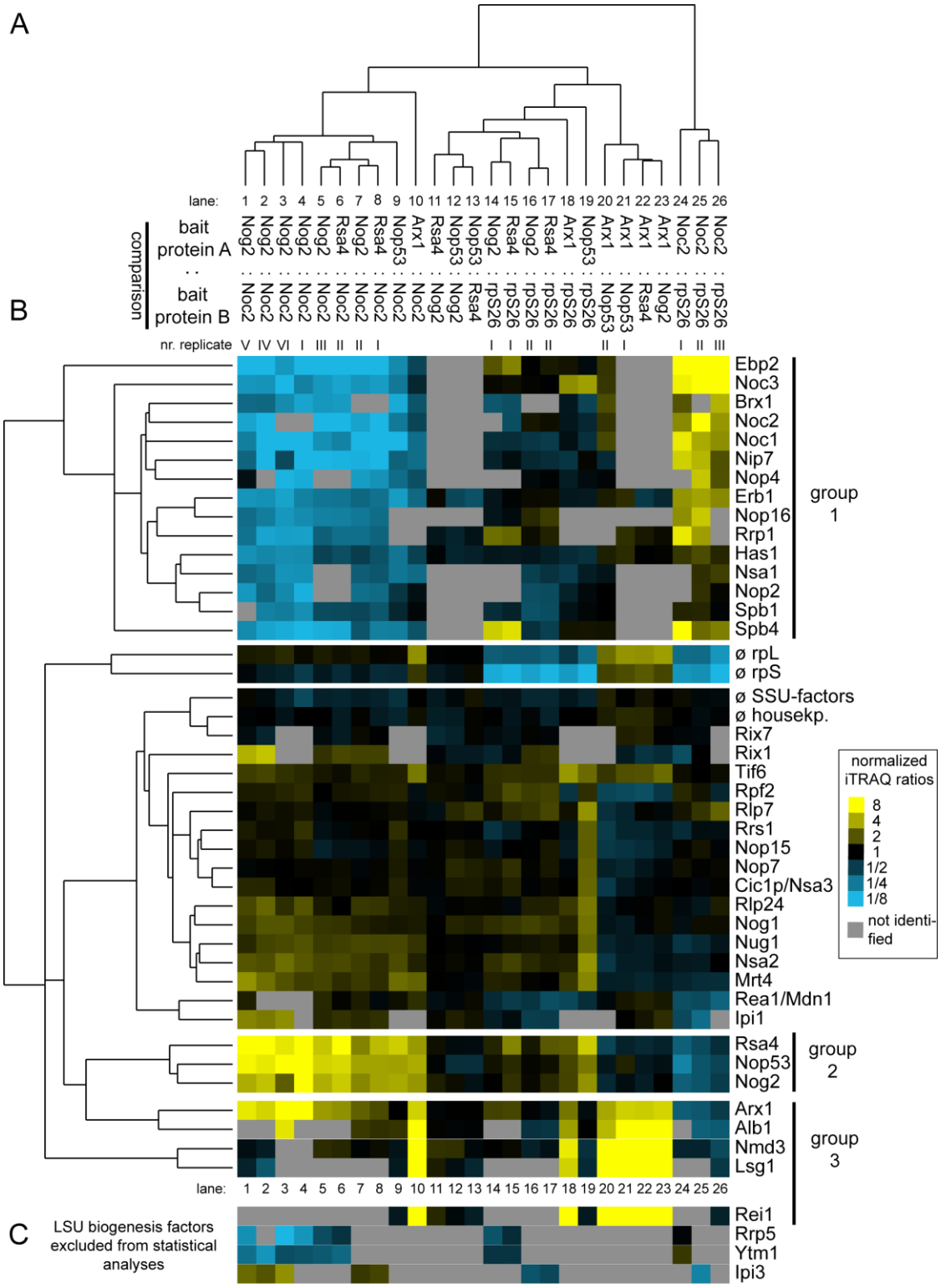

Figure 19 - Comparative analyses of the LSU biogenesis factor content in various affinity purified LSU (precursor) particles by semi-quantitative mass spectrometry.

(Pre-) ribosomal particles were affinity purified *ex-vivo* from total cellular extracts of yeast strains Y485, Y1878, Y1879, Y2398, Y2404, and Y2410 expressing FLAG-tagged rpS26 or TAP tagged ribosome biogenesis factors Nog2, Noc2, Rsa4, Nop53, or Arx1. Proteins present in the affinity purified fractions were compared by semi-quantitative mass spectrometry in the pair-wise combinations indicated in **A**) using iTRAQ reagents as described in the text, Figure 16 and sections 5.2.6, and 5.2.7. The resulting iTRAQ ratios of all LSU biogenesis factors that were identified in more than 50% of all pair wise comparisons were combined to one dataset which also included average ratios of identified housekeeping proteins, SSU biogenesis factors, LSU and SSU r-proteins. This dataset was further analyzed by statistical clustering methods as described in Figure 17 and sections 3.1, 5.2.8, and 5.2.9. In the self-organizing tree shown in **A**), most similar single comparisons are grouped in the same branches.

In the self-organizing tree on the left side of **B**) the similarity in behavior of the identified LSU biogenesis factors is analyzed. The normalized iTRAQ ratios for each of the proteins measured in the respective pair-wise particle comparison are visualized as a heat map in **B**). Blue colors represent a low and yellow colors a high average iTRAQ ratio of the respective protein in each comparison (see color code on the right side). A gray color indicates that the respective protein was not identified in the individual experiment shown in this lane. Groups of proteins clustering in one branch which are discussed in more detail in the results part of the manuscript are labeled by bars on the right. In **C**) the average iTRAQ ratios of a few LSU biogenesis factors are shown which were excluded from the statistical analyses since they were detected in less than 50% of all pair-wise comparisons. Adapted from Ohmayer et al. (2013).

Next, the similarity of the identified LSU biogenesis factors was computed by similar hierarchical clustering analyses, but now focusing on the behavior of (normalized) average iTRAQ ratios of each LSU biogenesis factor included in the 26 pair wise comparisons. Again, the similarity of the LSU biogenesis factors was visualized in a dendrogram in which similar behaving biogenesis factors were grouped in the same branch (see Figure 19B). The individual ("log2-transformed" and normalized) average iTRAQ ratio of each LSU biogenesis factor in the respective pair-wise comparison was depicted in a heat map (Figure 19B). A black color indicates that the respective protein was equally present in each of the two purifications that were compared to each other whereas yellow and blue colors indicate that the individual protein was more or less abundant in either of the two purified particles (see color code in Figure 19B). In case a LSU biogenesis factor could not be identified in individual pair wise comparisons the respective square was colored in gray. Several groups of LSU biogenesis factors were showing a similar behavior within the 26 pair wise comparisons and were therefore put in the same branches. One group (group 1) was specifically enriched in pre-60S particles which were purified by Noc2-TAP (Figure 19B, lanes 1-10, and 24-26). Besides Noc2, this group consisted of factors as Noc1, Erb1, Has1, Ebp2, Brx1, or Spb1 and others for most of which previous studies clearly indicated an association with early pre-60S particles (Dembowski et al., 2013a; Hierlmeier et al., 2012; Miles et al., 2005; Shimoji et al., 2012 and citations therein). Interestingly, Noc3 which was described to form a mainly nucleoplasmic complex with Noc2 which associates to 66S pre-ribosomal particles (Milkereit et al., 2001) was also put in this group 1.

A group of three LSU biogenesis factors (Figure 19B, group 2) was put in one branch in these hierarchical clustering analyses and consisted of Nog2, Nop53, and Rsa4. The comparative analyses showed that each of these proteins was underrepresented in early pre-60S particles purified by Noc2-TAP indicating that they are bound to a later population of preribosomes from which Noc2 had already dissociated (Figure 19B, lanes 1-10). Analysis of the (pre-) rRNAs each of these three proteins co-purified (Figure 18A, lanes 7-9) and the results of former studies confirmed their association to a later maturated population of pre-60S particles. These studies also showed that their depletion resulted in a delay in nuclear processing of 27SB and 7S pre-rRNAs (de la Cruz et al., 2005; Granato et al., 2005; Saveanu et al., 2001; Sydorskyy et al., 2005; Thomson and Tollervey, 2005). Direct comparison of the pre-ribosomes associated with Nog2-TAP, Nop53-TAP, and Rsa4-TAP indicated that their (pre-)rRNA- (Figure 18A, lanes 7-9) and protein composition (Figure 19B, lanes 11-13) was highly similar and clearly differed from the ones associated with Noc2-TAP (see above).

A third group of LSU biogenesis factors arose from the hierarchical clustering analyses whose members were enriched in (pre-) ribosomal particles purified by Arx1-TAP (group 3 in Figure 19B, lanes 10,18, and 20-23). Besides Arx1 itself, it consisted of Alb1, Lsg1, Nmd3, and (if identified) Rei1 (Figure 19C). All of these proteins were described to be involved in late (cytoplasmic) maturation events and/or the nuclear-cytoplasmic translocation of late LSU precursors (Bradatsch et al., 2007; Gadal et al., 2001; Hedges et al., 2005; Ho et al., 2000; Hung et al., 2008; Lebreton et al., 2006a; Meyer et al., 2010).

As depicted in Figure 19C, several (selected) LSU biogenesis factors were not identified often enough to fulfill the criteria of the hierarchical cluster analyses (≥ 50% of all 26 analyses). When identified however, several members behaved as expected from previous studies. The heat map pattern of Rrp5 and Ytm1 for instance was, as expected, highly comparable to the one of the members of the “early” group1 (Hierlmeier et al., 2012; Miles et al., 2005). Finally, the groups of LSU- and SSU r-proteins, whose average iTRAQ ratios were also included in the statistical analyses, were clustered in a clearly separated branch. As expected, they were more abundant than all identified LSU biogenesis factors in all particles purified by rpS26-FLAG (Figure 19B, lanes 14-19 and 24-26).

In summary, these results were in good agreement with what was expected considering the maturation state of (pre-) ribosomal particles the chosen bait proteins were previously described to interact with. This systematic comparative approach therefore proved to be a robust tool to analyze the composition of LSU biogenesis factors of different affinity purified RNPs and was, as shown in the following, also applied to study the behavior of the 46 yeast LSU r-proteins.

In order to analyze the composition of the differently maturated pre-60S particles in terms of their LSU r-proteins, the average iTRAQ ratios of all identified LSU r-proteins from the same 26 pair-wise particle comparisons were combined to one large meta-dataset that was subjected to the same hierarchical clustering analyses applied to study the behavior of LSU biogenesis factors (as described above and depicted in Figure 19). Again, a hierarchical clustering analysis of the 26 datasets derived from the individual pair wise comparisons analyzing the similarity (or difference) in regard to each other showed that comparisons of the same type were grouped together in the same branches and therefore showed the highest similarity among each other (Figure 20A). This indicated that the differences in the relative amounts of the individual LSU r-proteins in the individual pair wise comparisons were reproducible and statistical relevant even if the arising clusters were not always as distinct as in the case of the LSU biogenesis factors (compare the general tree in Figures 19A to the one in Figure 20A). The weak, but detectable amounts of contaminating 80S ribosomes present in the different affinity purifications of the chosen TAP tagged LSU biogenesis factors (see faint 25S and 18S rRNA signals in Figure 18A) could (at least in part) explain the lower statistical significance of these results.

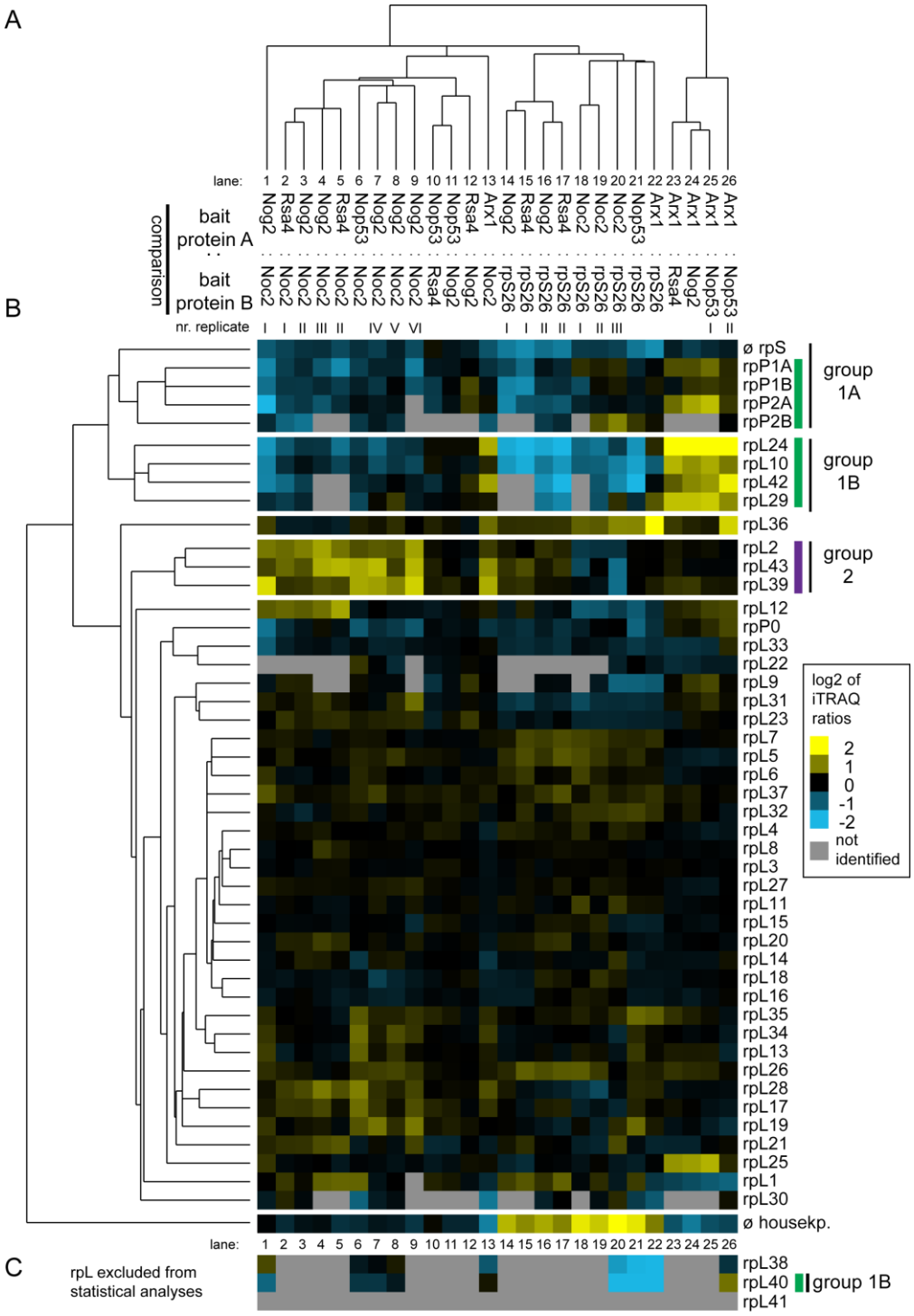

Figure 20 - Comparative analyses of the LSU r-protein content in various affinity purified LSU (precursor) particles by semi-quantitative mass spectrometry.

The experimental dataset generated as described in Figure 19 was analyzed in regard to iTRAQ ratios of all LSU r-proteins that were identified in more than 50% of all pair wise comparisons. This dataset was further analyzed by statistical clustering methods as described above. **A**) shows again a self-organizing tree with most similar single comparisons grouped in the same branches. Accordingly, the similarity in behavior of individual identified LSU r-proteins is shown on the left side of **B**). The normalized iTRAQ ratios for each protein measured in the respective pair wise particle comparison are visualized as a heat map in **B**). Blue colors represent a low and yellow colors a high average iTRAQ of each protein in the respective comparison (see color code on the right side). A gray color indicates that the respective protein was not identified in the individual experiment shown in this lane. Groups of proteins clustering in one branch which are discussed in more detail in (see text below) are labeled and highlighted with green and purple colors on the right in **B**). **C**) shows average iTRAQ ratios of the remaining LSU r-proteins that were excluded from the statistical analyses since they were detected in less than 50% of all pair wise comparisons. Adapted from Ohmayer et al. (2013).

With the exception of the LSU r-proteins rpL38, rpL40, and rpL41 all of the remaining 43 LSU r-proteins could be identified in at least 50% of the 26 pair-wise comparisons and were therefore included in the hierarchical cluster analyses (Figure 20B). Note that, in case two alleles are coding for a LSU r-protein, the average value of the respective iTRAQ ratios of both paralogues (if identified) was calculated due to the in general high sequence similarity of the respective paralogues (in most cases 98% or more sequence identity between rpLX A vs. rpLX B – see table 1). The only exceptions were the phospho-stalk proteins rpP1A/B and rpP2A/B whose paralogues have 50% and 55% sequence identity, respectively. Most of the identified peptides of rpP1A/B and rpP2A/B could therefore be clearly assigned to either of the two paralogues whereas for most of the peptides derived from all other LSU r-proteins this was not possible. The detection of a potential (albeit unlikely) different assembly behavior of a pair of two paralogues of a specific LSU r-protein was therefore (with the exception of rpP1A/B and rpP2A/B) not possible.

Besides the 43 regularly identified LSU r-proteins, the average iTRAQ ratios of all identified peptides derived from housekeeping proteins as well as those derived from SSU r-proteins were also included in the analyses. The housekeeping proteins, defined here as “background” proteins present to some extent in the affinity purified fractions, showed less similarity in regard to all LSU r-proteins and were therefore clustered in a clearly separated branch (Figure 20B), indicating that all identified LSU r-proteins behaved different than “background” proteins.

The analyses showed that the members of one group of LSU r-proteins (group 1A/B in Figure 20B) were enriched in mature 80S and late (pre-) ribosomes purified by rpS26-FLAG and Arx1-TAP, respectively. This behavior indicates that the stable incorporation of the respective LSU r-proteins into LSU precursors occurs at very late stages in LSU maturation. This first group consisted of rpP1A, rpP1B, rpP2A, and rpP2B (group 1A), as well as of rpL10, rpL24, rpL29, and rpL42 (group 1B). RpL40, which was in general hardly detectable due to its small size (52 amino acids long) and therefore excluded from the hierarchical cluster analyses, also showed, if identified, a comparable behavior as the members of group 1B (Figure 20C, lanes 20-22, and 26). Underrepresentation of the phospho-stalk proteins rpP0 and rpL12 in (early) LSU precursors was detectable in several of the pair wise comparisons, but was not as clear and statistical relevant as it was for the other members of this group (Figures 20B, lanes 13-26). Remarkably, four of the seven members of this “late” group (namely rpL24A/B, rpL29, rpP1A/B, and rpP2A/B) are encoded by non-essential genes (or pairs of genes) indicating a correlation between their specific late assembly and no essential role for LSU maturation and function in yeast (Baronas-Lowell and Warner, 1990; DeLabre et al., 2002; Remacha et al., 1995; Steffen et al., 2012). Two of the three essential members of this late group, rpL10 and rpL40, were previously shown to be not strictly required for any of the LSU pre-rRNA processing steps but for late, cytoplasmic maturation events enabling an efficient production of functional mature LSUs (Fernandez-Pevida et al., 2012; Pöll et al., 2009; West et al., 2005).

The pattern of rpL36 within the 26 pair-wise comparisons differed from the one of the other LSU r-proteins suggesting an “unusual” assembly behavior. Looking at the values of the (normalized) iTRAQ ratios of rpL36 however shows that the values were rather inconsistent, even within comparisons of the same type (see for example Arx1-TAP vs. Nop53-TAP comparisons in lanes 25 and 26 in Figure 20B). Therefore, no clear statement could be made for rpL36.

A second group consisting of the three LSU r-proteins rpL2, rpL39, and rpL43 was arising from the hierarchical cluster analyses (group 2 in Figure 20B). The members of this group differed from the rest by a specific underrepresentation in all “early” LSU precursors purified by Noc2-TAP in comparison to later (pre-) ribosomes (Figure 20B lanes 1-9, 13, and 18-20). The “early” LSU precursor populations that co-purified with Noc2-TAP contained only low amounts of the 7S pre-rRNA, which was present to much larger extents in the “later” LSU (precursors) purified by the other chosen LSU biogenesis factors Nog2, Nop53, Rsa4, and Arx1. Since the members of this group 2 were characterized by being underrepresented in the (small) 7S pre-rRNA-containing precursor populations purified by Noc2-TAP, the stabilized association of these three LSU r-proteins into nascent LSUs might coincide with the synthesis of the 7S pre-rRNA by cleavage in the ITS2 of 27SB pre-rRNA (see pre-rRNA processing scheme in Figure 6). Interestingly, depletion of the two essential members of this group, rpL2 and rpL43, resulted in a strong delay of 7S pre-rRNA processing (Pöll et al., 2009).

Finally, the remaining LSU r-proteins were grouped into one large branch which is subdivided into several smaller branches. However, the differences within these sub-branches seemed to be not highly significant and the heat-map pattern of most of the members tended to be less reproducible in pair-wise comparisons of the same kind. A group of LSU r-proteins seemed to be more underrepresented in “early”, Noc2-TAP purified LSU precursors than the other members of this large group indicating an above average stabilization of these proteins to LSU precursors from which Noc2 had dissociated, like it was observed for the members of group 2. This behavior was, however, not as strong and as reproducible as it was for the group 2 members (rpL2, rpL43, rpL39). Among them were for example rpL28 and rpL17 (Figure 20B, lanes 1-9) and, less consistent, rpL34, rpL35, rpL13, rpL19, and rpL26 (Figure 20B, lanes 6-9) or rpL21 (Figure 20B, lanes 1-5). Whether or to what extent these differences reflect above-average increases in affinities of these LSU r-proteins to LSU precursors (in this case before and after the processing of 27SB pre-rRNA) remains less clear with the data obtained with this approach (see discussion part for more details).

3.2.2 LSU r-protein association to LSU precursors addressed by affinity purification of tagged rpL and analysis of co-purified rRNA (precursors)

A different, complementary approach to study (and to confirm) the assembly behavior of certain LSU r-proteins observed in the comparative particle comparisons using semi quantitative mass spectrometry (see above in 3.2.1) will be described in the following.

Several essential LSU r-proteins were affinity purified *ex-vivo* from cell extracts and the co-purifying (pre-) rRNA content was isolated and subsequently analyzed in a comparative and quantitative way. Considering a specific LSU r-protein that is stably incorporated at late stages during LSU maturation, it could be expected to co-purify fewer amounts of early pre-rRNA species than other LSU r-proteins which are associating already to pre-60S particles of early maturation stages. The purification of the chosen candidates occurred via the FLAG epitope which was fused to the respective protein either N- or C-terminally. To ensure that the respective epitope tagged LSU r-protein is incorporated into (functional) LSUs *in vivo*, several criteria, that had to be fulfilled, were defined. First, the FLAG tagged variants of the selected r-proteins had to complement the lethal deletion(s) of the gene(s) coding for the respective r-proteins. To ensure this, only essential LSU r-proteins were chosen. Second, the FLAG-epitope fused r-protein had to be the only expressed variant of the respective r-protein and third, the growth of the particular yeast strains, as measured by the generation time, should be in the range of an untagged wild type strain. To this end, yeast strains were created each of which ectopically express a FLAG tagged version of one essential LSU r-protein (see 5.1.1 for more details including the observed generation time of the respective yeast strains). Cellular extracts of these yeast strains were used for affinity purifications using an anti-FLAG affinity matrix (in more detail described in 5.2.6.2). In addition, each of the in total 18 different affinity purifications were biologically reproduced using a buffer that contained different amounts of Potassium Chloride (in concentrations of 200 and 300 mM, respectively). As control to monitor the unspecific binding of LSU (precursors) to the anti FLAG affinity matrix, an untagged wild type yeast strain was included in the analyses. Out of the 16 chosen LSU r-proteins, FLAG tagged rpL10 and rpL40 belonged to the “late” group identified in the comparative proteomic studies described above (Figure 20B, group 1). RpL40 is expressed as a chimeric protein composed of rpL40 and a ubiquitin moiety. Two yeast strains were created that express either N-terminally FLAG tagged ubiquitin together with rpL40 or N-terminally FLAG tagged rpL40 without the ubiquitin moiety (which is cleaved off and not found in mature LSUs - Ben-Shem et al., 2011). RpL2 and rpL43, which were the two essential members of the group of LSU r-proteins, whose affinity to pre-60S particles seemed to increase concomitant with cleavage in the ITS2 (Figure 20B – group 2), were also included in these analyses.

The co-purified (pre-) rRNAs were isolated and analyzed by Northern blotting in a quantitative way. In order to determine the relative efficiencies of individual (pre-) rRNAs co-purifying with the respective r-proteins, the signal intensities of the affinity purified fractions were compared to the ones of a total cellular extract derived from a wild type strain (Figure 21, right “IP” panels). In addition, (pre-) rRNAs isolated from cellular extracts of each of the analyzed yeast strains were detected by Northern blotting to monitor whether the amounts and the relative distributions of the (pre-) rRNAs in the respective yeast trains were in the same range (Figure 21, left “Input” panels). Despite some variations, the levels of most of the analyzed (pre-) rRNAs in the “Input” (cellular extract) fractions were in a comparable range why a comparison of the signals of the different “IP” (=affinity purified) fractions to only one “Input” fraction (namely the one of a wild type yeast strain) was evaluated as reasonable and

justifiable (for technical reasons it was not possible to load both, “Input” and “IP” fractions of all analyzed yeast strains onto one gel).

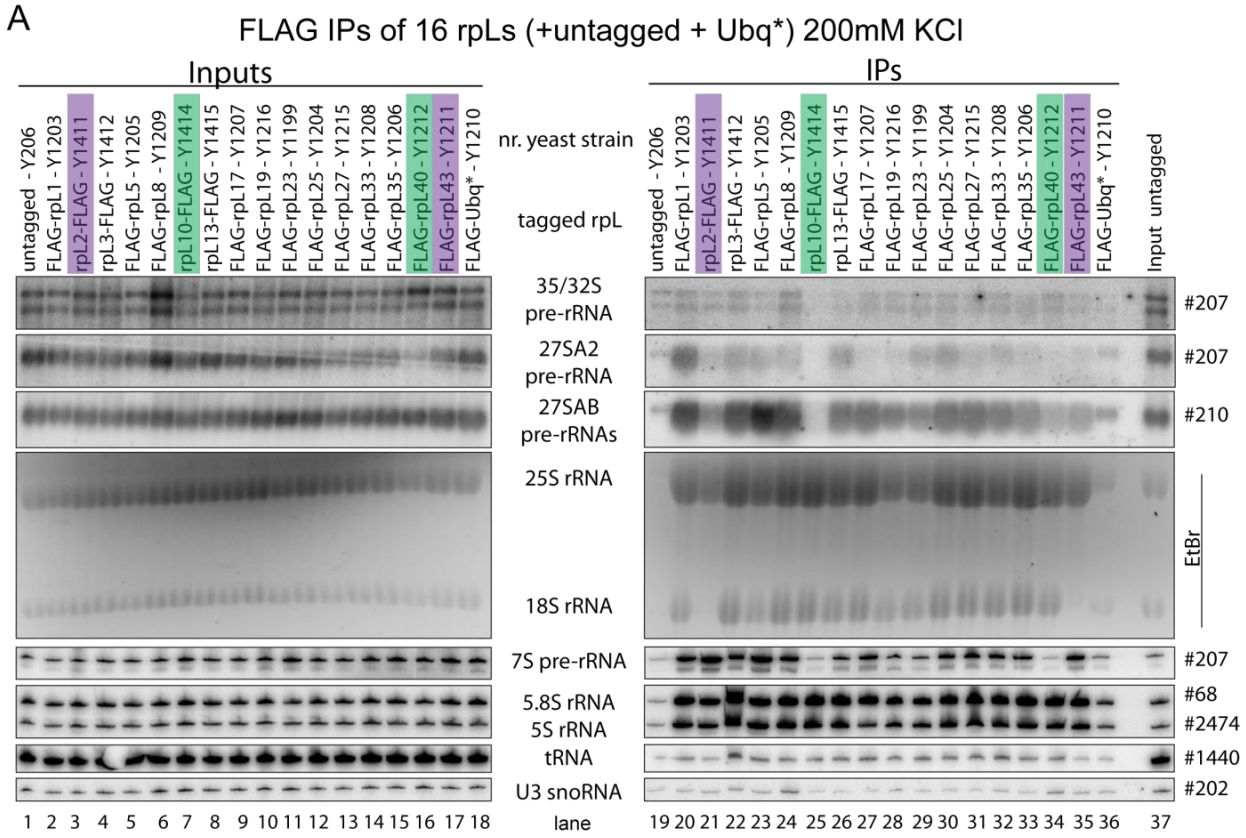

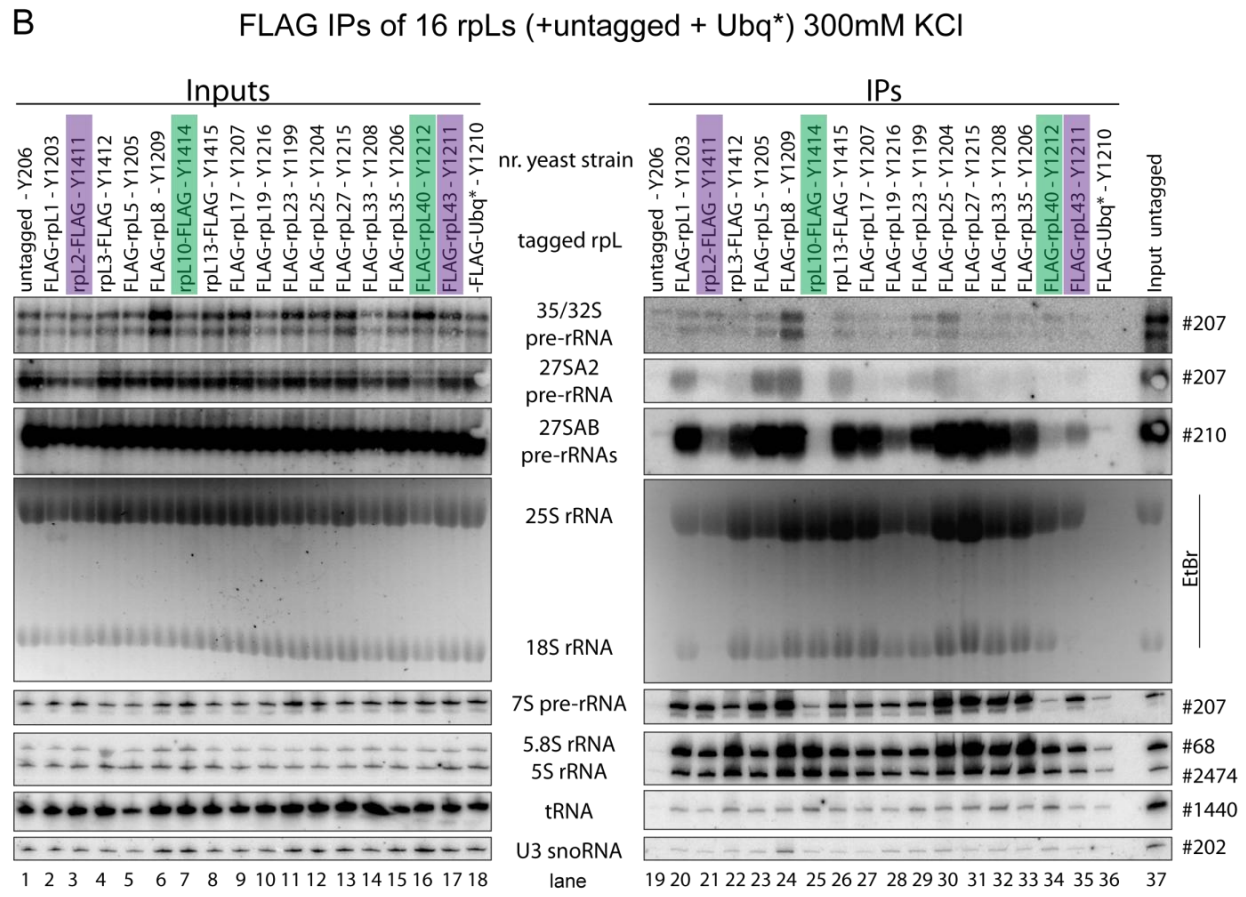

Figure 21 (previous page) - Analyses of (pre-) rRNAs co-purifying with selected FLAG tagged LSU r-proteins.

Cellular extracts of 16 yeast strains each of which ectopically expressing a FLAG tagged version of a LSU r-protein complementing the corresponding lethal gene deletion(s) were subjected to affinity purification using an anti-FLAG matrix as described in 5.2.6.2. An untagged wild type yeast strain and a yeast strain expressing a FLAG-tagged version of the Ubiquitin moiety of the Ubiquitin-rpL40A fusion protein ("FLAG-Ubq*") were included in the analyses. The (pre-) rRNA content of the total cellular extracts ("Input" lanes 1-18) or of parts of the affinity purified fractions ("IP" lanes 19-36) were analyzed by Northern Blotting using the indicated probes. A fraction of the cellular extract from an untagged yeast strain (lane 37) was used as reference to enable quantification of the relative amounts of the co-purified (pre-) rRNAs. The procedure was performed using two different concentrations of potassium chloride. The lysis buffers of the affinity purifications shown in **A)** and **B)** contained 200mM and 300mM potassium chloride, respectively. Equal signal intensities of the reference wild type Input and each IP fraction correspond to 1% co-purification efficiencies. The generation time of each yeast strain in YPD was determined as described in 5.2.1.5 and is listed in the table of the yeast strains shown in section 5.1.1. Adapted from Ohmayer et al. (2013).

To get an overview on the general assembly behavior of LSU r-proteins, the average co-purification efficiencies of the subsequently produced LSU rRNA precursors with the (in this approach tested) LSU r-proteins was calculated. In average, the in total 16 FLAG-tagged LSU r-proteins (the untagged wild type control and the Ubiquitin-tagged yeast strains were excluded here) co-purified the earliest precursor rRNAs (35S & 32S pre-rRNAs) to comparably weak extent at levels slightly above background while further processed pre-rRNAs were observed to be co-purified more efficiently (see Figure 21A&B and quantitation in Figure 22A). According to these observations, most of the tested LSU r-proteins seem to establish weak interactions with pre-ribosomes already at early stages which are stabilized with ongoing maturation of the LSU precursors, as measured by higher co-purification efficiencies. In line with this, the interaction of the tested LSU r-proteins to early pre-rRNAs could in average be more easily disrupted by higher salt concentrations (300mM vs. 200mM potassium chloride) than interaction with further maturated (pre-) rRNA species (see "IP" panels in Figures 21A&B and compare light gray to dark gray bars in Figure 22A).

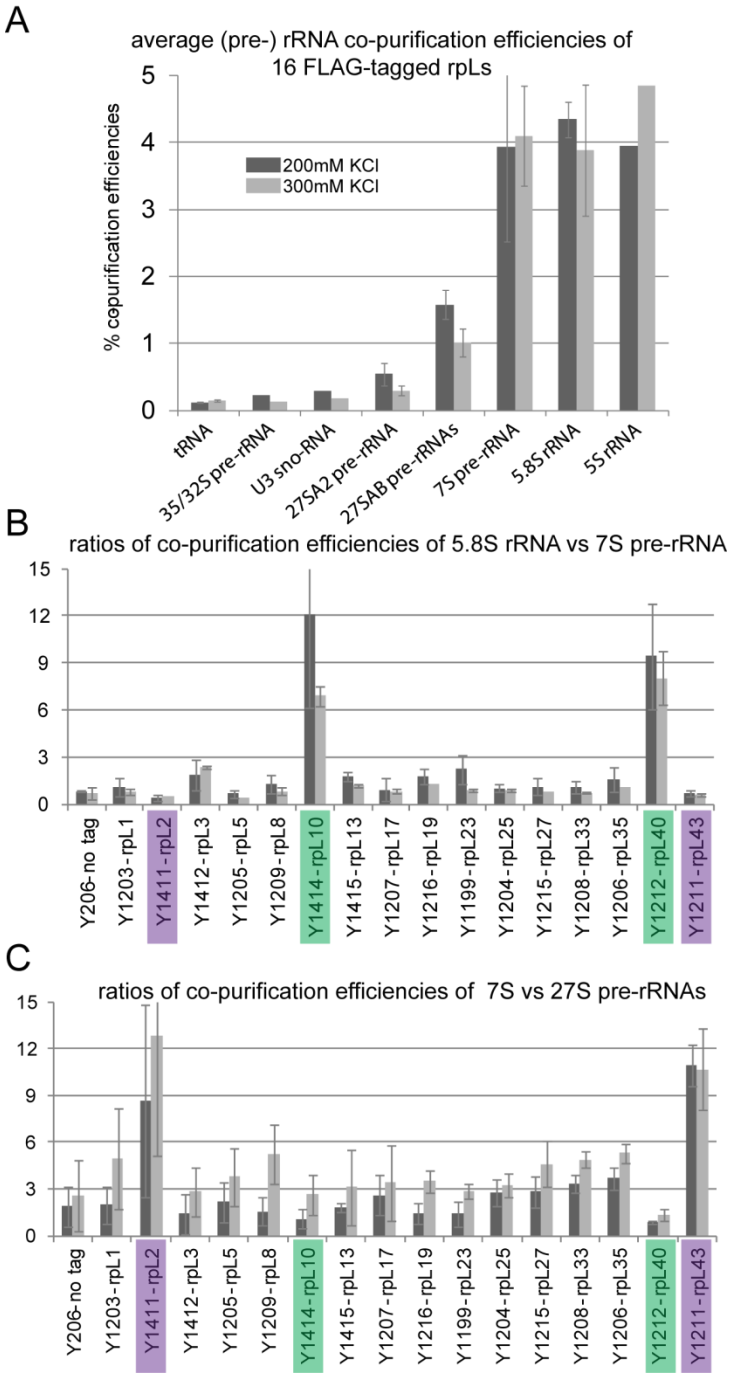

Figure 22 - Association of selected tagged LSU r-proteins with LSU precursor particles of different maturation states as indicated by co-purification of LSU (pre-) rRNAs.

Total cellular extracts of 16 yeast strains were prepared (indicated in **B)** and **C)**) each of which ectopically expressing a FLAG-tagged version of a LSU r-protein complementing the corresponding lethal gene deletion(s). Tagged proteins were affinity purified on a FLAG affinity matrix as described in section 5.2.6.2. (Pre-) rRNA species contained in cellular extracts (input fractions) and the corresponding purified fractions were analyzed by northern blotting (Figure 21A-B). In **A)** the average co-purification efficiencies of the indicated RNAs with the group of analyzed LSU r-proteins were determined by relating the respective signal intensities detected in purified fractions to the ones detected in the extract of a reference yeast strain. The quantifications shown in **A)** are derived from two reproduced northern blots of the same 16 affinity purifications for each concentration of potassium chloride (one of which is shown in Figure 21A-B). They exclude the untagged wild type (Figure 21A-B, lane 19) and the FLAG-Ubq* (Figure 21A-B, lane 36) strains. In **B)** is shown the ratio of the efficiency of 5.8S rRNA versus 7S pre-rRNA co-purification for each analyzed LSU r-protein. The ratios of the efficiencies of 7S pre-rRNA versus the 27S pre-rRNA co-purification are shown in **C)** for each analyzed LSU r-protein. Values obtained when purifications were performed using buffers containing 200 mM or 300 mM potassium chloride are represented as dark gray or light gray bars, respectively, in **A)** to **C)**. Adapted from Ohmayer et al. (2013).

These observations indicate that in average, the tested LSU r-proteins assemble with (pre-) ribosomes in a progressive way during their maturation. Early, in average weak interactions are stabilized in a multi-step fashion. Three of the 16 LSU r-proteins were previously analyzed in a comparable way as HA-, TAP-, or eGFP epitope tagged fusion proteins. In general, the results obtained in these studies were in agreement with the progressive assembly interpretation made here. Besides these three examples using HA-tagged rpL5 (Zhang et al., 2007), TAP-tagged rpL8 (Jakovljevic et al., 2012), and eGFP-tagged rpL35 (Babiano and de la Cruz, 2010), several other tested LSU r-proteins gave comparable results, even if in these studies the co-purification efficiencies were (if at all) only determined for a subset of rRNA (precursor) molecules. They include eGFP-tagged rpL17 and rpL37 (Gamalinda et al., 2013), HA-tagged rpL11 (Zhang et al., 2007), TAP-tagged rpL7 (Jakovljevic et al., 2012), and eGFP-tagged rpL26 (Babiano et al., 2012).

To address the specific assembly behavior of the two groups of LSU r-proteins observed in the proteomic approaches (see above), the efficiencies of the individual (pre-) rRNAs co-purifying with LSU r-proteins were analyzed in more detail and compared to each other (Figure 22B-C). Significant differences among the tested LSU r-proteins were observed when directly comparing the individual co-purification efficiencies of the 5.8S rRNA to its latest well detectable precursor, the 7S pre-rRNA. As shown in Figure 22B, rpL10 and rpL40 (the two members of the “late” group 1 in Figure 20B) showed the highest ratio of 5.8S rRNA versus 7S pre-rRNA co-purification efficiency among all tested r-proteins (see also “raw data” in Figure 21A&B, compare 5.8S rRNA to 7S pre-rRNA signals in “IP” panels). These observations were in agreement with the proteomic data and also argue for a stable association of these LSU r-proteins at very late stages in LSU maturation, namely after 7S pre-rRNA processing. Both, rpL10 and rpL40 were tested in a similar approach in previous studies in which comparable observations were made, even if the used epitope was different (TAP tag and HA tag, respectively versus FLAG tag used here) and no quantifications were shown (Fernandez-Pevida et al., 2012; Saveanu et al., 2001).

Focusing on one step “earlier” in the pre-rRNA processing pathway, namely the conversion of the 27SB pre-rRNA into the 7S (and 25.5S) pre-rRNAs by comparing the efficiencies of their co-purifcation to each of the tested tagged LSU r-proteins, gave the following results. RpL2 and rpL43 (both members of “group 2” in Figure 20B) were co-purifying the 7S pre-rRNA significantly better than the 27SB pre-rRNA. Even if a more efficient co-purification of the 7SB pre-rRNA (compared to the 27SB pre-rRNA) was observed for all of the tested LSU r-proteins, this effect was for none of them as strong as for rpL2 and rpL43 (see 3-4 fold higher 7S/27SB pre-rRNA ratios for rpL2 and rpL43 in Figure 22C). In agreement with the proteomic data, these observations argue for an above-average increased affinity of the members of this group 2 to LSU precursors after conversion of the 27SB pre-rRNA into the 7S and 25.5S pre-rRNAs (which occurs by an endonucleolytic cleavage in the ITS2 in the nucleus). However, both, tagged rpL2 and rpL43 were co-purifying earlier pre-rRNA intermediates as the 27SA2 or 35/32S pre-rRNAs to low, but above-background levels, indicating that some interactions to nascent LSUs are established already at earlier stages,

although they seem to be rather weak (Figure 21A, compare 35S/32S pre-rRNA signals of FLAG tagged rpL2 and rpL43 in the “IP” lane to the ones of the other r-proteins).

3.3 Analyses of pre-ribosomes after *in vivo* expression shut down of selected LSU r-proteins

3.3.1 Objectives and introduction to the approach

As introduced in section 2.3.3 and summarized in table 1, most essential LSU r-proteins are required for certain pre-rRNA processing events *in vivo*. According to their pre-rRNA processing phenotype, they can be categorized into four distinct classes (Figure 23, see also (Pöll et al., 2009). The first, “early” of these classes (class 1) is characterized by a strong delay in the formation of the 5’ end of the 5.8S rRNA sequences which occurs by successive processing of ITS1 sequences from 27SA2 and 27SA3 pre-rRNAs. The LSU r-proteins that were shown to exhibit this phenotype (rpL3, rpL4, rpL6, rpL7, rpL8, rpL15, rpL16, rpL18, rpL20, rpL32, and rpL33 (Gamalinda et al., 2014; Li et al., 2009; Pöll et al., 2009) are mainly bound to LSU rRNA domains I and II (Ben-Shem et al., 2011) (Figure 23). Please note that in this work, if not otherwise stated, the description of binding sites of LSU r-proteins (in the mature LSU) is based on the crystal structure of the yeast 80S ribosome which was published by the Yusupov group in 2011 (Ben-Shem et al., 2011) using the established nomenclature of the *Saccharomyces* genome database (SGD: http://www.yeastgenome.org/) and not the one suggested by the Yusupov group (Jenner et al., 2012). Both nomenclatures are summarized in table 1.

LSU r-proteins whose depletion results in a significant delay in ITS2 processing (at site C2) were assigned to the second, “middle” class (class 2). Among them are rpL9, rpL19, rpL23, rpL25, rpL27 rpL34, rpL35 (Pöll et al., 2009), rpL37 (Gamalinda et al., 2013), and (presumably) rpL31 (Gamalinda et al., 2014). In mature LSUs, most of them are bound in proximity to each other and they mainly establish contacts to LSU rRNA domains I (including 5.8S rRNA), III, and IV. RpL9 and rpL23 are located more distant of the others mainly contacting domains V and VI (rpL9), or domains IV, V, and VI (rpL23) (see Figure 23).

After *In vivo* expression shut down of members of the third, “late” class (class 3), 27SB pre-rRNAs can still be processed but the further processing of the resulting 7S pre-rRNA and/or nuclear export of pre-60S particles is disturbed. Among them are rpL2, rpL5, rpL10, rpL11, rpL13, rpL17, rpL21, rpL28, and rpL43 (Pöll et al., 2009 and citations therein). As depicted in Figure 23, the members of this class are not as clearly clustered in a certain morphological region of the LSU. Some members of this group are part of the 5S RNP, the major constituent of the central protuberance (rpL5, rpL11) while others (as rpL10 and rpL21) directly contact it. A structural feature that is shared by all members of this group is that they all show some interactions with LSU domains II and V, which build the platform for the incorporation of the 5S RNP. These commonly observed interactions seem to be crucial for the establishment of the final position of the central protuberance an event that is required for

the processing of the 3' end of late 5.8S rRNA precursors and/or nuclear export (Pöll et al., 2009).

Two essential LSU r-proteins, rpL1 and rpL40 were shown to be not strictly required for any pre-rRNA processing event nor for efficient nuclear export of pre-60S particles and were therefore categorized in class 4 (Pöll et al., 2009). Among the remaining, (yet) "uncategorized" LSU r-proteins are the non-essential ones and some essential ones, as rpL14, rpL30, rpL36, and rpL42, whose (potential) requirement for pre-rRNA processing of LSU precursors was not yet characterized.

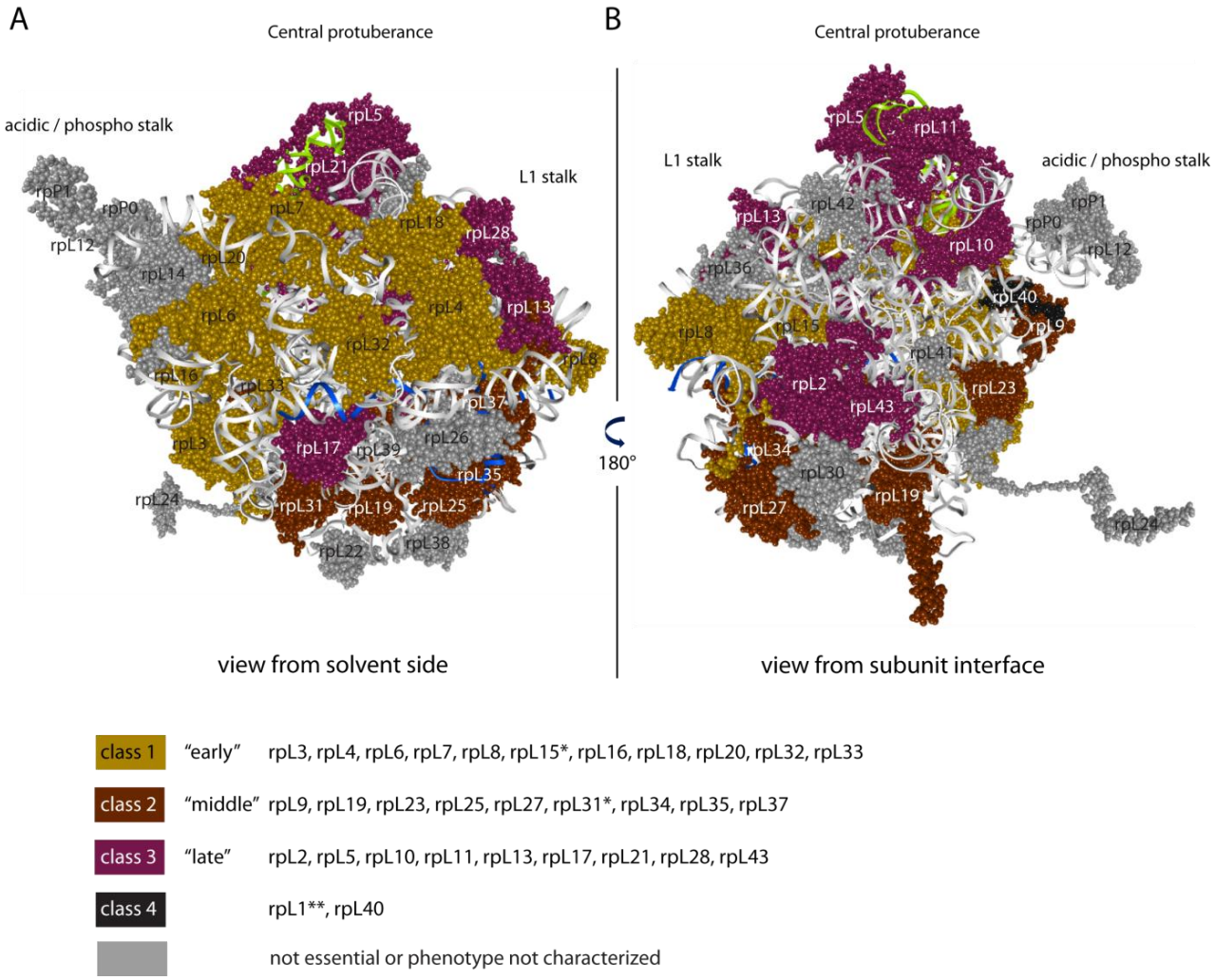

Figure 23 - Structure of the yeast LSU highlighting the LSU r-proteins according to their pre-rRNA processing phenotype class

The yeast LSU (Ben-Shem et al., 2011) is depicted as viewed from the solvent side **A)** or the subunit interface **B)**. The 25S rRNA is colored in gray, the 5S rRNA in green and the 5.8S rRNA in blue. LSU r-proteins that exhibit (according to Pöll et al. (2009)) an "early" (class 1) pre-rRNA processing phenotype are colored in orange, those with a "middle" (class 2) in dark brown, and those with a "late" (class 3) in purple. LSU r-proteins of class 4, which were described to be not strictly required for any pre-rRNA processing event are colored in black. Non-essential LSU r-proteins or those whose pre-rRNA processing phenotype is yet uncharacterized are colored in gray. (* phenotypes of rpL15 and rpL31 are not as certain, since not as properly analyzed – see table 1; ** Note that rpL1 is missing in the structure - its location is indicated as "L1 stalk".)

Aside from the described effects of *in vivo* depletion of LSU r-proteins on pre-rRNA processing and/or nuclear export, little is known on how the protein composition of these mutant pre-ribosomes might change when an essential LSU r-protein is missing. What became also evident in the studies addressing the pre-rRNA processing phenotypes of the individual r-proteins was that the mutant pre-60S particles are not strongly accumulating in the cell but efficiently degraded (see citations in the introduction in section 2.2.6).

The objective of this part of this work was to systematically analyze changes in the composition of (mutant) pre-60S particles which are still present (hence not yet degraded) in the cells after *in vivo* expression shut down of different LSU r-proteins. To this end, mutant preribosomes were affinity purified from cell extracts and their composition was analyzed and compared to the one of the respective wild type pre-ribosomal particles by semi quantitative mass spectrometry. Putative changes in the composition (in terms of other LSU r-proteins) of the mutant particles observed by this approach were then aimed to enable the decipherment of hierarchical assembly interrelationships among LSU r-proteins *in vivo*. As example, in case two r-proteins contact each other in the mature LSU, the question whether their assembly might occur independent or interdependent of each other can be addressed. In addition, possible effects on the interaction of the numerous LSU ribosome biogenesis factors with pre-60S particles should be detectable with this approach. Those effects could for example be a disturbed recruitment of certain biogenesis factors to, and/or a disturbed release of other factors from the mutant particles. Combining the results of these comparative studies with published data could help to shed more light on the molecular prerequisites required to enable certain maturation events as pre-rRNA processing or nuclear export. As simple example, in case a LSU biogenesis factor, that was shown to be required for a specific pre-rRNA processing event, is not recruited any more to the respective pre-60S particle after depletion of a specific LSU r-protein, the molecular cause of the pre-rRNA processing phenotype of this r-protein might (at least in parts) be explained.

Again, epitope tagged LSU biogenesis factors were used as bait proteins to purify the mutant particles. Depending on the respective depletion phenotype the LSU r-protein of interest exhibits, different LSU biogenesis factors were chosen as bait proteins. To analyze the consequence of *in vivo* depletion of LSU r-proteins showing an “early” (class 1) pre-rRNA processing phenotype, LSU biogenesis factors that start interacting with “early” pre-60S particles were chosen. Accordingly, the mutant pre-ribosomes made after depletion of “middle” (class 2) or “late” (class 3) acting LSU r-proteins were co-purified with LSU biogenesis factors that start interacting with pre-60S particles of early or intermediate pre-rRNA processing state and which remain bound until “late” LSU precursor populations. One important prerequisite to enable the detection of compositional changes of the mutant pre-ribosomes is that the binding of the respective LSU biogenesis factor chosen as bait protein is not affected by the lack of the depleted LSU r-protein. Therefore, in many cases, different bait proteins were used for the affinity purifications. To make the approach more resistant to possible “outliers” or artifacts (which might for example be observed when the contamination with mature LSUs or 80S ribosomes in single affinity purifications is above normal levels),

biological replicates of the respective comparisons were routinely created. In addition, aliquots of the affinity purified fractions were used to isolate and analyze the (pre-) rRNA content of the particles of interest. The following three sections will focus on changes in the protein composition of LSU precursors depleted of LSU r-proteins with an “early” (class 1 – section 3.3.2), “middle” (class 2 – section 3.3.3), and “late” (class 3 – section 3.3.4) pre-rRNA processing phenotype.

3.3.2 Changes in the protein composition of LSU precursor particles in r-protein expression mutants with an “early” (class 1) pre-rRNA processing phenotype

To analyze changes in the protein composition of LSU precursor particles in r-protein gene mutants exhibiting an “early” (class 1) pre-rRNA processing phenotype, two different TAP-tagged LSU biogenesis factors were chosen as bait proteins for their affinity purifications. One was Noc2-TAP which was used before to affinity purify the “early” pre-60S particles in the comparative analyses shown in section 3.2.1. It co-purified pre-ribosomes mainly containing 35S/32S and 27S pre-rRNAs (Figure 18 and Figure 24A, lanes 13-15). The other chosen biogenesis factor was Rpf2-TAP which was shown to start interacting with early, 35S pre-rRNA containing preribosomes as part of the “5S rRNA complex” which consists of the 5S rRNA, rpL5, rpL11 and the LSU biogenesis factor Rrs1 (Zhang et al., 2007). In contrast to Noc2, it remained bound until later, 7S pre-rRNA containing pre-60S particles (Figure 24B, lanes 13-15). Yeast strains which conditionally express the LSU r-protein of interest and which are in addition genetically modified to express a chromosomally encoded TAP-tagged version of Noc2 or Rpf2 were cultivated for four hours (sometimes in addition also for six or eight hours) in restrictive conditions in which *in vivo* expression of the respective LSU r-protein is shut down. Noc2-TAP or Rpf2-TAP and associating pre-ribosomes were purified from the cellular extracts of these yeast strains using an IgG matrix. As control, “wild type – like” yeast strains in which no LSU r-protein gene is under control of the inducible promoter and which express C-terminally TAP tagged Noc2 or Rpf2 were included. In total, the changes in the composition of pre-ribosomes after depletion of nine different “early” LSU r-proteins were analyzed. They included rpL3, rpL4, rpL7, rpL8, rpL16, rpL18, rpL20, rpL32, and rpL33. Parts of the cellular extract fraction (“Input”) and of the affinity purified fractions (“IP”) were used to isolate and subsequently analyze the RNA content by Northern blotting using specific probes for detection of the respective rRNA (precursors) (Figure 24).

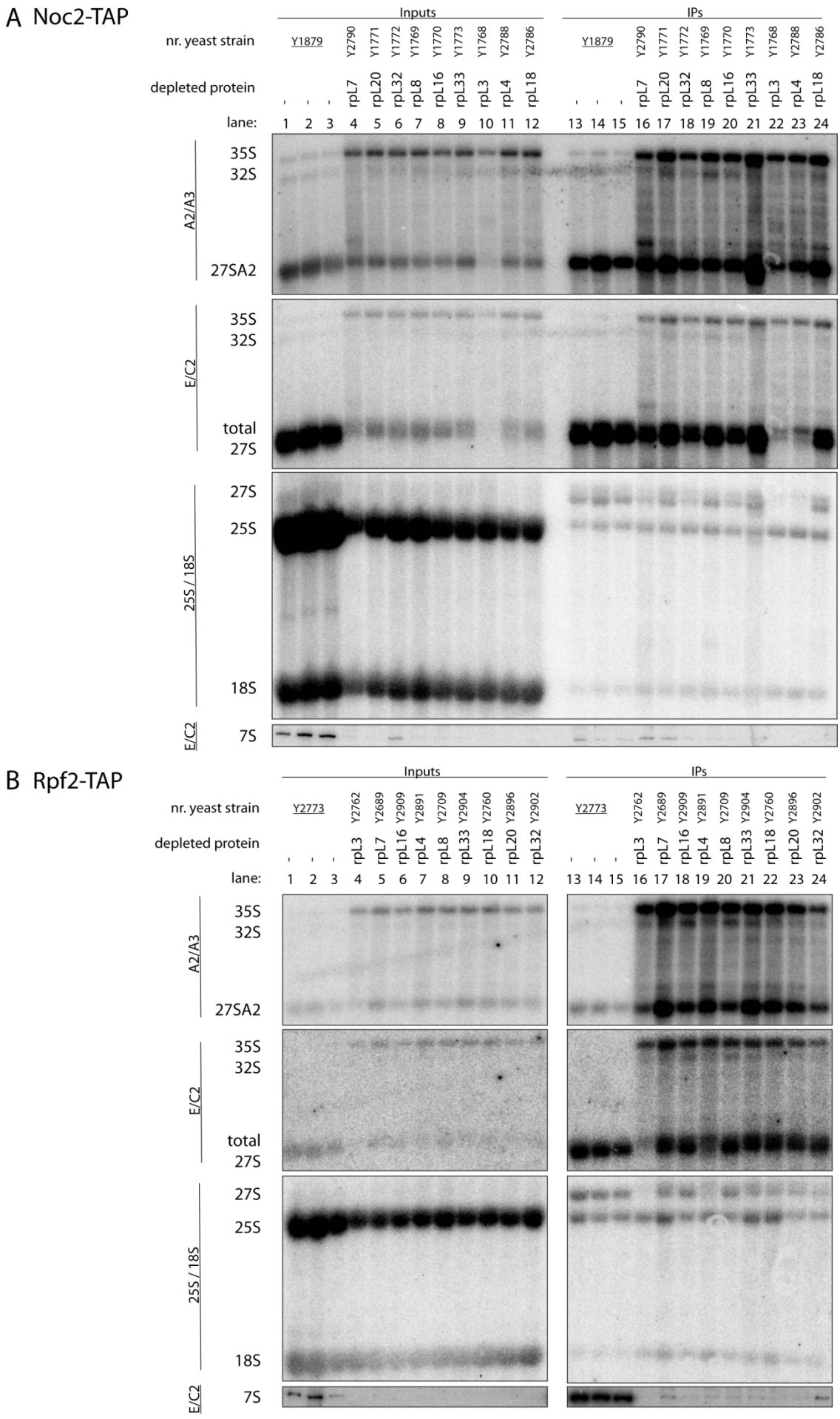
A Noc2-TAP
Inputs
IPs
nr. yeast strain
Y1879
Y2790
Y1771
Y1772
Y1769
Y1770
Y1773
Y1768
Y2788
Y2786
depleted protein
rpL7
rpL20
rpL32
rpL8
rpL16
rpL33
rpL3
rpL4
rpL18
lane:
1 2 3 4 5 6 7 8 9 10 11 12 13 14 15 16 17 18 19 20 21 22 23 24
A2/A3
35S
32S
27SA2
E/C2
35S
32S
total
27S
25S / 18S
27S
25S
18S
E/C2
7S
B Rpf2-TAP
Inputs
IPs
nr. yeast strain
Y2773
Y2762
Y2689
Y2909
Y2891
Y2709
Y2904
Y2760
Y2896
Y2902
depleted protein
rpL3
rpL7
rpL16
rpL4
rpL8
rpL33
rpL18
rpL20
rpL32
lane:
1 2 3 4 5 6 7 8 9 10 11 12 13 14 15 16 17 18 19 20 21 22 23 24
A2/A3
35S
32S
27SA2
E/C2
35S
32S
total
27S
25S / 18S
27S
25S
18S
E/C2
7S

Figure 24 (previous page) - Analyses of the (pre-) rRNA content of mutant pre-ribosomes depleted of various LSU r-proteins with an "early" pre-rRNA processing phenotype.

The indicated yeast strains expressing a chromosomally-encoded TAP-tagged version of the LSU biogenesis factors Noc2 (**A)**) or Rpf2 (**B)**) together with either the indicated (or no) LSU r-protein gene under control of the galactose-inducible GAL1/10 promoter were cultivated for four hours in glucose-containing medium to shut down expression of the respective LSU r-protein gene. Noc2-TAP or Rpf2-TAP and associated pre-ribosomal particles were then affinity purified from corresponding cellular extracts in a one-step purification as described in 5.2.6.1. The (pre-) rRNA content of total cellular extracts ("Input" lanes 1-12) or of parts of the affinity purified fractions (IP lanes 13-24) was analyzed by northern blotting. Detected (pre-) rRNAs and the used DNA oligonucleotide probe are indicated on the left. Equal signal intensities of the Input and IP fractions correspond to 4% co-purification efficiencies of the respective (pre-) rRNA.

The analysis of the (pre-) rRNAs isolated from the cellular extract ("Input") fractions confirmed the previously described "early" (class 1) pre-rRNA processing phenotype (Figure 24A-B, lanes 4-12). With the exception of rpL3, substantial amounts of 27SA2 pre-rRNAs could still be detected (Figure 24A-B, compare 27SA2 pre-rRNA signals in lanes 4-12 to the ones in lines 1-3). Analysis of total 27S pre-rRNAs (27SA2, 27SA3, and 27SB pre-rRNAs) however showed that the processing of the 27SA2 pre-rRNAs was significantly delayed after depletion of each of the nine LSU r-proteins (Figure 24A-B, compare total 27S pre-rRNA signals in lanes 4-12 to the ones in lanes 1-3). Consequently, levels of the further maturated 7S pre-rRNA were not or only to slight amounts detectable. In line with this, levels of the mature 25S (and 18S) rRNAs were also detected in lower amounts. As described before (Pöll et al., 2009), the decrease in levels of the 25S rRNA was stronger as the one of the 18S rRNA, since production of the SSU is not primarily affected the shift to the restrictive conditions (Figure 24A-B, compare 25S and 18S signals in lanes 4-12 the ones in lanes 1-3). In comparison to the cellular fractions from wild type cells, the steady state levels of the earliest precursors (35S/32S pre-rRNAs) were increasing in all analyzed mutants. In summary, the observed pre-rRNA processing phenotypes of each of the nine analyzed, "early" LSU r-proteins were in agreement with previously published data (Pöll et al., 2009 and citations therein). Depletion of rpL3 resulted in an even "earlier" pre-rRNA processing phenotype since levels of 27SA2 were significantly decreased after four hours shift to restrictive conditions what is in agreement with a previous study (Rosado et al., 2007b).

Comparison of the affinity purified ("IP") fractions of the LSU r-protein mutants to the ones of the respective wild type strains showed that the population of co-purified preribosomes containing the earliest 35S/32S pre-rRNAs increased after *in vivo* expression shut down of the analyzed r-proteins, what could be explained by the higher cellular steady state levels of these pre-rRNAs (see above). In the Noc2-TAP affinity purifications, the amounts of co-purified 27SA2 pre-rRNA containing particles were for most analyzed r-protein expression mutants in the range of the ones of wild type cells (Figure 24A, compare 27SA2 pre-rRNA signals in lanes 16-24 to the ones in lanes 13-15). Rpf2-TAP co-purified even more 27SA2 pre-rRNA containing pre-ribosomes after depletion of each analyzed r-protein (Figure 24B, compare lanes 16-24 to lanes 13-15). After depletion of rpL3, significantly fewer amounts of pre-ribosomes containing total 27S pre-rRNAs (27SA2, 27SA3 and $27SB_{l/s}$ species) were co-purified with both, Noc2-TAP and Rpf2-TAP (Figure 24A, lane 22; Figure 24B, lane 16), what is in agreement with the more reduced cellular levels of these species in this mutant (Figure 24A, compare lane 10 to lanes 4-12) . After depletion of rpL4 however, only Noc2-TAP but

not Rpf2-TAP, co-purified significantly fewer amounts of 27S pre-rRNA containing pre-ribosomes (Figure 24A, lane 23). This effect was reproducible in an independent Noc2-TAP purification (data not shown), but cannot be simply explained by reduced 27S pre-rRNA levels in the cellular extract fractions (Figure 24A, compare lane 11 to lanes 4-12). Therefore it might be possible that the association of Noc2, but not the one of Rpf2 to pre-ribosomes is specifically affected to some extent after depletion of rpL4 *in vivo*. Hybridization of the Northern Blots with probes detecting mature LSUs (25S rRNA) and SSUs (18S rRNAs), which can both be regarded as unspecific background, showed that all affinity purifications contained some amounts of contaminating mature LSUs and SSUs (Figures 24A-B, lines 13-24).

The rest of the affinity purified fractions were further processed (as described in section 5.2.7 and illustrated in Figure 16B) and subjected to semi quantitative mass spectrometry using iTRAQ. The protein composition of mutant pre-60S particles purified by Noc2-TAP or Rpf2-TAP was then compared to the ones of the respective “wild type” particles. The results of these studies are depicted in Figures 25-29.

In order to see whether the changes observed after *in vivo* expression shut down of the individual LSU r-proteins were reproducible (and therefore statistical relevant), the results of several biologically and/or technically reproduced pair-wise comparisons (mutant vs. wild type) were combined. The (normalized) average iTRAQ ratios of each identified LSU r-protein (Figures 25 & 26) or LSU biogenesis factor (Figures 28 & 29) were calculated and the proteins were ordered by these values (largest values first). Again, average iTRAQ ratios of identified housekeeping proteins, SSU r-proteins and SSU processome components were included. LSU r-proteins that were not (or not sufficiently frequent) identified are shown in the lower panels in Figures 25 & 26. Accordingly, LSU biogenesis factors that could not be identified in at least half of the pair-wise particle comparisons (or in average only with up to one peptide) are shown in the lower panels in Figures 28 & 29. Besides the highlighted LSU r-protein that had been depleted in the respective comparisons, other LSU r-proteins that either belong to the same phenotypic class (orange) or that showed specific assembly behavior (“late group” – green; “intermediate rpL2/43/39 group 2” – purple) are highlighted in Figures 25 & 26. Accordingly, LSU biogenesis factors that were shown to exhibit the same pre-rRNA processing phenotype are highlighted in orange in Figures 27 - 29.

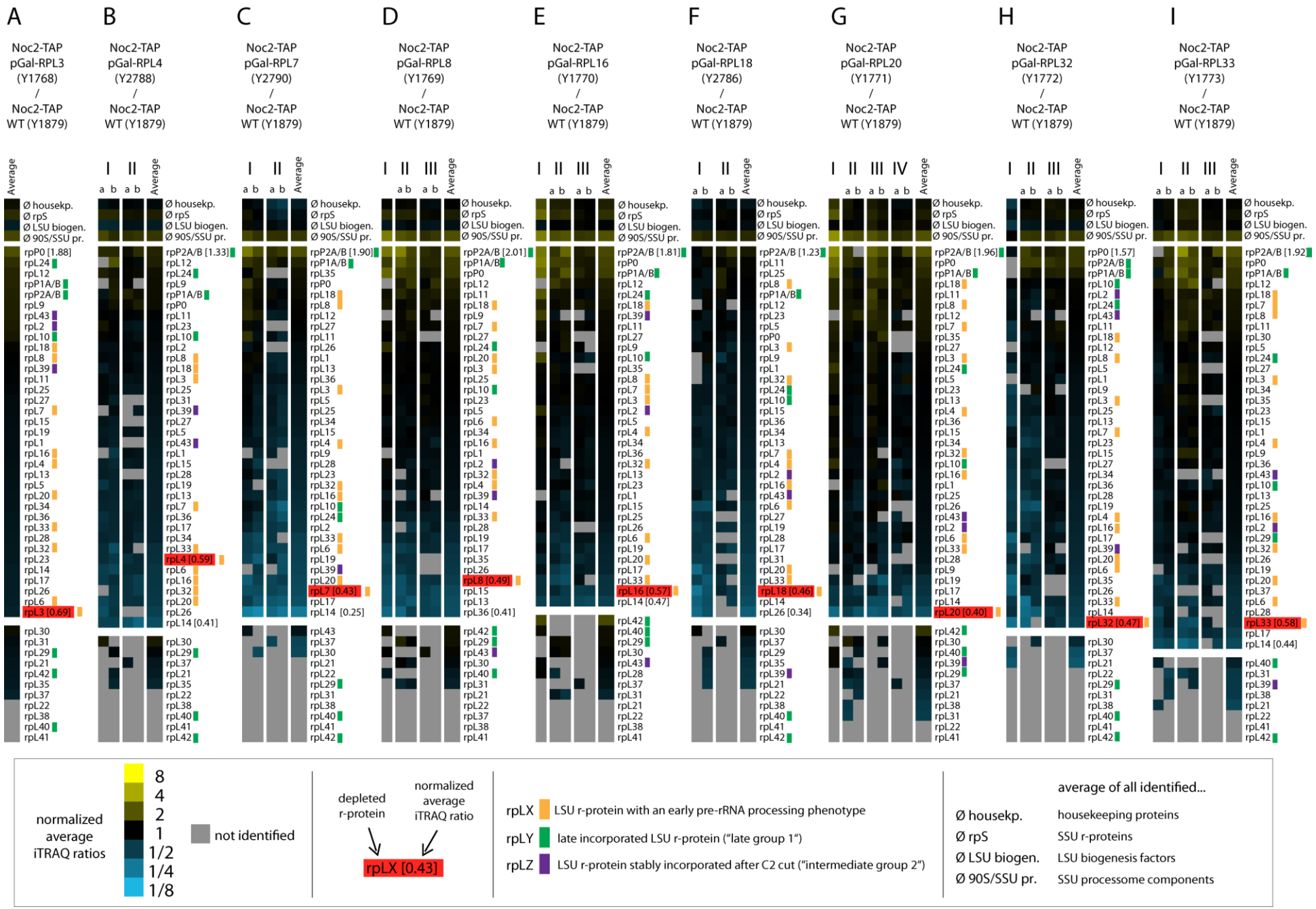
A
Noc2-TAP pGal-RPL3 (Y1768) / Noc2-TAP WT (Y1879)
B
Noc2-TAP pGal-RPL4 (Y2788) / Noc2-TAP WT (Y1879)
C
Noc2-TAP pGal-RPL7 (Y2790) / Noc2-TAP WT (Y1879)
D
Noc2-TAP pGal-RPL8 (Y1769) / Noc2-TAP WT (Y1879)
E
Noc2-TAP pGal-RPL16 (Y1770) / Noc2-TAP WT (Y1879)
F
Noc2-TAP pGal-RPL18 (Y2786) / Noc2-TAP WT (Y1879)
G
Noc2-TAP pGal-RPL20 (Y1771) / Noc2-TAP WT (Y1879)
H
Noc2-TAP pGal-RPL32 (Y1772) / Noc2-TAP WT (Y1879)
I
Noc2-TAP pGal-RPL33 (Y1773) / Noc2-TAP WT (Y1879)
Average
I II III IV
a b
Ø housekp.
Ø rpS
Ø LSU biogen.
Ø 90S/SSU pr.
rpP0 [1.88]
rpP2A/B [1.33]
rpP2A/B [1.90]
rpP2A/B [2.01]
rpP2A/B [1.81]
rpP2A/B [1.23]
rpP2A/B [1.96]
rpP0 [1.57]
rpP2A/B [1.92]
rpL3 [0.69]
rpL4 [0.59]
rpL7 [0.43]
rpL8 [0.49]
rpL16 [0.57]
rpL18 [0.46]
rpL20 [0.40]
rpL32 [0.47]
rpL33 [0.58]
rpL14 [0.41]
rpL14 [0.25]
rpL36 [0.41]
rpL14 [0.47]
rpL26 [0.34]
rpL14 [0.44]
normalized average iTRAQ ratios
8
4
2
1
1/2
1/4
1/8
not identified
depleted r-protein
normalized average iTRAQ ratio
rpLX [0.43]
rpLX LSU r-protein with an early pre-rRNA processing phenotype
rpLY late incorporated LSU r-protein ("late group 1")
rpLZ LSU r-protein stably incorporated after C2 cut ("intermediate group 2")
average of all identified...
Ø housekp. housekeeping proteins
Ø rpS SSU r-proteins
Ø LSU biogen. LSU biogenesis factors
Ø 90S/SSU pr. SSU processome components

Figure 25 - (previous page) Analyses of the changes of the LSU r-proteins levels in pre-60S particles purified via Noc2-TAP after *in vivo* depletion of selected "early" (class 1) ribosomal proteins.

The indicated yeast strains expressing a chromosomally-encoded TAP-tagged version of the LSU biogenesis factor Noc2 together with either the indicated (or no) LSU r-protein gene under control of the galactose-inducible GAL1/10 promoter were cultivated for four hours in glucose-containing medium to shut down expression of the respective LSU r-protein gene. Noc2-TAP associated pre-ribosomal particles were then affinity purified from corresponding cellular extracts in a one-step purification as described in 5.2.6.1. The changes in the protein composition of these affinity purified mutant pre-ribosomes in comparison to the respective wild type particles were analyzed by semi quantitative mass spectrometry using iTRAQ (see Figure 16 and sections 5.2.7, 5.2.8, and 5.2.9). Up to four biological replications of these pair-wise ("mutant vs. wild type") comparisons were analyzed (indicated by roman numbers above the heat map panels), from most of which in addition technical replicates were created ("a and b" above the heat maps). The resulting average iTRAQ ratios for each r-protein was calculated and is depicted in the right lane, assigned to as "average" for each mutant. LSU r-proteins, which were not or not often enough (in less than 50% of the individual pair-wise comparisons) identified are depicted in the lower panels. The color code of the heat map is shown in the box below. In addition to the LSU r-proteins, the average iTRAQ ratios of all identified housekeeping proteins, SSU r-proteins, LSU biogenesis factors, and 90S preribosome/SSU processome components were included and are shown in the upper panels. The depleted LSU r-protein and its average iTRAQ ratio are highlighted by a red box. In addition, the average range of the respective collection of pair wise comparisons (= highest and lowest average iTRAQ ratios) is indicated by the [iTRAQ ratios]. LSU r-proteins which have the same, "early" (class 1) pre-rRNA processing phenotype are highlighted with an orange box on the right of the respective LSU r-protein name. Those which were members of groups of LSU r-proteins showing a "specific" assembly behavior (Figures 20-22) are highlighted by green and purple boxes. See also legend box below the heat map panels. Note that the following Figures showing semi quantitaitive mass spectrometry data are similarly structured.

Figure 26 (next page) - Analyses of the changes of the LSU r-proteins levels in pre-60S particles purified via Rpf2-TAP after *in vivo* depletion of selected "early" (class 1) ribosomal proteins.

For details see legend of Figure 25 which is completely applicable to this Figure with a few exceptions. First, Rpf2-TAP was used as bait protein for all affinity purifications. Second, no technical replicates were created but the depletion time of the respective LSU r-protein could vary and is indicated above the heat map panels (in hours depletion). Third, in some of those pair- wise comparisons marked with an asterisk (*), the conditional yeast strain grown in permissive (Galactose containing) conditions was sometimes used as wild-type reference (instead of the Rpf2-TAP tagged wild-type with no RPL gene under control of the Gal inducible promoter).

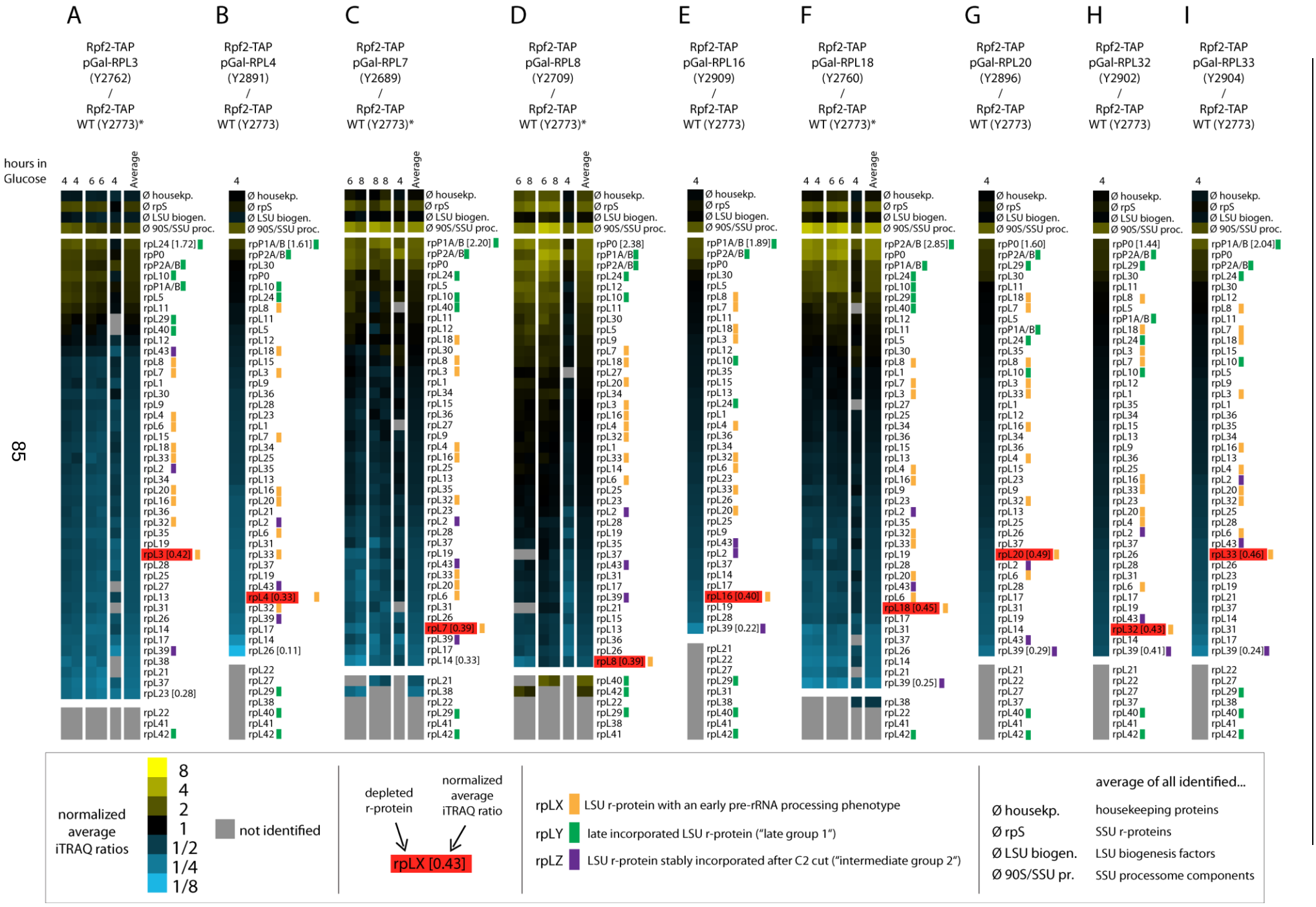
A
Rpf2-TAP pGal-RPL3 (Y2762) / Rpf2-TAP WT (Y2773)*
B
Rpf2-TAP pGal-RPL4 (Y2891) / Rpf2-TAP WT (Y2773)
C
Rpf2-TAP pGal-RPL7 (Y2689) / Rpf2-TAP WT (Y2773)*
D
Rpf2-TAP pGal-RPL8 (Y2709) / Rpf2-TAP WT (Y2773)*
E
Rpf2-TAP pGal-RPL16 (Y2909) / Rpf2-TAP WT (Y2773)
F
Rpf2-TAP pGal-RPL18 (Y2760) / Rpf2-TAP WT (Y2773)*
G
Rpf2-TAP pGal-RPL20 (Y2896) / Rpf2-TAP WT (Y2773)
H
Rpf2-TAP pGal-RPL32 (Y2902) / Rpf2-TAP WT (Y2773)
I
Rpf2-TAP pGal-RPL33 (Y2904) / Rpf2-TAP WT (Y2773)
hours in Glucose
Average
Ø housekp.
Ø rpS
Ø LSU biogen.
Ø 90S/SSU proc.
rpL3 [0.42]
rpL4 [0.33]
rpL7 [0.39]
rpL8 [0.39]
rpL16 [0.40]
rpL18 [0.45]
rpL20 [0.49]
rpL32 [0.43]
rpL33 [0.46]
normalized average iTRAQ ratios
8
4
2
1
1/2
1/4
1/8
not identified
depleted r-protein
normalized average iTRAQ ratio
rpLX [0.43]
rpLX LSU r-protein with an early pre-rRNA processing phenotype
rpLY late incorporated LSU r-protein ("late group 1")
rpLZ LSU r-protein stably incorporated after C2 cut ("intermediate group 2")
average of all identified...
Ø housekp. housekeeping proteins
Ø rpS SSU r-proteins
Ø LSU biogen. LSU biogenesis factors
Ø 90S/SSU pr. SSU processome components

In general, the depletion of the respective LSU r-protein should be confirmable by a significant underrepresentation in the purified mutant pre-ribosome in comparison to the respective wild type preribosome. As shown in Figures 25 and 26, this expected behavior could be observed in all cases. The average iTRAQ ratios of the depleted r-proteins, which were in most cases in a range between 0.3 and 0.5 indicate that the respective r-protein was clearly underrepresented, albeit not completely absent in the affinity purified fractions. The analyses of the (pre-) rRNAs present in the individual affinity purified fractions showed that the amounts of contaminating mature LSUs (as analyzed by its 25S rRNA) were in most cases almost in the same range as the "specifically" purified LSU precursors (Figure 24 A-B; compare 25S rRNA signals in "IP" lanes 13-24 to the 27S pre-rRNA signals detected with the same probe). Therefore, even if the depleted LSU r-protein was (in theory) completely absent from the population of specifically purified **pre-**ribosomal particles, the contaminating mature LSUs (which should still contain the actually depleted LSU r-protein) would only allow to detect in total a decrease of 50%. Therefore, in general, the observed changes in the LSU r-protein compositions were not very drastic (in a range between factor 0.25 and 2) but still very likely specific, since the depleted LSU r-protein was in all cases among the most underrepresented.

Another common observation was that changes in mutant preribosomes purified by Rpf2-TAP were in general seen for more LSU r-proteins than in the ones in mutant pre-ribosomes purified by Noc2-TAP (compare general heat map patterns in Figure 26 to the ones in Figure 25). These differences can be explained by the different populations of pre-60S particles Rpf2 and Noc2 were observed to associate with in the wild type situation. While Rpf2 remained bound to 7S pre-rRNA containing nuclear pre-60S particles, Noc2-TAP purified only minor amounts of 7S pre-rRNA indicating that it had been largely dissociated from these later population of pre-ribosomes (Figure 24A-B, compare 27S and 7S pre-rRNA signals in lanes 13-15 to the ones in lanes 1-3). Since this population of "late", 7S pre-rRNA containing pre-60S particles Rpf2-TAP normally co-purified was not produced any longer after depletion of the "early" LSU r-proteins, the total amounts of pre-ribosomes (and therefore the ones of the LSU r-proteins they contain) Rpf2-TAP co-purified decreased to greater extents than the ones Noc2-TAP co-purified. In line with this, levels of the LSU r-proteins whose affinity to pre-60S particles increased most after the production of the 7S pre-rRNA (Figure 20B) were observed to be more affected (decreased) in the mutant particles co-purified by Rpf2-TAP (Figure 26, highlighted in purple) as by Noc2-TAP (Figure 25, highlighted in purple). The members of the "late" group of LSU r-proteins (highlighted in green in Figures 25 & 26), which were observed to be underrepresented in all pre-60S particles (Figure 20B) can be largely regarded as "background" in all these analyses, since they should not be present in the affinity purified LSU precursors. In most cases, (if detected) their levels were unchanged or even increasing in the mutant pre-ribosomes. In comparison to most other LSU r-proteins their levels were among the highest, especially in those mutants in which the total amount of

pre-rRNAs was decreasing more than in the others (as observed after depletion of rpL3 or rpL4 – see for example 27S pre-rRNA signals in Figure 24A, lanes 22-23).

Before focusing on the differences in changes of the protein composition among the nine analyzed r-protein expression mutants, some other generally observed effects will be described in the following. As in all mutants the levels of 35S pre-rRNA were significantly increased, the levels of proteins contained in these “earliest” pre-ribosomes (90S pre-ribosome / SSU processome) were also, as expectable, increased. Both, the identified trans-acting SSU processome components (e.g. the UTPA/B/C complex components) and the SSU r-proteins (many of which were described to be present in the SSU processome) were found to be increased in comparison to the particles affinity purified from wild type cells (Figure 25 & 26, upper panels). In line with this, LSU ribosome biogenesis factors that function earlier in the 60S biogenesis pathway (before the processing of 27SA2/27SA3 pre-rRNAs) were unchanged or increased (e.g. Rrp5, Noc1 or Nop4 – Figures 28 and 29). On the other hand, LSU biogenesis factors that mainly interact with later, further maturated populations of pre-60S particles (e.g. Rsa4, Nog2, Nop53, Arx1 or Spb4) were underrepresented in the pre-ribosomes purified from the mutant cells (Figures 28 and 29). Some LSU r-proteins as rpL17, rpL19, rpL26, or (less consistent) rpL35, rpL28 and rpL37 tended to be underrepresented after depletion of either tested LSU r-protein, albeit to some variable extents (Figures 25 and 26).

In the following, differences in the changes of the protein composition among the nine analyzed LSU r-protein expression mutants will be outlined, first focusing on the LSU r-proteins (Figures 25 & 26). As mentioned above, all analyzed “early” LSU r-proteins except rpL3 (domain VI) are mainly bound to LSU rRNA domains I (rpL8) or II (rpL4, rpL7, rpL16, rpL20, rpL32, rpL33).

The preribosomes purified after depletion of rpL3 contained significantly less amounts of 27S pre-rRNA species since these were largely degraded (and/or not produced as much any longer) in the cellular extracts (Figure 24). Therefore, the affinity purified fractions mainly consisted of the earliest, 35S/32S pre-rRNAs preribosomes and, to a large portion, of contaminating mature LSUs (Figure 24A, lane 22; Figure 24B, lane 16 –compare 25S rRNA to 27S pre-rRNA signals). Due to these increased relative portions of “background”, no robust conclusions on the changes in the LSU r-protein compositions could be made in the case of the *RPL3* mutant. Interestingly, rpL3 itself was not observed to be underrepresented after depletion of any of the other analyzed “early” LSU r-proteins (Figures 25-26). This argues for a robust association of rpL3 to preribosomes of an early maturation state which seems to occur independently of other LSU r-proteins.

Depletion of rpL4 resulted in an underrepresentation of a large group of LSU r-proteins in the Rpf2-TAP purifications (Figure 26B). Remember that in the case of the Noc2-TAP purifications, the amounts of 27S pre-rRNA containing co-purified preribosomes were (in similarity to the *RPL3* mutant) reduced and the relative portions of contaminating mature

LSUs were increased what hampered robust and significant conclusions of the observed changes in the LSU r-protein composition of these purifications. As depicted in Figure 26B, rpL8, rpL18, and rpL3 were the least affected among the group of “early” LSU r-proteins what argues for an association of these r-proteins to nascent ribosomes independently of rpL4. The fact that rpL3 and rpL8 are located in mature LSUs rather distant of rpL4 contacting (in parts) different rRNA domains further supports the existence of these possible independencies (see also Figure 43C). Rpl18 on the other hand directly contacts rpL4 in mature LSUs and both proteins are bound to 25S rRNA domain II (Figure 43). However, their association seems to occur largely independent of each other since also in the inverted case of rpL18 depletion, rpL4 was only very mildly affected in the purified mutant preribosomes (Figures 25F and 26F).

After depletion of rpL7, besides rpL7 itself, a group of three LSU r-proteins (rpL6, rpL20, and rpL33) with an “early” pre-rRNA processing phenotype was specifically affected (Figures 25C, 26C). In the mature LSU all of them are bound in close proximity to rpL7 forming a “cluster” which establishes main contacts to domain II (and VI) (see also Figure 43). In addition, rpL14, which is part of the same cluster, was strongly affected after rpL7 depletion. RpL16 and rpL32, which are also bound in proximity of this group, were also affected, albeit to less extents. Again, rpL3, rpL8, and rpL18 were not or only very mildly affected indicating that they are able to establish stable interactions with nascent ribosome independently of also rpL7.

These observations suggest that the assembly of a group of LSU r-proteins consisting of rpL7, rpL6, rpL20, rpL33, rpL14 (and possibly rpL16 and rpL32) might occur in an interdependent manner *in vivo*. Whether or to which degree this putative interdependent assembly is true was, as far as possible, tested by depletion of rpL20, rpL33, rpL32, and rpL16. No appropriate yeast strains to shut down expression of rpL6 or rpL14 and analyze the consequence of their depletion existed were available. The results of the tested LSU r-protein mutants are shown in Figures 25 and 26 E,G,H,I. Among the most intensely affected LSU r-proteins of this group was, in all cases, rpL14, indicating that the stable incorporation of this (essential) LSU r-protein depends on each of the other members of this group. RpL7 on the other hand was not affected after depletion of either the other members of this group indicating that it is able to assemble independently and presumably before (“upstream”) of the others. Effects of the remaining members in regard to each other could be detected in the affinity purifications using both, Noc2-TAP and Rpf2-TAP as bait proteins, indicating a partial interdependent assembly behavior of these LSU r-proteins. Due to some variations within the single pair-wise comparisons it is challenging and presumably wrong to deduce any more detailed hierarchical interrelationships of the members of this group.

Rpl18, another “early” (class 1) LSU r-protein and domain II binder which is located also near the above described “cluster” (Figure 43) was not, or only slightly affected after depletion of any of the other tested members of this cluster (Figures 25, 26 C,E,G,H,I). Depletion of rpL18 itself however resulted in a significant reduction of levels of rpL6, rpL14, rpL20, rpL33, and

(less intense) rpL32 and rpL16 (Figures 25, 26 F). Only very mild effects on rpL7 could be detected confirming the largely independent assembly behavior of rpL7. As described above association rpL18 itself was not (or only slightly) affected in the other LSU r-protein expression mutants. Therefore, these data suggest that *in vivo*, the incorporation of rpL18 occurs also rather independent (hence "upstream") of the above described group of r-proteins which were underrepresented after its depletion.

Finally, changes in the r-protein composition of preribosomes purified from yeast cells depleted of rpL8, which is located distant of the other "early" LSU r-proteins mainly contacting domains I (including the 5.8SrRNA), III and V were analyzed by the same means (Figures 25D and 26D). Remarkably, none of the other LSU r-proteins which are described to exhibit the same "early" pre-rRNA processing phenotype were among the most affected ones. Instead, levels of an rpL8-specific group consisting of rpL13, rpL15, and rpL36 were significantly reduced. Interestingly, all of them are bound in proximity to rpL8 mainly in LSU rRNA domains I and V (Figure 43A). Like rpL7, the specific effect of rpL8 was therefore most pronounced in the direct neighborhood (and the same LSU rRNA domain) of its binding site. Whether or to what extent the assembly of the members of this group (rpL8, rpL13, rpL15, and rpL36), all of which are essential in yeast, might occur interdependent could unfortunately not be addressed since no yeast strains were available to conditionally express rpL15 and rpL36. The pre-rRNA processing phenotype of rpL36 is currently unknown and the one of rpL15 is only poorly characterized. Analyses of steady state levels of all (pre-) rRNA species purified from cells depleted of rpL15 however indicated that, with the exception of the 35S pre-rRNA, the levels all other pre-rRNA species were decreased arguing for an "early" (class 1) pre-rRNA processing phenotype (Li et al., 2009). Both, the experimental procedure and the time of rpL15 depletion were only poorly described, though. In addition, no direct comparison to any other depleted LSU r-protein was shown in this study what hampers a clear conclusion on the pre-rRNA processing phenotype of rpL15. *In vivo* expression shut down of rpL13 however did not result in the same pre-rRNA processing phenotype since substantial amounts of steady state 7S pre-rRNAs could still be detected after 4 hours depletion of rpL13 (Pöll et al., 2009). To some extent however, also earlier processing events seemed to be disturbed since the $27SB_s$ pre-rRNA steady state levels were reduced and the ones of its precursor, the 27SA3 pre-rRNA were increased as characteristic for the "early" LSU r-proteins (Gamalinda et al., 2014; Pöll et al., 2009). According to these data one can conclude that the binding of rpL8 does presumably not strictly depend on the presence of rpL13 since otherwise the pre-rRNA processing phenotype of rpL13 would have to be identical.

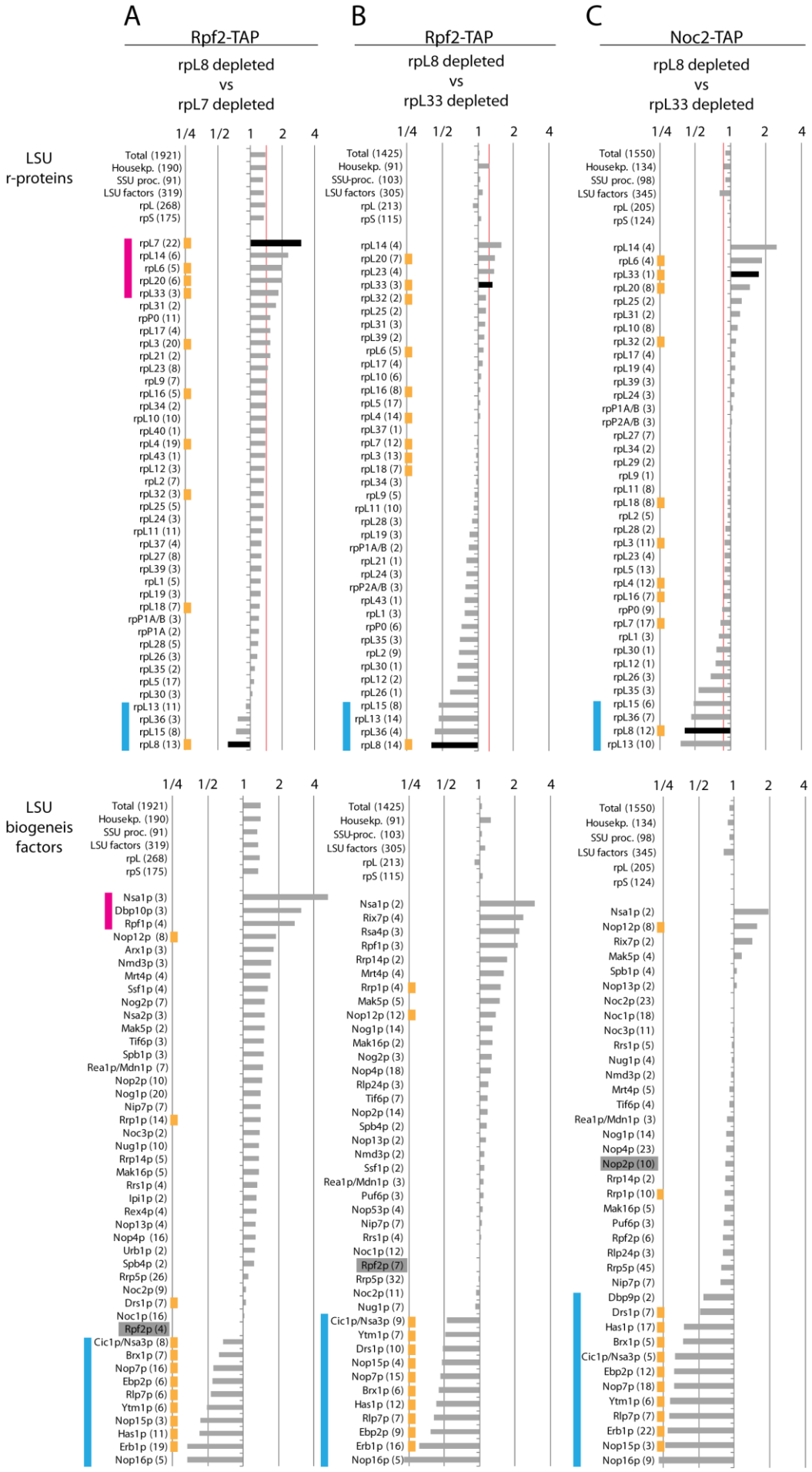
A
Rpf2-TAP
rpL8 depleted
vs
rpL7 depleted
B
Rpf2-TAP
rpL8 depleted
vs
rpL33 depleted
C
Noc2-TAP
rpL8 depleted
vs
rpL33 depleted
1/4 1/2 1 2 4
LSU
r-proteins
Total (1921)
Housekp. (190)
SSU proc. (91)
LSU factors (319)
rpL (268)
rpS (175)
rpL7 (22)
rpL14 (6)
rpL6 (5)
rpL20 (6)
rpL33 (3)
rpL31 (2)
rpP0 (11)
rpL17 (4)
rpL3 (20)
rpL21 (2)
rpL23 (8)
rpL9 (7)
rpL16 (5)
rpL34 (2)
rpL10 (10)
rpL40 (1)
rpL4 (19)
rpL43 (1)
rpL12 (3)
rpL2 (7)
rpL32 (3)
rpL25 (5)
rpL24 (3)
rpL11 (11)
rpL37 (4)
rpL27 (8)
rpL39 (3)
rpL1 (5)
rpL19 (3)
rpL18 (7)
rpP1A/B (3)
rpP1A (2)
rpL28 (5)
rpL26 (3)
rpL35 (2)
rpL5 (17)
rpL30 (3)
rpL13 (11)
rpL36 (3)
rpL15 (8)
rpL8 (13)
Total (1425)
Housekp. (91)
SSU-proc. (103)
LSU factors (305)
rpL (213)
rpS (115)
rpL14 (4)
rpL20 (7)
rpL23 (4)
rpL33 (3)
rpL32 (2)
rpL25 (2)
rpL31 (3)
rpL39 (2)
rpL6 (5)
rpL17 (4)
rpL10 (6)
rpL16 (8)
rpL5 (17)
rpL4 (14)
rpL37 (1)
rpL7 (12)
rpL3 (13)
rpL18 (7)
rpL34 (3)
rpL9 (5)
rpL11 (10)
rpL28 (3)
rpL19 (3)
rpP1A/B (2)
rpL21 (1)
rpL24 (3)
rpP2A/B (3)
rpL43 (1)
rpL1 (3)
rpP0 (6)
rpL35 (3)
rpL2 (9)
rpL30 (1)
rpL12 (2)
rpL26 (1)
rpL15 (8)
rpL13 (14)
rpL36 (4)
rpL8 (14)
Total (1550)
Housekp. (134)
SSU proc. (98)
LSU factors (345)
rpL (205)
rpS (124)
rpL14 (4)
rpL6 (4)
rpL33 (1)
rpL20 (8)
rpL25 (2)
rpL31 (2)
rpL10 (8)
rpL32 (2)
rpL17 (4)
rpL19 (4)
rpL39 (3)
rpL24 (3)
rpP1A/B (3)
rpP2A/B (3)
rpL27 (7)
rpL34 (2)
rpL29 (2)
rpL9 (1)
rpL11 (8)
rpL18 (8)
rpL2 (5)
rpL28 (2)
rpL3 (11)
rpL23 (4)
rpL5 (13)
rpL4 (12)
rpL16 (7)
rpP0 (9)
rpL7 (17)
rpL1 (3)
rpL30 (1)
rpL12 (1)
rpL26 (3)
rpL35 (3)
rpL15 (6)
rpL36 (7)
rpL8 (12)
rpL13 (10)
LSU
biogeneis
factors
Total (1921)
Housekp. (190)
SSU proc. (91)
LSU factors (319)
rpL (268)
rpS (175)
Nsa1p (3)
Dbp10p (3)
Rpf1p (4)
Nop12p (8)
Arx1p (3)
Nmd3p (3)
Mrt4p (4)
Ssf1p (4)
Nog2p (7)
Nsa2p (3)
Mak5p (2)
Tif6p (3)
Spb1p (3)
Rea1p/Mdn1p (7)
Nop2p (10)
Nog1p (20)
Nip7p (7)
Rrp1p (14)
Noc3p (2)
Nug1p (10)
Rrp14p (5)
Mak16p (5)
Rrs1p (4)
Ipi1p (2)
Rex4p (4)
Nop13p (4)
Nop4p (16)
Urb1p (2)
Spb4p (2)
Rrp5p (26)
Noc2p (9)
Drs1p (7)
Noc1p (16)
Rpf2p (4)
Cic1p/Nsa3p (8)
Brx1p (7)
Nop7p (16)
Ebp2p (6)
Rlp7p (6)
Ytm1p (6)
Nop15p (3)
Has1p (11)
Erb1p (19)
Nop16p (5)
Total (1425)
Housekp. (91)
SSU-proc. (103)
LSU factors (305)
rpL (213)
rpS (115)
Nsa1p (2)
Rix7p (4)
Rsa4p (3)
Rpf1p (3)
Rrp14p (2)
Mrt4p (4)
Rrp1p (4)
Mak5p (5)
Nop12p (12)
Nog1p (14)
Mak16p (2)
Nog2p (3)
Nop4p (18)
Rlp24p (3)
Tif6p (7)
Nop2p (14)
Spb4p (2)
Nop13p (2)
Nmd3p (2)
Ssf1p (2)
Rea1p/Mdn1p (3)
Puf6p (3)
Nop53p (4)
Nip7p (7)
Rrs1p (4)
Noc1p (12)
Rpf2p (7)
Rrp5p (32)
Noc2p (11)
Nug1p (7)
Cic1p/Nsa3p (9)
Ytm1p (7)
Drs1p (10)
Nop15p (4)
Nop7p (15)
Brx1p (6)
Has1p (12)
Rlp7p (7)
Ebp2p (9)
Erb1p (16)
Nop16p (5)
Total (1550)
Housekp. (134)
SSU proc. (98)
LSU factors (345)
rpL (205)
rpS (124)
Nsa1p (2)
Nop12p (8)
Rix7p (2)
Mak5p (4)
Spb1p (4)
Nop13p (2)
Noc2p (23)
Noc1p (18)
Noc3p (11)
Rrs1p (5)
Nug1p (4)
Nmd3p (2)
Mrt4p (5)
Tif6p (4)
Rea1p/Mdn1p (3)
Nog1p (14)
Nop4p (23)
Nop2p (10)
Rrp14p (2)
Rrp1p (10)
Mak16p (5)
Puf6p (3)
Rpf2p (6)
Rlp24p (3)
Rrp5p (45)
Nip7p (7)
Dbp9p (2)
Drs1p (7)
Has1p (17)
Brx1p (5)
Cic1p/Nsa3p (5)
Ebp2p (12)
Nop7p (18)
Ytm1p (6)
Rlp7p (7)
Erb1p (22)
Nop15p (3)
Nop16p (9)

Figure 27 (previous page) - Analysis of the differences of rpL8 depleted and rpL7/rpL33 depleted LSU precursors mutants by directly comparing their protein composition

Mutant preribosomes depleted of rpL8 were affinity purified as described before (Figures 24-26 and section 5.2.6.1) using either Noc2-TAP (**A)** and **C)**) or Rpf2-TAP (**B)**) as bait proteins. The levels of their LSU r-proteins (upper panels) or LSU biogenesis factors (lower panels) were directly compared to similarly purified preribosomes depleted of either rpL7 (**A)**) or rpL33 (**B)** and **C)**). iTRAQ ratios were normalized to the respective bait protein and are depicted in a log2 scale. In the upper panels, a red line indicated the "background" level as measured by the iTRAQ ratios of the identified housekeeping proteins. LSU r-proteins (upper panels) and LSU biogenesis factors ("A3 factors" – lower panels) with the same, early pre-rRNA processing phenotype are highlighted with orange boxes. LSU r-proteins and biogenesis factors that were specifically affected after depletion of rpL8 or rpL7/rpL33 are colored with blue and magenta boxes, respectively.

In order to verify the observed differences in the changes of the protein composition of preribosomes purified from cells depleted of rpL8 on the one hand and the members of the "rpL7 surrounding group" (rpL7, rpL6, rpL14, rpL16, rpL20, rpL32, rpL33) on the other hand, and to eventually better visualize these differences, the protein composition of rpL8 depleted particles was directly compared to the one of rpL7 or rpL33 depleted particles using the same semi quantitative pair-wise comparative approach. Again, the mutant preribosomes were co-purified by Rpf2-TAP and/or Noc2-TAP. The results of these analyses are depicted in Figure 27. As expected, the differences in the levels of the two depleted LSU r-proteins were most intense (rpL7 vs. rpL8 – Figure 27A) or among the most intense (rpL33 vs. rpL8 – Figure 27 B,C) in the direct pair-wise comparisons. In line with this, the LSU r-proteins which were specifically underrepresented in the *RPL8* mutants and the ones which were specifically underrepresented in the *RPL7* or *RPL33* mutants were clustering on the opposite sides among the group of all (identified) LSU r-proteins. In all cases, rpL13, rpL15, and rpL36 were clearly "clustering" with rpL8, strongly confirming the specificity of their underrepresentation in the *RPL8* mutant. On the other hand, rpL14, rpL20, and (less consistent) rpL6, rpL33, and rpL32 were most specifically affected in the *RPL7* or *RPL33* mutants. The before observed rather independent assembly behavior of rpL3, rpL4, rpL18, and rpL7 could be also observed in these direct comparisons in which the levels of these r-proteins were in the range of the mean level of all LSU r-proteins. In line with this, LSU r-proteins like rpL2, rpL43, rpL17, or rpL19 which tended to be affected in all cases (*RPL8* and *RPL7*/*RPL33* mutants) are positioned rather in the "middle" of the whole LSU r-protein group.

In summary, the presented data indicate that *in vivo* expression shut down of the analyzed "early" LSU r-proteins can be separated into specific (see above) and common effects, presumably mainly caused by the disturbed pre-rRNA processing at the level of 27SA2/ 27SA3 pre-rRNAs. LSU r-proteins whose association to the purified preribosomes was observed to be disturbed in all of the analyzed mutants might therefore be among the ones hat are establishing higher affinities to nascent preribosomes mainly after (or during) these disturbed pre-rRNA processing events. For the group consisting of rpL2, rpL43, and rpL39 clear evidences for an above-average affinity increase to pre-60S particles with processed 27S pre-rRNA species were provided from the experiments shown in section 0 (Figures 20 – 22). For the remaining LSU r-proteins that tended to be affected in all of the analyzed mutants (like rpL17, rpL19, rpL26) it might therefore be plausible that their affinity to preribosomes increases more than average during the processing of 27SA2pre-rRNA (via the 27SA3 pre-rRNA) to 27SB pre-rRNA. Alternatively their affinity to preribosomes of these

maturation states might in general be weaker and therefore more easily be disrupted after an essential LSU r-protein is depleted.

Besides the described differences in the changes of the LSU r-protein composition of preribosomes purified from the individual *RPL* mutant yeast cells, changes in the composition of LSU biogenesis factors in the purified preribosomes were analyzed as well. The results of these studies are depicted in Figures 27 (lower panels), 28, and 29. As mentioned above, some LSU biogenesis factors behaved similar in all analyzed expression mutants. The levels of those factors that function in earlier pre-rRNA processing steps, as Rrp5, Noc1, and Nop4, tended to be unchanged or even increased whereas factors that associate to further maturated pre-60S particles, as Rsa4, Nop53, Nog2, or Arx1 were underrepresented in all cases, especially when the preribosomes were purified with Rpf2-TAP (Figure 29). Another group of LSU biogenesis factors whose members were affected (if identified) after depletion of all tested "early" LSU r-proteins in the mutant preribosomes was arising also in the Noc2-TAP affinity purifications, in which the later (7S pre-rRNA) associating factors are normally not identified (Figure 28). It consisted of Nug1, Dbp10, Spb1, Spb4, Nsa1, and Nsa2, all of which are essential in yeast. They all were described to be involved in processing of 27SB pre-rRNAs and/or later pre-60S maturation events (Bassler et al., 2001; Burger et al., 2000; de la Cruz et al., 1998; García-Gómez et al., 2011; Kressler et al., 1999, 2008; Lebreton et al., 2006b). Therefore it seems unlikely that the "early" pre-rRNA processing phenotype that is shared by the analyzed LSU r-proteins is in general caused by a disturbed recruitment of one or more than one LSU biogenesis factors that are required for the same pre-rRNA processing events that are disturbed in the absence of the analyzed r-proteins.

Figure 28 (next page) - Analyses of the changes of the LSU biogenesis factor levels in pre-60S particles purified via Noc2-TAP after *in vivo* depletion of selected "early" (class 1) LSU r-proteins

The presented data derive from the same experiments which are described in detail in Figure 25 but now focusing on the changes of the levels of the identified LSU ribosome biogenesis factors. All iTRAQ ratios were normalized to the bait protein Noc2-TAP, which is highlighted by a gray box. In parenthesis, the number of different tryptic peptides by which the respective biogenesis factors was in average identified is given. The iTRAQ values of LSU biogenesis factors that were not or not always identified (or with only one peptide) are depicted in the lower panels. See legend box below the heat maps for more details.

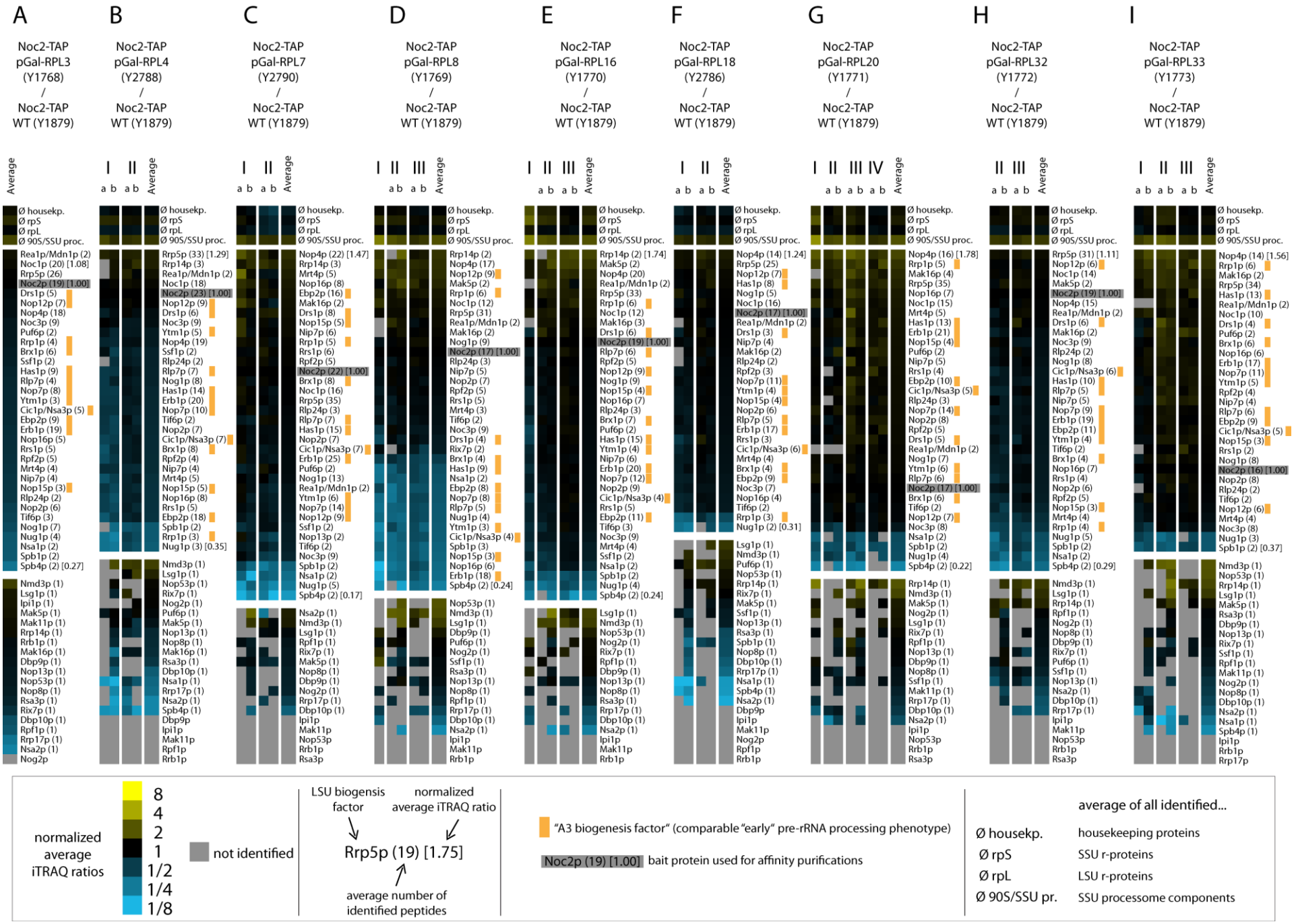
A
Noc2-TAP pGal-RPL3 (Y1768) / Noc2-TAP WT (Y1879)
B
Noc2-TAP pGal-RPL4 (Y2788) / Noc2-TAP WT (Y1879)
C
Noc2-TAP pGal-RPL7 (Y2790) / Noc2-TAP WT (Y1879)
D
Noc2-TAP pGal-RPL8 (Y1769) / Noc2-TAP WT (Y1879)
E
Noc2-TAP pGal-RPL16 (Y1770) / Noc2-TAP WT (Y1879)
F
Noc2-TAP pGal-RPL18 (Y2786) / Noc2-TAP WT (Y1879)
G
Noc2-TAP pGal-RPL20 (Y1771) / Noc2-TAP WT (Y1879)
H
Noc2-TAP pGal-RPL32 (Y1772) / Noc2-TAP WT (Y1879)
I
Noc2-TAP pGal-RPL33 (Y1773) / Noc2-TAP WT (Y1879)
normalized average iTRAQ ratios
8
4
2
1
1/2
1/4
1/8
not identified
LSU biogenesis factor
normalized average iTRAQ ratio
Rrp5p (19) [1.75]
average number of identified peptides
"A3 biogenesis factor" (comparable "early" pre-rRNA processing phenotype)
Noc2p (19) [1.00] bait protein used for affinity purifications
average of all identified...
Ø housekp. housekeeping proteins
Ø rpS SSU r-proteins
Ø rpL LSU r-proteins
Ø 90S/SSU pr. SSU processome components

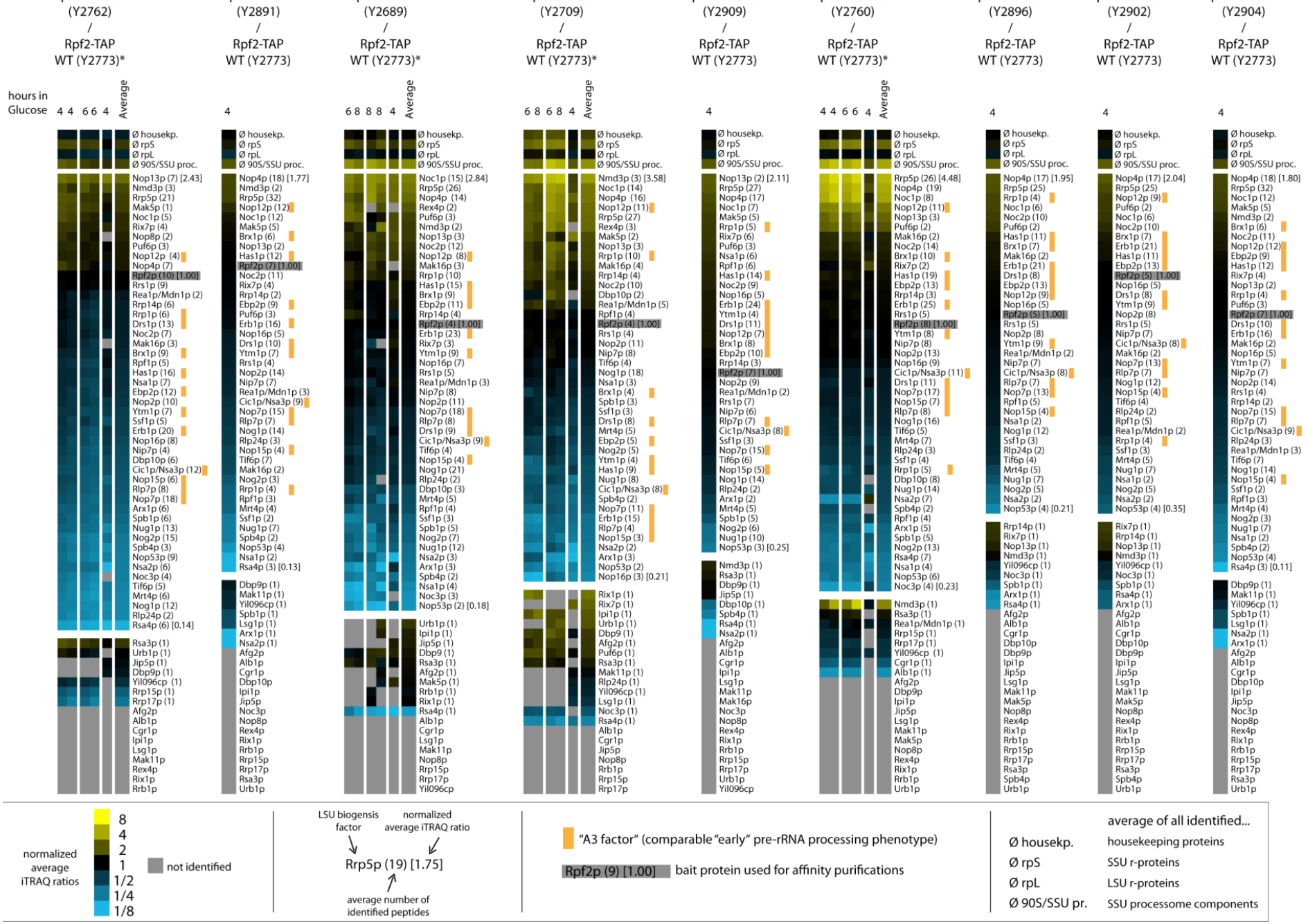
A
Rpf2-TAP pGal-RPL3 (Y2762) / Rpf2-TAP WT (Y2773)*
hours in Glucose
4 4 6 6 4 Average
B
Rpf2-TAP pGal-RPL4 (Y2891) / Rpf2-TAP WT (Y2773)
4
C
Rpf2-TAP pGal-RPL7 (Y2689) / Rpf2-TAP WT (Y2773)*
6 8 8 8 4 Average
D
Rpf2-TAP pGal-RPL8 (Y2709) / Rpf2-TAP WT (Y2773)*
6 8 6 8 4 Average
E
Rpf2-TAP pGal-RPL16 (Y2909) / Rpf2-TAP WT (Y2773)
4
F
Rpf2-TAP pGal-RPL18 (Y2760) / Rpf2-TAP WT (Y2773)*
4 4 6 6 4 Average
G
Rpf2-TAP pGal-RPL20 (Y2896) / Rpf2-TAP WT (Y2773)
4
H
Rpf2-TAP pGal-RPL32 (Y2902) / Rpf2-TAP WT (Y2773)
4
I
Rpf2-TAP pGal-RPL33 (Y2904) / Rpf2-TAP WT (Y2773)
4
normalized average iTRAQ ratios
8
4
2
1
1/2
1/4
1/8
not identified
LSU biogensis factor
normalized average iTRAQ ratio
Rrp5p (19) [1.75]
average number of identified peptides
"A3 factor" (comparable "early" pre-rRNA processing phenotype)
Rpf2p (9) [1.00] bait protein used for affinity purifications
average of all identified...
Ø housekp. housekeeping proteins
Ø rpS SSU r-proteins
Ø rpL LSU r-proteins
Ø 90S/SSU pr. SSU processome components

Figure 29 (previous page) - Analyses of the changes of the LSU biogenesis factor levels in pre-60S particles purified via Rpf2-TAP after *in vivo* depletion of selected "early" (class 1) LSU r-proteins

The presented data derive from the same experiments which are shown in Figure 26 but now focusing on the changes of the levels of the identified LSU ribosome biogenesis factors. All iTRAQ ratios were normalized to the bait protein Rpf2-TAP, which is highlighted by a gray box. In parenthesis, the number of different tryptic peptides by which the respective biogenesis factors was in average identified is given. The iTRAQ values of LSU biogenesis factors that were not or not always identified (or with only one peptide) are depicted in the lower panels. See legend box below the heat maps. For more experimental details see also legend of Figure 25.

An interesting question in these analyses was whether differences for some LSU biogenesis factors could be observed within the analyzed r-protein expression mutants, as they were observed for some LSU r-proteins. In case differences could be observed, several interesting conclusions might be deducible. If for example a certain LSU biogenesis factor co-behaves with certain LSU r-proteins (in terms of their changed levels in purified preribosomes after r-protein depletion) it is plausible that this LSU biogenesis factor might interact (directly or indirectly) with one or more of the respective LSU r-proteins on nascent ribosomes (even if the interaction of some ribosome biogenesis factors to (pre-)rRNA can occur independent of r-proteins). So far, the binding sites for only a few LSU biogenesis factors are described (see 2.2) whereas the position of all LSU r-proteins (in the mature LSU) is resolved in high resolution (Ben-Shem et al., 2011). If in addition this "co-affected" LSU biogenesis factor had the same pre-rRNA processing phenotype, the molecular reason for the pre-rRNA processing phenotype might be better understandable. A number of LSU biogenesis factors (sometimes also termed "A3 factors") that exhibit the same pre-rRNA processing phenotype have been described in the literature (see citations in section 2.2.6.2). In all of the pair wise particle comparisons, all of these described biogenesis factors could be identified reproducibly in the mass spectrometry analyses with numerous (≥3) different peptides what confirms the association of these factors to the analyzed "early" LSU precursors and also allowed the calculation of a more significant average iTRAQ ratio. As mentioned above, none of them was found to be strongly underrepresented in preribosomes purified from **all** LSU r-protein expression mutants. Therefore it is unlikely that the common "early" pre-rRNA processing phenotype of this group of LSU r-proteins is in all cases caused by the disturbed recruitment of one or more than of these "A3" biogenesis factors.

However, differences in the behavior of the identified LSU biogenesis factors (including the "A3 factors") were observed and will be described in the following. After depletion of the individual members of the above described "rpL7 cluster" (rpL7, rpL16, rpL20, rpL32, and rpL33), which are all bound in proximity to each other mainly in LSU domains II and VI, beside the above described commonly affected LSU biogenesis factors, no additional factors were strongly affected (Figures 28 and 29 C, E, G, H, I). The only exception was the *RPL32* mutant, whose purified preribosomes contained significantly reduced levels of Rrp1, a biogenesis factor that was described to be required for the efficient production of 27SB pre-rRNA (Figures 28H, 29H) (Horsey et al., 2004). Interestingly, the preribosomes purified from *RPL4* and *RPL18* mutants showed the same effect (Figures 28 and 29, B, F). The analyses shown above (Figures 25 and 26) indicated that the stable incorporation of rpL4 and rpL18 likely occurs independent of each other and of rpL32 but the association of rpL32 itself was

affected to some extents after depletion of rpL4 and rpL18. The fact that these three LSU r-proteins are bound in very close proximity to each other at one of the junctions of LSU domains I and II and the finding that the binding of Rrp1 was only significantly affected after depletion of these three LSU r-proteins suggests that the interaction site of Rrp1 to nascent preribosomes might be in proximity of this substructure possibly depending of its correct fold. Consequently, in these three mutants, the cause of the pre-rRNA processing phenotype might (at least in parts) be explained by their disturbed ability to bind the “A3 factor” Rrp1.

As described above, the preribosomes purified from rpL8 depleted cells differed most (in terms of the changes of their LSU r-protein levels) from the ones purified from cells depleted of the other tested LSU r-proteins (Figure 27A-C, upper panels). As shown in Figures 28D and 29D, these mutant preribosomes also differed most in terms of the changes of their LSU biogenesis factor content. The levels of ten of the 12 described “A3 factors” were significantly reduced in the preribosomes purified from the *RPL8* mutants. Among them were Erb1, Has1, Nop15, Ytm1, Rlp7, Ebp2, Nop7, Brx1, Cic1/Nsa3, and (a bit less consistent) Drs1. Only one additional (so far poorly characterized) LSU biogenesis factor, Nop16, was strongly underrepresented in the *RPL8* mutant. To confirm the specificity of the disturbed association of these 11 LSU biogenesis factors (10 “A3 factors” and Nop16) to preribosomes purified from rpL8 depleted cells they were again directly compared to preribosomes from rpL7, and rpL33 depleted cells, focusing now on the identified LSU biogenesis factors (Figure 27A-C, lower panels). These direct comparisons strongly confirmed the differences of the rpL8 depleted preribosomes in regard to preribosomes depleted of the other r-proteins, as they were also observed in terms of their LSU r-protein content (Figure 27A-C, upper panels).

Since rpL8 and the specifically affected group of LSU r-proteins (rpL13, rpL15, and rpL36) are bound in proximity to each other mainly contacting LSU domains I (with the 5.8S rRNA) and V, their reduced association might be the (direct or indirect) reason for the observed specific underrepresentation of the group of 10 “A3 factors” and Nop16. Some of them might be directly interacting with one or more of the affected LSU r-proteins or their binding might depend on the correct folding of LSU domain I substructures. The identification of the binding site for several of them was addressed by an RNA cross linking approach (CRAC) and could be dissolved for Erb1 (25S rRNA domain I) and Nop7 (25S rRNA domain III, in proximity to the contact area to domain I and the 5.8S rRNA) (Granneman et al., 2011). Nop15, Cic1/Nsa3 (Granneman et al., 2011), and Rlp7 (Dembowski et al., 2013b) were cross linking to ITS2 spacer sequences which are connecting the 3’ end of the 5.8S rRNA sequences to the 5’ end of the 25S rRNA sequences in premature ribosomes. Detailed structural information of the ITS2 sequences in preribosomes is lacking and limited to predictions from some chemical probing data but the position of its two ends are located very close to each other and in close proximity to rpL8 (in the mature LSU). Therefore it is plausible that rpL8 (and/or biogenesis factors interacting with rpL8) might be somehow required for the correct folding of the ITS2 substructures. In case it is depleted, the ITS2 structure might be de-stabilized resulting in the observed reduced ability of the “A3 factors” (Nop15, Cic1/Nsa3, and Rlp7) to bind to these structures in pre-mature 60S particles.

The levels of Nop12, the remaining factor of the described group of “A3 factors” were not (or only very mildly) reduced after depletion in either of the tested *RPL* mutants (Figures 28 - 29). In many cases its levels even increased in comparison to wild type preribosomes. Even if it is non-essential in yeast it was described to be involved in efficient production of 25S rRNA synthesis (Wu et al., 2001). Its binding site was also addressed (Granneman et al., 2011, see also Figure 9B) and it cross-linked to 5.8S rRNA sequences and domain I sequences of the 5’ end of the 25S rRNA which (in mature LSUs) are forming a helix with sequences of the 3’ end of the 5.8S rRNA.

This helix, which was termed “ITS2 proximal stem” (Peculis and Greer, 1998 and citations therein), is in very close proximity to rpL8 and rpL15 and is in parts directly contacting both. Still, the levels of Nop12 were not observed to be affected after depletion of rpL8 what clearly argues for an independent recruitment of Nop12 to early preribosomes in which the final conformation in this area is presumably not yet fully established. In fact, the conformation of the ITS2 (and the ITS2 proximal stem) was described to change during pre-rRNA processing from a rather open and accessible “ring” structure to a closed “hairpin” structure (Joseph et al., 1999; Peculis and Greer, 1998; Yeh and Lee, 1990).

In summary, the presented data provide clear evidences for different effects on the association of LSU ribosome biogenesis factors after deletion of “early” acting LSU r-proteins. While after depletion of rpL7, rpL16, rpL20, and rpL33 no strong effects on “A3-cluster –proteins” (LSU ribosome biogenesis factors that have the same early pre-rRNA processing phenotype) could be observed, depletion of rpL4, rpL18, and rpL32 resulted in a reduced association of Rrp1 to preribosomes. On the other hand, RPL8 expression shut down resulted in a reproducible and significant decrease in the levels of 11 specific LSU biogenesis factors, 10 of which belonging to the “A3-factor” group.

3.3.3 Changes in the protein composition of LSU precursor particles in r-protein expression mutants with a “middle” (class 2) pre-rRNA processing phenotype

Seven of the nine “class 2” LSU r-proteins after whose depletion steady state levels of 7S pre-rRNA significantly decrease when compared to the levels of its precursor, the 27SB pre-rRNA (resulting from a disturbed cleavage of 27SB pre-rRNAs in the ITS2 at site C2), are located in proximity to each other with main contacts to LSU rRNA domains III, I (5.8S), and IV (Figure 23). Among them are rpL19, rpL25, rpL27, rpL31, rpL34, rpL35, and rpL37. Even if structural information of pre-60S particles of “intermediate” maturation state is very limited, the two ends of the ITS2 (3’ end of 5.8S rRNA and 5’ end of 25S rRNA) are (in the mature LSU) positioned very close to each other and near these 7 LSU r-proteins. The remaining

two (rpL9 and rpL23) are positioned further apart from this cluster connecting LSU domains II, IV, and V (rpL9) or IV, V, and VI (rpL23) – see also Figure 44. In order to systematically analyze potential hierarchical interrelationships of these LSU r-proteins in regard to each other and to the other LSU r-proteins, changes in the composition of preribosomes purified from cells depleted of either of these LSU r-proteins were aimed to be characterized applying the same comparative approach used above (3.3.2).

Since the pre-rRNA processing phenotype of the LSU r-proteins expression mutants of this class (class 2) is "later" as the one of the above analyzed mutants (class 1), two different LSU biogenesis factors, that were shown to interact with "later" populations were used as bait protein for the affinity purifications. The first, Nog1 stays associated to intermediate to late LSU precursors (Saveanu et al., 2003). The second, Nop7 is interacting with the same intermediate to late nuclear LSU precursors but is, in contrast to Nog1, not exported to the cytoplasm (Altvater et al., 2012; Baßler et al., 2012; Bassler et al., 2010; Oeffinger et al., 2002). Yeast strains that conditionally express one of the LSU r-proteins of interest and in addition are genetically modified to express a chromosomally encoded TAP tagged version of Nog1 or Nop7 were created and grown for four or six hours in restrictive conditions to shut down expression of the respective LSU r-protein. Nog1-TAP (or Nop7-TAP) and associating preribosomes were affinity purified from the corresponding cellular extracts and their protein content was compared in a semi quantitative way to preribosomes from "wild type" yeast cells co-purified *ex-vivo* by Nog1-TAP (or Nop7-TAP). The results are depicted in Figures 30 -32. Again, parts of the cellular extract ("Input") and of the affinity purified ("IP") fractions were used to isolate and analyze the RNA content of by Northern blotting. After expression shut down of the 7 analyzed LSU r-proteins, the observed pre-rRNA processing phenotypes were consistent with the expected and above described ones. While steady state levels of 27S pre-rRNAs were similar or increased in comparison to the wild type situation, 7S pre-RNAs levels were significantly decreased (Figure 30A, compare 7S over 27S pre-rRNA ratios in lanes 2-5 to the one in lane 1; Figure 31A, compare lanes 3-4, 11-12, 19-20 to lanes 1-2, 9-10, 17-18). Importantly, the binding of the bait proteins to preribosomes was apparently not (or not strongly) affected after depletion of either of the analyzed r-proteins (Figures 30A; 31A).

Changes in the protein composition of the affinity purified preribosomes could be detected. The focus will first be set on the LSU r-proteins (Figures 30B-E; 31B-D) and then on the LSU biogenesis factors (Figure 32). As expectable, the depleted LSU r-protein was among the most underrepresented among all identified LSU r-proteins in each of the analyzed mutants (Figures 30B-E; 31B-D, highlighted by red boxes). In most cases, the association of a set of in part similar and in part specific LSU r-proteins was co-affected. Very consistently, levels of rpL2, rpL39, and rpL43 were reduced in all analyzed mutants (Figures 30B-E, and 31B-D, highlighted in purple). These three are the members of the group of LSU r-proteins whose affinity to preribosomes seemed to increase more than average after the processing of the 27S pre-rRNAs (Figures 20-22 "group 2"). The disturbed pre-rRNA processing at this step observed in these mutants could therefore explain their underrepresentation. Besides these

three, the association of some more LSU r-proteins tended to be affected in all cases, albeit to substantially less extents and also less consistent. Among them were rpL19, rpL31, rpL28, and (if identified) rpL21 and rpL29. Interestingly, the levels of the Phospho-stalk proteins rpP0, rpP1A/B, and rpP2A/B were in all cases higher in the mutant preribosomes than in the corresponding wild type preribosomes. Both, the results of this work (shown in Figure 20B) and previously published results (Bradatsch et al., 2012; Kemmler et al., 2009; Lo et al., 2009; Rodríguez-Mateos et al., 2009a) argued for a stable incorporation of the phospho stalk proteins at rather late, presumably mainly cytoplasmic LSU maturation stages. Whether this commonly observed effect (it was also observed in the analyses of the “early” LSU r-protein mutants; Figures 25 and 26) is significant or due to putative effects caused by the experimental procedure (for instance, cell compartmentalization is lost in the cellular extracts) remains unclear. It might also be plausible that in the case of a delayed maturation (pre-rRNA processing), as observed in the LSU r-protein expression mutants, the phospho stalk proteins are imported (or diffusing) into the nucleus and start associating with a nuclear population of preribosomes. For one of the ribosomal stalk components, rpP0 this behavior was recently described under certain conditions, why an “alternative”, nuclear pathway for the ribosomal stalk assembly was suggested (Francisco-Velilla et al., 2013; Rodríguez-Mateos et al., 2009a). Another common and noteworthy observation in all seven analyzed LSU r-protein expression mutants was that the group of 10 LSU r-proteins showing an “early” (class 1) pre-rRNA processing phenotype (see 3.3.2) was not (or only very moderately) affected indicating that their stable association to preribosomes does not depend on any of the tested “class 2” LSU r-proteins.

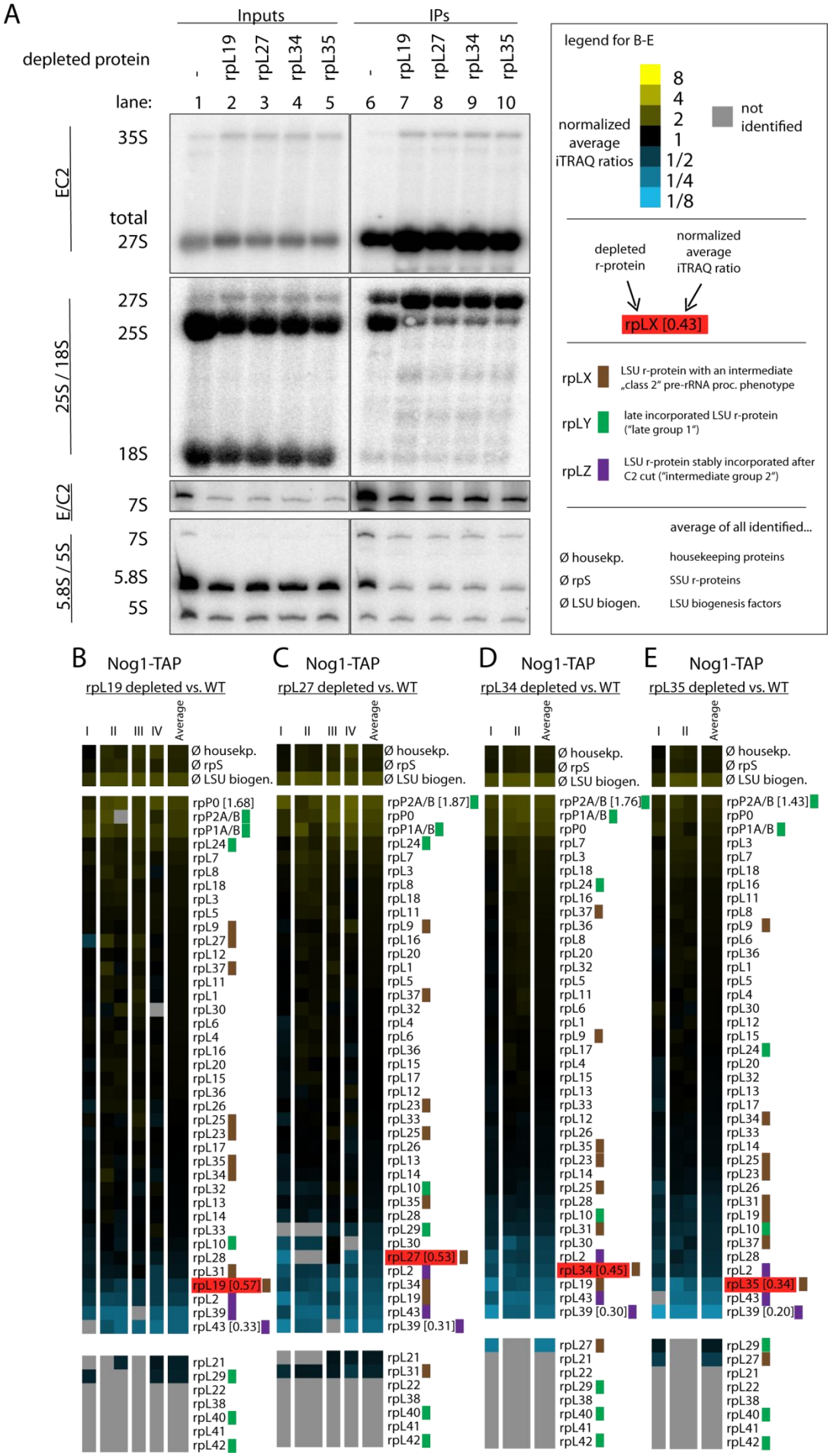
A
Inputs
IPs
depleted protein
-
rpL19
rpL27
rpL34
rpL35
lane:
1 2 3 4 5 6 7 8 9 10
EC2
35S
total
27S
25S / 18S
27S
25S
18S
E/C2
7S
5.8S / 5S
7S
5.8S
5S
legend for B-E
normalized average iTRAQ ratios
8
4
2
1
1/2
1/4
1/8
not identified
depleted r-protein
normalized average iTRAQ ratio
rpLX [0.43]
rpLX
LSU r-protein with an intermediate „class 2" pre-rRNA proc. phenotype
rpLY
late incorporated LSU r-protein ("late group 1")
rpLZ
LSU r-protein stably incorporated after C2 cut ("intermediate group 2")
average of all identified...
Ø housekp.
housekeeping proteins
Ø rpS
SSU r-proteins
Ø LSU biogen.
LSU biogenesis factors
B Nog1-TAP
rpL19 depleted vs. WT
C Nog1-TAP
rpL27 depleted vs. WT
D Nog1-TAP
rpL34 depleted vs. WT
E Nog1-TAP
rpL35 depleted vs. WT
I II III IV Average
Ø housekp.
Ø rpS
Ø LSU biogen.
rpP0 [1.68]
rpP2A/B
rpP1A/B
rpL24
rpL7
rpL8
rpL18
rpL3
rpL5
rpL9
rpL27
rpL12
rpL37
rpL11
rpL1
rpL30
rpL6
rpL4
rpL16
rpL20
rpL15
rpL36
rpL26
rpL25
rpL23
rpL17
rpL35
rpL34
rpL32
rpL13
rpL14
rpL33
rpL10
rpL28
rpL31
rpL19 [0.57]
rpL2
rpL39
rpL43 [0.33]
rpL21
rpL29
rpL22
rpL38
rpL40
rpL41
rpL42
rpP2A/B [1.87]
rpP0
rpP1A/B
rpL24
rpL7
rpL3
rpL8
rpL18
rpL11
rpL9
rpL16
rpL20
rpL1
rpL5
rpL37
rpL32
rpL4
rpL6
rpL36
rpL15
rpL17
rpL12
rpL23
rpL33
rpL25
rpL26
rpL13
rpL14
rpL10
rpL35
rpL28
rpL29
rpL30
rpL27 [0.53]
rpL2
rpL34
rpL19
rpL43
rpL39 [0.31]
rpL21
rpL31
rpL22
rpL38
rpL40
rpL41
rpL42
rpP2A/B [1.76]
rpP1A/B
rpP0
rpL7
rpL3
rpL18
rpL24
rpL16
rpL37
rpL36
rpL8
rpL20
rpL32
rpL5
rpL11
rpL6
rpL1
rpL9
rpL17
rpL4
rpL15
rpL13
rpL33
rpL12
rpL26
rpL35
rpL23
rpL14
rpL25
rpL28
rpL10
rpL31
rpL30
rpL2
rpL34 [0.45]
rpL19
rpL43
rpL39 [0.30]
rpL27
rpL21
rpL22
rpL29
rpL38
rpL40
rpL41
rpL42
rpP2A/B [1.43]
rpP0
rpP1A/B
rpL3
rpL7
rpL18
rpL16
rpL11
rpL8
rpL9
rpL6
rpL36
rpL1
rpL5
rpL4
rpL30
rpL12
rpL15
rpL24
rpL20
rpL32
rpL13
rpL17
rpL34
rpL33
rpL14
rpL25
rpL23
rpL26
rpL31
rpL19
rpL10
rpL37
rpL28
rpL2
rpL35 [0.34]
rpL43
rpL39 [0.20]
rpL29
rpL27
rpL21
rpL22
rpL38
rpL40
rpL41
rpL42

Figure 30 (previous page) - Analyses of the (pre-) rRNA content and changes in LSU r-protein levels of mutant preribosomes depleted of various LSU r-proteins with a "middle" (class 2) pre-rRNA processing phenotype.

LSU precursors of intermediate to late maturation stages were affinity purified *ex vivo* from wild type cells or cells depleted for four hours of the indicated LSU r-proteins using Nog1-TAP as bait protein in a similar way as described in the legends of Figures 24 and 25 and in section 5.2.6.1. The analysis of the (pre-) rRNA content is depicted in **A)**. **B)-E)** show the changes in LSU r-protein levels of preribosomes purified from rpL19, rpL27, rpL34, or rpL35 depleted cells, in comparison to the respective Nog1-TAP wild type particles. The depleted protein is highlighted by a red box and the remaining class 2 LSU r-proteins are marked in brown, see legend box for more details.

Figure 31 (next page) - Analyses of the (pre-) rRNA content and changes in LSU r-protein levels mutant preribosomes depleted of other LSU r-proteins with a "middle" (class 2) pre-rRNA processing phenotype.

The same experimental procedure as described in the legend of Figure 30 was applied with the following modifications. Here, Nop7-TAP was used as bait protein for the affinity purifications. The corresponding wild type LSU precursors were purified from cellular extracts of the same yeast strains which were grown to the same OD_{600} in permissive conditions (galactose containing medium). The depletion time (growth in restrictive conditions (= glucose containing medium)) are indicated above the northern blots in **A)** and above the heat maps in **B)-D)**. See legend box on the right, section 5.2.6.1 and legends of Figures 24, 25, and 30 for more details. Parts of the presented data are published in Gamalinda et al. (2014).

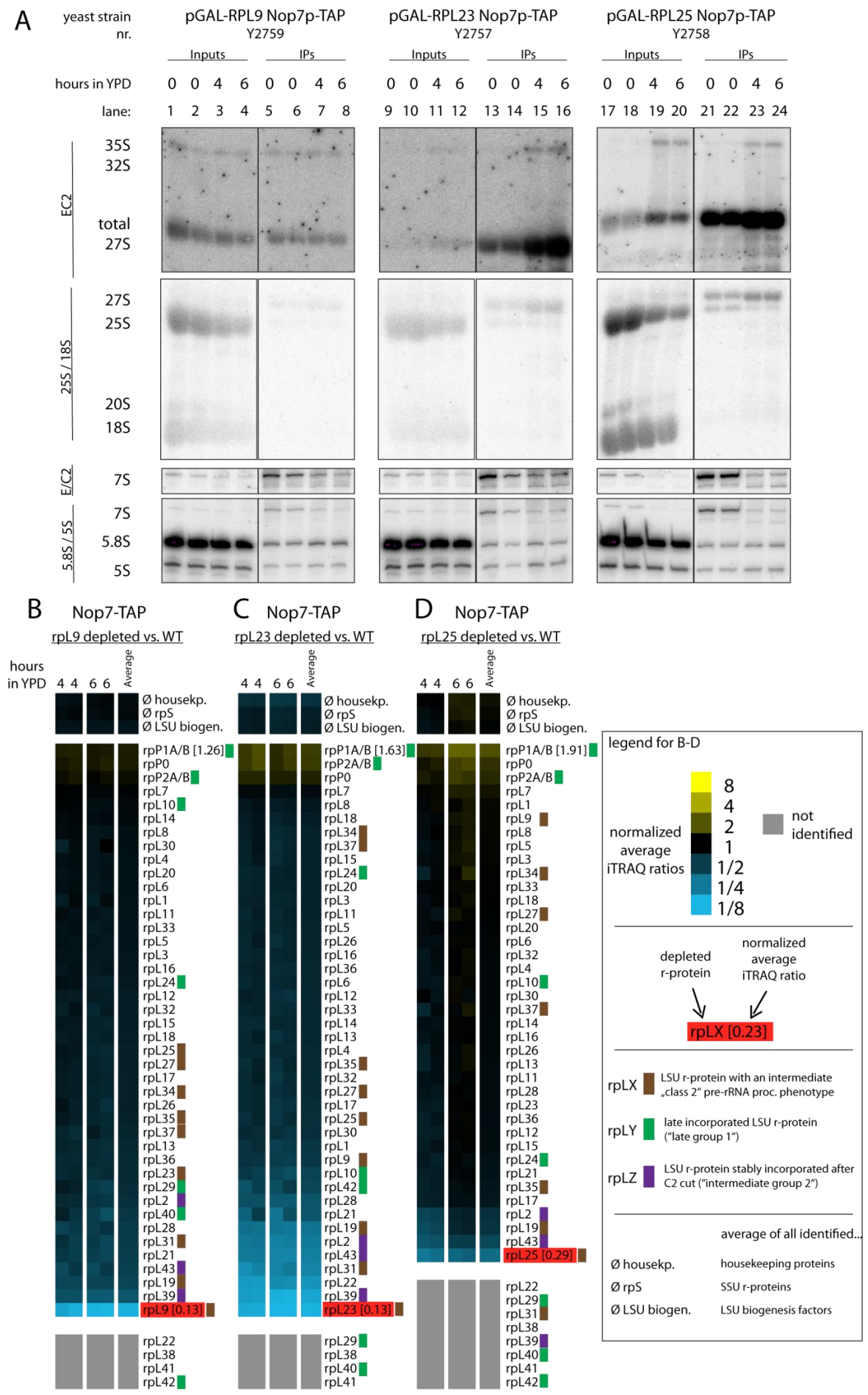
A
yeast strain nr.
pGAL-RPL9 Nop7p-TAP Y2759
pGAL-RPL23 Nop7p-TAP Y2757
pGAL-RPL25 Nop7p-TAP Y2758
Inputs
IPs
hours in YPD
lane:
EC2
35S
32S
total 27S
25S / 18S
27S
25S
20S
18S
E/C2
7S
5.8S / 5S
7S
5.8S
5S
B Nop7-TAP rpL9 depleted vs. WT
C Nop7-TAP rpL23 depleted vs. WT
D Nop7-TAP rpL25 depleted vs. WT
hours in YPD
Average
Ø housekp.
Ø rpS
Ø LSU biogen.
rpL9 [0.13]
rpL23 [0.13]
rpL25 [0.29]
legend for B-D
normalized average iTRAQ ratios
not identified
depleted r-protein
normalized average iTRAQ ratio
rpLX [0.23]
rpLX LSU r-protein with an intermediate „class 2" pre-rRNA proc. phenotype
rpLY late incorporated LSU r-protein ("late group 1")
rpLZ LSU r-protein stably incorporated after C2 cut ("intermediate group 2")
average of all identified...
Ø housekp. housekeeping proteins
Ø rpS SSU r-proteins
Ø LSU biogen. LSU biogenesis factors

Besides these commonly observed effects on certain LSU r-proteins, additional, specific effects were observed and will be described in the following. While association of rpL19 was affected in all analyzed mutants (to varying extents), its own depletion did not show clear effects on any of the six other tested LSU r-protein of this phenotypic class (Figure 30B). The only clear effects could be detected for those LSU r-proteins which were commonly underrepresented (as the rpL2/43/39 group, rpL31, rpL28, and, less stringent, rpL21, and rpL29). This finding that the association of rpL19 to mutant preribosomes seems to be disturbed after depletion of all tested LSU r-proteins of this phenotypic class suggests that its stabilized incorporation into pre-60S particles might occur at later, "downstream" stages, possibly concomitant with the cleavage in the ITS2 (as suggested for the rpL2/39/43 group).

The comparative proteomic analyzes on differently maturated preribosomes shown above (see 3.2.1 and Figure 20B) to some extent support this idea since rpL19 was, beside the rpL2/39/43 group among the most underrepresented in "pre C2" (27SB pre-rRNA containing) versus "post C2" (25.5S and 7S pre-rRNAs containing) pre-60S particles (Figure 20B, lanes 1-9). These evidences were, however much less clear as for rpL2, rpL43, and rpL39. In addition, the results of the complementary approach of directly affinity purifying selected LSU r-proteins and quantifying the co-purified pre-rRNA species (shown in section 3.2.2 and Figures 21-22) did not provide any further evidences for this hypothesis since the 7S over 27S pre-rRNA ratio of FLAG-rpL19 was not higher than the one of most of the other tested LSU r-proteins (Figures 21 and 22C). In the mature ribosome, rpL19, which has a rather "stretched" than globular conformation, contacts LSU rRNA domains III, IV, and VI, those LSU domains to which the LSU r-proteins of this phenotypic class are mainly bound. In addition, its C-terminus protrudes into the SSU with more than 40 amino acids (Figure 23). Whether this conformation of the C-terminus of rpL19 is already established when it is incorporated to LSU precursors is unclear, though. The establishment of its contacts to all of the three LSU rRNA domains might be important for its stable association to preribosomes. In case one or more than one of these contacts get (partially) disrupted (or cannot be established any longer), as possible consequence of depletion of LSU r-proteins, its affinity to the mutant preribosomes might be weakened. Interestingly, in line with this, rpL31, whose binding was (as the one of rpL19) affected in all tested mutants, contacts the same three LSU rRNA domains (see also Figure 44).

The association of both, rpL25 and rpL35 to preribosomes was only moderately affected after depletion of any of the other tested LSU r-proteins suggesting that their assembly largely occurs independently. Since (in the mature LSU) both proteins contact each other via a large contact area it appears plausible that their assembly might occur interdependent of each other. However, depletion of rpL35 affected levels of rpL25 only very mildly and not stronger than the ones of a larger group of other LSU r-proteins (Figure 30E). The observations in case of rpL25 depletion were very similar, only showing weak effects on levels of rpL35 which were also seen for a larger group of LSU r-proteins (Figure 31D). Together, these observations suggest that the assembly of both, rpL25 and rpL35 largely occurs

independently of each other and of other LSU r-proteins, even if they contact each other in mature LSUs.

Rpl37, whose association to the analyzed mutant preribosomes was only observed to be reproducibly weakened after depletion of rpL35, but not after depletion of the other members of this phenotypic class, is bound to LSU domains I (5.8S), II, and III in proximity to rpL35 (Figures 30, 31). Both directly contact each other via a small contact surface (see also Figure 44C). Whether this rather weak, but specific effect of rpL35 depletion on rpL37 association is invertible, (hence also observable for rpL35 association after rpL37 depletion) remains unclear since no appropriate yeast strain to test this hypothesis was available.

After depletion of rpL27, besides the commonly affected r-proteins, strong effects were seen on levels of rpL34 and rpL30 (Figure 30C). Interestingly, these three LSU r-proteins directly contact each other in LSU domains III and V (Figure 44). RpL34 depletion showed the same effect: beside the commonly affected group of r-proteins these three, directly interacting proteins were affected most (Figure 30E, see lower panel). Whether or not rpL30, which is essential in yeast, is required for stable association of rpL27 and rpL34 could not be tested since the appropriate conditional yeast strain remains to be created. Altogether these data suggest that in this case the stable incorporation of a group of directly interacting proteins seems to be interdependent.

Neither rpL9 (which interacts with LSU domains II, V, and VI) nor rpL23 (LSU domains IV, V, and VI) are in close proximity of other LSU r-proteins with the same pre-rRNA processing phenotype. They also don't directly contact each other (Figure 44). In addition, among all members of this phenotypic class, these two are most distant (almost on the "opposite" side) from the two ends of the ITS2 (3' end of 5.8S rRNA and 5' end of 25S rRNA), whose processing is disturbed (at site C2) after their depletion. Still, they do exhibit this phenotype, even if they are that far apart and surrounded by LSU r-proteins that have a different or no pre-rRNA processing phenotype. After depletion of rpL9, besides rpL9 itself, whose levels were strongly reduced (to about 1/8 in average), levels of all other identified LSU r-proteins (except the phospho stalk proteins) were also reduced, albeit to much less extents (Figure 31B). This argues for a slightly reduced co-purification efficiency of preribosomes via Nop7-TAP in the *RPL9* mutant. However, no evidences for a more pronounced reduction of the levels of any of the other LSU r-proteins with this phenotype were provided by these experiments. Depletion of rpL23 also resulted in a strong reduction in levels of rpL23 itself (average iTRAQ ratio of 0.13), but in addition, the levels of the group of commonly affected LSU r-proteins (rpL2/39/43 group, rpL19, rpL31 (rpL21, rpL28)) were also strongly reduced (Figure 31C). Levels of rpL22, which is bound to LSU domain III in proximity to rpL19 and rpL31 (Figure 23), were also strongly reduced but in all other analyzed mutants of this phenotype it was never identified. Therefore it remains unclear whether rpL22 is (as rpL19 and rpL31) also commonly affected or only (as observed) after depletion of rpL23. In contrast to rpL19, both, rpL22 and rpL31 are not strictly required for any pre-rRNA processing events since they are non-essential in yeast.

In summary, the observed changes in the LSU r-protein composition of preribosomes purified *ex-vivo* from cells depleted of the "class2" LSU r-protein expression mutants can be grouped into two different categories. While the association of a specific group of LSU r-proteins (rpL2, rpL39, rpL43, rpL19, rpL31, rpL28, rpL21, and rpL29) to the mutant preribosomes was affected in all analyzed expression mutants, some specific effects were observed. The general observation in these cases was that all of the specifically affected LSU r-proteins are located (in mature ribosomes) in close proximity to the LSU r-protein that had been depleted, often being bound to the same LSU rRNA domain or even directly contacting it. The members of the commonly affected group are only in some cases, but not always in proximity of the depleted r-protein. Therefore it appears plausible, that their underrepresentation might not be a direct consequence of the lack of the depleted r-protein itself but rather be explained by the disturbed pre-rRNA processing event, which is similar in all cases. These so to speak "phenotype specific" effects were also observed in the studies addressing the group of LSU r-protein with an "early" pre-rRNA processing phenotype shown above (section 3.3.2 and Figures 25-27).

Besides the observed changes in the LSU r-protein composition of preribosomes purified *ex vivo* from cells depleted of the LSU r-proteins of this class, the changes in levels of LSU biogenesis factors were also addressed (Figure 32). A group of LSU biogenesis factors was observed to be substantially underrepresented in preribosomes purified from all analyzed expression mutants. It consists of Nop53, Nog2, Rsa4, Arx1, and (if identified) Bud20, all of which are involved in "downstream" maturation events, as 7S pre-rRNA processing or nuclear export of pre-60S particles (Altvater et al., 2012; Baßler et al., 2012; Bradatsch et al., 2007; de la Cruz et al., 2005; Granato et al., 2005; Hung et al., 2008; Saveanu et al., 2001; Sydorskyy et al., 2005; Thomson and Tollervey, 2005). Interestingly, none of those LSU biogenesis factors that have been described to be required for 27S pre-rRNA processing (see 2.2.6.3 and citations therein) was affected in each of the seven analyzed LSU r-protein expression mutants of this phenotypic class. Levels of Spb4, a putative ATP-dependent RNA helicase which is also required for this pre-rRNA processing event (de la Cruz et al., 1998) tended to be (in parts strongly) affected after depletion of several (*RPL9, RPL23, RPL25, RPL34*), but not all (e.g. *RPL19*, *RPL35*) LSU r-protein expression mutants. Its identification by mass spectrometry was difficult and in most cases limited to only one peptide, what hampered more robust calculations of average iTRAQ ratios. According to these data, it appears therefore unlikely that the pre-rRNA processing phenotype all these LSU r-proteins share is simply due to the disturbed recruitment of one or more trans-acting LSU biogenesis factors that were shown to be required for the pre-rRNA processing step that is inhibited. However, significant differences in the changes of the LSU biogenesis factor composition could be observed within the seven analyzed *RPL* mutants that will be described in the following.

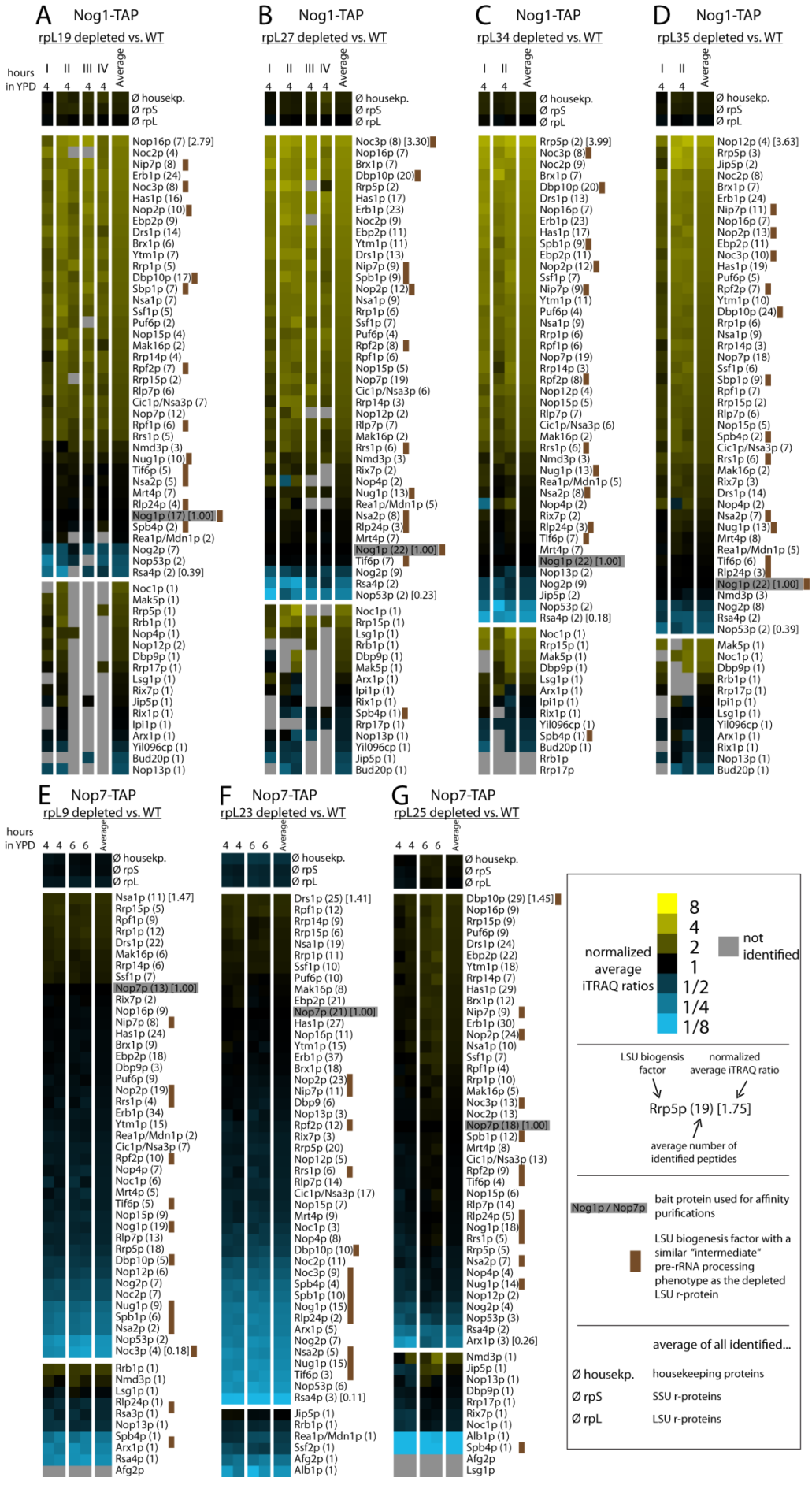
A Nog1-TAP
rpL19 depleted vs. WT
B Nog1-TAP
rpL27 depleted vs. WT
C Nog1-TAP
rpL34 depleted vs. WT
D Nog1-TAP
rpL35 depleted vs. WT
E Nop7-TAP
rpL9 depleted vs. WT
F Nop7-TAP
rpL23 depleted vs. WT
G Nop7-TAP
rpL25 depleted vs. WT
hours in YPD
Average
Ø housekp.
Ø rpS
Ø rpL
normalized average iTRAQ ratios
8
4
2
1
1/2
1/4
1/8
not identified
LSU biogensis factor
normalized average iTRAQ ratio
Rrp5p (19) [1.75]
average number of identified peptides
Nog1p / Nop7p
bait protein used for affinity purifications
LSU biogenesis factor with a similar "intermediate" pre-rRNA processing phenotype as the depleted LSU r-protein
average of all identified...
housekeeping proteins
SSU r-proteins
LSU r-proteins

Figure 32 (previous page) - Analyses of the changes of the LSU biogenesis factor levels in LSU precursors purified via Nog1-TAP or Nop7-TAP after *in vivo* depletion of selected "middle" (class 2) LSU r-proteins.

All shown data of this figure derive from experiments described and shown in Figures 30 and 31. Depicted here are the levels of all identified LSU ribosome biogenesis factors after depletion of the indicated LSU r-protein. All iTRAQ ratios were normalized to the used bait protein (Nog1-TAP in **A)** - **D)** or Nop7-TAP in **E)** - **G)**). The average number of identified peptides is given in parentheses. LSU biogenesis factors that have the same pre-rRNA processing phenotype as the depleted LSU r-protein (class 2) are highlighted in brown. See legends of previous Figures and box on the right for more details. Parts of the presented data are published in Gamalinda et al. (2014).

After depletion of rpL27 and rpL34 (which directly interact with each other and whose expression mutants behaved very similar in terms of the changes of their LSU r-protein compositions – see above) the preribosomal levels of one essential LSU biogenesis factor, the WD repeat protein Jip5, were observed to be specifically affected, albeit its detection was generally difficult and limited to 0-2 peptides (Figure 32B, C). On the other hand, in preribosomes purified from the *RPL35* mutant its levels were more than two-fold enriched (Figure 32D) while in the remaining mutants its levels were (if it was identified) rather unchanged (Figure 32A, E, F, G, see lower panels). The role of Jip5 in ribosome biogenesis was not investigated in detail but one study provided evidence for its physical interaction with ribosomal subunit (precursors) even if the majority of the Jip5-TAP population seemed to be in the free, non (pre-)ribosome co-sedimenting fractions of lower density (Li et al., 2009). In this study the pre-rRNA processing phenotype of Jip5 was also investigated and it was characterized by an accumulation of 27S/7S pre-rRNAs over the 5.8S rRNA suggesting a function in late nuclear stages of LSU maturation. The finding that only parts of TAP-tagged Jip5 co-sedimented with LSU (precursors) (Li et al., 2009) suggest that it might be interacting for a relatively short time and hence only present in a relatively small population of pre-60S particles co-purified by factors as Nog1-TAP or Nop7-TAP what is in line with its poor detection by mass spectrometry observed here. Alternatively, its affinity to (pre-)ribosomes might be very weak and therefore easily be disrupted in the biochemical procedures. Nonetheless, its apparently more reduced levels in the *RPL27* and *RPL34* mutants suggest that its interaction with preribosomes might occur via the neighborhood of rpL27 and rpL34 and presumably depend on the correct conformation of this structural neighborhood.

More clear and significant differences in the changes of the LSU r-protein composition were observed for the *RPL9* and the *RPL23* mutants (Figure 32E, F). Beside the commonly affected group of LSU biogenesis factors, some additional LSU biogenesis factors were observed to be reduced in both mutants, some only in the *RPL23* mutant. After rpL9 depletion, levels of Nug1, Spb1, Nsa2, and, most intensely, Noc3 were strongly reduced. After depletion of rpL23 the same group was affected and in addition the levels of Tif6, Rlp24, and Nog1 decreased significantly. In the other analyzed LSU r-protein expression mutants of this class their levels were unchanged or in the case of Noc3 (and Spb1) even substantially increased (Figure 32A-D, G). Interestingly, with the exception of Noc3, all of these LSU r-proteins have been described to be required for efficient processing of 27SB pre-rRNAs (Bassler et al., 2001; Basu et al., 2001; Kallstrom et al., 2003; Kressler et al., 1999; Lebreton et al., 2006b; Saveanu et al., 2003; Senger et al., 2001).

The specific underrepresentation of Rlp24 and Tif6 which was observed in preribosomes purified from rpL23 depleted yeast cells (Figure 32F), as well as the one of Noc3 observed in rpL9 (and rpL23) depleted preribosomes (Figures 32E,F) was addressed in more detail. The human homologue of the ribosomal subunit anti-association factor Tif6, (eukaryotic translation initiation factor 6 - eiF6), was localized by cryo-EM at the interface of the LSU (Gartmann et al., 2010; Valenzuela et al., 1982). According to these structural data its binding occurs largely via direct contacts to rpL23 what can explain its observed specific underrepresentation in preribosomes purified from cells depleted of rpL23 (Figure 32F). Besides its role as anti association factor it is required for efficient LSU maturation (Basu et al., 2001; Senger et al., 2001). To directly test its apparently reduced ability to interact with nuclear pre-60S particles depleted of rpL23, Tif6-TAP was affinity purified from cell expressing or not expressing RPL23 and the co-purified (pre-) rRNAs were isolated and analyzed by Northern blotting (Figure 33B). While association of Tif6-TAP to 27S pre-rRNA containing preribosomes was indeed significantly disturbed after rpL23 depletion (Figure 33B, compare 27S pre-rRNA ratios of lanes 11-12 / 7-8 the ones of lanes 9-10 / 5-6), its binding to mature LSUs was not detectably affected (Figure 33B, compare ratios of 25S and 5.8S rRNA of the same lanes). The specific underrepresentation of Rlp24 in preribosomes purified from cells depleted of rpL23 (Figure 32F) was aimed to be tested by the similar complementary approach using Rlp24-TAP as bait protein (Figure 33A). Surprisingly, the SDS-PAGE and Western blot analyses of the protein content of the cell extracts from the Rlp24-TAP tagged *RPL23* mutant showed that levels of Rlp24-TAP were specifically reduced after shift to restrictive conditions (Figure 33A, compare lanes 3-4 to lanes 1-2). Whether this potential degradation of Rlp24 is the reason for or the consequence of its presumably reduced association to preribosomes depleted of rpL23 is unclear. It is also possible that expression of RLP24 is tightly coupled to the one of RPL23 (or regulated by levels of rpL23) and therefore simply less expressed after shift to restrictive conditions. Due to the high sequence homology between Rlp24 and rpL24 it was suggested to act as “nuclear placeholder” for the late incorporated rpL24 (Saveanu et al., 2003) which is directly contacting rpL23 in the mature LSU. Therefore it appears reasonable that indeed, its affinity to preribosomes is reduced as consequence of a missing structural component (rpL23) that is presumably directly contacting it. The third LSU biogenesis factor whose association to preribosomes was specifically affected after rpL23 depletion, Nog1, was described to physically interact with Rlp24 (Saveanu et al., 2003) strongly suggesting that its binding site is also near rpL23 what would also explain its reduced association in this mutant. Indeed, in the recently published cryo-EM structure of a late LSU precursor electron densities corresponding to parts of Nog1 were identified in close proximity to densities corresponding to Tif6 (see Figure 12B and Leidig et al., 2013).

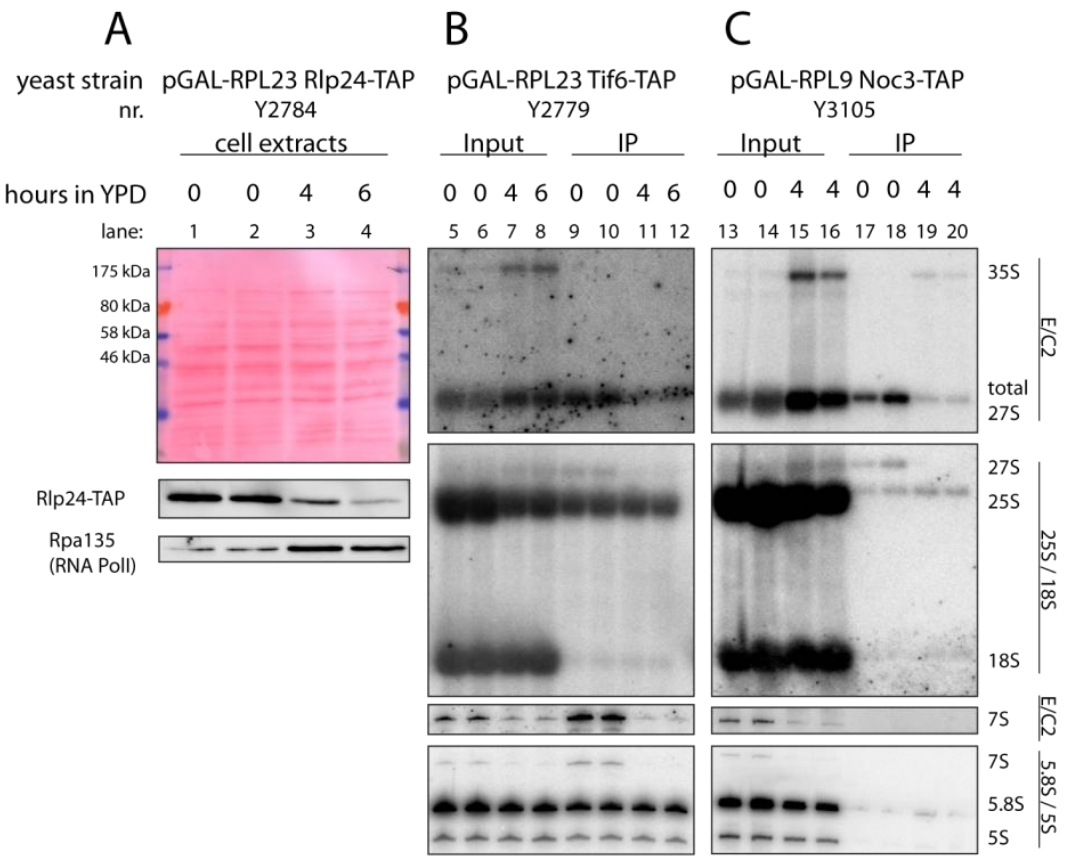
A
B
C
yeast strain
nr.
pGAL-RPL23 Rlp24-TAP
Y2784
pGAL-RPL23 Tif6-TAP
Y2779
pGAL-RPL9 Noc3-TAP
Y3105
cell extracts
Input
IP
Input
IP
hours in YPD
0 0 4 6
0 0 4 6 0 0 4 6
0 0 4 4 0 0 4 4
lane:
1 2 3 4
5 6 7 8 9 10 11 12
13 14 15 16 17 18 19 20
175 kDa
80 kDa
58 kDa
46 kDa
Rlp24-TAP
Rpa135
(RNA PolI)
35S
total
27S
27S
25S
18S
7S
7S
5.8S
5S
E/C2
25S / 18S
E/C2
5.8S / 5S

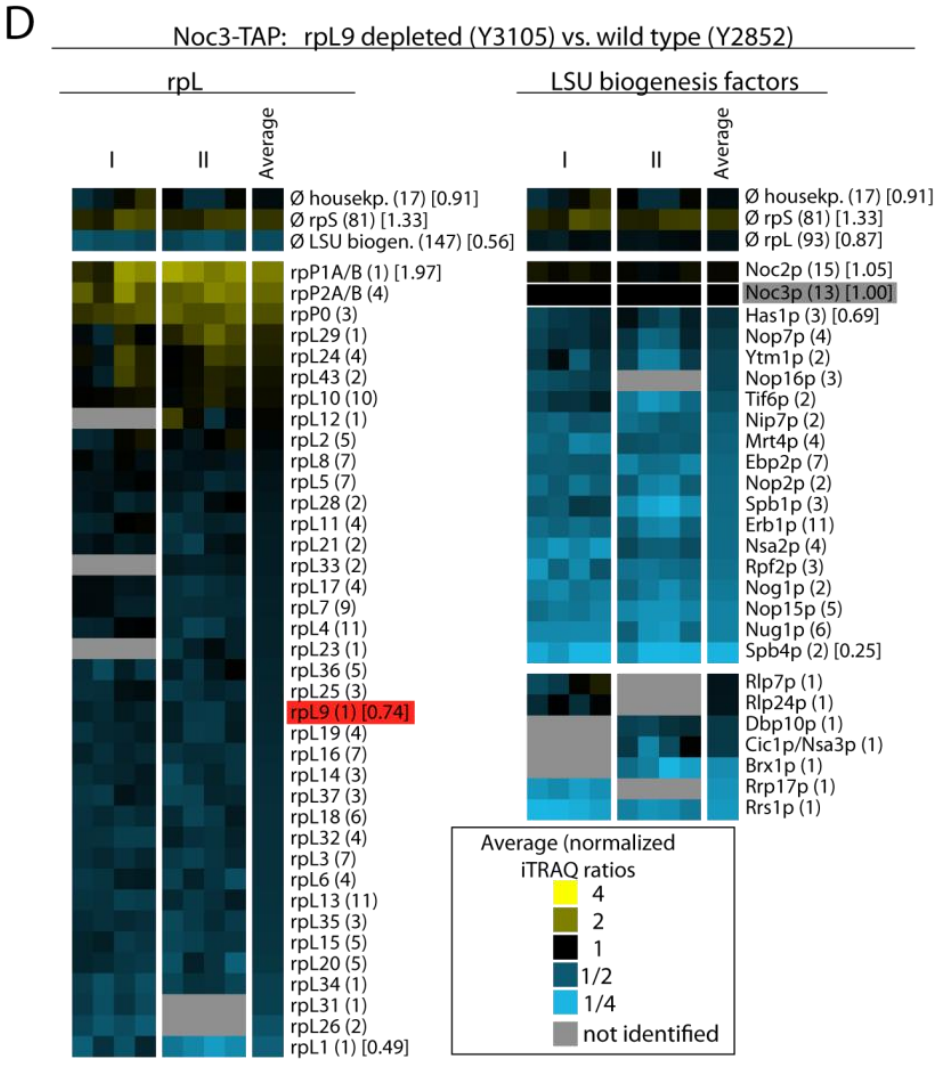
D
Noc3-TAP: rpL9 depleted (Y3105) vs. wild type (Y2852)
rpL
LSU biogenesis factors
I
II
Average
Ø housekp. (17) [0.91]
Ø rpS (81) [1.33]
Ø LSU biogen. (147) [0.56]
rpP1A/B (1) [1.97]
rpP2A/B (4)
rpP0 (3)
rpL29 (1)
rpL24 (4)
rpL43 (2)
rpL10 (10)
rpL12 (1)
rpL2 (5)
rpL8 (7)
rpL5 (7)
rpL28 (2)
rpL11 (4)
rpL21 (2)
rpL33 (2)
rpL17 (4)
rpL7 (9)
rpL4 (11)
rpL23 (1)
rpL36 (5)
rpL25 (3)
rpL9 (1) [0.74]
rpL19 (4)
rpL16 (7)
rpL14 (3)
rpL37 (3)
rpL18 (6)
rpL32 (4)
rpL3 (7)
rpL6 (4)
rpL13 (11)
rpL35 (3)
rpL15 (5)
rpL20 (5)
rpL34 (1)
rpL31 (1)
rpL26 (2)
rpL1 (1) [0.49]
Ø housekp. (17) [0.91]
Ø rpS (81) [1.33]
Ø rpL (93) [0.87]
Noc2p (15) [1.05]
Noc3p (13) [1.00]
Has1p (3) [0.69]
Nop7p (4)
Ytm1p (2)
Nop16p (3)
Tif6p (2)
Nip7p (2)
Mrt4p (4)
Ebp2p (7)
Nop2p (2)
Spb1p (3)
Erb1p (11)
Nsa2p (4)
Rpf2p (3)
Nog1p (2)
Nop15p (5)
Nug1p (6)
Spb4p (2) [0.25]
Rlp7p (1)
Rlp24p (1)
Dbp10p (1)
Cic1p/Nsa3p (1)
Brx1p (1)
Rrp17p (1)
Rrs1p (1)
Average (normalized iTRAQ ratios
4
2
1
1/2
1/4
not identified

Figure 33 (previous page) - Results from complementary approaches of the *RPL23* and *RPL9* mutants to confirm some unique features of these mutants identified previously.

A) The total protein content of extracts from Rlp24-TAP tagged yeast cells expressing or not expressing RPL23 were analyzed by western blot. To illustrate the total protein levels, the membrane was Ponceau stained after the transfer (upper panel). Levels of Rlp24-TAP and Rpa135 were analyzed using specific antibodies (see 5.1.6). **B)** Analysis of the (pre-) rRNA content of cellular extracts (Input) and Tif6-TAP affinity purified fractions (IP) of yeast cells depleted for the indicated hours (or not depleted) of rpL23 by northern blotting as described previously. **C)** Analysis of the (pre-) rRNA content of cellular extracts (Input) and Noc3-TAP affinity purified fractions (IP) of yeast cells depleted for the indicated hours (or not depleted) of rpL9 by northern blotting as described previously. **D)** shows the changes in LSU r-protein (left) or LSU biogenesis factor (right) levels of Noc3-TAP affinity purified LSU precursors after *in vivo* depletion of rpL9 for four hours. All iTRAQ ratios were normalized to the bait protein Noc3-TAP. See legends of previous Figures for more details.

The levels of Noc3, which interacts with Noc2 in a complex that is also stable when it is not associated with preribosomes (Milkereit et al., 2001), were reduced in preribosomes purified from both, the *RPL9* and the *RPL23* mutants (Figure 32 E&F). A temperature sensitive *noc3* mutant strain was initially described to have a rather "early" pre-rRNA processing phenotype with decreased steady state levels of all precursor rRNAs except the 35S pre-rRNA (Milkereit et al., 2001). Studies on a conditional *NOC3* mutant, which were performed in our laboratories, however indicated that substantial amounts of 27S pre-rRNAs could still be produced after Noc3 depletion but that the "downstream" processing events (ITS2 cleavage and processing) were significantly disturbed (T. Hierlmeier, unpublished data). Therefore, Noc3 seems to belong to the same "phenotypic class" as the other LSU biogenesis factors specifically affected after rpL9 and rpL23 depletion, which exhibit this pre-rRNA processing phenotype, too. A direct affinity purification of TAP tagged Noc3 after depletion of rpL9 (after which the effect was more pronounced as after depletion of rpL23) further confirmed its reduced affinity to these mutant preribosomes (Figure 33C, D). Levels of co-purified 27S pre-rRNAs (Figure 33C, compare lanes 19-20 to lanes 17-18), LSU r-proteins, and biogenesis factors (Figure 33D) were significantly reduced. Due to substantial amounts of "background" LSUs (Figure 33C, see 25S rRNA panel) the effect is more pronounced within the group of LSU biogenesis factors. The only identified LSU biogenesis factors whose levels were not decreased in the *RPL9* mutant was Noc2, what further confirms the described existence of a stable, preribosome independent Noc2/Noc3 complex (Milkereit et al., 2001).

In summary, the presented data provide clear evidences for specific changes in the LSU biogenesis factor composition in preribosomes purified from cells depleted of different "class2" LSU r-proteins. As done for the LSU r-proteins (see above) the observed effects can again be ordered into two classes. While the first, "phenotype specific" class consists of LSU biogenesis factors which were commonly affected (no matter which LSU r-protein of this class had been depleted) the second, "local" class was characterized by specific effects on (groups of) LSU biogenesis factors that were only observed in several mutants. The specificity of these effects could be due to rather "local" changes in the structural neighborhoods of the depleted r-protein, as observed in the case of Tif6, Rlp24, and Nog1 in the *RPL23* mutant or Jip5 in the *RPL27* and *RPL34* mutants (see above).

3.3.4 Changes in the protein composition of LSU precursor particles in r-protein expression mutants with a "late" (class 3) pre-rRNA processing phenotype

The consequence of *in vivo* expression shut down of essential LSU r-protein with a "late" (class 3) pre-rRNA processing phenotype on the composition of pre-60S particles was addressed by the same means as described in the previous two sections. Six expression mutants of LSU r-proteins (rpL2, rpL43, rpL21, rpL28, rpL11, and rpL10) were analyzed in more detail described in the following. Again, yeast strains that conditionally express one of these six "class 3" LSU r-proteins and that in addition express chromosomally encoded TAP tagged versions of LSU biogenesis factors Nog1 or Nop7 were created. Cellular extracts were prepared and used to affinity purify Nog1-TAP or Nop7-TAP and associated preribosomes. The (pre-) rRNA and protein composition of these mutant preribosomes was analyzed and compared to the ones purified from the respective wild type cells. The (pre-) rRNA composition and the changes of the LSU r-protein composition of preribosomes purified from mutants of *RPL2*, *RPL43*, *RPL21*, and *RPL28* are depicted in Figure 34. The ones of *RPL11* and *RPL10* are depicted in Figure 35. The changes in the composition of LSU biogenesis factors in preribosomes purified from *RPL2*, *RPL43*, *RPL21*, and *RPL28* mutants are shown in Figure 37 and the ones of *RPL11* and *RPL10* in Figure 35. Figures 36, 38, and 39 summarize results of a more direct characterization of the (in Figure 34 and 37) observed disturbed preribosomal association of certain LSU biogenesis factors (Nog2 and Rsa4) or LSU r-proteins (rpL2) after depletion of some of the six analyzed LSU r-proteins. Figure 40 shows the results of a more detailed characterization of the consequence of rpL21 depletion on the altered association of certain LSU biogenesis factors including Nog1, Nog2, Rsa4, Nop7, and Nop53.

As defined for LSU r-proteins of this phenotypic class, steady state levels of 7S pre-rRNAs were not (strongly) decreased after depletion of any of the six LSU r-proteins (Figure 34A, Figure 35A and C, see 7S pre-rRNA signals in "Input" lanes). However, as expected, steady state levels of the mature 25S and 5.8S rRNAs were decreased even if these changes were not that obvious due to the huge amount of mature LSUs or 80S ribosomes in the cell extracts. In the affinity purified fractions of Nog1-TAP and Nop7-TAP, high amounts of both, the 27S and 7S pre-rRNAs were detected in all cases. In addition, the preribosomes purified by Nog1-TAP from rpL21, rpL10, and (to less extents) rpL28 depleted cells, contained increased amounts of presumably nascent 25S/25.5S and 5.8S/6S (pre-) rRNAs (Figure 34A, lanes 8, 15-16). These increased amounts indicate that after depletion of rpL21, rpL10 (and rpL28) the further processing of 7S pre-rRNAs is less tight blocked as after depletion of rpL2 or rpL43, as previously observed (Pöll et al., 2009).

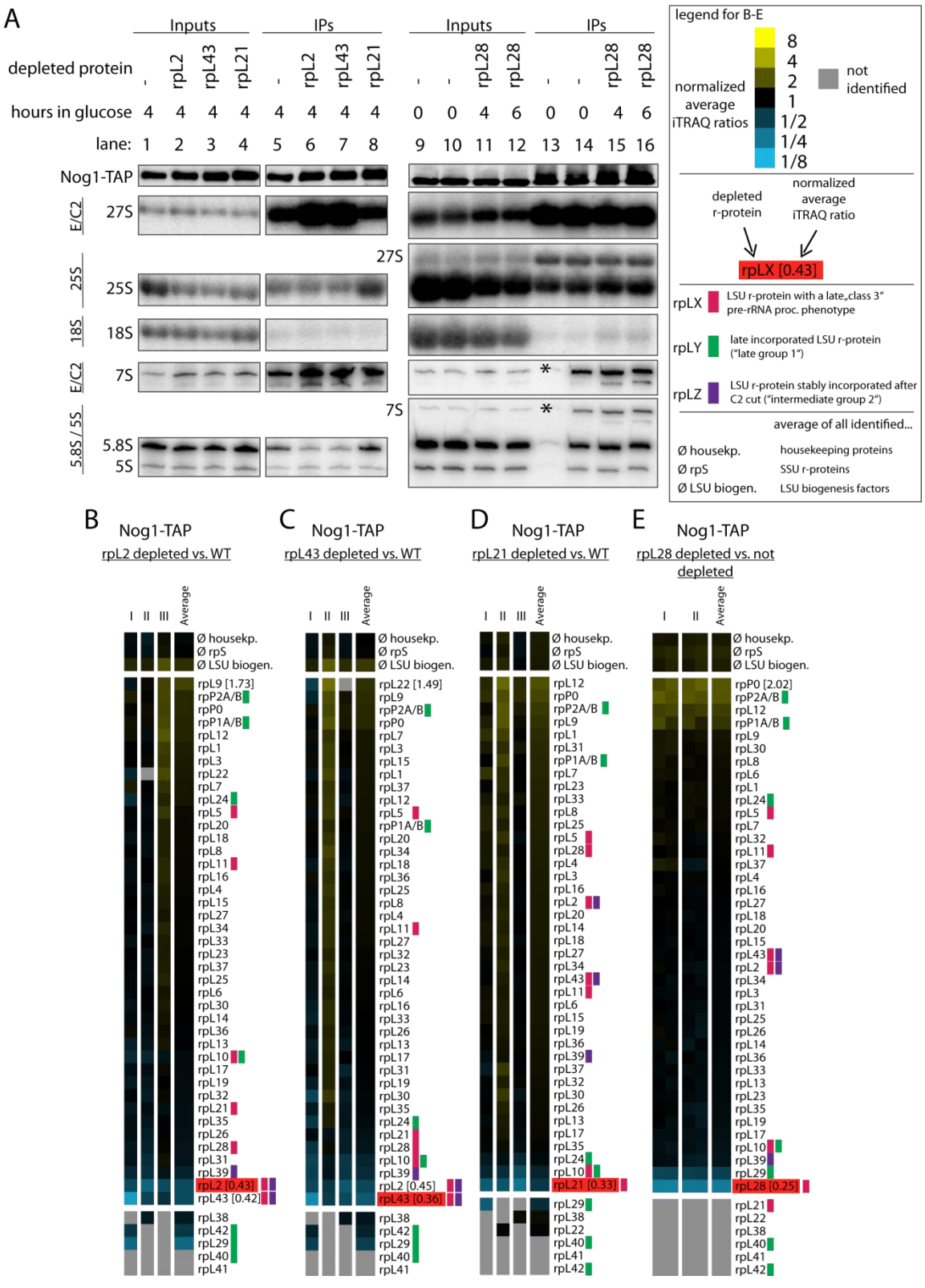

Figure 34 - Analyses of the (pre-) rRNA content and changes in LSU r-protein levels of mutant preribosomes depleted of various LSU r-proteins with a "late" (class 3) pre-rRNA processing phenotype.

LSU precursors of intermediate to late maturation stages were affinity purified *ex vivo* from wild type cells or cells depleted of the indicated LSU r-proteins for four or six hours using Nog1-TAP in as bait protein in a similar way as described in the legend of Figure 30. The analysis of the (pre-) rRNA content is depicted in **A)**. Asterisks in lane 13 indicate that the RNA sample was lost during the extraction procedure (in lane 14 a biological replicate is shown). **B)**-**E)** show the changes in LSU r-protein levels of preribosomes purified from rpL2, rpL43, rpL21, or rpL28 depleted cells in comparison to the respective Nog1-TAP wild type particles. The depleted protein is highlighted by a red box and the remaining class 3 LSU r-proteins are marked in magenta, see legend box for more details. Parts of the presented data are published in Ohmayer et al. (2013).

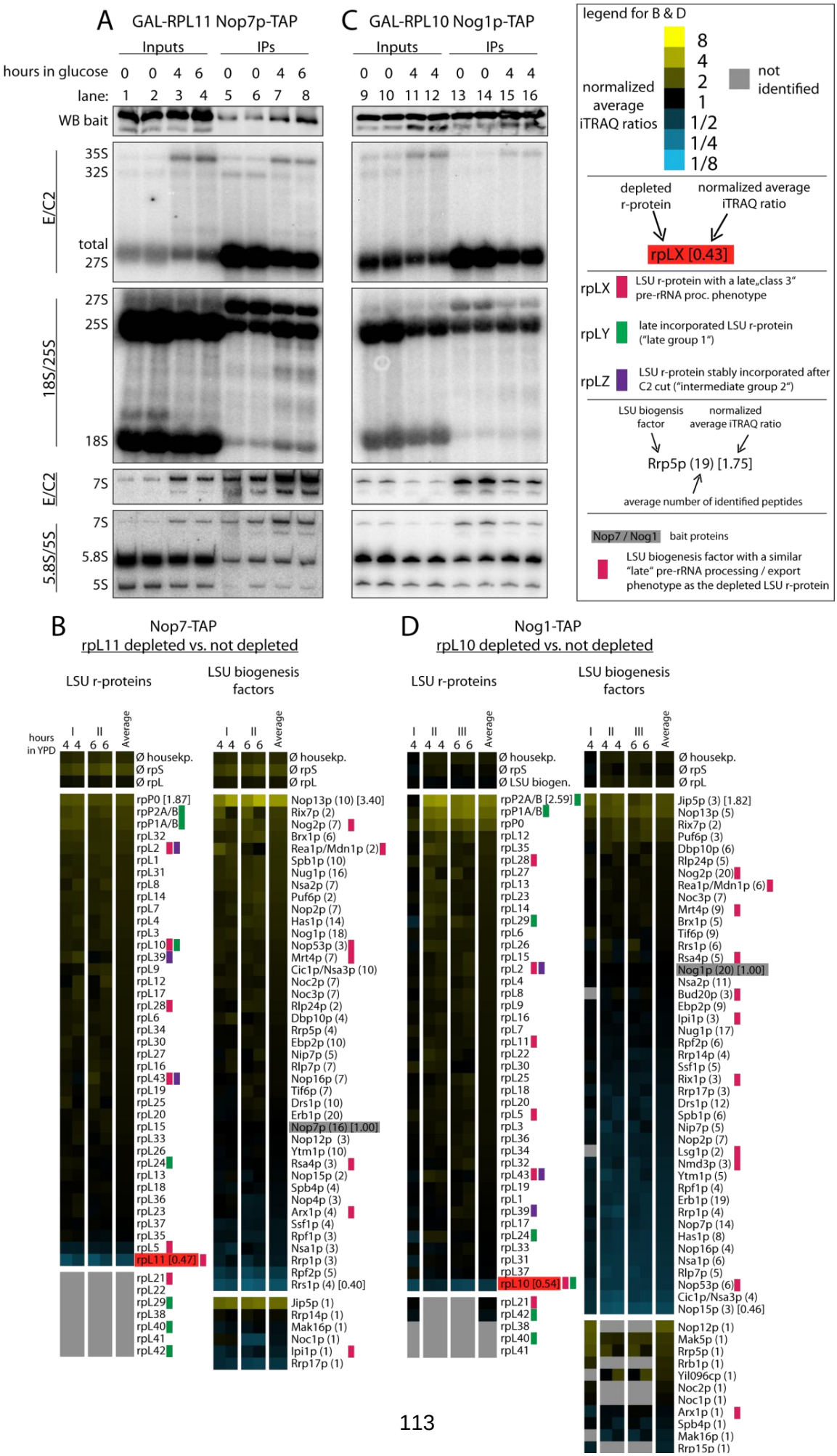
A GAL-RPL11 Nop7p-TAP
C GAL-RPL10 Nog1p-TAP
Inputs
IPs
hours in glucose
lane:
WB bait
E/C2
35S
32S
total
27S
18S/25S
27S
25S
18S
7S
5.8S/5S
5.8S
5S
legend for B & D
normalized average iTRAQ ratios
not identified
depleted r-protein
normalized average iTRAQ ratio
rpLX [0.43]
rpLX
LSU r-protein with a late„class 3" pre-rRNA proc. phenotype
rpLY
late incorporated LSU r-protein ("late group 1")
rpLZ
LSU r-protein stably incorporated after C2 cut ("intermediate group 2")
LSU biogensis factor
normalized average iTRAQ ratio
Rrp5p (19) [1.75]
average number of identified peptides
Nop7 / Nog1
bait proteins
LSU biogenesis factor with a similar "late" pre-rRNA processing / export phenotype as the depleted LSU r-protein
B Nop7-TAP
rpL11 depleted vs. not depleted
D Nog1-TAP
rpL10 depleted vs. not depleted
LSU r-proteins
LSU biogenesis factors
hours in YPD
Average
Ø housekp.
Ø rpS
Ø rpL
Ø LSU biogen.
rpP0 [1.87]
rpP2A/B
rpP1A/B
rpL32
rpL2
rpL1
rpL31
rpL8
rpL14
rpL7
rpL4
rpL3
rpL10
rpL39
rpL9
rpL12
rpL17
rpL28
rpL6
rpL34
rpL30
rpL27
rpL16
rpL43
rpL19
rpL25
rpL20
rpL15
rpL33
rpL26
rpL24
rpL13
rpL18
rpL36
rpL23
rpL37
rpL35
rpL5
rpL11 [0.47]
rpL21
rpL22
rpL29
rpL38
rpL40
rpL41
rpL42
Nop13p (10) [3.40]
Rix7p (2)
Nog2p (7)
Brx1p (6)
Rea1p/Mdn1p (2)
Spb1p (10)
Nug1p (16)
Nsa2p (7)
Puf6p (2)
Nop2p (7)
Has1p (14)
Nog1p (18)
Nop53p (3)
Mrt4p (7)
Cic1p/Nsa3p (10)
Noc2p (7)
Noc3p (7)
Rlp24p (2)
Dbp10p (4)
Rrp5p (4)
Ebp2p (10)
Nip7p (5)
Rlp7p (7)
Nop16p (7)
Tif6p (7)
Drs1p (10)
Erb1p (20)
Nop7p (16) [1.00]
Nop12p (3)
Ytm1p (10)
Rsa4p (3)
Nop15p (2)
Spb4p (4)
Nop4p (3)
Arx1p (4)
Ssf1p (4)
Rpf1p (3)
Nsa1p (3)
Rrp1p (3)
Rpf2p (5)
Rrs1p (4) [0.40]
Jip5p (1)
Rrp14p (1)
Mak16p (1)
Noc1p (1)
Ipi1p (1)
Rrp17p (1)
rpP2A/B [2.59]
rpP1A/B
rpP0
rpL12
rpL35
rpL28
rpL27
rpL13
rpL23
rpL14
rpL29
rpL6
rpL26
rpL15
rpL2
rpL4
rpL8
rpL9
rpL16
rpL7
rpL11
rpL22
rpL30
rpL25
rpL18
rpL20
rpL5
rpL3
rpL36
rpL34
rpL32
rpL43
rpL19
rpL1
rpL39
rpL17
rpL24
rpL33
rpL31
rpL37
rpL10 [0.54]
rpL21
rpL42
rpL38
rpL40
rpL41
Jip5p (3) [1.82]
Nop13p (5)
Rix7p (2)
Puf6p (3)
Dbp10p (6)
Rlp24p (5)
Nog2p (20)
Rea1p/Mdn1p (6)
Noc3p (7)
Mrt4p (9)
Brx1p (5)
Tif6p (9)
Rrs1p (6)
Rsa4p (5)
Nog1p (20) [1.00]
Nsa2p (11)
Bud20p (3)
Ebp2p (9)
Ipi1p (3)
Nug1p (17)
Rpf2p (6)
Rrp14p (4)
Ssf1p (5)
Rix1p (3)
Rrp17p (3)
Drs1p (12)
Spb1p (6)
Nip7p (5)
Nop2p (7)
Lsg1p (2)
Nmd3p (3)
Ytm1p (5)
Rpf1p (4)
Erb1p (19)
Rrp1p (4)
Nop7p (14)
Has1p (8)
Nop16p (4)
Nsa1p (6)
Rlp7p (5)
Nop53p (6)
Cic1p/Nsa3p (4)
Nop15p (3) [0.46]
Nop12p (1)
Mak5p (1)
Rrp5p (1)
Rrb1p (1)
Yil096cp (1)
Noc2p (1)
Noc1p (1)
Arx1p (1)
Spb4p (1)
Mak16p (1)
Rrp15p (1)

Figure 35 (previous page) - Analyses of the (pre-) rRNA content and changes in LSU r-protein and LSU biogenesis factor levels of mutant preribosomes depleted of rpL11 or rpL10 that exhibit a "late" (class 3) pre-rRNA processing phenotype.

LSU precursors of intermediate to late maturation stages were affinity purified *ex vivo* from wild type cells or cells depleted for four or six hours of rpL11 (**A)** and **B)**) or rpL10 (**C)** and **D)**) using Nop7-TAP and Nog1-TAP, respectively as bait protein, were analyzed in a similar way as described in Figure 34. The analysis of the (pre-) rRNA content is depicted in **A)** and **C)**. Parts **B)** and **D)** show the changes in LSU r-protein levels (left) and LSU biogenesis factors levels (right) of preribosomes purified from rpL11 and rpL10 depleted cells, respectively in comparison to the respective Nop7-TAP or Nog1-TAP wild type particles. The depleted protein is highlighted by a red box and the remaining class 3 LSU r-proteins are marked in magenta, see legend box and previous Figure legends for more details. Parts of the presented data are published in Gamalinda et al. (2014).

Differences in the changes of the LSU r-protein levels in preribosomes purified from the different LSU r-protein mutants were observed. As expected, the depleted LSU r-protein was among the most underrepresented in all cases (Figures 34B-E and 35B&D). After depletion of both, rpL2 and rpL43, levels of three LSU r-proteins, rpL2, rpL43, and rpL39 were most affected (Figure 34A-B). These three are the members of "group 2" (Figure 20B) that was characterized by a strong increase of their affinities to preribosomes concomitant processing of 27SB pre-rRNA containing preribosomes (see also Figure 22C). As mentioned before, rpL2 and rpL43 are located at the subunit interface of the LSU directly contacting each other while rpL39 is bound between LSU domain I (5.8S rRNA) and III (Ben-Shem et al., 2011). The observed reduced association of rpL2 to preribosomes depleted of rpL43 was directly addressed using ectopically expressed FLAG-tagged rpL2 as bait protein to affinity purify (pre-) ribosomes from cells in which expression of rpL43 or rpL21 (or no LSU r-protein) had been shut down (Figure 36). Co-purification efficiencies of 7S pre-rRNA and 5.8S rRNA with FLAG-rpL2 and FLAG rpL3 was analyzed by Northern blotting (Figure 36A). Quantification of the 7S pre-rRNA co-purification efficiencies confirmed the reduced association of FLAG-rpL2 to preribosomes purified from rpL43 depleted cells while association of FLAG-rpL3 was not affected (Figure 36B). The efficiency of 5.8S rRNA containing mature LSUs co-purifying with FLAG-rpL2 was, however, not reduced. Therefore, reduced yields of the FLAG-rpL2 affinity purification (e.g. due to technical problems) can be excluded as reason for its reduced association to 7S pre-rRNA containing preribosomes. Beside the rpL2/rpL43/rpL39 group, the levels of several other LSU r-proteins were reduced in the preribosomes purified from rpL2 and rpL43 depleted cells (Figure 34A-B). These decreases were not as strong and less consistent, though. Among the most consistently reduced LSU r-proteins were rpL10, rpL29, rpL42, rpL28, and rpL21, the essential of which (rpL10, rpL21, rpL28) have (as rpL2 and rpL43) a late, "class 3" pre-rRNA processing phenotype. RpL10, rpL29, and rpL42 were in addition members of the group of LSU r-proteins with strong evidences for being incorporated at very late stages in LSU maturation (see results in part 0 and citations therein).

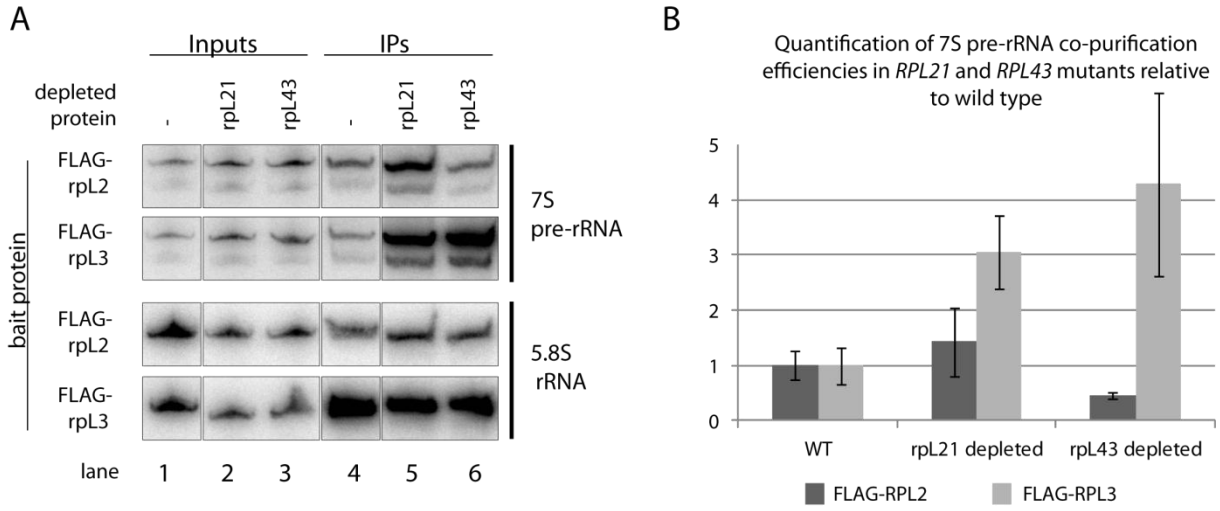

Figure 36 - Impact of *in vivo* depletion of rpL21 or rpL43 on association of FLAG tagged rpL2 and rpL3 with 7S pre-rRNA containing LSU precursors and mature LSUs.

Yeast strains which ectopically express either rpL43 (Y1103) or rpL21 (Y1100) under the control of the GAL1/10 promoter and a wild type yeast strain (Y207) were transformed with plasmids coding for a FLAG tagged version of rpL2 (TK1028) or rpL3 (TK1029) under control of the RPS28 promoter. Transformants were cultivated in galactose-containing medium and shifted for 4 hours to glucose containing medium to shut down the expression of the respective r-protein gene. Cellular extracts of these strains were subjected to affinity purification using an anti-FLAG matrix as described in 5.2.6.2. **A)** The (pre-) rRNA content of the total cellular extracts ("Input" lanes 1-3) or of parts of the affinity purified fractions ("IP" lanes 4-6) was analyzed by northern blotting. Changes in co-purification efficiencies of the 7S pre-rRNA after shutting down the expression of RPL43 or RPL21 were quantified in **B)** in relation to the amount of 7S pre-rRNA co-purified in the reference wild type strain. Relative amounts of the 7S pre-rRNA co-purified via rpL2-FLAG and rpL3-FLAG are shown in dark and light gray, respectively. Quantification was performed from two biological replicates. The standard deviations are indicated as error bars. Modified from Ohmayer et al. (2013).

Depletion of rpL21 resulted in a different pattern: none of the three LSU r-proteins which were most affected after rpL2 or rpL43 depletion (rpL2, rpL43, rpL39) was significantly reduced in the Nog1-TAP purified preribosomes (Figure 34D). The association of FLAG tagged rpL2 (and rpL3) to preribosomes from cells depleted of rpL21 was not reduced but significantly higher as measured by increased co-purification efficiencies of 7S pre-rRNA (Figure 36) what is in agreement with the semi quantitative mass spectrometry data (Figure 34D). Only levels of a smaller group consisting of rpL21 itself, rpL10, rpL24, and (if identified) rpL29 were reduced (Figure 34D). Remarkably, rpL10, rpL24, and rpL29 are all members of the group of LSU r-proteins which are stably incorporated into LSU precursors at very late maturation stages (see results in section 0 and citations therein). This tendency of an underrepresentation of late incorporated LSU r-proteins was also observed after depletion of rpL28, albeit less intense and also less consistent (Figure 34E). Depletion of rpL11 only affected levels of rpL5 (Figure 35B, left panel), which is, together with rpL11, the 5S rRNA, and the biogenesis factors Rpf2 and Rrs1 part of the "5S RNP" that was described to be incorporated into early preribosomes as "pre-assembled" RNP (Zhang et al., 2007). In line with this, both, Rpf2 and Rrs1 were the two most intensely reduced LSU biogenesis factors among all identified ones (Figure 35B, right panel). Depletion of rpL10 resulted only in mild changes in the LSU r-protein composition of Nog1-TAP purified LSU precursors (Figure 35D, left panel) indicating that rpL10 is not strictly required for the stable association of any other LSU r-protein. Some of the putative "candidate" LSU r-proteins (which are also late incorporated and which one could therefore suspect to be affected), as rpL40 or rpL42, could

however not at all be identified (or only in one of the experiments) (Figure 35D). A potential impact of rpL10 incorporation on association of both, rpL40, and rpL42, can therefore not be excluded.

As done for the LSU r-proteins with an “earlier” (class 1 and 2) pre-rRNA processing phenotype (see previous two sections), the changes in the LSU biogenesis factor composition of the affinity purified preribosomes was also addressed in each of these six mutants (Figures 35B&D and 37). In general, the pattern of the *RPL2* and *RPL43* mutants was very similar and largely differed from the one of the other four mutants (compare pattern in Figure 37A&B to the ones in Figures 37C&D, and 35B&D). The levels of most of the identified LSU biogenesis factors were unaffected or even increased after depletion of rpL2 or rpL43. Among them were LSU biogenesis factors that function in earlier pre-60S maturation steps as the Noc1/Noc2/Rrp5 module, the “A3 factors”, or also some of the factors involved in C2 cleavage (“B factors”). The observed behavior of some of those factors (and also some LSU r-proteins) was also addressed by Western blot analyses what largely confirmed the data derived from the mass spectrometry analyses (Ohmayer et al., 2013). In line with this, Noc2-TAP co-purified significantly higher amounts of 7S pre-rRNA after depletion of both, rpL2 and rpL43 (diploma thesis Martina Sauert and shown in Ohmayer et al., 2013). The observed increased levels of LSU biogenesis factors co-purifying with Nog1-TAP after rpL2 or rpL43 depletion might indicate a distortion of their release. As introduced in section 2.2.6.4, the cleavage in the ITS2 of 27SB pre-rRNA containing preribosomes was described to be accompanied by the release of many early factors for some of which a “mechanochemical” mechanism involving the action of NTPases was shown (see citations in 2.2.6.4).

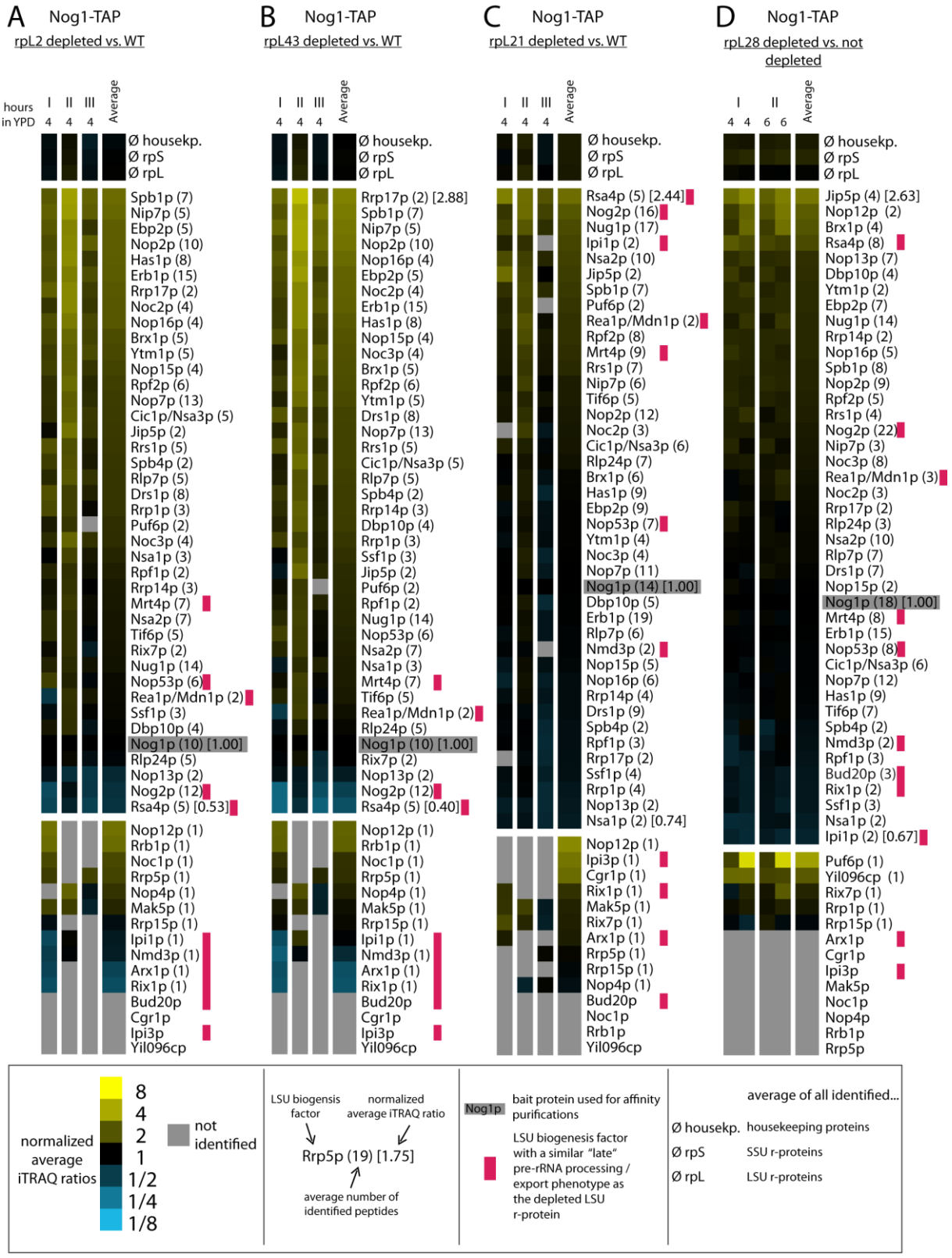

Figure 37 - Analyses of the changes of the LSU biogenesis factor levels in LSU precursors purified via Nog1-TAP after *in vivo* depletion of selected "late" (class 3) LSU r-proteins.

All shown data derive from the experiments shown in Figure 34. Depicted here are the levels of all identified LSU ribosome biogenesis factors after depletion of the indicated LSU r-protein. All iTRAQ ratios were normalized to the bait protein Nog1-TAP. The average number of identified peptides is given in parentheses. LSU biogenesis factors that have a similar "late" pre-rRNA processing phenotype as the depleted LSU r-protein (class 3) are highlighted in magenta. See legends of previous Figures and box for more details. Parts of the presented data are published in Ohmayer et al. (2013).

On the other hand, association of a group of factors was reduced in the *RPL2* and *RPL43* mutants. Among these factors were Nog2, Rsa4, Nop13, and, in addition (albeit identified less confidently with only one peptide in average) Arx1, Nmd3, Ipi1, and Rix1/Ipi2 (Figure 37A&B, see also lower panels). Interestingly, as mentioned above, both, Nog2 and Rsa4 depletion was previously shown to result in delay in nuclear processing of 27SB and 7S pre-rRNAs (de la Cruz et al., 2005; Granato et al., 2005; Saveanu et al., 2001; Sydorskyy et al., 2005; Thomson and Tollervey, 2005). The depletion phenotype of these two biogenesis factors is therefore similar to the one of rpL2 and rpL43. Two of the five remaining factors whose levels were reduced after *in vivo* depletion of rpL2 and rpL43, Nop13 and Arx1, are encoded by non-essential genes while the remaining three, Nmd3, Ipi1, and Rix1/Ipi2 are essential in yeast. Nmd3 functions as export adapter for the nuclear export of LSU precursors (Hedges et al., 2005; West et al., 2005) and both, Ipi1 and Rix1/Ipi2 are members of the "Rix1 complex" (Rix1/Ipi2, Ipi1, Ipi3) that was described to be required for efficient 7S pre-rRNA processing and nuclear export (Galani et al., 2004).

After rpL21 depletion, with the exception of Nmd3, all of the above described LSU biogenesis factors whose association to preribosomes purified from rpL2 and rpL43 depleted cells was significantly reduced, co-purified equally well with Nog1-TAP or even accumulated up to more than two fold (Figure 37C, see also lower panel). This strongly suggests that the assembly of rpL21, whose pre-rRNA processing phenotype was characterized by a less tight block of nuclear 7S pre-rRNA processing (see above and Figure 34A), is not required for association of Rsa4, Nog2, or the Rix1 complex, but rather for the efficient release of these LSU biogenesis factors.

Rpl28 depletion also resulted in increased levels of Nog2 and Rsa4 but the levels of the members of the Rix1 complex and several other late acting LSU biogenesis factors as Bud20, Nmd3, or (only mildly) Nop53 and Mrt4 were reduced (Figure 37D).

As mentioned above, rpL11 depletion resulted in rather moderate changes in levels of LSU biogenesis factors (Figure 35B). Rpf2 and Rrs1, both components of the 5S RNP which contains also rpL5 and rpL11 (Zhang et al., 2007), were the two most affected factors. Since in this case, the strictly nuclear Nop7-TAP was used as bait protein for the affinity purifications, a direct comparison of the changes of the LSU biogenesis factor composition after rpL11 depletion to the changes observed after depletion of the other five analyzed "class 3" LSU r-proteins (for which the "shuttling" factor Nog1 was TAP tagged) is difficult and will not be done in more detail.

The consequences of rpL10 depletion on the changes in the LSU biogenesis factor composition of Nog1-TAP purified preribosomes are depicted in Figure 35D. According to the observed data, association of a larger group of factors was reduced. Among them were, on the one hand, early acting factors as Cic1/Nsa3, Rlp7, Has1 and the other "A3 factors" and on the other hand some late acting factors as Nmd3, Lsg1, or Arx1. The analyses of the (pre-) rRNAs co-purifying with Nog1-TAP showed that the population of preribosomes Nog1-TAP

interacts with seemed to change after depletion of rpL10. In contrast to the *RPL2*, *RPL43*, and *RPL28* mutants, the 25(.5)S / 27S (pre-) rRNA ratio and the 5.8S(6S) / 7S (pre-) rRNA ratio of the affinity purification fractions were significantly shifted towards the mature 25S and 5.8S rRNAs (Figure 35C, compare 25S/27S and 5.8S/7S ratios in lanes 15-16 to the ones in lanes 13-14). This might reflect a disturbed release of Nog1-TAP from the mutant preribosomes what presumably complicates the interpretation of the obtained data. The above mentioned reduced levels of the early acting "A3 factors" observed after *in vivo* depletion of rpL10 are in agreement with these (pre-) rRNA data. In any case, alternative approaches to investigate the effects of rpL10 depletion on the composition of late pre-60S particles are required to (possibly) confirm the observed effects on the Nog1-TAP purified preribosomes. The evidences that a number of late acting LSU biogenesis factors (as Arx1, Nmd3, Tif6, Alb1, Rei1, or Lsg1 (Merl et al., 2010)) can apparently associate to mature LSUs further hamper these approaches, since therefore, their use as bait proteins for affinity purification of rpL10 depleted preribosomes is limited. A more direct way to visualize the (potential) compositional changes in LSU precursors depleted of rpL10 might be the creation of a high resolved cryo-EM structure as recently done for late wild-type LSU precursors (Bradatsch et al., 2012; Leidig et al., 2014).

The previously observed altered association of Nog2 and Rsa4 to preribosomes purified from cells depleted of rpL25 (and other "class 2" LSU r-proteins – see Figure 32), rpL2, rpL43, and rpL21 (Figure 37A-C) was aimed to be addressed more directly by affinity purifying both proteins from the respective mutant strains and analyze the co-purified RNPs by the same methods used before (Northern blotting and semi quantitative mass spectrometry). While the association of Nog2 and Rsa4 to preribosomes purified from cells depleted of rpL25, rpL2, and rpL43 (and others) was strongly reduced, they accumulated in preribosomes purified from rpL21 and rpL28 depleted cells (see above). Yeast strains that conditionally express one of the four LSU r-proteins (rpL25, rpL2, rpL43, rpL21) and the corresponding wild type strain were genetically modified to express chromosomally encoded versions of Nog2-TAP or Rsa4-TAP. The results of the analyses of the changes of the (pre-) rRNA- and protein composition of Nog2-TAP and Rsa4-TAP affinity purified particles are depicted in Figures 38 and 39 respectively. To better highlight the differences in the (pre-) rRNA composition of the respective preribosomes co-purified by Nog2-TAP or Rsa4-TAP, the co-purification efficiencies of the 27S and 7S pre-rRNAs and the ones of the 25.5S/25S and 6S/5.8S (pre-) rRNAs of these preribosomes were calculated based on the quantified Northern blotting data (Figures 38B, 39B). Levels of internal background, as determined by quantification of the co-purification efficiencies of the 20S pre-RNA of SSU precursors, was included to visualize the levels unspecific amounts of the (pre-) rRNA of interest (indicated by a red line in Figures 38B and 39B; raw data not shown).

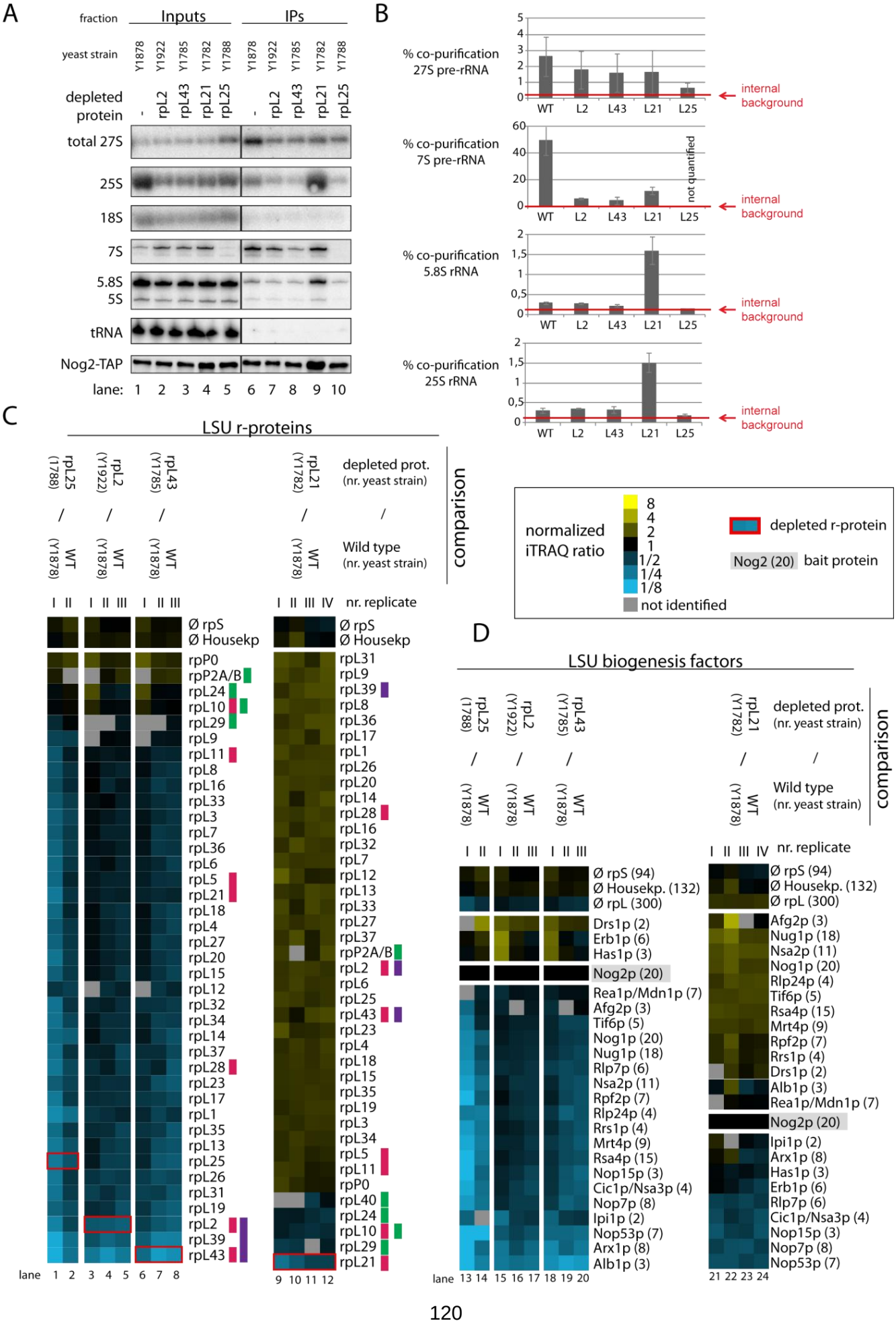
A
fraction
Inputs
IPs
yeast strain
Y1878
Y1922
Y1785
Y1782
Y1788
depleted protein
-
rpL2
rpL43
rpL21
rpL25
total 27S
25S
18S
7S
5.8S
5S
tRNA
Nog2-TAP
lane: 1 2 3 4 5 6 7 8 9 10
B
% co-purification 27S pre-rRNA
% co-purification 7S pre-rRNA
% co-purification 5.8S rRNA
% co-purification 25S rRNA
WT
L2
L43
L21
L25
internal background
not quantified
C
LSU r-proteins
rpL25 (1788) / WT (Y1878)
rpL2 (Y1922) / WT (Y1878)
rpL43 (Y1785) / WT (Y1878)
rpL21 (Y1782) / WT (Y1878)
depleted prot. (nr. yeast strain) / Wild type (nr. yeast strain)
comparison
normalized iTRAQ ratio
8
4
2
1
1/2
1/4
1/8
not identified
depleted r-protein
Nog2 (20) bait protein
I II III IV nr. replicate
Ø rpS
Ø Housekp
rpP0
rpP2A/B
rpL24
rpL10
rpL29
rpL9
rpL11
rpL8
rpL16
rpL33
rpL3
rpL7
rpL36
rpL6
rpL5
rpL21
rpL18
rpL4
rpL27
rpL20
rpL15
rpL12
rpL32
rpL34
rpL14
rpL37
rpL28
rpL23
rpL17
rpL1
rpL35
rpL13
rpL25
rpL26
rpL31
rpL19
rpL2
rpL39
rpL43
rpL31
rpL9
rpL39
rpL8
rpL36
rpL17
rpL1
rpL26
rpL20
rpL14
rpL28
rpL16
rpL32
rpL7
rpL12
rpL13
rpL33
rpL27
rpL37
rpP2A/B
rpL2
rpL6
rpL25
rpL43
rpL23
rpL4
rpL18
rpL15
rpL35
rpL19
rpL3
rpL34
rpL5
rpL11
rpP0
rpL40
rpL24
rpL10
rpL29
rpL21
lane 1 2 3 4 5 6 7 8
9 10 11 12
D
LSU biogenesis factors
Ø rpS (94)
Ø Housekp. (132)
Ø rpL (300)
Drs1p (2)
Erb1p (6)
Has1p (3)
Nog2p (20)
Rea1p/Mdn1p (7)
Afg2p (3)
Tif6p (5)
Nog1p (20)
Nug1p (18)
Rlp7p (6)
Nsa2p (11)
Rpf2p (7)
Rlp24p (4)
Rrs1p (4)
Mrt4p (9)
Rsa4p (15)
Nop15p (3)
Cic1p/Nsa3p (4)
Nop7p (8)
Ipi1p (2)
Nop53p (7)
Arx1p (8)
Alb1p (3)
lane 13 14 15 16 17 18 19 20
Ø rpS (94)
Ø Housekp. (132)
Ø rpL (300)
Afg2p (3)
Nug1p (18)
Nsa2p (11)
Nog1p (20)
Rlp24p (4)
Tif6p (5)
Rsa4p (15)
Mrt4p (9)
Rpf2p (7)
Rrs1p (4)
Drs1p (2)
Alb1p (3)
Rea1p/Mdn1p (7)
Nog2p (20)
Ipi1p (2)
Arx1p (8)
Has1p (3)
Erb1p (6)
Rlp7p (6)
Cic1p/Nsa3p (4)
Nop15p (3)
Nop7p (8)
Nop53p (7)
21 22 23 24

Figure 38 (previous page) - Analyses of the (pre-) rRNA content and changes in levels of LSU r-proteins and ribosome biogenesis factors of LSU precursors purified via Nog2-TAP after *in vivo* depletion of selected class 2 or 3 LSU r-proteins.

LSU precursors of intermediate to late maturation stages were affinity purified *ex vivo* from wild type cells or cells depleted for four hours of the indicated LSU r-protein using Nog2-TAP as bait protein and analyzed in a similar way as described in the previous Figure legends. The (pre-) rRNA content of total cellular extracts (Input lanes 1-5) or of the affinity purified fractions (IP lanes 6-10) are shown in **A)**. Equal signal intensities of the Input and IP fractions correspond to 1% (35S, 27S pre-rRNAs and 25S and 18S rRNAs) or 10% (7S pre-rRNA, 5.8S, 5S rRNAs and glutamyl-tRNA) co-purification efficiencies, respectively. Purification efficiencies of the bait protein Nog2-TAP were monitored by western blotting (see panel designated Nog2-TAP). Equal signal intensities in the western blot analyses indicate 25% purification efficiency of Nog2-TAP. Quantitation of the co-purification efficiencies (in %) of the 7S, 27S, 25S and 5.8S (pre-) rRNAs are shown in **B)**. Red bars in **B)** designate internal background levels of the affinity purification procedure as measured by co-purification efficiencies of 20S pre-rRNA (data not shown). The iTRAQ ratio for each LSU r-protein **C)** or LSU biogenesis factor **D)** which was identified by more than one peptide (except rpL43, rpL29 and rpL40, marked by a (*)) in more than 70% of all pair-wise comparisons are displayed as a heat map (see color code). In **C)** the iTRAQ ratios of the LSU r-protein whose expression had been shut down are highlighted by red boxes. LSU r-proteins with a “late” (class 3) pre-rRNA processing phenotype are highlighted in magenta. Those that stably assembly at late or intermediate stages (groups 1 and 2 in Figure 20B) are highlighted in green and purple, respectively. Modified from Ohmayer et al. (2013).

Figure 39 (next page) - Analyses of the (pre-) rRNA content and changes in levels of LSU r-proteins and ribosome biogenesis factors of LSU precursors purified via Rsa4-TAP after *in vivo* depletion of selected class 2 or 3 LSU r-proteins.

LSU precursors of intermediate to late maturation stages were affinity purified *ex vivo* from wild type cells or cells depleted for four hours of the indicated LSU r-protein using Rsa4-TAP as bait protein and analyzed in a similar way as described in the previous Figure 38. Modified from Ohmayer et al. (2013).

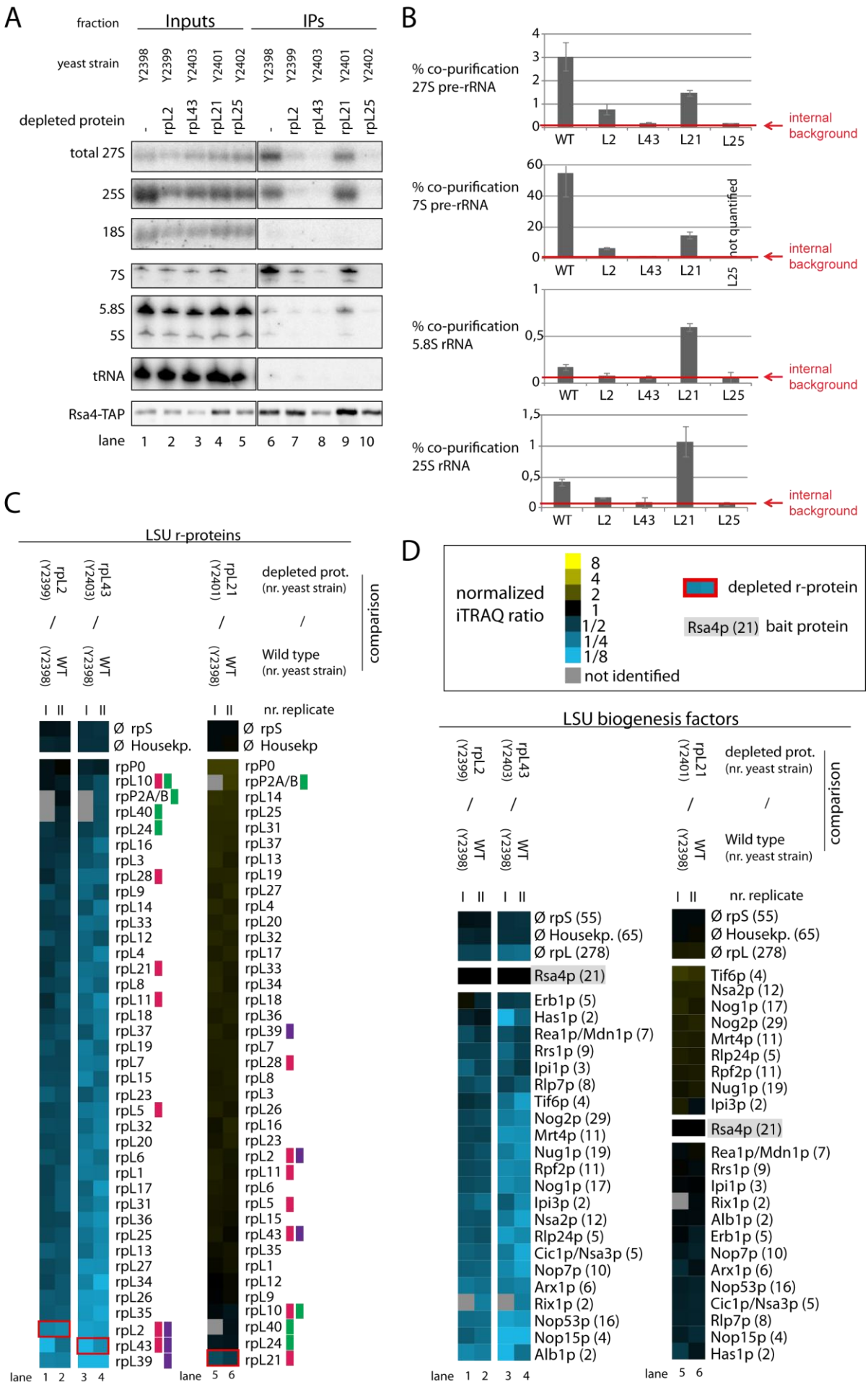
A
fraction
Inputs
IPs
yeast strain
Y2398
Y2399
Y2403
Y2401
Y2402
depleted protein
-
rpL2
rpL43
rpL21
rpL25
total 27S
25S
18S
7S
5.8S
5S
tRNA
Rsa4-TAP
lane 1 2 3 4 5 6 7 8 9 10
B
% co-purification 27S pre-rRNA
% co-purification 7S pre-rRNA
% co-purification 5.8S rRNA
% co-purification 25S rRNA
WT L2 L43 L21 L25
internal background
not quantified
C
LSU r-proteins
depleted prot. (nr. yeast strain)
comparison
Wild type (nr. yeast strain)
nr. replicate
Ø rpS
Ø Housekp.
lane 1 2 3 4 5 6
D
normalized iTRAQ ratio
8
4
2
1
1/2
1/4
1/8
not identified
depleted r-protein
Rsa4p (21) bait protein
LSU biogenesis factors
Ø rpS (55)
Ø Housekp. (65)
Ø rpL (278)
Rsa4p (21)
Erb1p (5)
Has1p (2)
Rea1p/Mdn1p (7)
Rrs1p (9)
Ipi1p (3)
Rlp7p (8)
Tif6p (4)
Nog2p (29)
Mrt4p (11)
Nug1p (19)
Rpf2p (11)
Nog1p (17)
Ipi3p (2)
Nsa2p (12)
Rlp24p (5)
Cic1p/Nsa3p (5)
Nop7p (10)
Arx1p (6)
Rix1p (2)
Nop53p (16)
Nop15p (4)
Alb1p (2)

As expected from the previously obtained semi quantitative MS data, the efficiencies of 27S and 7S pre-rRNAs co-purifying with Nog2-TAP or Rsa4-TAP were significantly reduced after depletion of rpL25, rpL2, and rpL43 (Figures 38A-B, 39A-B). These reduced efficiencies reflect the reduced association of Nog2-TAP and Rsa4-TAP to intermediate (and late) nuclear pre-60S particles as observed before. However, depletion of rpL21, after which no reduced association (but a significant increase) of Nog2 or Rsa4 to Nog1-TAP purified preribosomes was observed before (Figure 37C), also resulted in decreased co-purification efficiencies of both 27S and 7S pre-rRNAs (Figures 38A-B and 39A-B). These, on a first glance conflicting results of an increased preribosomal association of Nog2 and Rsa4 on the one hand (Nog1-TAP purified and MS analyzed preribosomes) and a reduced co-purification of pre-60S containing pre-rRNAs on the other hand can be dissolved when focusing on the co-purification efficiencies of Nog2-TAP and Rsa4-TAP of the later 5.8S and 25.5/25S (pre-) rRNAs (Figures 38A and 39A, respectively). The efficiencies of 5.8S and 25.5/25S (pre-) rRNAs co-purifying with both, Nog2-TAP and Rsa4-TAP were strongly increased (≥ factor 3) in the *RPL21* mutant (Figures 38B, 39B). The observed increase of Nog2 and Rsa4 levels in this mutant can therefore be explained by a stable association of both factors to late (nuclear) LSU precursors that contain mature 5.8S rRNAs and 25.5S pre-rRNAs or 25S rRNAs, which strongly accumulate after depletion of rpL21.

The analyses using semi quantitative mass spectrometry which were performed with parts of the affinity purified fractions to analyze the changes in the protein composition of the mutant preribosomes co-purified by Nog2-TAP and Rsa4-TAP further confirmed the data obtained from the (pre-) rRNA analyses (Figures 38C-D, 39C-D). The reduced association of Nog2-TAP and Rsa4-TAP to preribosomes from rpL25, rpL2, and rpL43 depleted cells was largely confirmed by reduced levels of most LSU r-proteins and LSU biogenesis factors (Figures 38C-D, 39C-D). Consistent with the previous results (Figures 32G and 37A-B) the reduced association to these mutant preribosomes was more pronounced for Rsa4-TAP than for Nog2-TAP (compare general patterns (lower iTRAQ ratios) in Figures 39C-D to the ones in Figures 38C-D).

As observed before in preribosomes purified by Nog1-TAP (Figure 34D), the main effects of rpL21 depletion on the LSU r-protein composition were seen on rpL21 itself and, to a weaker extent, on rpL10, rpL24, rpL40, and (when detected) rpL29 (Figures 38C, 39C). Some LSU biogenesis factors that are recruited to “early” preribosomes as the “A3 factors” Nop7, Nop15, Cic1/Nsa3, Rlp7, Erb1 or Has1 were strongly underrepresented in preribosomes purified by Nog2-TAP from rpL21 depleted cells (Figure 38D, lanes 21-24). The same effect was seen for Nop53, which is required for later pre-rRNA processing steps and which mainly binds to LSU precursors of intermediate to late maturation stages (Figure 18A and (Granato et al., 2005)). In contrast to the Nog2-TAP purified LSU precursors, these effects were less evident in preribosomes co-purifying with Nog1-TAP or Rsa4-TAP from rpL21 depleted cells (Figures 37C and 39D). These observations suggested that Nog2 preferentially associates with specific sub-populations of rpL21 depleted LSU precursor particles which partially released the above described “A3 factors” (Nop7, Nop15, Cic1/Nsa3, Rlp7, Erb1 or Has1)

and Nop53. To better visualize this apparently different behavior of Nog2, the (pre-) rRNAs co-purifying with Nog2-TAP, Rsa4-TAP and Nog1-TAP from rpL21 depleted cells were directly compared to each other (Figure 40). As expectable from the previous results, the ratio of late nascent (6S)/5.8S (pre-) rRNA over 7S pre-rRNA of the Nog2-TAP purified particles was significantly higher than the one of Nog1-TAP or Rsa4-TAP (Figure 40A) further confirming the preferential binding of Nog2 to a "later" preribosomal sub-population of rpL21 depleted cells. The above suggested partial release of a set of LSU biogenesis factors (including Nop7 and Nop53) from LSU precursors in rpL21 depleted cells was also directly addressed via affinity purification of TAP tagged Nop7 and Nop53 (Figure 40B). Co-purification efficiencies of 7S pre-rRNAs and 5.8S rRNAs using Nop7-TAP and Nop53-TAP (and in addition Nog1-TAP, NBog2-TAP, and Rsa4-TAP) as bait proteins in cells in which rpL21 was either expressed ("wild type") or repressed were calculated based on the quantified signals of the Northern blotting analyses (Figure 40C). Tagged Nop7 and Nop53 co-purified 7S (and 27S) pre-rRNAs of rpL21 depleted cells equally efficient as of wild type cells (Figure 40C, raw data in Figure 40B). However, in contrast to Nog1, Rsa4, and especially Nog2, efficiencies of (nascent) 5.8S rRNAs co-purifying with tagged Nop7 or Nop53 did not increase over background (Figure 40C, for the raw data used for quantifications see Figures 34A, 38A, 39A, and 40B) after *in vivo* expression shut down of RPL21. In summary, the presented data further indicate that a group of LSU biogenesis factors including Nop53, Nop7 and (presumably) other earlier acting "A3 factors" as Nop15, Cic1/Nsa3, Rlp7, Erb1 or Has1 partially dissociate from a late nascent nuclear LSU precursor population that is still produced in the absence of rpL21. On the other hand, the release of a group of factors including Nog1, Rsa4, Nog2 (and possibly Nug1, Nsa2, Rrs1, Rpf2 and a few others) from the same late nascent pre-60S populations seems to be disturbed (Figures 37C, 38D, 39D).

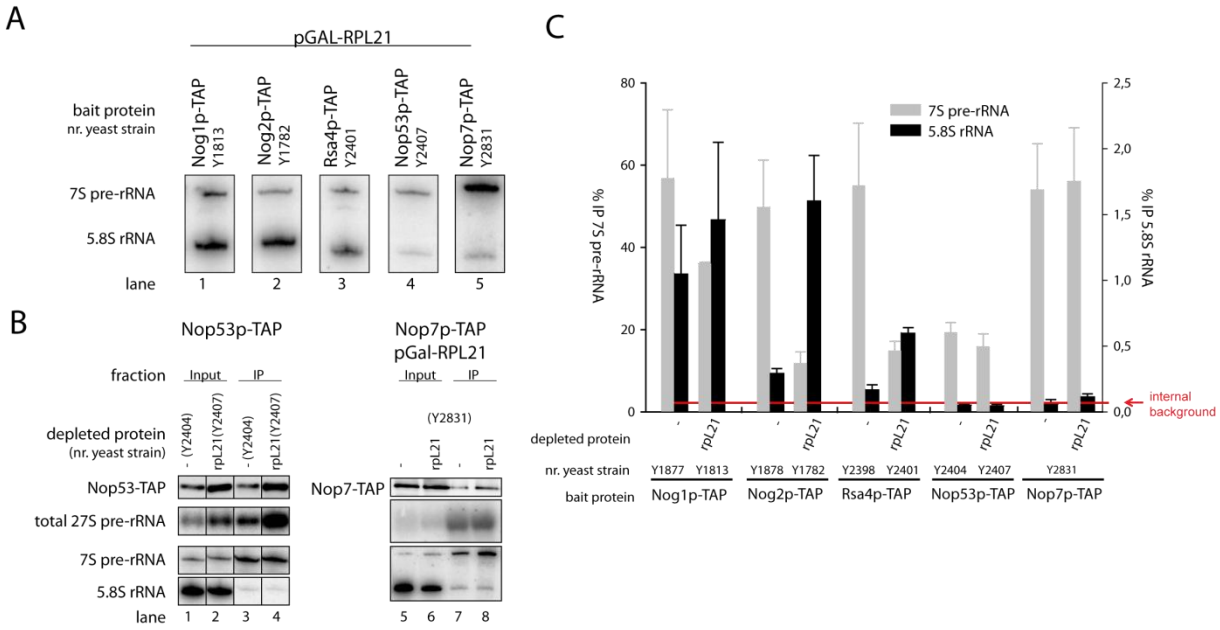

Figure 40 - (Pre-) rRNA composition of different preribosomal particle populations affinity purified after *in vivo* depletion of rpL21.

The indicated derivates of a wild type yeast strain and of a strain in which rpL21 expression is under control of the GAL1/10 promoter were created which express a chromosomally encoded TAP-tagged version of the LSU biogenesis factors Nog1, Nog2, Rsa4, Nop53 or Nop7. Strains were cultivated for four hours in glucose-containing medium to shut down (or not) expression of RPL21. The TAP-tagged proteins and associated preribosomal particles were then affinity purified from corresponding cellular extracts as described above. **A)** shows the relative amounts of 5.8S rRNA and 7S pre-rRNA in the affinity purified fractions as detected northern blotting using a probe which is complementary to 5.8 rRNA sequences. Lanes 1-3 (using tagged Nog1, Nog2, and Rsa4, respectively, are derived from the experiments shown in Figures 34, 38, and 39, respectively. In **B)** the (pre-) rRNA content of total cellular extracts (Input) or fractions affinity purified via Nop53-TAP or Nop7-TAP (IP) from cells expressing (or not expressing) RPL21 are shown. Purification efficiencies of the bait proteins were monitored by western blotting (see panel designated WB bait). **C)** Shows a quantitation of the average co-purifications efficiencies of 5.8S rRNA and 7S pre-rRNAs with the indicated tagged LSU biogenesis factors in presence or upon depletion of rpL21 seen in two independent experiments. The scale for the 7S pre-rRNA co-purification efficiency is on the left side, the one for the 5.8S rRNA is on the right side. The internal background level of the experiments, as measured by the (unspecific) efficiency of 20S pre-rRNA co-purification, is indicated by a red line (raw data not shown).The scale for the internal background is the one of 5.8S rRNA on the right. Adapted from Ohmayer et al. (2013).

4 Discussion

4.1 General features of the assembly of LSU r-proteins in yeast

As described in section 3.2.2, the assembly characteristics of a number of essential LSU r-proteins was addressed by affinity purifying FLAG tagged versions of in total 16 LSU r-proteins *ex vivo* from cell extracts followed by comparative quantitative analyses of the co-purified rRNA (precursor) molecules (Figures 21 and 22). In average, the earliest pre-rRNAs were co-purified to rather low efficiencies which were, however, still above background levels. Further maturated preribosomal particles were co-purified with significantly higher efficiencies indicating that (in average) the affinities of the tested LSU r-proteins to the respective preribosomes increase in a step wise fashion. In sum, these results suggest that in yeast the rather loose associations of many LSU r-proteins to early LSU precursors are progressively converted to more stable interactions during the course of LSU maturation. In line with this, the (in average) weak interactions of LSU r-proteins to early LSU precursors could more easily be disrupted by higher salt concentrations while the more stable associations to later LSU precursors (or mature LSUs) remained largely unaffected (Figures 21 and 22).

A study investigating the interaction of tagged SSU r-proteins with SSU precursors of different maturation states provided evidences for a similar, progressive assembly behavior of the tested r-proteins (Ferreira-Cerca et al., 2007). In addition, some of the extensive factor-free *in vitro* reconstitution studies on prokaryotic ribosomal subunits introduced in section 2.3.1.1 suggested similar conclusions. *E.coli* SSU r-protein S4 was reported to stabilize a weak initial *in vitro* interaction to 16S rRNA (fragments) into a more robust one by “rearranging” (folding) the initial labile complex to a more stable one (Mayerle et al., 2011). The “induced fit” like mechanism of the formation of final r-protein - rRNA interactions which was suggested in an earlier study of the Woodson laboratory also argues for a progressively stabilization of r-protein r-RNA interactions in the course of the maturation of ribosomal subunits (Adilakshmi et al., 2008; Woodson, 2011). Complementary approaches performed by the Williamson laboratories investigating different *in vitro* SSU assembly intermediates applying fluorescence triple correlation spectroscopy resulted in similar conclusions (Ridgeway et al., 2012 and citations therein).

Altogether these findings suggest that the assembly process of many r-proteins, at the end of which a stable association to the respective ribosomal subunit is established, occurs in several steps after each of which the association becomes more robust. Assembly of many r-proteins therefore should not be regarded as a simple one-step event, but rather as a multi-step process.

4.2 Specific assembly behavior of a subset of LSU r-proteins

In contrast to the above described “typical” assembly characteristics of most LSU r-proteins, the results shown in sections 3.2.1and 3.2.2 indicate a different, specific assembly behavior for a subset of LSU r-proteins which significantly differs from the one of most other LSU r-proteins. Two groups of LSU r-proteins showed a unique assembly behavior which will be discussed in the following two sub-sections.

4.2.1 Late incorporation of a specific group of LSU r-proteins

The first of these two groups consists of the essential LSU r-proteins rpL10, rpL40, and rpL42 and the non-essential r-proteins rpL24, rpL29, rpP1A/B, and rpP2A/B. All of these “late” LSU r-proteins were characterized by a clear underrepresentation in most of the analyzed pre-60S particles in comparison to mature LSUs, as measured by the pair wise comparative analyses of differently maturated (pre-) 60S particles applying semi quantitative mass spectrometry shown in section 3.2.1 (Figure 20). In addition, the “late” assembly of two essential members of this group, rpL10 and rpL40, was confirmed in a complementary approach described in section 3.2.2 (Figures 21 and 22). FLAG epitope fused versions of a number of essential LSU r-proteins were affinity purified *ex-vivo* from cellular extracts and the maturation state of the co-purified (pre-) ribosomal particles was investigated by analyzing the rRNA (precursors) by Northern blotting. Among all tested LSU r-proteins, both, FLAG tagged rpL10 and rpL40 co-purified all rRNA precursor species to very low extents while mature rRNAs were co-purified much more efficiently. Accordingly, the ratios of the co-purification efficiencies of the 5.8S rRNA versus its latest well detectable precursor, the 7S pre-rRNA were by far higher for rpL10-FLAG and FLAG-rpL40 than for all other tested LSU r-proteins (Figure 21 and quantification in Figure 22B). As introduced in section 2.3.2.2, the *in vivo* assembly behavior of eukaryotic LSU r-proteins was started to be analyzed already almost 40 years ago by several means including metabolic labeling techniques and, more recently, affinity purifications of LSU (precursors) analyzed by mass spectrometry and/or Northern blotting (see section 2.3.2.2 and citations therein). Very consistently with the results obtained in the probably more systematic approaches applied here, evidences for a rather late assembly behavior all the members of this “late” group were already provided in some of these studies. While the late assembly behavior of rpL10 and rpL24 was very consistently described in several studies on eukaryotic LSUs from several organisms (yeast, mouse, human), evidence for late assembly of the other members (rpL29, rpL40, rpL42, rpP1A/B, and rpP2A/B) was found less consistent in the literature (see citations in the introduction-section 2.3.2.2).

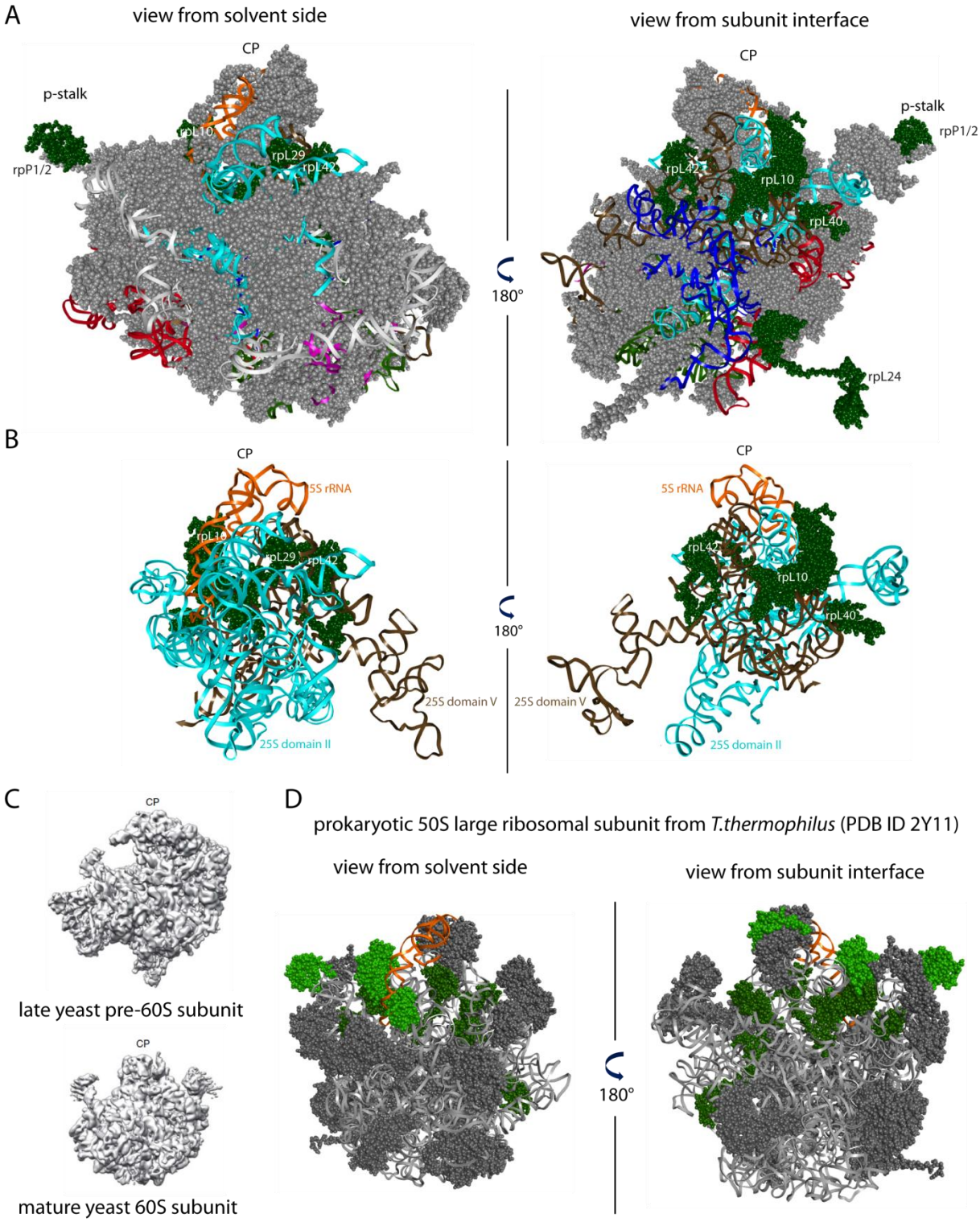

Figure 41 - Illustration of the late incorporated LSU r-proteins on a mature eukaryotic (yeast) and prokaryotic (*t.thermophilus*) large subunit highlighting their contacts to LSU rRNA domains.

The members of the group of LSU r-proteins which are incorporated at late stages (group 1 in Figure 20B) in LSU maturation rpL10, rpL24, rpL29, rpL40, rpL42, rpP1A/B, and rpP2A/B are colored in green. The remaining yeast LSU r-proteins are colored in gray in part **A)**, in which the yeast crystal structure (Ben-Shem et al. (2011)) is depicted from two perspectives. LSU rRNA secondary structure domains are colored in magenta (5.8S rRNA), gray, cyan, green, blue, brown, and red (25S rRNA domain I – VI), and orange (5S rRNA), respectively. In **B)** the LSU is depicted from the same perspectives but only showing the "late" LSU r-proteins, the 5S rRNA, and 25S rRNA domain II and V to better visualize the location of rpL10, rpL29, rpL40, and rpL42, in or around the central protuberance establishing many contacts to 25S rRNA domains II and V. In **C)**, the recently published cryo-EM structure of a late pre-60S particle (upper structure) in which the orientation of the central protuberance (the "5S

RNP" and parts of domains II and V) differ significantly to their final location in the mature LSU (lower structure). Adapted from Leidig et al. (2014). In **D),** the structure of a prokaryotic 50S ribosomal subunit from *T.thermophilus* (PDB file 2Y11) is shown. 23S rRNA is colored in gray, 5S rRNA in orange and most LSU r-proteins in gray. Those r-proteins that were identified in two recent studies to be incorporated at late maturation stages (Chen and Williamson, 2012) and/or to be underrepresented in mutant 45S LSU precursors (Jomaa et al., 2013) are colored in different shades of green. *B.subtilis* L16, L27, L28, L33, L35, and L36 and their *E.coli* homologues that were identified in both studies to be late incorporated / underrepresented in LSU precursors (see above) are colored in dark green. *E.coli* L30, L10, L25, and L31 which were additionally identified to be late incorporated by the Williamson lab are colored in light green.

The location of the members of this late group on the mature yeast LSU is depicted in Figure 41 (Ben-Shem et al., 2011). With the exception of rpL24 and the phospho stalk proteins rpP1 and rpP2, all remaining "late" LSU r-proteins (rpL10, rpL29, rpL40, and rpL42) are located in and/or around the central protuberance ("CP" in Figure 41A-B) which consists of the 5S rRNA, parts of 25S rRNA domains II and V and several additional r-proteins, including rpL5, rpL11, and rpL21 (Figure 41A-B). In contrast to these "late" LSU r-proteins, the 5S rRNA and the two r-proteins rpL5 and rpL11 were described to be recruited as the "5S RNP" (which also contains the two LSU biogenesis factors Rpf2 and Rrs1) to LSU precursors of early maturation stages (Zhang et al., 2007). The location of most of the "late" LSU r-proteins around the "core" of the central protuberance therefore suggests that the establishment of the "final" orientation of this structural feature involves some late LSU r-protein assembly events. The very recent publication of a sub-nanometer resolved cryo-EM structure (8.7Å) of a late (Arx1-TAP or Arx1-TAP/Rsa4-FLAG) affinity purified LSU precursor particle strikingly confirmed these predictions (Leidig et al., 2014 and Figure 41C). The densities corresponding to LSU r-proteins rpL10, rpL29, rpL40, and rpL42 were missing in the structure of the late Arx1 particle while those densities of the "5S RNP" (5S rRNA, rpL5, rpL11) and some helices of the neighboring LSU rRNA domains II and V (helices 38, and 82-88) were described to be in a largely different conformation. Therefore, the "5S RNP" was suggested to perform a "semicircular" movement during late stages of pre-60S maturation to adopt its final position – an event that is apparently followed (or accompanied) by the assembly of the above listed "late" LSU r-proteins (and the release of some LSU biogenesis factors positioned in or near this structural feature as Rsa4 and Nog1). Interestingly, the remaining members of the late group, rpL24, rpP1A/B, and rpP2A/B were also described to be absent from the premature Arx1 particle, confirming their late incorporation (Leidig et al., 2014). In addition to those three, densities corresponding to rpP0 were described to be largely "occupied" by its "placeholder", the LSU biogenesis factor Mrt4 which shares some homology with rpP0 (Rodríguez-Mateos et al., 2009a, 2009b). The results shown in Figure 20 pointed into the same direction, namely a partial underrepresentation of rpP0 in the analyzed LSU precursors, which was, however, less strong and consistent why rpP0 was not clustered into the same branch as the other members of the "late" group of LSU r-proteins. Furthermore, the non-essential domain IV binder rpL41, whose tryptic peptides cannot be identified by the applied mass spectrometry based approach (due to its small size of only 25 amino acids and its inappropriate sequence), could not be detected in the late pre-60S particle (Leidig et al., 2014). This indicates that it is indeed not yet incorporated into this late Arx1 particle. Alternatively it might already be associated but (still) have a flexible conformation.

In addition, the proposed exchangeability of rpL10 and the phospho proteins, as well as the partial underrepresentation of the latter in LSUs from stationary cells and 80S ribosomes versus “polysomal ribosomes” (see section 2.3.2.2 and citations therein) does not argue against a potential dynamic structural variability of the central protuberance and the phospho stalk even in mature LSUs.

Remarkably, recent studies on the assembly of prokaryotic (*E.coli* and *Bacillus subtilis*) LSUs provided evidences for very similar conclusions, even if both, the composition of prokaryotic ribosomal subunits and their maturation differ from the ones of their eukaryotic counterparts (only about half of the r-proteins are conserved between pro- and eukaryotes, different biogenesis factors are involved, no cell compartmentalization in prokaryotes, etc…). As already mentioned in the introduction section 2.3.2.1, the Williamson group combined an *in vivo* stable isotope pulse-labeling approach with quantitative mass spectrometry and identified a group of r-proteins being late incorporated (Chen and Williamson, 2012, see also Figure 14C-D). Interestingly, and in line with the above discussed conclusions, many of these late prokaryotic LSU r-proteins (including L16, L25, L27, L30, L31, L33, and L35) are located at or near the central protuberance (Figure 41D and Schmeing et al., 2011). Based on these initial data and on recently published structural information of a late 45S LSU precursor isolated from *Bacillus subtilis* cells, from which several r-proteins (including most of the previously identified) were underrepresented, the authors concluded that the final conformation of “key functional sites”, one of which is the central protuberance, are established late in the assembly process of prokaryotic 50S subunits (Jomaa et al., 2013).

In sum, the late assembly behavior of all members of this group of LSU r-proteins identified in this work are in agreement with very recent and extensive previous studies starting almost 40 years ago. In addition, despite all the differences in composition of pro- and eukaryotic ribosomes and their biogenesis (see above), they seem to share the late establishment of the final conformation of the central protuberance, which might be dynamic even in mature LSUs during the translational cycle (see above).

4.2.2 Pronounced increase of the affinity of rpL2, rpL43, and rpL39 concomitant with ITS2 processing

The second group that was characterized by a clearly distinct assembly behavior consists of the two essential LSU r-proteins rpL2 and rpL43 and the non-essential rpL39. The results shown in sections 3.2.1 and 3.2.2 (Figures 20-22) indicated that the binding strength of these proteins increased more than the one of the other LSU r-proteins during or shortly after the first processing event in the ITS2 (at site C2) of 27SB pre-rRNA containing LSU precursors in the nucleus. However, both, FLAG tagged rpL2 and rpL43 co-purified the earlier, 35S pre-rRNA or 27S pre-rRNA containing preribosomes to comparably weak, but detectable extents indicating that they already start interacting with early preribosomes, albeit with very low

affinities (Figures 21-22). Even if most of the other LSU r-proteins were characterized by a similar behavior, namely clearly increased affinities to preribosomes of later maturation stages, the affinity of none of them increased after this processing event as strong as for rpL2 and rpL43. In line with this, rpL2, rpL39, and rpL43 tended to be reproducibly underrepresented in mutant preribosomes whose maturation was inhibited at early or intermediate ("pre – C2 cut") stages by depletion of LSU r-proteins with an "early" or "middle" pre-rRNA processing phenotype (sections 3.3.2 and 3.3.3, see for example Figures 26, 30, or 31).

Interestingly, L2, (homologue of rpL2, see also table 1), the only prokaryotic homologue of this group was reported to be underrepresented in pre-mature ribosomes isolated from *E.coli* cellular extracts (Nierhaus et al., 1973). In the previously described stable isotope pulse labeling approach by the Williamson laboratories *E.coli* L2 was grouped into the fourth of six groups (Chen and Williamson, 2012, see also Figure 14C-D). This does not argue against the conclusions drawn above that its interaction with early preribosomes is very weak at early stages (and therefore presumably not detectable in this approach) but stabilized more than average at later maturation stages. Even if *E.coli* L2 was initially described to be able to bind to 23S rRNA independently of other r-proteins in a defined factor free LSU *in vitro* reconstitution system positioning it as primary binder in the prokaryotic LSU *in vitro* assembly map (see assembly map in Figure 13B, Herold and Nierhaus, 1987 and citations therein), more detailed studies indicate that in some defined situations its stable association to the 23S rRNA can depend on the previous binding of other r-proteins (Marquardt et al., 1979; Roth and Nierhaus, 1980).

Figure 42 (next page) - Location of rpL2, rpL43, and rpL39 on the mature yeast 60S ribosomal subunit and illustration of their main contacts to different LSU rRNA domains.

The rRNAs of the yeast LSU and the LSU r-protein rpL2, rpL43, and rpL39 are depicted in **A)** as published by Ben-Shem et al., 2011. The colors of the rRNA (secodondary structure domains) are as described in Figure 41 (see also color code in part **B)**). rpL2, and rpL43 are colored in light and dark gray, respectively. RpL39 is colored in black. Again the LSU is depicted as viewed from two different perspectives. The position of ITS2 sequences (in preribosomes, as indicated by the 3' end of the 5.8S rRNA and the 5'end of the 25S rRNA) is shown. The direct contacts of rRNA sequences of 25S rRNA domains II, III, IV, and V to the rpL2/rpL43 dimer (right) or of the 5.8S rRNA and 25S rRNA domains I and III to rpL39 (left) are highlighted by yellow colors in **C)**. These contacts of rpL39 or the rpL2/rpL43 dimer to the LSU domains is illustrated in a simplified way in **B)**. Each black lines corresponds to one direct contact of rpL39 (left) or the rpL2/rpL43 dimer (right) to (stretches) of the respective LSU rRNA domains. The lengths of colored boxes corresponding to the LSU rRNA (domains) depicted in **B)** are in proportion to their real length (in yeast).

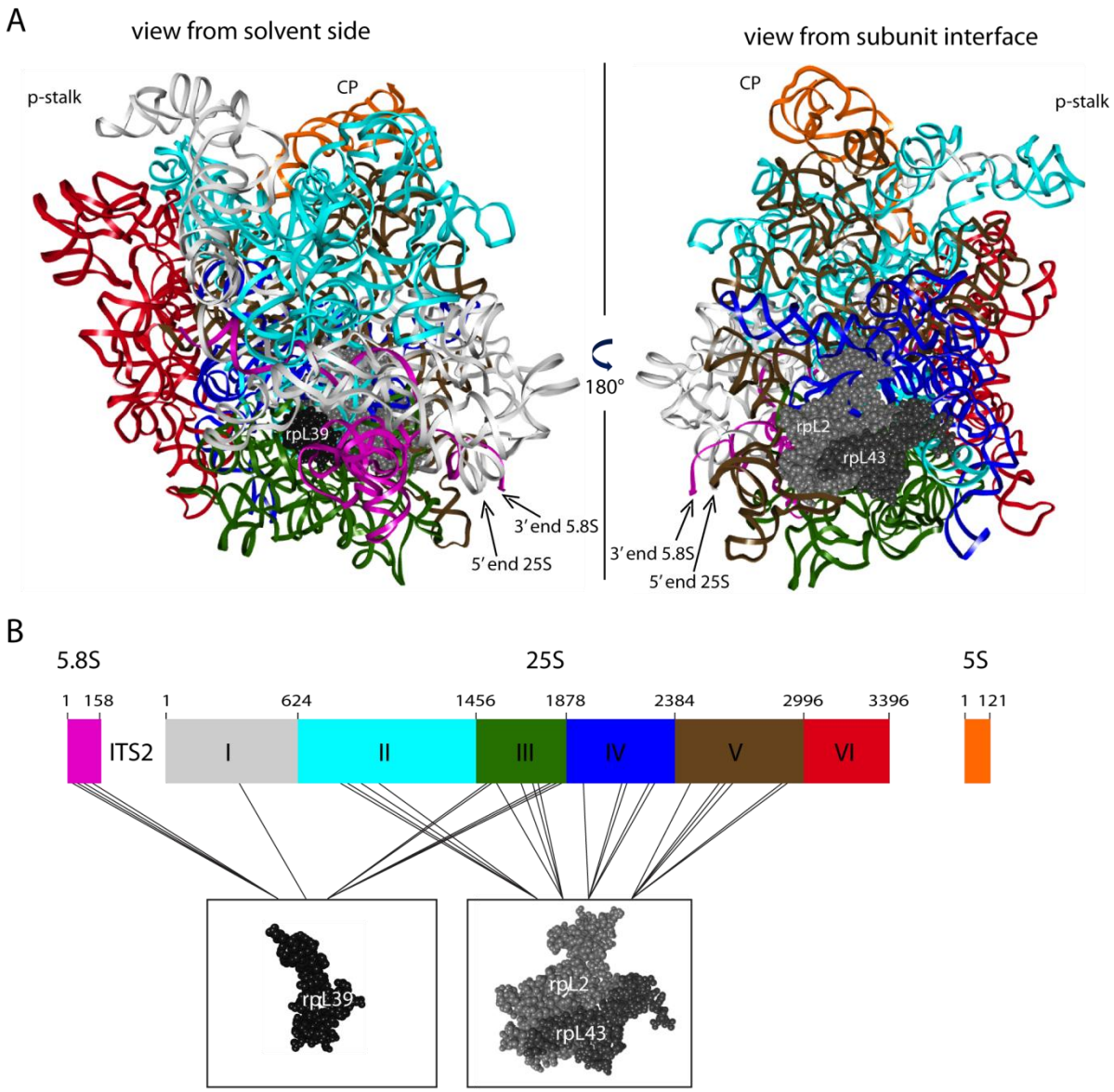
A
view from solvent side
view from subunit interface
p-stalk
CP
CP
p-stalk
180°
rpL39
rpL2
rpL43
3′ end 5.8S
5′ end 25S
3′ end 5.8S
5′ end 25S
B
5.8S
25S
5S
1 158
1
624
1456
1878
2384
2996
3396
1 121
ITS2
I
II
III
IV
V
VI
rpL39
rpL2
rpL43
C
5.8S rRNA
domain I
domain III
rpL39
domain II
domain IV
domain V
rpL2
rpL43
domain III
rpL39
rpL2
rpL43

As illustrated in the yeast LSU structure shown in Figure 42, the location of both, pro- and eukaryotic L2 / rpL2 is at the subunit interface side. In both cases, L2 / rpL2 directly contact four of the six LSU secondary structure domains (23S/25S rRNA domains II, III, IV, and V) via distinct interaction interfaces which are (for yeast) highlighted and schematically illustrated in Figure 42B-C (Schmeing et al., 2011; Schuwirth et al., 2005; Ben-Shem et al., 2011). Combining the previous data deduced from the prokaryotic *in vitro* LSU reconstitution studies and the pro- and eukaryotic *in vivo* data (latter of which were obtained in this work) with the structural information of both, pro- and eukaryotic LSUs one can hypothesize that at early stages, the establishment of a few of the numerous interactions of L2 / rpL2 with (a) certain LSU rRNA domain(s) is sufficient for its detectable, but comparably weak association to early or intermediate LSU precursors. Indeed, the “primary in vitro binding site” of *E.coli* L2 was described to consist of parts of LSU domain IV (Egebjerg et al., 1991; Klein et al., 2004). The here observed above-average increased association to later, “post ITS2 processed” nuclear LSU precursors might be derived from the establishment of the additional interaction interfaces of rpL2 (or a putative rpL2/rpL43 dimer) with all four 25S rRNA domains as found in the mature LSU (see Figure 42B-C).

A conformational change of nuclear LSU precursors which eventually leads to the establishment of the stable incorporation of rpL2 and rpL43 and which might occur concomitant with the endonucleolytic cleavage of ITS2 sequences at site C2 is one possible explanation of the observed results. These likely occurring conformational changes might be accompanied by the binding, “action” and/or release of certain LSU biogenesis factors. One of these factors could be the GTPase Nog2, which has the same “late” pre-rRNA processing phenotype as rpL2 and rpL43 (Saveanu et al., 2001) and which was recently reported to cross-link to parts of rRNA domains of the subunit interface (mainly domains IV and V) that are in part very close to the location of rpL2 (e.g. helix 71 in domain IV, Matsuo et al., 2013). Indeed, Nog2 was observed to be underrepresented in mutant preribosomes in which the ITS2 processing was inhibited (see results shown in Figures 37 and 38). This potential link of ITS2 processing, Nog2 association (presumably including the “action” of its GTPase activity) and stabilized incorporation of rpL2/rpL43/rpL39 is an interesting example of how r-protein assembly and maturation events are coupled *in vivo*.

The third member of this group, the non-essential rpL39 is not located at the subunit interface of the LSU but rather on the opposite side between domains I (incl. the 5.8S rRNA) and III, directly contacting these domains with several interaction interfaces (Figure 42C). Since it is not required for cell growth, it was not included in the affinity purifications of FLAG epitope tagged LSU r-proteins (Figures 21-22), why the presumably pronounced increase of its affinity to ITS2 processed preribosomes could not be directly tested. However it clearly showed a very similar behavior as rpL2 and rpL43 in all analyses on both, “wild type-like” and mutant preribosomes in which semi quantitative mass spectrometry was applied (see for example Figures 20, 26, 30, 31, 34). These results open up the possibility of similar conformational changes in the LSU domains rpL39 interacts with (domain I (including the 5.8S rRNA) and III) which might take place during or shortly after the ITS2 processing of

27SB pre-rRNA containing nuclear LSU precursors. As illustrated in the structure shown in Figure 42A, both ends of the ITS2 sequence (3' end of 5.8S rRNA and 5' end of 25S rRNA) are in proximity of rpL39. In addition and in contrast to most other LSU r-proteins, rpL39 seems to be largely "buried" by the rRNA domains it interacts with. A presumably more "open" state of these domains in "pre-ITS2 processed" LSU precursors might therefore be converted to the more "closed" conformation found in mature LSUs, in which rpL39 connects these LSU domains with each other what could lead to its apparently stabilized association. In contrast to rpL2 and rpL43, the binding of rpL39 seems to be not strictly required for these potentially occurring events, though, since it is non-essential under normal laboratory conditions.

4.2.3 Outlook for possible future approaches and their challenges

As described above, some of the structural predictions made in this work which are based on biochemical approaches were recently confirmed in the case of the late occurring structural rearrangement of the central protuberance which seems to be accompanied by the incorporation of the members of the "late" group of LSU r-proteins (section 4.2.1). Whether or not other predictions on structural changes of LSU precursors made in the previous sections might be confirmed by structural data in the near future remains less clear. One such yet unconfirmed prediction is a possible conversion of a more open like structure of "pre-C2 cut" LSU precursors into the more defined one of "post-C2 cut" LSU precursors what seems to coincide with (or be followed by) the stabilized incorporation of certain LSU r-proteins as rpL2 and rpL43 (see above). The recent advancements in the cryo EM field (as more efficient particle sorting, improved algorithms to compute structural information etc…) might allow the creation of sufficiently resolved structural information of LSU precursors of "early" or "intermediate" maturation state, even if this seems to be more challenging. One of the main reasons for that is that many different LSU precursor populations have to be distinguished from each other. The association of a large number of trans-acting biogenesis factors (and/or RNPs), the presence of spacer rRNA sequences and the in general presumably weaker interaction strengths (which are more fragile during the purification and therefore require mild buffer conditions) probably further hamper these studies. In addition, the in the previous section described flexibility of several LSU rRNA domains (which in general seem to adopt a rather "open" like conformation in LSU precursors of an earlier maturation state) complicates their detection by cryo-EM (and also crystallography).

Besides this, improved biochemical approaches could help to better understand the dynamics of the association of r-proteins to earlier preribosomes. The detection of potential differences in the r-protein composition of the earliest (35S pre-rRNA to 27SA2 pre-rRNA containing) LSU precursors could not be addressed here, since the biogenesis factor Noc2, which was used as bait protein to co-purify these "early" particles stayed associated with all these "early" assembly intermediates. The inclusion of additional biogenesis factors which exclusively bind to 35S or 27SA2 pre-rRNA containing preribosomes could be one way to address potential "early" LSU r-protein assembly events. The creation of yeast strains

expressing a combination of two differently epitope tagged biogenesis factors (e.g. TAP and FLAG tag) whose cell extracts could be subjected to two sequential affinity purification steps could also help to increase the “resolution” of the early assembly intermediates.

Reducing the “background” of contaminating mature LSUs, which was present in all affinity purifications and therefore clearly limiting the pair-wise comparative approaches analyzed by semi quantitative mass spectrometry is another possible strategy to enable the detection of weaker compositional changes. The separation of nuclear fractions from the cytoplasm prior to the affinity purification of epitope tagged proteins might help to reduce this contaminating background of cytoplasmic mature ribosomes. Another way is the use of stable isotope labeled amino acids, using for example N14/N15 containing nitrogen compounds as sole source of nitrogen. The resulting tryptic peptides of the differently isotope labeled proteins behave similar in liquid chromatography but can be distinguished by mass spectrometry opening up the use of quantitative mass spectrometry based approaches, as already applied to study the assembly of prokaryotic ribosomes (Chen and Williamson, 2012; Chen et al., 2012; Jomaa et al., 2013). Combining the stable isotope labeling with a pulse (e.g. shift of an appropriate yeast culture from N15 containing to N14 containing medium), after which the “newly” produced r-proteins can be distinguished from the previously present pool of r-proteins mainly incorporated into mature ribosomal subunits, is an alternative and promising strategy. Initially performed experiments gave promising results (P. Milkereit). Based on this approach, several other questions, as the potential exchangeability of LSU r-proteins during the translational cycle (see above) could rather easily be addressed.

Finally, the use of a different approach based on structural probing of (pre-) ribosomal particles focusing on the analyses of the conformational dynamics can be used to complement the here applied methodology. One way is based on the fusion of proteins with a micrococcal nuclease (MNase) resulting in a fusion protein that can be used as molecular probe after being incorporated *in vivo* into complex RNPs as the ribosome. The conditional ribonuclease activity can be activated what results in an induced cleavage of RNA regions which are accessible for the fusion protein within the local environment of the RNP of interest. The potential of this approach was shown to be applicable to obtain specific RNA cleavage events in as complex RNPs as the ribosome (Ohmayer et al., 2012) and could therefore also be applied to study the sophisticated conformational dynamics of ribosomal precursor particles. Initial studies resulted in promising, yet unpublished results (C. Müller and A. Limmer). In addition to these tethered structure probing approaches, the potential of more broadly used “general” (undirected) structure probing approaches as the hydroxyl radical induced cleavage of RNA could also be used to obtain helpful structural information. In addition, cross-linking based approaches followed by reverse transcription of the cross linked rRNA (“CRAC”) was intensely used in the last few years to systematically investigate the binding sites of the numerous trans-acting ribosome biogenesis factors what will certainly be continued (Granneman et al., 2009, see also 2.2.6.2 and citations therein).

4.3 Hierarchical interrelationships among LSU r-protein assembly events in yeast

Besides studying the *in vivo* assembly characteristics of LSU r-proteins in the "wild type" situation (see above), the second main goal of this work was to decipher how some of LSU r-protein assembly events are controlled *in vivo* and how they might depend on each other. Therefore, as described in sections 3.3.2, 3.3.3, and 3.3.4 the changes in the protein composition of mutant LSU precursors depleted of one of in total 22 different essential LSU r-proteins was systematically analyzed by comparing the levels of LSU r-proteins in the mutant LSU precursors to the respective wild type particles by mass spectrometry in a semi quantitative way. According to the pre-rRNA processing status of the *RPL* mutants, the LSU r-proteins had previously been classified into four distinct classes of pre-rRNA phenotypes. The 22 LSU r-protein expression mutants analyzed in this work belonged to pre-rRNA processing classes I, II, and III. Hence, pre-rRNA processing was inhibited at "early", "middle" or "late" maturation stages of nascent LSUs. Nine "early" (class 1) expression mutants (*RPL3, RPL4, RPL7, RPL8, RPL16, RPL18, RPL20, RPL32, and RPL33*), seven "middle" (class 2) mutants (*RPL9, RPL19, RPL23, RPL25, RPL27, RPL34, and RPL35*), and six "late" (class 3) mutants (*RPL2, RPL10, RPL11, RPL21, RPL28, and RPL43*) were analyzed in more detail as shown in sections 3.3.2, 3.3.3, and 3.3.4, respectively. In general, and in agreement with previous studies, the expression shut down of most of the analyzed r-proteins lead to a destabilization of the resulting LSU precursors which were subjected to an efficient degradation, as indicated by reduced levels of LSUs and no extreme accumulation of pre-rRNAs. Consequently only changes in the protein composition of mutant LSU precursors which were not (yet) degraded could be identified in the applied approach. In general, presumably due to some amounts of contaminating mature LSUs in all affinity purifications, the observed effects on the levels of LSU r-proteins were not very drastic (levels of the depleted LSU r-protein were normally not below about 1/8 - 1/2 of the wild type situation). Furthermore, the degree of effects on the other LSU r-proteins led to the conclusion that they were normally not completely absent from the mutant preribosomes. The observed effects rather argue for the inhibition of a specific step in the above described progressive assembly process of most LSU r-proteins.

In most cases, the observed effects on other LSU r-proteins could be categorized into two distinct classes. Many of the strongest effects on other LSU r-proteins were specifically seen in individual LSU r-protein mutants. In these cases, levels of LSU r-proteins that bind in the neighborhood of the depleted r-protein, either directly contacting it or being bound to the same LSU rRNA domain, were reduced. A second, more general class of effects was observed which can be related to the distortion of the respective maturation event (as pre-rRNA processing or nuclear export). Examples of the first class of observed effects can be found in *RPL* mutants of all three phenotypic classes, some of which will be illustrated in the following.

Concerning the group of analyzed class 1 LSU r-proteins (section 3.3.2), differences in the effects on other LSU r-proteins were among the most distinct between the *RPL8* mutant and the *RPL7* (group of) mutant(s). While rpL8 depletion resulted in strongly reduced levels of rpL8 itself, rpL13, rpL15, and rpL36, depletion of rpL7 resulted in strongly reduced levels of rpL7 itself, rpL6, rpL14, rpL20, rpL16, and rpL33. As already mentioned in section 3.3.2, the members of each of the two groups form “cluster” on the LSU which are clearly separated from each other (Figure 43A). The members of the “rpL8 – group” mainly contact LSU rRNA domains I (including the 5.8S rRNA) with some slight contacts to domains III, and V, respectively (not shown), while the members of the “rpL7 group” contact LSU rRNA domains I, VI, and mainly II. The hierarchical interrelationships among the members of these groups could only in parts be tested. According to the obtained data, rpL7 is required for the stable association of all the members of this group but its own association was not strongly affected after depletion of any of the other tested members of this group, hence it seems to be the most “upstream” member of this group. On the other hand, stable association of rpL16, rpL33, and rpL20 seemed to be partially interdependent. RpL20, and especially rpL14 seemed to be among the most “downstream” LSU r-proteins of this group, meaning that their assembly presumably requires the previous assembly of all the other LSU r-proteins bound in this LSU neighborhood. The possible molecular reason of the common “early” pre-rRNA processing phenotype which is shared by all the class 1 LSU r-proteins will be discussed in section 4.5.

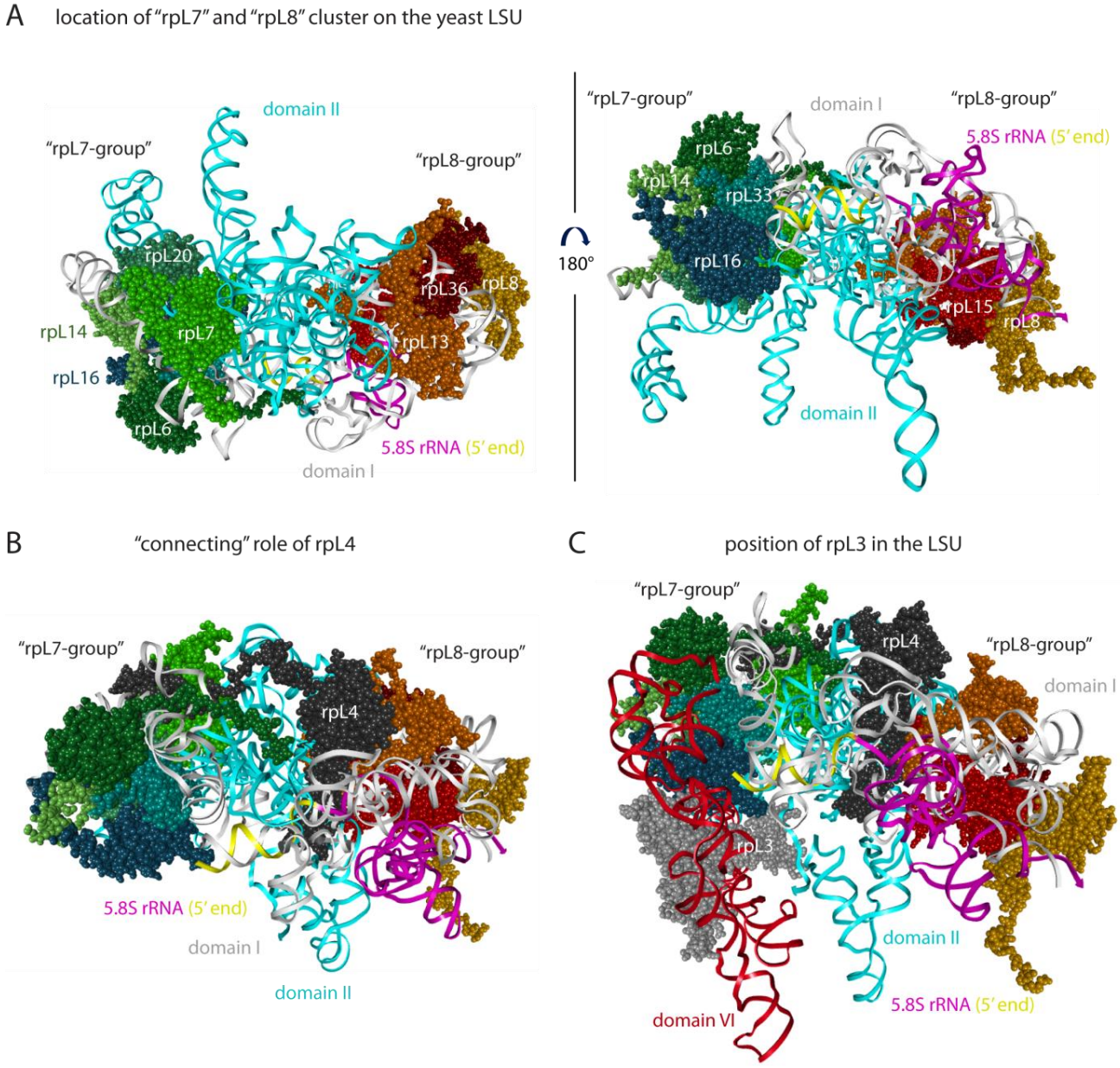

Figure 43 - The location of early required LSU r-proteins on the LSU can explain their hierarchical interdependencies

Parts of the yeast LSU (Ben-Shem et al., 2011) are shown to illustrate the location of most of the class 1 LSU r-proteins aiming to explain the observed hierarchical interrelationships among them. **A)** shows LSU rRNA domains I (gray), including the 5.8S rRNA - magenta), and II (cyan) and the members of the rpL7 (colored in shades of green and blue) and the rpL8 (colored in shades of orange and red) "cluster" from two different perspectives. The 5' end (20 nucleotides) of the 5.8S rRNA (magenta) which forms a helix with parts of domain I and whose creation (by exonucleolytic processing of ITS1 sequences) is disturbed after depletion of the class 1 LSU r-proteins is highlighted in yellow. **B)** illustrates the conformation of rpL4 (dark gray) and its location "between" the rpL7 and rpL8 cluster. **C)** illustrates the location of rpL3 (light gray) which mainly contacts LSU rRNA domain VI.

The reason for the observed more pronounced effect of rpL4 depletion on the other LSU r-proteins might also be found in the structure of rpL4 and its location in the LSU (Figure 43B). RpL4, which is the second largest LSU r-protein, adapts a rather “stretched” conformation and is located in between the rpL7 and rpL8 “cluster” with numerous direct contacts to rRNA domains I and II and several members of both cluster (rpL20/rpL7/rpL6 and rpL13/rpL15). Its presumably important role in orienting and stabilizing these sub-structures of the LSU might therefore explain the more pronounced and “broad” effects on other LSU r-proteins which result in the observed reduced levels of 27SB pre-rRNAs caused by increased turn-over rates of these deficient preribosomes.

According to the even more “drastic” pre-rRNA processing phenotype of rpL3 (which is the largest LSU r-protein) and the most pronounced degrees of preribosomal degradation one could suspect a similar “central” position of it. In the mature LSU however, it almost exclusively interacts with LSU rRNA domain VI and only directly contacts rpL16 but no other members of the class 1 LSU r-proteins (Figure 43C). The potential cause for its requirement in the earliest LSU maturation events resulting in its “drastic” phenotype will also be discussed in section 4.5.

Regarding the second (class 2) group of LSU r-proteins (which exhibit an intermediate pre-rRNA processing phenotype), similar effects could be observed some of which will be presented in the following. As shown in section 3.3.3, the seven class 2 LSU r-protein expression mutants which were analyzed in this work, shared a group of LSU r-proteins whose levels were strongly reduced. The strongest effects among these were seen on rpL2, rpL43, and rpL39 for which strong evidences could be provided that their association increases in a pronounced way after the ITS2 processing (at site C2 – see above). Since exactly this pre-rRNA processing event was strongly disturbed in the class 2 LSU r-protein mutants, it is consequential that these three LSU r-proteins were constantly among strongly affected. Their location in the mature LSU and the presumably increased association after a suggested conformational change between the “pre-“ vs. “post” ITS2 processed LSU precursors was discussed in the previous section 4.2.2 (Figure 42).

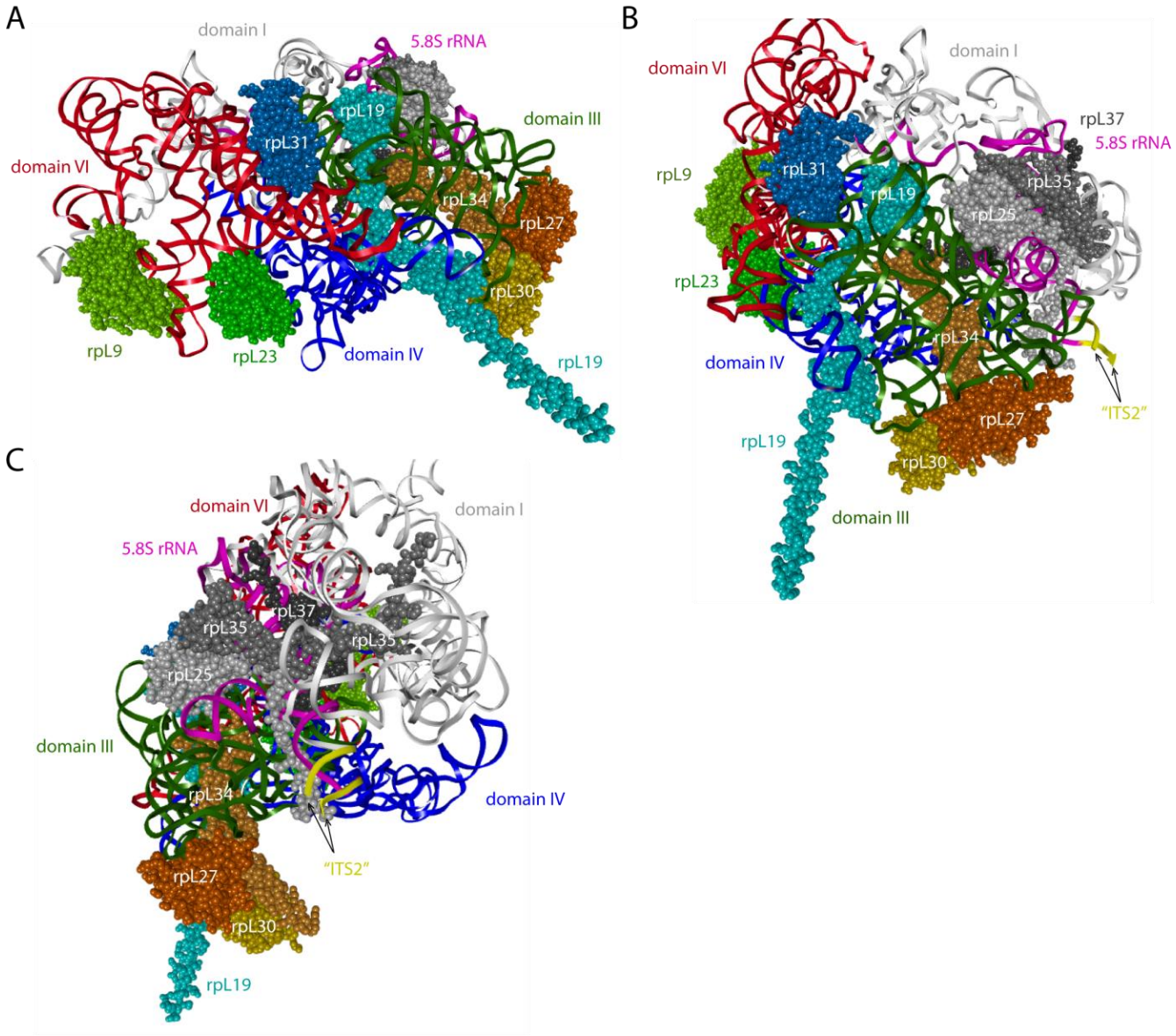

Figure 44 - Illustration of the location of the class 2 LSU r-proteins on the mature LSU highlighting cluster showing some features of interdependencies.

Parts of the yeast LSU (Ben-Shem et al., 2011) are shown to illustrate the location of most of the class 2 LSU r-proteins. LSU rRNA domains I (including the 5.8S rRNA), III, IV, and VI and some LSU r-proteins are shown in the indicated colors. Three different perspectives were chosen in **A)**, **B)**, and **C)**. RpL31 and rpL19, which were affected in all mutants, are colored in shades of blue, rpL27/rpL34/rpL30 and rpL25/rpL35/rpL37 which showed some degrees of interdependent assembly behavior are colored in shades of orange and gray, respectively. rpL9 and rpL23, which are located further apart from the other members of this class (mainly bound to rRNA domains VI) are colored in shades of green. The position of ITS2 sequences (whose endonucleolytic processing is disturbed in the preribosomes depleted of the class 2 LSU r-proteins) is indicated by yellow colors highlighting the 3' end of 5.8S rRNA and 5' end of 25S rRNA sequences, respectively.

As mentioned before, most of the members of this phenotypic class are located in proximity to each other mainly contacting LSU rRNA domains I (including the 5.8S rRNA), III, IV, and VI. Interestingly, two of the LSU r-proteins whose levels were also affected in all analyzed mutants of this class are located in this area. Both of them (rpL19 and rpL31) have been described to be involved in the pre-rRNA processing step that is inhibited in these mutants, although rpL31 was found to be a non-essential r-protein whose depletion is only lethal in combination with rpL39 depletion (Peisker et al., 2008). With the exception of the commonly

affected LSU r-proteins (rpL2, rpL43, rpL39, rpL31), depletion of rpL19 did not show any strong effects on other LSU r-proteins indicating that its stable association occurs rather "downstream" of the other class 2 LSU r-proteins and requires their previous binding. The other, specific effects that were seen after depletion of the remaining tested class 2 LSU r-protein mutants can very consistently be correlated to their location in the LSU. Groups of class 2 LSU r-proteins that showed interdependent assembly behavior can be defined which are illustrated in Figure 44. The three "domain III binders" rpL27, rpL34, and rpL30 showed (as far as tested) interdependent assembly characteristics: depletion of rpL27 and rpL34 clearly affected the association of each other and of rpL30. These specific effects were not seen at all (or much less pronounced) in the other tested mutants of this class. The fact that these three r-proteins are bound in close proximity to each other and contact the same LSU rRNA domain is another example of the often observed "local" effects (Figure 44). The specific effect of rpL35 depletion on rpL37 levels can also be explained by their close proximity (Figure 44C). The nearby bound rpL25 behaved largely independent, though and was not strongly affected after depletion of rpL35 (Figure 30). The probable proximity of many of the class 2 LSU r-proteins to the ITS2 sequences (the 3' end of the 5.8S rRNA and the 5' end of the 25S rRNA are in close proximity to each other and to many class 2 LSU r-proteins, see highlighted in Figure 44) might in part explain the molecular reason for their pre-rRNA processing phenotype, what will be discussed in section 4.5.

Finally, the "late" (class 3) LSU r-proteins six of which were analyzed in the same way in this work showed to some extents interdependent assembly behavior. Depletion of rpL11 lead to strong and specifically reduced levels of rpL5 which is, like rpL11 part of the 5S RNP (Zhang et al., 2007). Other LSU r-proteins were however not affected in the *RPL11* mutant (Figure 35). Depletion of rpL2 and rpL43 resulted in strong effects on each other and on rpL39. Due to the strong interdependency of the rpL2/rpL43 dimer (Figure 34) and their very similar behavior in the previously discussed experiments, their assembly might occur in a coordinated way in which both might even already interact before they are recruited to preribosomes. It is plausible that already their nuclear import might, as recently suggested for rpL5 and rpL11, occur in a "synchronized" way (Kressler et al., 2012b). However, no direct evidences for this hypothesis could be provided in this work why it remains largely speculative. Additional, albeit much less pronounced effects of rpL2 or rpL43 depletion on other LSU r-proteins were observed for some "late" incorporated LSU r-proteins many of which are bound at or near the central protuberance (as rpL10). This effect is in agreement with the above suggested (and recently confirmed) late establishment of the final orientation of the central protuberance which involves assembly of these "late" LSU r-proteins (Leidig et al., 2014). Since the LSU maturation is inhibited "upstream" of this event in the *RPL2* and *RPL43* mutants, the observed effects on levels of these late incorporated LSU r-proteins can be explained. The observed effects of rpL21 depletion on late LSU r-proteins can be explained by the same means. The detection of effects of rpL10 depletion on the levels of other LSU r-protein was hampered by the here applied experimental approach most likely due to changes in the association of the chosen bait protein Nog1-TAP. In addition, not all

"candidates" for being affected (late incorporated LSU r-proteins and/or LSU r-protein bound near rpL10) could be identified by the mass spectrometry based readout.

In sum, the here summarized observations illustrate the above suggested two categories of effects. First, most of the effects which were specifically observed for individual *RPL* mutants can be explained by the location of the affected LSU r-proteins in the neighborhood of the depleted one, either directly contacting it or being bound to the same LSU rRNA domain(s). The lack of the depleted LSU r-protein leads to a partial destabilization of its direct neighborhood and/or the associated LSU rRNA domain(s) what can lead to some long-range effects. The second category of effects can be correlated to the depletion phenotype of the respective *RPL* mutants: the largely inhibited maturation at different stages of the deficient LSU precursors (pre-rRNA processing or nuclear export) leads to the commonly observed reduced binding ability of those LSU r-proteins that are stably incorporated at later maturation stages. The only exceptions in these cases were the phospho stalk proteins rpP0, rpP1 and rpP2 whose levels tended to be even increased in most of the *RPL* mutants. As previously described, an "alternative", nuclear assembly pathway was suggested for rpP0 which might explain these effects (Francisco-Velilla et al., 2013; Rodríguez-Mateos et al., 2009a).

4.4 Comparison of the observed *in vivo* hierarchies of r-protein assembly events to previous prokaryotic *in vitro* studies

The obtained results of the extensive studies on *RPL* mutants summarized in the previous section provided evidence that several yeast r-protein assembly events occur *in vivo* in a cooperative way and are in part controlled by hierarchical relationships among each other. In this section these observations will be compared to the results of previous extensive studies on the factor free *in vitro* assembly of prokaryotic ribosomal subunits (see section 2.3.1.1) highlighting the main similarities and differences.

Concerning the SSU, evidences for similarities in the hierarchy of SSU r-proteins assembly events of the head domain between yeast (*in vivo*) and the prokaryotic *in vitro* assembly system were shown (Ferreira-Cerca et al., 2007). In this study, depletion of yeast rpS5 and rpS15, whose prokaryotic homologues S7 and S19 were described as primary and secondary *in vitro* binders of the SSU head domain, respectively, were shown to affect assembly events of the SSU head domain which were (in the *in vitro* SSU assembly map) indeed described as being "downstream" (see also Figures 13A and 14B). On the other hand, not all of the "predicted" interrelationships among SSU r-protein assembly events according the prokaryotic *in vitro* assembly map could be observed in yeast *in vivo*: depletion of yeast rpS5 did not affect assembly of rpS0, what would have been predicted from the assembly map of their prokaryotic homologues S7 and S2, respectively.

The prokaryotic *in vitro* assembly map of the LSU on the other hand, whose rRNA domains are not as separated in space as they are in the SSU but heavily "intertwined" with each

other, appears much more sophisticated showing many “horizontal” connections between LSU r-proteins being (mainly) bound to different rRNA domains (see Figures 13B, 14D). Since only about half of the eukaryotic LSU r-proteins have prokaryotic homologues, the direct comparison of the *in vivo* hierarchies obtained in this work to the *in vitro* hierarchies is limited to those LSU r-proteins that are shared by both domains of life. Those yeast LSU r-proteins that affected the stability of the early yeast LSU precursors most (resulting in reduced levels of almost all other LSU r-proteins), rpL3 and rpL4, have homologues in *E.coli* (L3 and L4, respectively). A “stimulatory” effect of *E.coli* L3 on the stabilized association of a group of primary rRNA binders was indeed described *in vitro* (see Figure 13B and section 2.3.1.1). *E.coli* L4 also showed some effects on the association of other *E.coli* LSU r-proteins *in vitro* including L2 (homologue of yeast rpL2), L22 (yeast rpL17) and L29 (yeast rpL35) which were also observed for their yeast homologues *in vivo* in this work. In addition, the here observed effect of yeast rpL11 depletion on levels of rpL5 was seen *in vitro* (with *E.coli* homologues L5, and L18, respectively).

On the other hand, many of the “predicted” effects (based on the prokaryotic *in vitro* assembly maps) were not observed in yeast *in vivo* and some of the effects observed *in vivo* (in yeast) were not described *in vitro* (*E.coli*). Depletion of the class 2 yeast LSU r-proteins rpL9 (*E.coli* L6), rpL35 (L29), rpL25 (L23), and rpL23 (L14) showed very strong effects on the levels of rpL2 (L2) none of which was seen *in vitro* (*in E.coli*). Depletion of the yeast class 1 LSU r-protein rpL7 (L30) resulted in reduced association of a large group of LSU r-proteins including rpL16 (L13). *In vitro* however, *E.coli* L30 was described as being rather downstream in one assembly tree and not being required for the association of any other r-protein what is in large contrast to its apparent role *in vivo* in yeast. *E.coli* L15 (homologue of yeast rpL28) was described to be required for the stable association of a number of r-proteins *in vitro* and therefore adapting a “central position” in the LSU *in vitro* assembly map (see Figure 13B). *In vivo* however, depletion of yeast rpL28 only slightly affected levels of other LSU r-proteins why its role considerably differs from what it would be predicted (Figure 34D). The predicted requirement of L2 (homologue of yeast rpL2) binding for L15 (rpL28) association was not as evident *in vivo* and only characterized by a rather mild effect (Figure 34B). The additional requirement of *E.coli* L2 (rpL2) binding for association of L5 (rpL11) was not seen at all *in vivo* in yeast. Another difference in both systems is the lack of detected effects of yeast rpL26 (*E.coli* L24) depletion on assembly of rpL17 (L22) and rpL35 (L29) (Babiano et al., 2012). All in all one can conclude that the hierarchical interrelationships of LSU r-protein assembly events largely differ in the prokaryotic *in vitro* assembly map and the here tested yeast LSU expression mutants.

As described previously, the expression shut down of essential yeast LSU r-proteins (especially the ones that are required for early maturation events) lead to a rather quick and efficient degradation of the deficient LSU precursors. It cannot be excluded that certain populations of misassembled LSU precursors are in some cases degraded faster than other why they would be underrepresented (“lost”) in the applied experimental approach in which only those mutant LSU precursors that were not yet degraded could be analyzed. This

potential “selective degradation” is unlikely to occur in the *in vitro* assembly systems what might to some extents explain the observed large differences of both systems.

Some of the here observed effects might also be the result of a potentially coupled expression of r-protein genes (which might be achieved for example by feedback regulation loops). Only about half of the r-proteins are conserved between pro- and eukaryotes and different species (within the same domains of life) show some variations in the sequence of r-proteins and rRNA. Therefore it can also not be excluded that these differences might specifically affect the hierarchical interrelationships among certain r-protein assembly events in certain species. Another significant difference is that the here performed yeast r-protein expression mutant studies resemble “single omission” experiments meaning that (most likely) only the actually depleted LSU r-protein is absent while the other LSU r-proteins are still produced. On the other hand, hierarchical interrelationships among r-protein assembly events in the *in vitro* assembly maps were deduced from experiments in which in most cases only a defined subset of components (r-proteins and rRNAs) were mixed together. This setup clearly does not fully mimic the situation *in vivo* what might have been especially relevant in those cases in which r-proteins contact different rRNA domains (like rpL2 / L2 as described in the previous section and illustrated in Figure 42). In addition, other aspects of ribosome biogenesis *in vivo* were not reflected in the experimental setup *in vitro*. They include the involvement of numerous ribosome biogenesis factors, the presence of different (pre-) rRNA processing and modification states and the presumable beginning of some initial r-protein assembly events already during the ongoing production of rRNA (and, in eukaryotes, the cell compartmentalization).

4.5 Correlation of LSU r-protein assembly events with maturation events of the LSU precursors including pre-rRNA processing and transient interaction of ribosome biogenesis factors

As discussed above, the stable association of LSU r-proteins often requires the previous binding of other LSU r-proteins. These hierarchical interrelationships are not limited to r-protein assembly events but can be extended to the transient interaction to the numerous ribosome biogenesis factors whose (often altered) association to mutant preribosomes was also systematically analyzed in this work. In the literature, some examples for an impact of r-protein assembly events on the recruitment or the release of certain biogenesis factors are described (Bussiere et al., 2012; Gamalinda et al., 2013; Jakob et al., 2012; Lo et al., 2010; Zhang et al., 2007). Furthermore, some LSU biogenesis factors were described to influence the assembly states of certain LSU r-proteins (Jakob et al., 2012; Lo et al., 2009; Sahasranaman et al., 2011; Zhang et al., 2007). In addition, the pre-rRNA processing phenotype of most LSU biogenesis factors is known. The more recently published studies investigating the binding sites of ribosome biogenesis factors by cross linking and cryo-EM approaches can also contribute to better understand the molecular prerequisites for some pre-60S maturation events. In the following two sub-sections, examples of (potential) links between LSU r-protein assembly events, the association (recruitment or release) of ribosome

biogenesis factors and maturation events (pre-rRNA processing and nuclear export) will be discussed, again starting with early pre-rRNA processing events which are disturbed after depletion of class 1 LSU r-proteins (4.5.1). In section 4.5.2 a the assembly of “middle” acting LSU r-proteins will be correlated to the ITS2 processing of 27SB pre-rRNA containing LSU precursors, including their requirement for association of certain biogenesis factors.

4.5.1 Correlation of the assembly of “early” acting (class 1) LSU r-proteins to maturation of the 5’ end of 5.8S rRNA precursors

As described above and illustrated in Figures 43 and 45, the “early”, class 1 LSU r-proteins are mainly bound to LSU domains I, II, and VI. Two local “cluster” of LSU r-proteins were emerging from the depletion analyses which were specifically affected after depletion of rpL7 and rpL8, respectively. As shown in Figures 25 and 26 and illustrated in Figure 43, depletion of rpL7 (and several members of the “rpL7 cluster”) apparently disturbed the local environment of rpL7 and the integrity of the fold of parts of LSU rRNA domain II. Depletion of rpL8 on the other hand resulted in the distortion of parts of LSU domain I. Since the “early” pre-rRNA processing phenotype (which is characterized by a disturbed creation of the 5’ end of the 5.8S rRNA by an exonucleolytic trimming of ITS1 sequences) is shared by all the class 1 LSU r-proteins, the integrity of both domains is apparently important to enable this processing event, as suggested previously (Pöll et al., 2009). A number of LSU biogenesis factors (“A3 factors”) were also described to be required for this event (see citations in section 2.2.6.2). Interestingly, the association of none of these factors seemed to be inhibited in all of the nine analyzed class 1 LSU r-proteins mutants why the pre-rRNA processing phenotype is apparently not simply the result of a general inhibited “action” of essential LSU biogenesis factor(s). While after depletion of rpL7 (and the analyzed members of the “rpL7 group”) the level of no “A3 factors” in the mutant preribosomes was significantly reduced, rpL8 depletion resulted in significantly reduced levels of ten “A3 factors” what could (in part) explain the pre-rRNA processing phenotype of rpL8. Several of these factors, whose binding sites were investigated by UV cross-linking experiments (see citations in sections 2.2.6.2 and 3.3.2), apparently bind near this cluster in parts of domain I and ITS2 sequences, whose ends (3’ end of 5.8S rRNA and 5’ end of 25S rRNA) are indicated in Figure 45A and C). The association of one of the remaining “A3 factors”, Rrp1, was only significantly affected after depletion of rpL4, rpL18, and rpL32, which are bound in proximity to each other between the rpL7 and rpL8 groups (Figure 45A-B). It is therefore plausible that Rrp1 binds near these three LSU r-proteins and requires their association what could partly explain the pre-rRNA processing phenotype of rpL18 and rpL32 after whose depletion the effects on the levels of the other class 1 were not as strong (Figures 25 and 26). In sum, both, the proper folding state of LSU domains I (including the 5’ end of the 5.8S rRNA) and II as well as the recruitment of several “A3 factors” (which in parts seems to depend on the integrity of these domains) seem to be required to enable the proper trimming of ITS1 sequences (stopping at the 5’ end of the 5.8S rRNA at site B1s).

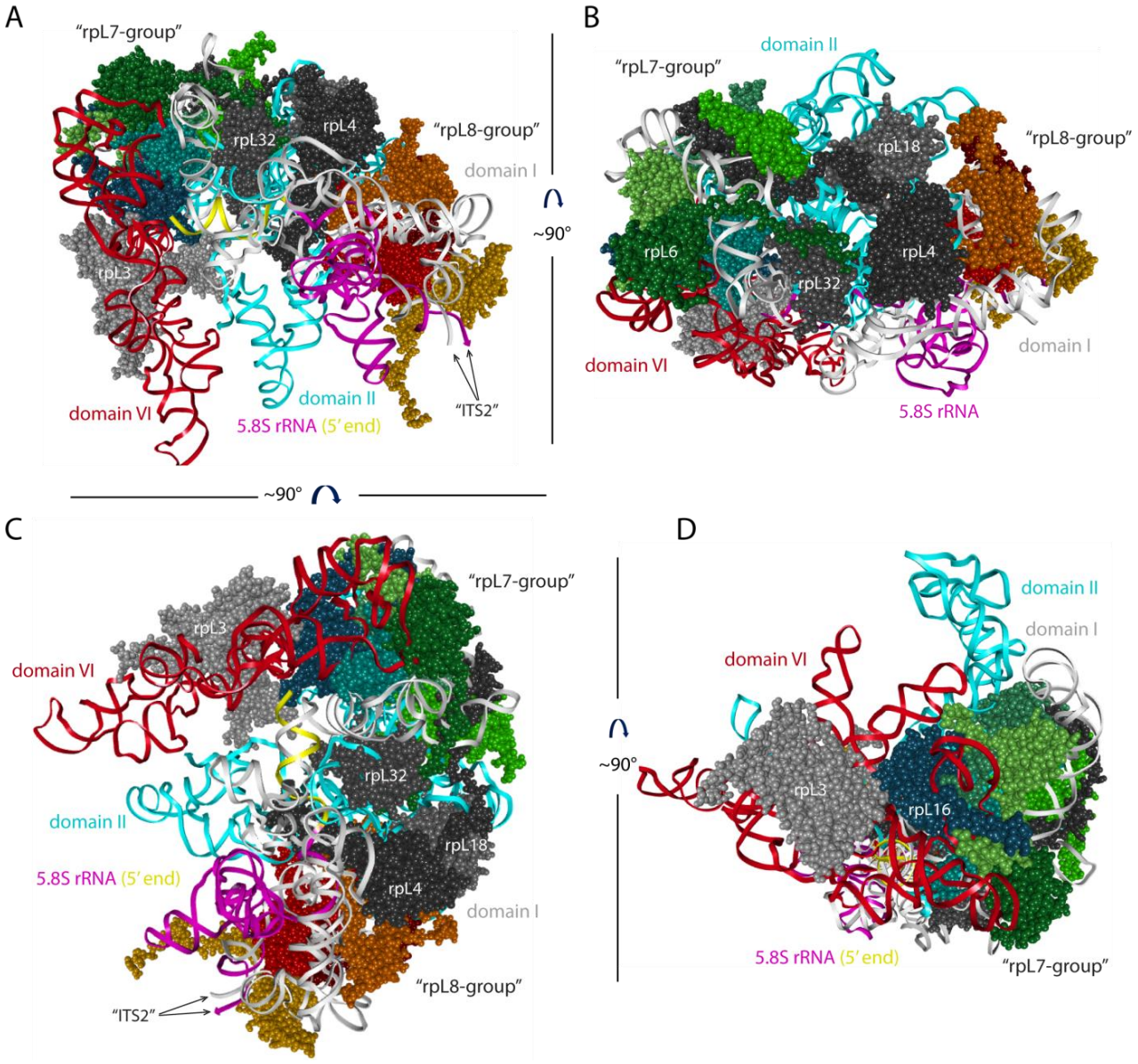

Figure 45 - Class 1 LSU r-proteins seem to be required for the integrity of LSU domains I, II, and the correct positioning of domain VI what might be crucial for the correct processing of ITS1 sequences in early LSU precursors

Parts of the yeast LSU (Ben-Shem et al., 2011) are depicted from different perspectives aiming to illustrate the location of class 1 LSU r-proteins relative to the 5' end of the 5.8S rRNA whose creation is inhibited in these mutants. The 5' end of the 5.8S rRNA, which forms a helical structure with parts of domain I is highlighted in yellow (20 nucleotides). RpL8 and LSU r-proteins specifically affected after its depletion are highlighted in orange and red colors ("rpL8-group"). The ends of the ITS2 sequences to which some "A3 factors" were described to bind are indicated by arrows. The orientation of domain VI (red) in relation to the 5' end of the 5.8S rRNA is best visible in **A)** and **C)**. The location of rpL4, rpL18, and rpL32 "in between the "rpL7-group" (green and blue colors) and the "rpL8-group" whose binding might constitute a "platform" for the "A3 factor" Rrp1 is best visible in **B)**. **D)** shows a "top view" of the same structure seen from domain VI illustrating that domain VI "covers" the crucial processing site (yellow) like a lid.

As already mentioned above (Figure 9D and Pöll et al., 2009), the observed pre-rRNA processing phenotype observed after depletion of the class 1 LSU r-proteins and the "A3 factors" might not necessarily be caused by a disturbed ITS1 trimming per se but rather be result of a lack of the inhibition of the exonucleolytic digest at the correct position (at site

B1s). Mutant pre-60S particles in which the prerequisites for a proper ITS1 trimming are not fulfilled were therefore suggested to be further digested by the exonuclease Rat1 (and presumably Rrp17) and finally turned over (Pöll et al., 2009). As mentioned previously, the incorporation of several LSU r-proteins, including rpL17, which is located directly "on top" of the crucial site B1s was speculated to be required as sort of "roadblock" to stop the exonucleolytic trimming of ITS1 sequences at the correct position (Sahasranaman et al., 2011). However, rpL17 depletion does not show the same class 1 pre-rRNA processing phenotype (but a later one) and therefore rpL17 cannot be crucial for this event. Instead, the 5' end of the 5.8S rRNA (= site B1s), is in the mature LSU part of a helix of 5.8S and domain I rRNA sequences (Figure 45A and C). As also mentioned above and illustrated in Figure 9C, there are evidences that this helical structure is not yet established in ITS1 containing preribosomes. The establishment of this helical structure which is presumably disturbed after depletion of the class 1 LSU r-proteins and the "A3 factors" might rather be required to stop the 5'-3' ITS1 digest at the correct position. In fact, the 5' end of the 5.8S rRNA is surrounded by parts of the "rpL7 cluster" and, very interestingly, parts of LSU domain VI which is "covering" this crucial site like a "lid" (Figure 45C). As discussed before, rpL3, the largest yeast LSU r-protein almost exclusively interacts with LSU domain VI connecting several helices within domain VI to each other. The establishment of these interactions seems to be crucial since its depletion lead to the most drastic pre-rRNA processing phenotype among all tested LSU r-proteins. Interestingly, several class 1 LSU r-proteins of the "rpL7 – cluster" (mainly rpL20, rpL33, rpL6, and rpL16) are bound at or near the interface of domains II and VI. The establishment of the interaction between these two domains might be triggered by the assembly of these LSU r-proteins what could lead to the correct orientation of domain VI relative to domain II and I (including 5.8S rRNA sequences and its 5' end). In case the development of these sub-structures is disturbed, what seems to happen after depletion of the "rpL7-cluster" proteins, the orientation of domain VI "on top" of the site B1s might not be possible any more what could result in an inhibited restriction of the exonucleolytic activity of Rat1 (and Rrp17) which is necessary once their processing has reached the site B1s. This potential inability to restrict the 5'-3' exonucleases might result in the above described turnover of the mutant LSU precursors by a degradation of their pre-rRNAs (Pöll et al., 2009).

4.5.2 Correlation of assembly of "middle" acting (class 2) LSU r-proteins to ITS2 processing of 27SB pre-rRNA containing LSU precursors

Nine LSU r-proteins were described to be required for the efficient ITS2 cleavage of the 27SB pre-rRNA of nuclear LSU precursors. Seven of them (rpL19, rpL25, rpL27, rpL31, rpL34, rpL35, rpL37 – highlighted in yellow in Figure 46) are located near the boundary of the ITS2 (3' end of the 5.8S rRNA and 5' end of the 25S rRNA) interacting mainly with domains III (rpL27, rpL34), domains III, IV and VI (rpL19, rpL31), or domains I (including 5.8S rRNA) and III (rpL25) or domain I (and 5.8SrRNA - rpL35 and rpL37). Beside a commonly affected group of LSU r-proteins, their individual depletion resulted in specific effects on the

association of other LSU r-proteins which are in many cases bound in the direct neighborhood of the depleted LSU r-protein (see sections 3.3.3, 4.3, and illustrated in Figure 44). Interestingly, the analyses of the ribosome biogenesis factors interacting with these mutant preribosomes revealed that the association of no biogenesis factor that was described to be required for ITS2 cleavage ("B factors") was strongly disturbed in all of these seven *RPL* mutants. Therefore, the shared pre-rRNA processing phenotype cannot easily explained by the reduced association of a required factor.

Alternatively, (some of) these seven LSU r-proteins might be involved in the actual cleavage event not by recruiting LSU biogenesis factors but by contributing to the establishment of proper conformations of LSU (pre-) rRNA domains. One option is that ITS2 spacer sequences might directly interact with some of the class 2 LSU r-proteins and that these interactions are required for the cleavage at site C2. Even if the exact spatial orientation of the ITS2 is not know, its 2D conformation was described to change during LSU maturation from a rather open and accessible "ring"-structure to a closed "hairpin"-structure (Joseph et al., 1999; Peculis and Greer, 1998; Yeh and Lee, 1990). In one recently published study the authors analyzed putative structural changes in the ITS2 by *in vivo* structure probing (using DMS) after depletion of rpL35 and rpL37 (Gamalinda et al., 2013). Both, rpL35 and rpL37 are located between the 5.8S rRNA and LSU rRNA domain I near the boundary of the ITS2 (see Figure 44C). The results indicated that depletion of rpL35 or rpL37 did "not significantly perturb the overall structure of ITS2" (Gamalinda et al., 2013), why it is likely not (strongly) interacting with these LSU r-proteins.

Another option is that the ITS2 rather folds into the opposing direction towards domain III (illustrated best in Figure 44C) where the class 2 LSU r-proteins rpL27 and rpL34 are located. RpL27, rpL34, and potentially rpL30 (which all showed, as far as tested, an interdependent assembly behavior – Figure 30 C-D) might therefore directly interact with ITS2 sequences and be required for the establishment of a proper fold to enable the cleavage (see illustration in Figure 46). Of course this hypothesis needs to be tested by structure probing approaches e.g. by using DMS or the before mentioned tethered structure probing approach in which a nuclease is fused to the r-protein of interest (see section 4.2.3 and Ohmayer et al., 2012).

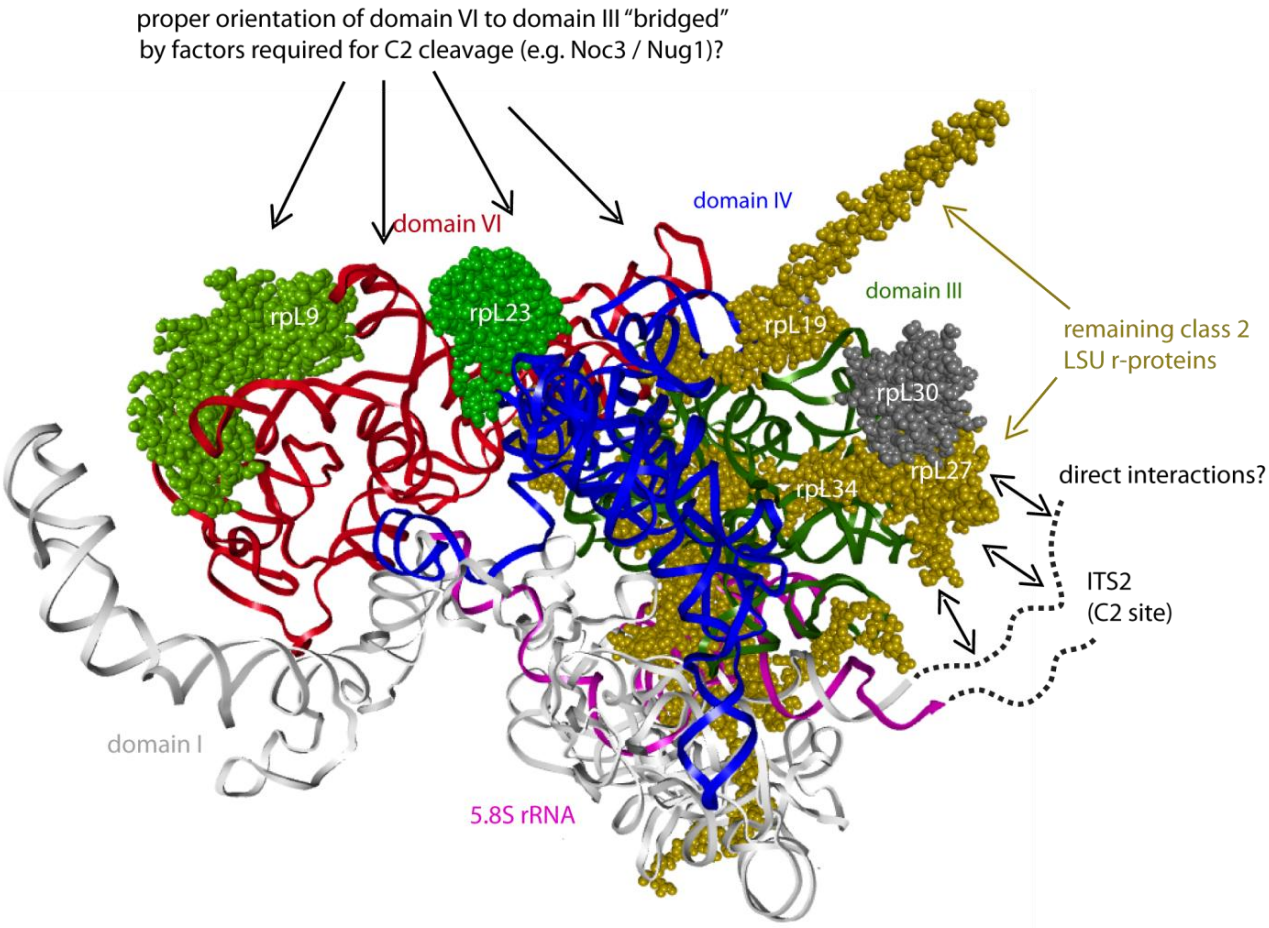

Figure 46 - Some class 2 LSU r-proteins might be involved in ITS2 cleavage of intermediately maturated (27SB pre-rRNA containing) nuclear LSU precursors while others could be involved in the recruitment of certain required biogenesis factors

Parts of the yeast LSU (Ben-Shem et al.; 2011) is depicted highlighting the location of the class 2 LSU r-proteins relative to each other and to the boundaries of the ITS2. LSU rRNA domains I (incl. the 5.8S rRNA), III, IV, and VI are highlighted in the indicated colors. "Class 2" LSU r-proteins are highlighted in yellow (rpL19, rpL25, rpL27, rpL31, rpL34, rpL35, and rpL37) and shades of green (rpL9 and rpL23), respectively. The possible locations of ITS2 sequences are indicated in dashed lines including possible interactions with LSU domain III binders. The parts of domain VI (and VI) where factors as Noc3 might connect these domains to domain III are indicated by arrows. See text for more detailed explanations.

The remaining class 2 LSU r-proteins, rpL9 and rpL23, are not bound near the ITS2 boundaries (but mainly interacting with domains VI, and IV) why it appears unlikely that they are directly contacting ITS2 sequences in LSU precursors. As observed for all "class 2" *RPL* mutants, their depletion resulted in reduced levels of "class 2" LSU r-proteins rpL19 and rpL31 which are located "in between" rpL9/rpL23 and the domain III binders rpL27/rpL34 "linking" LSU domain III to domains VI and IV (see Figure 44A).

Interestingly, and in contrast to the other five "class 2" LSU r-proteins depletion of rpL9 and rpL23 resulted in (partially) strongly reduced association of several LSU biogenesis factors that were described to be required for efficient ITS2 cleavage. Among them are Tif6, Rlp24, Nog1, Spb1, Spb4, Dbp10, Nsa2, Nug1, and Noc3 in the case of the *RPL23* mutant (Figures 32F, and 33A-B) and Spb1, Nsa2, Nug1 and Noc3 in the *RPL9* mutant (Figures 32E and

33C-D). In the case of rpL23, the observed effects on association Tif6, Rlp24 and Nog1 might be explained by the loss of direct interactions between rpL23 and these biogenesis factors (see citations in section 3.3.3). The binding sites for the remaining biogenesis factors whose association was specifically disturbed after depletion of rpL9 and rpL23 are still unknown but it seems likely that (at least some of them) might also bind near this neighborhood. One of them, Noc3 was recently investigated in more detail in our laboratories (T. Hierlmeier, unpublished data). As mentioned before, depletion of Noc3 resulted in the same pre-rRNA processing phenotype. Quantitative proteome analyses indicated that the LSU precursors purified from cells depleted of Noc3 were also depleted of the same group of LSU r-proteins whose binding was commonly affected in all “class 2” LSU r-proteins, including rpL19 and rpL31. However, levels of rpL9 or rpL23 were unaffected indicating that their incorporation into preribosomes occurs independently and (most likely) prior to Noc3 association. Therefore it is plausible that factors as Noc3 (or maybe Nug1) are “bridging” rpL9/rpL23 in LSU domains VI (and IV) to LSU domain III, an event that seems to be required for stable incorporation of rpL19 and rpL31 (illustrated in Figure 46). This potential role of these “B factors” in “bridging” several LSU domains to each other could also explain the depletion phenotype of the more distant rpL9 and rpL23. Future analyses will have to be performed to test these hypotheses; the determination of the binding sites of the remaining “B factors” will likely be among the most straightforward approaches.

5 Material and Methods

5.1 Materials

5.1.1 Yeast strains

Nr.	name	Plasmid	Genotype	origin / strategy	generation time in minutes (medium)*
Y206	BY4741	-	his3-1, leu2-0, ura3-0, met15-0	Euroscarf	102 (in YPD)
Y207	BY4742	-	his3-1, leu2-0, ura3-0, met15-0	Euroscarf	133 (in YPG)
Y265	RPS26-Shuffle	TK306	his3-1, leu2-0, ura3-0, met15-0, lys2-0, YER131w::kanMX4, YGL189c::HIS3Mx6	Ferreira-Cerca et al., 2005	
Y485	pGAL-RPS26-FLAG	TK391	his3-1, leu2-0, ura3-0, met15-0, lys2-0, YER131w::kanMX4, YGL189c::HIS3Mx6	Plasmid TK391 was transformed into Y265 - selection on YNB-LEU and FoA (Ohmayer et al., 2013)	181 (in YPG)
Y927	pGAL-RPL10	TK808	his3-1, leu2-0, ura3-0, YLR075w::kanMX4	Pöll et al., 2009	
Y928	pGAL-RPL23	TK812	his3-1, leu2-0, ura3-0, YBL087c::HIS3, YER117w::kanMX4	Pöll et al., 2009	
Y930	pGAL-RPL34	TK814	his3-0, leu2-0, ura3-0, YIL052c::HIS3, YER056c-a::kanMX4	Pöll et al., 2009	
Y931	pGAL-RPL16	TK810	his3-1, leu2-0, ura3-0, YNL069c::kanMX4, YIL133c::HIS3	Pöll et al., 2009	
Y932	pGAL-RPL20	TK821	his3-0, leu2-0, ura3-0, YOR312c::HIS3, YMR242c::kanMX4	Pöll et al., 2009	
Y933	pGAL-RPL1	TK818	his3-1, leu2-0, ura3-0, YGL135W::kanMX4, YPL220w::HIS3	Pöll et al., 2009	
Y965	pGAL-RPL2	TK819	his3-1, leu2-0, ura3-0, YIL018w::kanMX4, YFR031c-a::HIS3	Pöll et al., 2009	
Y966	pGAL-RPL3	TK822	his3-1, leu2-0, ura3-0, YOR063w::kanMX4	Pöll et al., 2009	
Y967	pGAL-RPL13	TK823	his3-1, leu2-0, ura3-0, YMR142c::kanMX4, YDL082w::HIS3	Pöll et al., 2009	
Y1026	pGAL-RPL25	TK865	his3-1, leu2-0, ura3-0, YOL127w::kanMX4	Pöll et al., 2009	
Y1058	Shuffle-RPL40				
Y1082	pGal-RPL27	TK855	his3-1, leu2-0, ura3-0, YDR471w::HIS3MX6, YHR010w::kanMX4	Pöll et al., 2009	
Y1092	pGAL-RPL5	TK852	his3-1, leu2-0, ura3-0, YPL131w::kanMX4	Pöll et al., 2009	
Y1093	pGAL-RPL28	TK856	his3-1, leu2-0, ura3-0, YGL103w::kanMX4	Pöll et al., 2009	

Y1094	pGAL-RPL35	TK857	his3-1, leu2-0, ura3-0, YDL191w::kanMX4, YDL136w::HIS3	Pöll et al., 2009	
Y1095	pGAL-RPL17	TK846	his3-1, leu2-0, ura3-0, YKL180w::kanMX4, YJL177w::HIS3MX6	Pöll et al., 2009	
Y1096	pGAL-RPL33	TK813	his3-1, leu2-0, ura3-0, YPL143w::kanMX4, YOR234c::HIS3MX6	Pöll et al., 2009	
Y1097	pGAL-RPL8B	TK882	his3-1, leu2-0, ura3-0, met15-0, lys2-0, YHL033c::HIS3MX6, YLL045c::kanMX4	Pöll et al., 2009	
Y1098	pGAL-RPL9	TK883	his3-0, leu2D0, lys2D0/LYS2, ura3D0, met15D0/MET15, YNL067w::kanMX4, YGL147c::HIS3MX6	Pöll et al., 2009	
Y1099	pGAL-RPL19B	TK884	his3-1, leu2-0, ura3-0, met15D0/MET15D0, lys2-0, YBR084c-a::HIS3MX6, YBL027w::kanMX4	Pöll et al., 2009	
Y1100	pGAL-RPL21A	TK885	his3-1, leu2-0, ura3-0, met15-0, lys2-0, YBR191w::HIS3MX6, YPL079w::kanMX4	Pöll et al., 2009	
Y1101	pGAL-Ubq-RPL40A	TK887	his3-1, leu2-0, ura3-0, met15D0/MET15, YIL148w::HIS3MX6, YKR094c::kanMX4	Plasmid TK887 was transformed into Y1058 (see Pöll et al., 2009 for strategy) (Ohmayer et al., 2013)	
Y1102	pGAL-RPL32	TK880	his3-1, leu2-0, ura3-0, YBL092w::kanMX4	Pöll et al., 2009	
Y1103	pGAL-RPL43	TK881	his3-1, leu2-0, ura3-0, lys2-0, YJR094w-a::HIS3MX6, YPR043w::kanMX4	Pöll et al., 2009	
Y1104	pGAL-RPL40A (minus Ubq)	TK888	his3-1, leu2-0, ura3-0, met15D0/MET15, YIL148w::HIS3MX6, YKR094c::kanMX4	Pöll et al., 2009	
Y1199	pRPS28-FLAG-RPL23	TK942	his3-1, leu2-0, ura3-0, YBL087c::HIS3, YER117w::kanMX4	Plasmid TK942 was transformed into Y928, cells were grown on Glucose containing medium (Ohmayer et al., 2013)	136 (in YPD)
Y1203	pRPS28-FLAG-RPL1	TK945	his3-1, leu2-0, ura3-0, YGL135W::kanMX4, YPL220w::HIS3	Plasmid TK945 was transformed into Y933, cells were grown on Glucose containing medium (Ohmayer et al., 2013)	118 (in YPD)
Y1204	pRPS28-FLAG-RPL25	TK959	his3-1, leu2-0, ura3-0, YOL127w::kanMX4	Plasmid TK959 was transformed into Y1026, cells were grown on Glucose containing medium (Ohmayer et al., 2013)	111 (in YPD)
Y1205	pRPS28-FLAG-RPL5	TK952	his3-1, leu2-0, ura3-0, YPL131w::kanMX4	Plasmid TK952 was transformed into Y1092, cells were grown on Glucose containing medium (Ohmayer et al., 2013)	103 (in YPD)
Y1206	pRPS28-FLAG-RPL35	TK957	his3-1, leu2-0, ura3-0, YDL191w::kanMX4, YDL136w::HIS3	Plasmid TK957 was transformed into Y1094, cells were grown on Glucose containing medium (Ohmayer et al., 2013)	101 (in YPD)
Y1207	pRPS28-FLAG-RPL17	TK951	his3-1, leu2-0, ura3-0, YKL180w::kanMX4, YJL177w::HIS3MX6	Plasmid TK951 was transformed into Y1095, cells were grown on Glucose containing medium (Ohmayer et al., 2013)	105 (in YPD)

Y1208	pRPS28-FLAG-RPL33	TK943	his3-1, leu2-0, ura3-0, YPL143w::kanMX4, YOR234c::HIS3MX6	Plasmid TK943 was transformed into Y1096, cells were grown on Glucose containing medium (Ohmayer et al., 2013)	100 (in YPD)
Y1209	pRPS28-FLAG-RPL8B	TK963	his3-1, leu2-0, ura3-0, met15-0, lys2-0, YHL033c::HIS3MX6, YLL045c::kanMX4	Plasmid TK963 was transformed into Y1097, cells were grown on Glucose containing medium (Ohmayer et al., 2013)	112 (in YPD)
Y1210	pRPS28-FLAG-Ubq-RPL40A	TK968	his3-1, leu2-0, ura3-0, met15D0/MET15, YIL148w::HIS3MX6, YKR094c::kanMX4	Plasmid TK968 was transformed into Y1101, cells were grown on Glucose containing medium (Ohmayer et al., 2013)	96 (in YPD)
Y1211	pRPS28-FLAG-RPL43A	TK962	his3-1, leu2-0, ura3-0, lys2-0, YJR094w-a::HIS3MX6, YPR043w::kanMX4	Plasmid TK962 was transformed into Y1103, cells were grown on Glucose containing medium (Ohmayer et al., 2013)	104 (in YPD)
Y1212	pRPS28-FLAG-RPL40A (minus Ubq)	TK969	his3-1, leu2-0, ura3-0, met15D0/MET15, YIL148w::HIS3MX6, YKR094c::kanMX4	Plasmid TK969 was transformed into Y1104, cells were grown on Glucose containing medium - lacks Ubq moiety; FLAG tag N-terminally fused to rpL40A (Ohmayer et al., 2013)	202 (in YPD)
Y1215	pRPS28-FLAG-RPL27	TK955	his3-1, leu2-0, ura3-0, YDR471w::HIS3MX6, YHR010w::kanMX4	Plasmid TK955 was transformed into Y1082, cells were grown on Glucose containing medium (Ohmayer et al., 2013)	108 (in YPD)
Y1216	pRPS28-FLAG-RPL19B	TK965	his3-1, leu2-0, ura3-0, met15D0/MET15D0, lys2-0, YBR084c-a::HIS3MX6, YBL027w::kanMX4	Plasmid TK965 was transformed into Y1099, cells were grown on Glucose containing medium (Ohmayer et al., 2013)	101 (in YPD)
Y1411	pRPS28-RPL2-Flag	TK1028	his3-1, leu2-0, ura3-0, YIL018w::kanMX4, YFR031c-a::HIS3	Plasmid TK1028 was transformed into Y965, cells were grown on Glucose containing medium (Ohmayer et al., 2013)	133 (in YPD)
Y1412	pRPS28-RPL3-Flag	TK1029	his3-1, leu2-0, ura3-0, YOR063w::kanMX4	Plasmid TK1029 was transformed into Y966, cells were grown on Glucose containing medium (Ohmayer et al., 2013)	106 (in YPD)
Y1414	pRPS28-RPL10-Flag	TK1031	his3-1, leu2-0, ura3-0, YLR075w::kanMX4	Plasmid TK1031 was transformed into Y927, cells were grown on Glucose containing medium (Ohmayer et al., 2013)	102 (in YPD)
Y1415	pRPS28-RPL13-Flag	TK1032	his3-1, leu2-0, ura3-0, YMR142c::kanMX4, YDL082w::HIS3	Plasmid TK1032 was transformed into Y967, cells were grown on Glucose containing medium (Ohmayer et al., 2013)	106 (in YPD)
Y1433	pRPS28-eGFP-RPL1	TK1041	his3-1, leu2-0, ura3-0, YGL135W::kanMX4, YPL220w::HIS3	Plasmid TK1041 was transformed into Y933, cells were grown on Glucose containing medium (Ohmayer et al., 2013)	160 (in YPD)
Y1435	pRPS28-eGFP-RPL5	TK1045	his3-1, leu2-0, ura3-0, YPL131w::kanMX4	Plasmid TK1045 was transformed into Y1092, cells were grown on Glucose containing medium (Ohmayer et al., 2013)	128 (in YPD)
Y1438	pRPS28-eGFP-RPL33	TK1039	his3-1, leu2-0, ura3-0, YPL143w::kanMX4, YOR234c::HIS3MX6	Plasmid TK1039 was transformed into Y1096, cells were grown on Glucose containing medium (Ohmayer et al., 2013)	133 (in YPD)

Y1606	pGAl-RPL4	-	ura3-52, trp1-d101, lys2-801, his3-d200, leu2-d1, rpl4b::kanmx6, GAL-3HA-RPL4A (TRP1)	John Woolford laboratories (JW8402) (Pöll et al., 2009)	
Y1607	pGAL-RPL7	-	ura3-52, trp1-d101, lys2-801, his3-d200, leu2-d1, RPL7::KanmX6, GAL-3HA-RPL7A (Trp1)	John Woolford laboratories (Pöll et al., 2009)	
Y1608	pGAL-RPL18	-	ura3-52, trp1-d101, lys2-801, his3-d200, leu2-d1, rpl18b::kanmx6, GAL-3HA-RPL18A (TRP1)	John Woolford laboratories (Pöll et al., 2009)	
Y1768	pGAL-RPL3 Noc2-TAP	TK822	his3-1, leu2-0, ura3-0, YOR063w::kanMX4, YOR206W-TAP (URA3-KL)	strain Y966 was transformed with a PCR product on pBS1539 with primers 621/622 (Julius Ossowski)	
Y1769	pGAL-RPL8 NOC2-TAP	TK882	his3-1, leu2-0, met15-0, lys2-0, ura3-0, YHL033c::HIS3MX6, YLL045c::kanMX4, YOR206W-TAP (URA3-KL)	strain Y1097 was transformed with a PCR product on pBS1539 with primers 621/622 (Julius Ossowski)	
Y1770	pGAL-RPL16 NOC2-TAP	TK810	his3-1, leu2-0, ura3-0, YNL069c::kanMX4, YIL133c::HIS3, YOR206W-TAP (URA3-KL)	strain Y931 was transformed with a PCR product on PBS1539 with primers 621/622 (Julius Ossowski)	
Y1771	pGAL-RPL20 NOC2-TAP	TK821	his3-0, leu2-0, ura3-0, YOR312c::HIS3, YMR242c::kanMX4, YOR206W-TAP (URA3-KL)	strain Y932 was transformed with a PCR product on pBS1539 with primers 621/622 (Julius Ossowski)	
Y1772	pGAL-RPL32 NOC2-TAP	TK880	his3-1, leu2-0, ura3-0, YBL092w::kanMX4, YOR206W-TAP (URA3-KL)	strain Y1102 was transformed with a PCR product on pBS1539 with primers 621/622 (Julius Ossowski)	
Y1773	pGAL-RPL33 NOC2-TAP	TK813	his3-1, leu2-0, ura3-0, YPL143w::kanMX4, YOR234c::HIS3MX6, YOR206W-TAP (URA3-KL)	strain Y1096 was transformed with a PCR product on pBS1539 with primers 621/622 (Julius Ossowski)	
Y1782	pGAL-RPL21A NOG2-TAP	TK885	his3-1, leu2-0, ura3-0, met15-0, lys2-0, YBR191w::HIS3MX6, YPL079w::kanMX4, nog2::NOG2-TAP-URA3	strain Y1100 was transformed with a PCR product on pBS1539 with primers O2661/O2162 (Ohmayer et al., 2013)	
Y1785	pGAL-RPL43 NOG2-TAP	TK881	his3-1, leu2-0, ura3-0, lys2-0, YJR094w-a::HIS3MX6, YPR043w::kanMX4, nog2::NOG2-TAP-URA3	strain Y1103 was transformed with a PCR product on pBS1539 with primers 2661/2162 (Ohmayer et al., 2013)	
Y1788	pGAL-RPL25 NOG2-TAP	TK865	his3-1, leu2-0, ura3-0, YOL127w::kanMX4, nog2::NOG2-TAP-URA3	strain Y1026 was transformed with a PCR product on pBS1539 with primers 2661/2162 (Ohmayer et al., 2013)	
Y1813	pGAL-RPL21A NOG1-TAP	TK885	his3-1, leu2-0, ura3-0, met15-0, lys2-0, YBR191w::HIS3MX6, YPL079w::kanMX4, nog1::NOG1-TAP-URA3	strain Y1100 was transformed with a PCR product on pBS1539 with primers 2659/2160 (Ohmayer et al., 2013)	
Y1814	pGAL-RPL28 NOG1-TAP	TK856	his3-1, leu2-0, ura3-0, YGL103w::kanMX4, YPL093W-TAP (Kl URA3)	strain Y1093 was transformed with a PCR product on pBS1539 with primers 2159/2160 (Gisela Pöll)	
Y1816	pGAL-RPL25 NOG1-TAP	TK865	his3-1, leu2-0, ura3-0, YOL127w::kanMX4, nog1::NOG1-TAP-URA3	strainY1026 was transformed with a PCR product on pBS1539 with primers 2659/2160) (Ohmayer et al., 2013)	

Y1817	pGAL-RPL43 NOG1-TAP	TK881	his3-1, leu2-0, ura3-0, lys2-0, YJR094w-a::HIS3MX6, YPR043w::kanMX4, nog1::NOG1-TAP-URA3	strain Y1103 was transformed with a PCR product on pBS1539 with primers 2659/2160 (Ohmayer et al., 2013)	
Y1877	BY4742 NOG1-TAP	-	his3-1, leu2-0, ura3-0, lys2-0, nog1::NOG1-TAP-URA3	strain Y207 was transformed with a PCR product on pBS1539 with primers 2659/2160 (Ohmayer et al., 2013)	
Y1878	BY4742 NOG2-TAP	-	his3-1, leu2-0, ura3-0, lys2-0, nog2::NOG2-TAP-URA3	strain Y207 was transformed with a PCR product on pBS1539 with primers 2661/2162 (Ohmayer et al., 2013)	
Y1879	BY4742 NOC2-TAP	-	his3-1, leu2-0, ura3-0, lys2-0, noc2::NOC2-TAP-URA3	strain Y207 was transformed with a PCR product on pBS1539 with primers 621/622 (Ohmayer et al., 2013)	
Y1917	pGAL-RPL2 NOC2-TAP	TK819	his3-1, leu2-0, ura3-0, YIL018w::kanMX4, YFR031c-a::HIS3, noc2::NOC2-TAP-URA3	strain Y965 was transformed with a PCR product on pBS1539 with primers 621/622 (Ohmayer et al., 2013)	
Y1918	pGAL-RPL10 NOG1-TAP	TK808	his3-1, leu2-0, ura3-0, YLR075w::kanMX4, YPL093W-TAP (Kl URA3)	strain Y927 was transformed with a PCR product on pBS1539 with primers 2159/2160 (Julius Ossowski)	
Y1921	pGAL-RPL2 NOG1-TAP	TK819	his3-1, leu2-0, ura3-0, YIL018w::kanMX4, YFR031c-a::HIS3, nog1::NOG1-TAP-URA3	strain Y965 was transformed with a PCR product on pBS1539 with primers 2659/2160 (Ohmayer et al., 2013)	
Y1922	pGAL-RPL2 NOG2-TAP	TK819	his3-1, leu2-0, ura3-0, YIL018w::kanMX4, YFR031c-a::HIS3, nog2::NOG2-TAP-URA3	strain Y965 was transformed with a PCR product on pBS1539 with primers 2661/2162 (Ohmayer et al., 2013)	
Y1924	pGAL-RPL35 NOG1-TAP	TK857	his3-1, leu2-0, ura3-0, YDL191w::kanMX4, YDL136w::HIS3, YPL093W-TAP (Kl URA3)	strain Y1094 was transformed with a PCR product on pBS1539 with primers 2159/2160 (Julius Ossowski)	
Y1959	pGAL-RPL19 NOG1-TAP	TK884	his3-1, leu2-0, ura3-0, met15D0/MET15D0, lys2-0, YBR084c-a::HIS3MX6, YBL027w::kanMX4, YPL093W-TAP (Kl URA3)	strain Y1099 was transformed with a PCR product on pBS1539 with primers 2159/2160 (Julius Ossowski)	
Y2103	pGAL-RPL43A NOC2-TAP	TK881	his3-1, leu2-0, ura3-0, lys2-0, YJR094w-a::HIS3MX6, YPR043w::kanMX4, , noc2::NOC2-TAP-URA3	strain Y1103 was transformed with a PCR product on pBS1539 with primers 621/622 (Ohmayer et al., 2013)	
Y2398	BY4742 RSA4-TAP	-	his3-1, leu2-0, ura3-0, lys2-0, rsa4::RSA4-TAP-URA3	strain Y207 was transformed with a PCR product on pBS1539 with primers 2932/2933 (Ohmayer et al., 2013)	
Y2399	pGAL-RPL2 RSA4-TAP	TK819	his3-1, leu2-0, ura3-0, YIL018w::kanMX4, YFR031c-a::HIS3, rsa4::RSA4-TAP-URA3	strain Y965 was transformed with a PCR product on pBS1539 with primers 2932/2933 (Ohmayer et al., 2013)	
Y2401	pGAL-RPL21A RSA4-TAP	TK885	his3-1, leu2-0, ura3-0, met15-0, lys2-0, YBR191w::HIS3MX6, YPL079w::kanMX4, rsa4::RSA4-TAP-URA3	strain Y1100 was transformed with a PCR product on pBS1539 with primers 2932/2933 (Ohmayer et al., 2013)	
Y2402	pGAL-RPL25 RSA4-TAP	TK865	his3-1, leu2-0, ura3-0, YOL127w::kanMX4, rsa4::RSA4-TAP-URA3	strain Y1026 was transformed with a PCR product on pBS1539 with primers 2932/2933 (Ohmayer et al., 2013)	

Y2403	pGAL-RPL43A RSA4-TAP	TK881	his3-1, leu2-0, ura3-0, lys2-0, YJR094w-a::HIS3MX6, YPR043w::kanMX4, rsa4::RSA4-TAP-URA3	strain Y1103 was transformed with a PCR product on pBS1539 with primers 2932/2933 (Ohmayer et al., 2013)	
Y2404	BY4742 NOP53-TAP	-	his3-1, leu2-0, ura3-0, lys2-0, nop53::NOP53-TAP-URA3	strain Y207 was transformed with a PCR product on pBS1539 with primers 2934/2935 (Ohmayer et al., 2013)	
Y2407	pGAL-RPL21A NOP53-TAP	TK885	his3-1, leu2-0, ura3-0, met15-0, lys2-0, YBR191w::HIS3MX6, YPL079w::kanMX4, nop53::NOP53-TAP-URA3	strain Y1100 was transformed with a PCR product on pBS1539 with primers 2934/2935 (Ohmayer et al., 2013)	
Y2410	BY4742 ARX1-TAP	-	his3-1, leu2-0, ura3-0, lys2-0, arx1::ARX1-TAP-URA3	strain Y207 was transformed with a PCR product on pBS1539 with primers 2936/2937 (Ohmayer et al., 2013)	
Y2689	pGAL-RPL7 RPF2-TAP	-	ura3-52, trp1-d101, lys2-801, his3-d200, leu2-d1, RPL7::KanmX6, GAL-3HA-RPL7A (Trp1), YKR081C-TAP (Kl URA3)	John Woolford laboratories (JW8492) (Jacovljevic et al., 2012)	
Y2709	pGAL-RPL8 RPF2-TAP	TK882	his3-1, leu2-0, ura3-0, met15-0, lys2-0, YHL033c::HIS3MX6, YLL045c::kanMX4, YKR081C-TAP (Kl URA3)	John Woolford laboratories (JW8493) (Jacovljevic et al., 2012)	
Y2757	pGAL-RPL23 NOP7-TAP	TK812	his3-1, leu2-0, ura3-0, YBL087c::HIS3, YER117w::kanMX4, nop7::NOP7-TAP-URA3	John Woolford laboratories (JW8328) (Gamalinda et al., 2014)	
Y2758	pGAL-RPL25 NOP7-TAP	TK865	his3-1, leu2-0, ura3-0, YOL127w::kanMX4, nop7::NOP7-TAP-URA3	John Woolford laboratories (JWY8419) (Gamalinda et al., 2014)	
Y2759	pGAL-RPL9 NOP7-TAP	TK883	his3-0, leu2D0, lys2D0/LYS2, ura3D0, met15D0/MET15, YNL067w::kanMX4, YGL147c::HIS3MX6, nop7::NOP7-TAP-URA3	John Woolford laboratories (JW8436) (Gamalinda et al., 2014)	
Y2760	pGAL-RPL18 RPF2-TAP	-	ura3-52, trp1-d101, lys2-801, his3-d200, leu2-d1, rpl18b::kanmx6, GAL-3HA-RPL18A (TRP1), YKR081C-TAP (Kl URA3)	John Woolford laboratories (JW8534) (Gamalinda et al., 2014)	
Y2762	pGAL-RPL3 RPF2-TAP	TK822	his3-1, leu2-0, ura3-0, YOR063w::kanMX4, YKR081C-TAP (Kl URA3)	John Woolford laboratories (JW8692) (Gamalinda et al. 2014)	
Y2773	BY4742 RPF2-TAP	-	his3-0, leu2-0, ura3-0, lys2-0, YKR081C-TAP (Kl URA3)	strain Y207 was transformed with a PCR product on pBS1539 with primers 227/237	
Y2779	pGAL-RPL23 TIF6-TAP	TK812	his3-1, leu2-0, ura3-0, YBL087c::HIS3, YER117w::kanMX4, YPR016C-TAP (URA3-0-KL)	John Woolford laboratories; derivate of strain strain Y928	
Y2784	pGAL-RPL23 RLP24-TAP	TK812	his3-1, leu2-0, ura3-0, YBL087c::HIS3, YER117w::kanMX4, YLR009W-TAP (URA3-0-KL)	John Woolford laboratories; derivate of strain strain Y928	
Y2786	pGAL-RPL18 NOC2-TAP	-	ura3-52, trp1-d101, lys2-801, his3-d200, leu2-d1, rpl18b::kanmx6, GAL-3HA-RPL18A (TRP1), YOR206W-TAP (URA3-KL)	strain Y1608 was transformed with a PCR product on pBS1539 with primers 621/622	

Y2788	pGAL-RPL4 NOC2-TAP	-	ura3-52, trp1-d101, lys2-801, his3-d200, leu2-d1, rpl4b::kanmx6, GAL-3HA-RPL4A (TRP1), YOR206W-TAP (URA3-KL)	strain Y1606 was transfromed with a PCR product on pBS1539 with primers 621/622	
Y2790	pGAL-RPL7 NOC2-TAP	-	ura3-52, trp1-d101, lys2-801, his3-d200, leu2-d1, RPL7::KanmX6, GAL-3HA-RPL7A (Trp1), YOR206W-TAP (URA3-KL)	strain Y1607 was transformed with a PCR product on pBS1539 with primers 621/622	
Y2830	pGAL-RPL11 NOP7-TAP	pRS316-RPL5-HA URA3	see Gamalinda et al., 2014; Genes dev	John Woolford laboratories (JW8112) (Gamalinda et al., 2014)	
Y2831	pGal-RPL21A NOP7-TAP	TK885	his3-1, leu2-0, ura3-0, met15-0, lys2-0, YBR191w::HIS3MX6, YPL079w::kanMX4, nop7::NOP7-TAP-URA3, YGR103W-TAP (KanMX6),	strain Y1100 was transformed with a PCR product on pBS1539 with primers 638/639 (Ohmayer et al., 2013)	
Y2852	BY4742 NOC3-TAP	-	his3-0, leu2-0, ura3-0, lys2-0, YLR002C-TAP (Kl URA3)	strain Y207 was transformed with a PCR product on pBS1539 with primers 3670/3671	
Y2891	pGAL-RPL4 RPF2-TAP	-	ura3-52, trp1-d101, lys2-801, his3-d200, leu2-d1, rpl4b::kanmx6, GAL-3HA-RPL4A (TRP1), YKR081C-TAP (KI URA3)	strain Y1606 was transfromed with a PCR product on pBS1539 with primers 227/237	
Y2896	pGAL-RPL20 RPF2-TAP	TK821	his3-0, leu2-0, ura3-0, YOR312c::HIS3, YMR242c::kanMX4, YKR081C-TAP (KI URA3)	strain Y932 was transformed with a PCR product on pBS1539 with primers 227/237	
Y2899	pGAL-RPL27 NOG1-TAP	TK855	his3-1, leu2-0, ura3-0, YDR471w::HIS3MX6, YHR010w::kanMX4, YPL093W-TAP (Kl URA3)	strain Y1082 was transformed with a PCR on pBS1539 with primers 2159/2160	
Y2902	pGAL-RPL32 RPF2-TAP	TK880	his3-1, leu2-0, ura3-0, YBL092w::kanMX4, YKR081C-TAP (KI URA3)	strain Y1102 was transformed with a PCR product on pBS1539 with primers 227/237	
Y2904	pGAL-RPL33 RPF2-TAP	TK813	his3-1, leu2-0, ura3-0, YPL143w::kanMX4, YOR234c::HIS3MX6	strain Y1096 was transformed with a PCR product on pBS1539 with primers 227/237	
Y2907	pGAL-RPL34 NOG1-TAP	TK814	his3-0, leu2-0, ura3-0, YIL052c::HIS3, YER056c-a::kanMX4, YPL093W-TAP (Kl URA3)	strain Y930 was transformed with a PCR product on pBS1539 with primers 2159/2160	
Y2909	pGAL-RPL16 RPF2-TAP	TK810	his3-1, leu2-0, ura3-0, YNL069c::kanMX4, YIL133c::HIS3, YKR081C-TAP (KI URA3)	strain Y931 was transformed with a PCR product on PBS1539 with primers 227/237	
Y3105	pGAL-RPL9 NOC3-TAP	TK883	his3-0, leu2D0, lys2D0/LYS2, ura3D0, met15D0/MET15, YNL067w::kanMX4, YGL147c::HIS3MX6, YLR002C-TAP (Kl URA3)	strain Y1098 was transformed with a PCR product on pBS1539 with primers 367073671	

* Determination of generation time was performed as described in section 5.2.1.5 and (Ohmayer et al., 2012).

5.1.2 Plasmids

Nr.	Name	Yeast marker	origin / cloning strategy
	YEPlac195	URA3	
	pBS1539	URA3	Euroscarf
	pYM12		Knop et al., 1999
	Ycplac33	URA3	
TK230	YCplac111GAL	LEU2	Ferreira-Cerca et al., Mol. Cell 20 (2), p. 263-275
TK349	YEplac195-pRPS28-short-FLAG	URA3	product of a PCR with genomic DNA and primer O581/O582 (=RPS28 promoter from positions -245 until +1) EcoRI/BamHI digested and cloned into Yeplac195 (Ohmayer et al., 2013)
TK391	pGAL-RPS26-FLAG	LEU2	product of a PCR reaction with yeast genomic DNA as template and primers O618/O496 was cloned BamHI/PstI in TK230 (Ohmayer et al., 2013)
TK487	pRPS28-RPS24-FLAG	URA3	Ferreira-Cerca et al., 2007 (suppl. data)
TK584	Yep-pRPS28KpnI-Ct-FLAG	URA3	Oligonucletides O947 and O948 were hybridised, phosphorylated and cloned into BamHI/PstI digested K487 (Ohmayer et al., 2013)
TK789	YEplac195-MCS	URA3	TK349 was EcoRI/HindIII digested, filled with Klenow and blunt ligated (Ohmayer et al., 2013)
TK792	YEplac195 pRPS28 FLAG modified	URA3	product of a PCR with K349 as template and primers O1266/O1267 was cloned KasI into K789 (Ohmayer et al., 2013)
TK808	pGAL-RPL10	LEU2	Pöll et al., 2009
TK810	pGAL-RPL16	LEU2	Pöll et al., 2009
TK812	pGAL-RPL23	LEU2	Pöll et al., 2009
TK813	pGAL-RPL33	LEU2	Pöll et al., 2009
TK814	pGAL-RPL34	LEU2	Pöll et al., 2009
TK818	pGAL-RPL1B	LEU2	Pöll et al., 2009
TK819	pGAL-RPL2	LEU2	Pöll et al., 2009
TK821	pGAL-RPL20	LEU2	Pöll et al., 2009
TK822	pGAL-RPL3	LEU2	Pöll et al., 2009
TK823	pGAL-RPL13A	LEU2	Pöll et al., 2009
TK846	pGAL-RPL17A	LEU2	Pöll et al., 2009
TK852	pGAL-RPL5	LEU2	Pöll et al., 2009
TK855	pGAL-RPL27A	LEU2	Pöll et al., 2009
TK856	pGAL-RPL28	LEU2	Pöll et al., 2009
TK857	pGAL-RPL35A	LEU2	Pöll et al., 2009
TK865	pGAL-RPL25	LEU2	Pöll et al., 2009
TK865	pGAL-RPL25	LEU2	Pöll et al., 2009
TK880	YCplac111GAL-RPL32	LEU2	Pöll et al., 2009
TK881	YCplac111GAL-RPL43	LEU2	Pöll et al., 2009
TK882	YCplac111GAL-RPL8B	LEU2	Pöll et al., 2009
TK883	YCplac111GAL-RPL9A	LEU2	Pöll et al., 2009

TK884	YCplac111GAL-RPL19B	LEU2	Pöll et al., 2009
TK885	YCplac111GAL-RPL21A	LEU2	Pöll et al., 2009
TK887	YCplac111GAL-Ubq-RPL40A	LEU2	product of a PCR with genomic DNA and primers O1438/O1424 was BamHI/PstI digested and cloned into TK792 (Ohmayer et al., 2013)
TK888	YCplac111GAL-RPL40A-minus Ubq moiety	LEU2	Pöll et al., 2009 (suppl. data)
TK942	YEp-pRPS28-FLAG-RPL23	URA3	BamHI / PstI cassette from TK812 was cloned into TK792 (Ohmayer et al., 2013)
TK943	YEp-pRPS28-FLAG-RPL33	URA3	BamHI / PstI cassette from TK813 was cloned into TK792 (Ohmayer et al., 2013)
TK945	YEp-pRPS28-FLAG-RPL1B	URA3	BamHI / PstI cassette from TK818 was cloned into TK792 (Ohmayer et al., 2013)
TK951	YEp-pRPS28-FLAG-RPL17A	URA3	BamHI / PstI cassette from TK846 was cloned into TK792 (Ohmayer et al., 2013)
TK952	YEp-pRPS28-FLAG-RPL5	URA3	BamHI / PstI cassette from TK852 was cloned into TK792 (Ohmayer et al., 2013)
TK955	YEp-pRPS28-FLAG-RPL27A	URA3	BamHI / PstI cassette from TK855 was cloned into TK792 (Ohmayer et al., 2013)
TK957	YEp-pRPS28-FLAG-RPL35A	URA3	BamHI / PstI cassette from TK857 was cloned into TK792 (Ohmayer et al., 2013)
TK959	YEp-pRPS28-FLAG-RPL25	URA3	BamHI / PstI cassette from TK865 was cloned into TK792 (Ohmayer et al., 2013)
TK962	YEp-pRPS28-FLAG-RPL43	URA3	BamHI / PstI cassette from TK881 was cloned into TK792 (Ohmayer et al., 2013)
TK963	YEp-pRPS28-FLAG-RPL8B	URA3	BamHI / PstI cassette from TK882 was cloned into TK792 (Ohmayer et al., 2013)
TK965	YEp-pRPS28-FLAG-RPL19B	URA3	BamHI / PstI cassette from TK884 was cloned into TK792 (Ohmayer et al., 2013)
TK968	YEp-pRPS28-FLAG-Ubq-RPL40A	URA3	BamHI / PstI cassette from TK887 was cloned into TK792 (Ohmayer et al., 2013)
TK969	YEp-pRPS28-FLAG-RPL40A minus Ubq moiety	URA3	BamHI / PstI cassette from TK888 was cloned into TK792; lacks N-terminal ubiquitine moiety. FLAG tag N-terminally fused to rpL40A (Ohmayer et al., 2013)
TK1028	pRPS28-RPL2-Flag	URA3	product of a PCR with TK819 as template and primers O1664/O1273 was BamHI/PstI cloned into TK487 (Ohmayer et al., 2013)
TK1029	pRPS28-RPL3-Flag	URA3	product of a PCR with TK822 as template and primers O1665/O1274 was BamHI/PstI cloned into TK487 (Ohmayer et al., 2013)
TK1031	pRPS28-RPL10-Flag	URA3	product of a PCR with TK808 as template and primers O1663/O1279 was BamHI/PstI cloned into TK487 (Ohmayer et al., 2013)
TK1032	pRPS28-RPL13-Flag	URA3	product of a PCR with TK823 as template and primers O1667/O1280 was BamHI/PstI cloned into TK487 (Ohmayer et al., 2013)

5.1.3 Oligonucleotides

Nr.	name	sequence (5´ to 3´ direction)
227	RPF2-TAP fw	CAGTGCCACTGATATTGAGCCCTCTGCTAAAAGACAGAAGAAATCCATGG AAAAGAGAAG
237	RPF2-TAP rev	CTCCTCTCTTAGATTATCATATAATATACAAAGTTTATGGGTCTACGACTCA CTATAGGG
496	GalRPS26A_F_Bam	CGCCGCGGATCCATGCCAAAGAAGAGAGCT
581	RPS28B-Prom-F2	TTTTTTGAATTCGCTTATTCATGTTCGAATC
582	RPS28B-Prom-Rv-FLAG	TTTTTTGGATCCGGTACCCTTATCGTCGTCATCCTTGTAATCCATTGCTGC TCTTTTATGCTTTGC
618	RPS-Flag-Ct-PstI	TTTTTTCTGCAGTTACTTATCGTCGTCATCCTTGTAATCCATTAAAGCCTTC TTGGCGGCATC
621	NOC2-TAP fw	AAGTGATGATGACAACGAAGATGTTGAAATGTCAGACGCT TCCATGGAAAAGAGAAG
622	NOC2-TAP rev	CTATTGAATTCAAGACAAAAAATCAAATCTTGCTGAGTTGTACGACTCACT ATAGGG
638	NOP7-TAP fw	GCCAAACAAAAAGCTAAACTGAATAAACTAGATTCCAAGAAATCCATGGAA AAGAGAAG
639	NOP7-TAP rev	AGACAAAATTTTTGAGAGGCTATTGGAAAAGAAGAGAAAATACGACTCACT ATAGGG
947	Yc-KpnI-Up	GATCTGGTACCGGATCCTCTAGAGTCGACCTGCA
948	Yc-KpnI-Do	GGTCGACTCTAGAGGATCCGGTACCA
1266	pRPS28_mod_for	CTTGGCGCCGAATTCATGCATGCTTATTCATGTTCGAA
1267	pRPS28_mod_rev	GAAGGCGCCGAATTCAAGCTTGCATGCCTGC
1273	RPL2B-Start-BAM	TTTTTTGGATCCATGGGTAGAGTTATTCGTAACCAA
1274	RPL3-Start-BAM	TTTTTTGGATCCATGTCTCACAGAAAGTACGAAG
1279	RPL10-Start-BAM	TTTTTTGGATCCATGGCTAGAAGACCAGCTAG
1280	RPL13-Start-BAM	TTTTTTGGATCCATGGCCATTTCCAAGAATTTACCA
1424	RPL40A-Do2-Pst	TTTTTTCTGCAGATACCACCGCTACGCGTTGAC
1438	RPL40A-Gal-Bam	TTTTTTGGATCCATGCAAATTTTTGTCAAGACTTTGACTG
1663	RPL10-ORf-Rev	TTTTTTCTGCAGAGCTTGAGCAGCAAAGTATTC
1664	RPL2B-Orf-Rev	TTTTTTCTGCAGATCTTGGGTCTTTTGAGAACC
1665	RPL3-Orf-Rev	TTTTTTCTGCAGCAAGTCCTTCTTCAAAGTACC
1667	RPL13-Orf-Rev	TTTTTTCTGCAGTTTCTTCTTTTCAGCTTCAGC
2159	NOG1-TAP fw	CAAAGCATTTATTCAGTGGTAAGCGTGGTGTCGGTAAGACAGATTTCCGT TCCATGGAAAAGAGAAG
2160	NOG1-TAP rev	TCTCTACTTCTTATTCTTTCTTTTGCATGTACTTTAAAAAAAATATGATACGA CTCACTATAGGG
2161	NOG2-TAP fw	AGGAAGGGGAAGAAAAACCAAAGAAGAAAGAAGTTGAGAAGACGGCATC CATGGAAAAGAGAAG
2162	NOG2-TAP rev	TCACTTGTAATCTTAAATTAATATTATACACCGGTTGTCCGTTTTTACCTTA CGACTCACTATAGGG
2932	RSA4-TAP fw	CGACTGGAGTGTCGACGGTAAAAGAGTGTGTAGTGGTGGGAAAGACAAG ATGGTAAGATTGTGGACGCATTCCATGGAAAAGAGAAG
2933	RSA4-TAP rev	AAATGCAGTTCTATATCACAGTTATATAATATTTATATGTGCATGTATGTTA CTTGTCTTTGCACATAACTACGACTCACTATAGGG
2934	NOP53-TAP fw	AGTGCCCGTTAGGAAAGGTAGAAAGTATAAGCAGAAAATCACTGAAAAGT GGACACATAAGGACTTCAAATCCATGGAAAAGAGAAG
2935	NOP53-TAP rev	ATCTCACTTGATGAATCCACGTATCAAGGACAACCTTTTCATGGAAACATA TACTGTAAAACAAAAAACTTACGACTCACTATAGGG
2936	ARX1-TAP fw	GGAAACGCAGCCAATGAAGCAGAAGAGTGTTGAGACATCAAATGGCGGA GTTGAAGAAACCATGAAAATGTCCATGGAAAAGAGAAG
2937	ARX1-TAP rev	AATATTCTATTTTACATTTTATGATATACTTATATTATTTATATACTAGCTTTA GAAATGATGAAGTTTCTACGACTCACTATAGGG
3670	NOC3-TAP fw	AAAGCATTATTGTCCTGTAGTTACAAAGGGGCTACGCTCTCTATCATCTAG ATCTAAAGAGTGTTCTAAATCCATGGAAAAGAGAAG
3671	NOC3-TAP rev	ACTCGACACGGCAAAAATGATTGGCTAACGATAATCGTGGCTCTTTATATA CTTAATATATAGGATCTAGTACGACTCACTATAGGG

5.1.4 Probes (DNA oligonucleotides used as RNA probes)

number	name	sequence (5´ to 3´ direction)
68	5.8S rRNA probe	TTTCGCTGCGTTCTTCAT
202	U3 sno-RNA probe	CCAACTTGTCAGACTGCCATT
205	18S rRNA probe	CATGGCTTAATCTTTGAGAC
207	A2/A3 probe	TGTTACCTCTGGGCCC
210	E/C2 probe	GGCCAGCAATTTCAAGTTA
212	25SrRNA probe	CTCCGCTTATTGATATGC
1440	Glutamyl-tRNA probe	CGGTCTCCACGGTGAAAGC
1819	D/A2 probe	GTAAAAGCTCTCATGCTCTTGCC
2474	5S rRNA probe	TTAACTACAGTTGATCGG

5.1.5 Enzymes

Enzyme	Origin
GoTaq Polymerase	Bio-Rad
Herculase II Fusion DNA Polymerase	Stratagene
Restriction Endonucleases	New England Biolabs
RNasin® Plus RNase inhibitor	Promega
T4 DNA Ligase	New England Biolabs
T4 Polynucleotide Kinase	New England Biolabs
Taq DNA Polymerase	New England Biolabs
Trypsin, sequencing grade	Roche

5.1.6 Antibodies (used for Western blotting)

Antibody	Species	Dilution	Origin
PAP (peroxidase anti-peroxidase)	rabbit	1:5000	Sigma-Aldrich
α-Flag	rabbit	1:1000	Sigma-Aldrich
α-RPA135 (RNA Polymerase I subunit)	rabbit	1:5000	(Buhler et al., 1980)
α-rabbit IgG (H+L) (peroxidase-conjugated)	goat	1:5000	Jackson IR/ Dianova

5.1.7 Chemicals

All chemicals were purchased at the highest available purity from Sigma-Aldrich, Merck, Fluka, Roth or J.T.Baker, except agarose electrophoresis grade (Invitrogen), bromine phenol blue (Serva), Ficoll (Serva), gentamycin (PAA), Tris ultrapure (USB Corporation) and Tween 20 (Serva). Isotope labelled γ-32P-ATP was purchased from Hartmann Analytic. Ingredients for growth media were purchased from BD Biosciences (Bacto Agar, Bacto Peptone, Bacto Tryptone and Bacto Yeast Extract), Q-Biogene, Bio101, Inc. or Sunrise Science Products (Complete supplement mixtures (CSM), Yeast nitrogen base (YNB), amino acids, adenine)

and Sigma-Aldrich (D(+)-glucose, D(+)-galactose, amino acids and uracil). Water was always purified with an Elga Purelab Ultra device prior to use to achieve a resistivity of 18.2 MΩ-cm.

5.1.8 Media and buffers

Medium	Composition
YPD (yeast extract, peptone, dextrose)	1% (w/v) yeast extract 2% (w/v) peptone 2% (w/v) glucose
YPG (yeast extract, peptone, galactose)	1% (w/v) yeast extract 2% (w/v) peptone 2% (w/v) galactose
SDC/SGC	6,7 g/l YNB (yeast nitrogen base) CSM dropout according to label 2 % (w/v) sugar (glucose for SDC, galactose for SGC) amino acid supplements according to the list below
LB (lysogeny broth)	1% (w/v) tryptone 0.5% (w/v) yeast extract 0.5% (w/v) NaCl
LB_{Amp}	LB + 100 µg/ml ampicillin
SOB medium	2% (w/v) tryptone 0.5% (w/v) yeast extract 0.5 g/l NaCl 0.19 g/l KCl 2.03 g/l MgCl2 x 6 H2O pH 7.0 with NaOH

The solvent was H_2O, if not indicated otherwise. The pH values were measured RT. All media was sterilized for 20 minutes at 110°C. Supplements were added after cooling to approximately 60°C. For plate media 2% (w/v) agarose were added before autoclaving.

Amino acid supplementation according to Bio101RSystems (mg/liter)

Adenine: 10*; Arginine: 50; Aspartic Acid: 80; Histidine: 20; Isoleucine: 50; Leucine: 100; Lysine: 50; Methionine: 20**; Phenylalanine: 50; Threonine: 100**; Tryptophan: 50; Tyrosine: 50; Uracil: 20; Valine: 140;

* Minimum quantity for healthy growth and yet optimized to promote red color in certain adenine auxotrophs. CSM formulations are available that contain 20 or 40 mg/liter of adenine.

** 80 mg/liter of Homoserine is substituted for Threonine in mixtures where Methionine is dropped-out.

Buffer	Ingredients	Concentration
10x PBS	NaCl KCl KH_2PO_4 Na_2HPO_4 pH 7.4 with NaOH	1.37 M 27 mM 18 mM 0.1 M
1x PBST	NaCl KCl KH_2PO_4 Tween-20	0.137 M 2.7 mM 1.8 mM 0.05% (v/v)

10xTBS	NaCl KCl Tris pH7.4	1,35M 27mM 125mM
4x lower tris (SDS-PAGE)	Tris SDS pH 8.8 with HCl	1.5 M 0.4% (w/v)
4x upper tris (SDS-PAGE)	Tris SDS bromophenol blue pH 6.8 with HCl	0.5 M 0.4% (w/v)
4x protein sample buffer (Laemmli buffer)	Tris pH 6.8 glycerol SDS β-mercaptoethanol bromophenol blue	0.25 M 40% (v/v) 8.4% (w/v) 0.57 M
4/3 16% Acrylamid + urea (100ml)	Rotiphorese Gel 30 Urea	71,1ml 6M (36,06g)
4/3 4% Acryalamid + urea (100ml)	Rotiphorese Gel30 Urea H_2O	17,7ml 6M (36,06g) 53,4ml
HU buffer	Tris pH 6.8 SDS EDTA pH 8.0 β-mercaptoethanol urea bromophenol blue	0.2 M 5% (w/v) 1 mM 0.21 M 8 M
10x electrophoresis buffer	Tris glycine SDS	0.25 M 1.92 M 1% (w/v)
transfer buffer (Western Blot)	Tris glycine methanol SDS	25 mM 192 mM 20% (v/v) 0,05% (w/v)
Ponceau staining solution	Ponceau S HOAc	0.5% (w/v) 1% (v/v)
Coomassie staining solution	Coomassie Brilliant Blue R 250 methanol HOAc	0.1% (w/v) 45% (v/v) 10% (v/v)
destaining solution (Coomassie)	methanol HOAc	45% (v/v) 10% (v/v)
100x protease inhibitors (PIs)	benzamidine PMSF solvent: ethanol store at -20°C	0.2 M 0.1 M
10x DNA loading buffer	Tris-HCl pH 8.0 EDTA pH 8.0 glycerol bromophenol blue xylene cyanol	4 mM 0.4 mM 60% (v/v)
5x TBE buffer	Tris boric acid EDTA pH 8.0	445 mM 445 mM 10 mM
AE buffer	NaOAc pH 5.3 EDTA pH 8.0	50 mM 10 mM
RNA solubilization buffer (for agarose gel samples)	formamide (deionised) formaldehyde MOPS buffer Bromphenol blue store at -20°C	50% (v/v) 8% (v/v) 1x
RNA solubilization buffer (for acryl amide gel samples)	formamide (deionised) TBE check pH; should be pH 7 Xylen cyanol Bromphenol blue store at -20°C	80% (v/v) 0.1x

20x SSC	NaCl tri-sodium-citrate dihydrate pH 7.0 with HCl	3 M 0.3 M
10x MOPS buffer	sodium acetate trihydrate MOPS EDTA pH 8.0 pH 7.0 with NaOH	20 mM 0.2 M 10 mM
RNA hybridisation buffer	Formamide SSC SDS Denhard's solution	50% (v/v) 5x 0.5% (w/v) 5x
50x Denhard's solution	Ficoll (Typ 400) Polyvinylpyrrolidone (avg. MW 40000) BSA (Fraction V, Sigma Alrich) store at -20°C	10mg/ml 10mg/ml 10mg/ml
buffer A200/300	Tris/HCl pH 8 KCl $Mg(OAc)_2$ Protease inhibitors RNAsin	20mM 200mM / 300mM 5mM 1x 0.04 U / ml
buffer A200/300 +T/T	Tris–HCl pH 8 KCl $Mg(OAc)_2$ Protease inhibitors RNAsin Triton X-100 Tween-20	20mM 200mM / 300mM 5mM 1x 0.04 U / ml 0.5% (w/v) 0.1% (w/v)
buffer AC	NH_4OAC $MgCl_2$ pH ad 7.4 with HOAc	100 mM 0.1 mM
TELit	Tris pH 8.0 LiOAc EDTA pH 8.0 pH 8.0 with HOAc	10 mM 100 mM 1 mM
LitSorb	sorbitol solvent: TELit autoclave	1 M
LitPEG	polyethylene glycol (PEG3350) solvent: TELit autoclave	40% (w/v)
ampicilin stock solution	ampicilin store at -20°C	100 mg/ml
Tfb I buffer	KAc MnCl2 KCl glycerol pH 5,8 with 0,2 M HOAc sterile filtration	30 mM 50 mM 100 mM 15% (v/v)
TfB II buffer	MOPS CaCl2 KCl glycerol pH 7,0 with 1M NaOH sterile filtration	10 mM 75 mM 10 mM 15% (v/v)

5.1.9 Kits

Kit	**Origin**
Herculase II Fusion enzyme (with dNTP combo)	Agilent
iTRAQ® Reagent multiplex kit	Applied biosystems (AB Sciex)
peqGOLD Plasmid Miniprep Kits	Peqlab
pGEMT easy Kit	Promega
QIAEX II gel extraction kit	Qiagen
QIAquick PCR Purification Kit	Qiagen

5.1.10 Consumables

Material	Origin
1 kb DNA ladder	New England Biolabs
100 bp DNA ladder	New England Biolabs
6 peptide mixture (P/N 4368762) f. calibration	AB Sciex
96-well plates	Sarstedt
α-cyano-4-hydroxy cinnamic acid (matrix)	Sigma Aldirch
Acclaim™ 3µm PepMap100 C18 Nano LC Columns with nanoViper™ Fittings (75µm x 150 mm) (P/N 164568)	Thermo Scientific
ANTI-FLAG M2 Affinity Gel	Sigma Aldirch
BcMag™ Epoxy-Activated magnetic beads	Bioclone Inc.
Blotting papers MN 827 B	Millipore
BM Chemiluminescence Blotting Substrate (POD)	Roche
ColorPlus Prestained Protein Marker, Broad Range (7-175 kDa)	New England Biolabs
Extra Thick Blot Paper	Bio-Rad
Extran® MA 01 alkaline	Merck
Filter paper 3mm	Whatman
Gene pulser cuvettes (2mm)	Bio-Rad
Glass beads (Ø 0.75-1 mm)	Roth
Glow writer	Diversified biotech
Glycogen	Ambion
IgG SepharoseTM 6 Fast Flow	GE Healthcare
Immobilion-P Membrane PVDF 0,45 µm	Millipore
Inoculation loops (1µl)	Sarstedt
Membrane PositiveTM	MP Biomedicals
Micro Bio-Spin 6 Columns	Bio-Rad
Milk powder	Sukofin
MobiCol microspin column	MoBiTec
NuPAGE® 4-12% Bis-Tris Gel	Life technologies
Polamét (metal care)	Anti-black
Poly-Prep Chromatography columns (10ml)	Bio-Rad
Precision Wipes (11x21cm)	Kimberly-Clark
Protein Assay “Dye Reagent Concentrate”	Bio-Rad
Protein Marker, Broad Range (2-212 kDa)	New England Biolabs
rabbit IgG(I5006-100MG lyophilized powder)	Sigma-Aldrich
Safe-lock tubes 1,5ml (for mass spectrometry)	Eppendorf
Salmon Sperm DNA (10 mg/ml)	Invitrogen
SimplyBlue™ SafeStain	Invitrogen
SpeedVac concentrator	Eppendorf
SYBR Safe DNA Gel stain	Invitrogen
Ultima Gold Liquid scintillation cocktail	Perkin Elmer
µ-Precolumn (300µm x 5mm) C18PepMap100, 5µm, 100Å (P/N 160454)	Thermo Scientific

5.1.11 Equipment

Device	Manufacturer
4800 Proteomics Analyzer MALDI-TOF/TOF	Applied Biosystems (Ab Sciex)
Avanti J-26 XP centrifuge	Beckman Coulter
AxioCam MR CCD camera	Zeiss

Axiovert 200M microscope	Zeiss
Biofuge Fresco refrigerated tabletop centrifuge	Hereaus
Biofuge Pico tabletop centrifuge	Hereaus
C412 centrifuge	Jouan
Centrikon T-324 centrifuge	Kontron Instruments
CT422 refrigerated centrifuge	Jouan
Electrophoresis system model 45-2010-i	Peqlab Biotechnologie GmbH
Trans Blot Cell	Biorad
FLA-3000 phosphor imager	Fujifilm
IKA-Vibrax VXR	IKA
Incubators	Memmert
LAS-3000 chemiluminescence imager	Fujifilm
MicroPulser electroporation apparatus	Bio-Rad
NanoDrop ND-1000 spectrophotometer	Peqlab Biotechnologie GmbH
Phosphoimager screens	Fujifilm
Power Pac 3000 power supplies	Bio-Rad
Probot	LC Packings (Dionex)
Shake incubators Multitron / Minitron	Infors
Speed Vac Concentrator	Savant
Superose 12 PC 3.2/30	GE Healthcare
Szintillation counter „1600 TR-Packard“	Packard
TECAN infinite F500 reader	TECAN
Thermomixer compact	Eppendorf
Trans-Blot SD Semi-Dry Transfer Cell	Bio-Rad
UltiMate 3000 NanoHPLC	LC Packings (Dionex)
Ultrospec 3100pro spectrophotometer	Amersham
UV systeme (gel documentation)	INTAS
Vacuum blotter	Biorad
Drystar	H. Hoelzel

5.1.12 Software

Software	**Producer**
4000 Series Explorer v.3.6	Applied Biosystems
Acrobat 7.0 Professional v.7.0.9	Adobe
Chromelion V.6.80	LC Packings (Dionex)
Cluster 3.0	Michael Eisen lab (Stanford University)
Data Explorer v.4.5 C	Applied Biosystems
Discovery Studio 4.0 Client	Accelrys
GPS Explorer v.3.5	Applied Biosystems
i-control V1.5	TECAN
Illustrator CS3	Adobe
Image Reader FLA-3000 V1.8	Fujifilm
Image Reader LAS-3000 V2.2	Fujifilm
Mascot	Matrix Science
Microsoft Office 2007	Microsoft
Multi Gauge V3.0	Fujifilm

Photoshop CS3	Adobe
Protein Pilot	Applied Biosystems
SigmaPlot	Systat
Java Treeview V1.1.6r2	Alok (http://jtreeview.sourceforge.net)
VectorNTI	Invitrogen
µcarrier V.2.0	LC Packings (Dionex)
Zotero (4.0.19)	http://zotero.org (Center f. History and new media)

5.2 Methods

5.2.1 Work with *S.cerevisiae* (yeast)

5.2.1.1 Cultivation and harvest of yeast strains

Strains of the yeast *Saccharomyces cerevisiae* were cultivated using standard microbiological methods (Amberg and Cold Spring Harbor Laboratory, 2005). Liquid cultures were grown in the appropriate medium at 30°C, unless stated otherwise. Cell growth was monitored by measuring the absorbance at 600 nm (optical density OD_{600}). Cells from liquid cultures were harvested at ~5000 x g at room temperature. Resulting cell pellets were dissolved in cold water, transferred to a 50ml tube and centrifuged at 5000 x g for 5 minutes at 4°C. For cultivation on solid agar plates containing the appropriate medium, single colonies or small aliquots of glycerol stocks were streaked out using sterile inoculation loops in order to obtain colonies derived from single yeast cells. Short-term storage of yeast strains was accomplished by keeping the agar plates at 4°C, for long-term storage see section 5.2.1.6.

5.2.1.2 Preparation of transformation competent yeast cells

50 ml of an exponentially growing yeast culture (OD600 ~ 0.5-0.7) were harvested by centrifugation for 5 min at 4000 rpm and RT. Cells were first washed with 25 ml sterile H_2O and then with 5 ml LitSorb before resuspending in 360 µl LitSorb. 40 µl of Salmon Sperm DNA, which were previously incubated for 5 min at 99°C and immediately chilled on ice, were added to the cell suspension. After mixing, 50 µl aliquots were transferred to 0.5 ml tubes and stored at -80°C.

5.2.1.3 Transformation of competent yeast cells with DNA

An aliquot (50µl) of competent yeast cells was thawed on ice. DNA to be transformed (100 ng of plasmid DNA or 5-10 µg of linear DNA for integration into the genome) was added and the sample was mixed. After addition of six volumes of LitPEG, the suspension was mixed thoroughly and incubated for at least 30 min (30 min – 3 hours) at RT. Sterile DMSO was added to the sample (1/9 of the total volume), followed by incubation at 42°C for 15 min and centrifugation for 1 min at 3000 rpm and RT. When selecting for auxotrophic markers (*e.g. TRP1*, *LEU2*, *URA3*), the cell pellet was directly resuspended in 100 µl sterile H_2O and plated on SCD- or SCG-plates lacking the corresponding marker. If selection for antibiotic

resistance (*e.g.* geneticin, hygromycin B) was required, the cell pellet was resuspended in 5 ml YPD or YPG and incubated for 2-3 generation times at 30°C while shaking to allow the expression of the marker before plating on the respective selection media. Since selection for antibiotic resistance often results in a high number of transient transformants, these plates were replica-plated on fresh selection media to further isolate positive clones.

5.2.1.4 Generation of yeast strains expressing epitope tag fusion proteins

Yeast strains expressing endogenously encoded FLAG or tandem affinity purification (TAP) tag fusion proteins were constructed by transformation of PCR based tagging cassettes (5.2.1.3) and homologous recombination as widely-used and described (Knop et al., 1999; Puig et al., 2001), using different auxotrophy (typically *URA3*, *LEU2* or *TRP1*) or resistance markers for selection. The plasmids and oligonucleotides used are listed in sections 5.1.2 and 5.1.3, respectively. The resulting strains are listed in 5.1.1.

5.2.1.5 Determination of generation time (as listed in 5.1.1)

The purpose of the measurement of the generation times in this work was to estimate relative differences of certain yeast strains to the corresponding wild type yeast strains. To this end, an automatized procedure using small volumes of yeast cultures was applied as described in the following (and in Ohmayer et al., 2012). The yeast strain of interest was grown overnight in the medium of interest (YPD or YPG) and then diluted to an OD_{600} of 0.02 in 0.2 ml of the respective fresh medium in a covered sterile 96 well plate. Cells were incubated at 30°C in a TECAN infinite F500 reader with measurements taken in kinetic cycle mode (shaking for a duration of 25 seconds per cycle in orbital shaking mode with an amplitude of 5 mm, wait time of 30 seconds before measurement of the OD_{612}, total cycle length of 15 minutes). Growth measurements using larger culture volumes incubated at 30°C in Erlenmeyer flasks on a rotary shaker (as it is usually done) gave identical results in regard to these **relative** changes in generation times (absolute numbers differed, however).

5.2.1.6 Purification of genomic DNA from yeast

A yeast culture was grown overnight in 5 ml YPD. Cells were harvested by centrifugation and resuspended in 500 µl H_2O. Cells were centrifuged again and resuspended in 500 µl 1M sorbitol, 0.1M EDTA. 3µl of 2% zymolyase (10mM Tris-HCl pH8.0, 5% glucose, 2% zymolyase) were added and incubated for 60 min at 37°C. The spheroblasts were centrifuged at 5000 x g for 5 min (table-top centrifuge). After addition of 500 µl IR buffer and 50 µl 10% SDS, the samples were vortexed until lysis was complete (about 1 min at full speed). Samples were incubated for 30 min at 65°C. For precipitation of nucleic acids, 200 µl of 5 M KOAc were added and samples were kept on ice for 20 min. Samples were centrifuged at 16600 x g for 20 min at 4°C, the resulting supernatant was transferred to a new microtube. 1.5 µl of RNAseA (100 mg/ml) was added and samples were incubated at RT over night. After addition of 750 µl isopropanol, DNA was precipitated at RT for 5 min and pelleted (13000 rpm, 5 min in a table-top centrifuge). The pellet was washed once with ice-

cold 70% EtOH and centrifuged again (13000 rpm, 5 min in a table-top centrifuge). The supernatant was discarded and the DNA pellet air-dried to eliminate remnants of ethanol. The dry pellet was resuspended in 50 µl TE buffer.

5.2.1.7 Long-term storage of yeast strains

2 ml of an overnight culture of the yeast strain to be stored were mixed with 1 ml sterile 50% (v/v) glycerol and separated into two aliquots. Glycerol stocks were stored at -80°C.

5.2.2 Work with *E.coli*

5.2.2.1 Cultivation of bacterial strains

Liquid cultures were grown in LB medium supplemented with the required antibiotics at 37°C. Cell growth was monitored by measuring the absorbance (optical density) at 600 nm (OD600). For cultivation on solid agar plates containing LB medium and the required antibiotics, single colonies or small aliquots of glycerol stocks were streaked out using sterile disposable inoculation loops in order to obtain colonies derived from single bacterial cells. Plates were incubated upside down at 37°C for not longer than 1 day. Short-term storage of bacterial strains was accomplished by keeping the agar plates at 4°C.

5.2.2.2 Preparation of electro competent bacterial cells

The *E. coli* strain XL1-Blue was used as a host for amplification of plasmid DNA. In order to increase the efficiency of plasmid DNA uptake, competent cells for electroporation were prepared. Cells were grown in 400 ml SOB medium at 37°C to mid-log phase (OD600 ~ 0.35-0.6), chilled on ice for 15 min, and centrifuged for 10 min at 6000 rpm and 4°C. To reduce the ionic strength of the cell suspension, cells were washed three times with cold sterile H_2O and once with sterile 10% (v/v) glycerol. After resuspending the cells in 1.5 ml sterile 10% (v/v) glycerol, 50 µl aliquots were transferred to 1.5 ml tubes and stored at -80°C.

5.2.2.3 Transformation of competent bacterial cells with DNA by electroporation

An aliquot of electro competent bacterial cells (see above) was thawed on ice. DNA to be transformed (1 ng of plasmid DNA or 1-2 µl of a ligation sample) was added and the sample was mixed. After pipetting the suspension into a cold 0.2 cm electroporation cuvette, pulsing was performed with program EC2 in a MicroPulser electroporation apparatus. Immediately after the pulse, 1 ml LB medium was added and the sample was transferred to a 1.5 ml tube following incubation for 30-60 min at 37°C. 100 µl of the cell suspension were plated on LB supplemented with the required antibiotics and incubated overnight at 37°C. The residual cells were centrifuged for 1 min at 5000 rpm and RT. About 900 µl of the supernatant were discarded and the pellet was resuspended in the remaining liquid, plated as above, and incubated overnight at 37°C

5.2.2.4 Preparation of chemical competent cells

200 ml SOB medium were inoculated from a stationary *E. coli* culture to an OD 600 = 0.2 and incubated at 37°C to a final OD600 ~ 0.5 – 0.6. Cells were harvested in 50 ml tubes by centrifugation (4500 rpm, 10 min, 4°C). Each cell pellet was resuspended in 15 ml cold Tfb-I buffer, incubated on ice for 20 min and centrifuged as above. The cell pellets were resuspended and combined in a total volume of 4 ml cold Tfb-II buffer and incubated on ice for 20 min. 100 µl aliquots of the cell suspension were stored at – 80°C.

5.2.2.5 Transformation of competent bacterial cells with DNA by heat shock

An aliquot of chemical competent bacterial cells (see above) was thawed on ice. DNA to be transformed (10 - 100 ng of plasmid DNA) was added; the sample was mixed and incubated on ice for 5 min. After a heat shock step (42°C, 40 sec), the sample was incubated on ice for another 3 min. Subsequently, 1 ml LB medium was added and the sample was incubated for 30-60 min at 37°C. 100 µl of the cell suspension were plated on LB supplemented with the required antibiotics and incubated overnight at 37°C. The residual cells were centrifuged for 1 min at 5000 rpm and RT. About 900 µl of the supernatant were discarded and the pellet was resuspended in the remaining liquid, plated as above and incubated overnight at 37°C.

5.2.2.6 Purification of plasmid DNA from *E.coli* ("mini-preparation")

Plasmid DNA was isolated from 3-5 ml *E. coli* cultures with the peqGOLD Plasmid Miniprep Kit (Peqlab) according to the manufacturer's instructions. If larger amounts of plasmid were required the procedure was extended to a larger *E.coli* culture that was further processed similarly (as several single "mini preparations").

5.2.3 Work with DNA

5.2.3.1 Native agarose gel electrophoresis of DNA

Native agarose gel electrophoresis was used to separate DNA fragments. Depending on the fragment size, electrophoresis was performed with gels composed of 0.8%, 1% or 1.2% (w/v) agarose and 0.5x TBE buffer and containing 0.1 µg/ml ethidium bromide or appropriate amounts of SYBR safe stain. 0.5x TBE was used as electrophoresis buffer and gels were run at 100-150 V. For length determination, 0.5 µg of a DNA standard (1 kb ladder or 100 bp ladder) was used in a concentration of 50 µg/ml in 1x DNA loading buffer. DNA fragments were visualized by exposing the gel to UV light (254 nm).

5.2.3.2 Purification of DNA fragments from agarose gel

DNA fragments of interest were cut out from agarose gels and eluted using the QIAEX II gel extraction kit (Qiagen) following the instructions provided by the manufacturer.

5.2.3.3 Polymerase chain reaction (PCR)

The annealing temperatures for all primers used in PCR were estimated with the VectorNTI software from the Invitrogen company. For amplification of DNA fragments used for cloning, proofreading PCR was performed using Herculase II fusion polymerase (Agilent) with yeast genomic DNA (~ 500 ng) or plasmid DNA (~ 50 ng) as templates in 50µl reactions (0.25 µM of reverse and forward primers, 0.25 mM each dNTP). Annealing temperatures and amplification times were individually adjusted according to the manufacturer's manual. 5% of each PCR was analyzed by agarose gel electrophoresis and subsequently purified with Qiaquick PCR purification kit (Qiagen) according to the manufacturer or precipitated with ethanol (see below) for cloning or integration, respectively. For "screening" of a large number of ligated plasmids transformed in *E.coli*, the Go-Taq Polyermase (Bio-Rad) was used, following the manufacturer's instructions.

5.2.3.4 Ethanol precipitation of DNA

To precipitate DNA from PCR reactions, 1/10 of 10M LiCl was added to the aqueous PCR product. DNA was precipitated by addition of 2.5 volumes of 100% ethanol; to precipitate small amounts of DNA, glycogen (5µl of 20mg/ml stock solution) was supplemented. Samples were kept at -20°C for at least 1 hour. DNA was pelleted at 13000 rpm for 20 minutes at 4°C. To remove excess salt, the pellet was briefly washed with ice-cold 70% ethanol. The supernatant was discarded, the pellet air-dried and dissolved in TE or water.

5.2.3.5 Quantification of DNA using UV spectroscopy

Concentration of DNA samples dissolved in water was measured by UV spectroscopy at 260 nm (1 OD260 = 50 µg/ml) using a NanoDrop ND-1000 spectrophotometer. To determine contamination with proteins, absorbance at 280 nm was additionally measured. The ratio of OD260/OD280 of pure DNA is between 1.8 and 2.0.

5.2.3.6 Digestion of DNA with restriction endonucleases

A variety of restriction endonucleases were used to digest DNA in order to prepare defined DNA fragments for cloning or to check for presence and correct orientation of inserted DNA fragments. Digestion of DNA with the restriction endonucleases was done following the manufacturer's instructions. After digestion, the DNA fragments were separated on agarose gels and subsequently further processed as described above.

5.2.3.7 Adenylation of PCR products

Proofreading polymerases yield blunt ended PCR products. However, for subsequent ligation into the pGEMT easy vector system (Promega), a 3' A overhang is required, which can be introduced by the Taq Polymerase. To this end, the ethanol precipitated PCR product was incubated in a 30 µl reaction containing 0.25 mM dATP, 1x Thermo-Pol buffer (NEB) and 2.5 U Taq polymerase (NEB) for 5 min at 72°C. The adenylated PCR product was subsequently

purified using the QIAquick PCR Purification Kit (Quiagen) according to the manufacturer's instructions.

5.2.3.8 Dephosphorylation of DNA fragments

Re-ligation of the target plasmid ("backbone") can interfere with efficient ligation of the desired insert DNA into the plasmid. This problem can be minimized by dephosphorylation of the plasmid DNA after restriction enzyme digest. Digested plasmid DNA was incubated in 1x Antarctic phosphatase buffer (NEB) with 5 U Antarctic phosphatase at 37°C for 1 h, followed by incubation at 65°C for 5 min to inactivate the enzyme. The dephosphorylated plasmid DNA was directly used for ligation reactions without further purification.

5.2.3.9 DNA ligation

In order to clone DNA sequences into plasmids, the quantity (and purity) of purified DNA fragments digested with restriction endonucleases was measured by UV spectroscopy (see above). A fivefold molar excess of insert DNA compared to the plasmid DNA fragment (unless lengths of "backbone" and "insert" were similar) was incubated in a 20 µl ligation reaction using 400 U T4 DNA ligase (NEB) for 2 h at RT or overnight at 16°C. 1-2 µl of the ligation reaction were used for transformation of competent bacterial cells (see above). Cloning of adenylated PCR products into the pGEMT vector system (Promega) was done according to the manual using a threefold molar excess of insert to vector DNA.

5.2.3.10 Sequencing of DNA

DNA sequencing was performed by the GENEART/(Thermo Fischer) company and the service of primer synthesis was provided by Eurofins MWG Operon. Obtained sequences were compared to desired sequence using alignment tools of the VectorNTI software.

5.2.4 Work with RNA

5.2.4.1 RNA extraction

RNA extractions were essentially performed as described previously (Schmitt et al., 1990). Samples from which RNA should be extracted (cell pellets, aliquots of cell lysates, affinity purified material) were resuspended or diluted in 500 µl AE buffer and mixed with 500 µl phenol equilibrated in AE buffer and 50 µl of 10% (w/v) SDS. The samples were incubated in a thermomixer for 7 min at 1400 rpm and 65°C and afterwards chilled on ice for 3 min. After centrifugation for 2 min at 13000 rpm and 4°C, 3x 150 µl of the aqueous phase was collected and mixed with 500 µl phenol equilibrated in AE buffer by vortexing. The samples were again centrifuged and 3x 120 µl of the supernatant were mixed with 500 µl chloroform by vortexing. Phases were separated by centrifugation and the RNA in 3x 100 µl of the supernatant was precipitated by addition of 750 µl NaOAc-EtOH mix (composed of 1 volume 3 M NaOAc pH 5.3 and 25 volumes of ethanol) and incubation for at least 30 min at -20°C. In case that RNA should subsequently be analyzed in different gel systems, the sample was split in

appropriate ratios (usually 1/3 for acryl amide, 2/3 for agarose gels) prior to incubation at -20°C. The precipitated RNA was pelleted by centrifugation for 20min at 14000 rpm and 4°C, washed once with 70% cold Ethanol and dissolved in MOPS (for agarose gels) and TBE (for acryl amide gels) based solubilization buffer (5.1.8), respectively. Prior to use the dissolved RNA was denatured by incubation for 15 min at 65°C, followed by incubation on ice for 5 minutes. It was stored at -20°C.

5.2.4.2 Denaturing agarose gel electrophoresis of RNA with high molecular weight

Denaturing agarose gel electrophoresis was used to separate RNA species longer than 1000 bases (25S and 18S rRNAs and their respective precursor molecules). In this work electrophoresis was routinely performed with gels composed of 1.2% (w/v) agarose, 2% (v/v) formaldehyde, and 1x MOPS buffer containing 0.5 µg/ml ethidium bromide. The electrophoresis buffer was composed of 1x MOPS buffer and 2% (v/v) formaldehyde. Gels were run for 14-16 h at 40 V.

5.2.4.3 Denaturing agarose gel electrophoresis of RNA with low molecular weight

Denaturing acryl amide gel electrophoresis was used to separate RNA species between 100 and 500 bases (tRNA, 5S, 5.8S rRNAs and 7S pre-rRNA). In this work, electrophoresis was routinely performed with gels composed of 6% (w/v) acryl amide (acryl amide: bis-acryl amide 37.5:1), 7 M urea and 0.5x TBE. Before loading of the RNA sample, the pockets of the acryl amid gel were thoroughly flushed with 0.5x TBE to remove the dissolved urea. The electrophoresis buffer was 0.5x TBE. Gels were run for 75 – 90 min at 150 V.

5.2.4.4 Northern blotting (passive capillary transfer)

RNAs separated on agarose or acryl amid gels (see above) were transferred and immobilized on positively charged membranes (Positive™ MPBiomedicals) using different methods depending on the gel system. Passive capillary transfer was used for agarose gels. Prior to transfer, the agarose gels were washed once for 5 min in milli-Q water, once 20 min in 0.05 M NaOH to partially hydrolyze the RNAs and facilitate the transfer of larger RNAs, and were further equilibrated 20 min in 10xSSC. Transfer of the RNAs from the agarose gel to the membrane was then achieved over-night by drawing the transfer buffer (10xSSC) from the reservoir upward through the gel into a stack of pumping paper. The RNAs were eluted from the gel and deposited onto the positively charged membrane with the help of the buffer stream. To cross-link the transferred RNA to the membranes they were exposed (after drying at RT) for 30 seconds on each side with UV light (254) using the “INTAS UV system” gel-documentation device.

5.2.4.5 Northern blotting (electro transfer)

RNAs separated on acryl amide gels were transferred and immobilized on positively charged membranes (Positive™ MPBiomedicals) by electro transfer. Prior to transfer, the gels were

stained with 0.5 µg/ml ethidium bromide solution in 0.5x TBE for 5-10 min. The RNAs were transferred from the gel onto the positively charged membrane in 0.5x TBE using a wet tank blotting apparatus (Biorad) and applying a voltage of 50 V for 90 min. To cross-link the transferred RNA to the membranes they were exposed (after drying at RT) for 30 seconds on each side with UV light (254) using the “INTAS UV system” gel-documentation device.

5.2.4.6 Radioactive probe labeling and detection of RNA

Different RNA species immobilized on the membranes (see above) were detected using specific DNA oligonucleotides as probes. Probes used in this work are listed in section 5.1.4. The 5’ ends of all oligo-probes were labeled with P-32. 100 pmol of oligo-probe were incubated with 50 mCi of γ-^{32}P-ATP (Hartmann Analytik), in 1x PNK buffer (NEB) and 10 U of T4 polynucleotide kinase (NEB) in a total volume of 15 µl for 45 min at 37°C. Reactions were stopped by addition of 1ml of 0.5M EDTA pH 8. After addition of 50 µl H_2O, labeled probes were purified from non-incorporated nucleotides using a size exclusion column (Spin6-Biorad). Incorporated radioactivity was estimated by counting 1 µl of purified labeled probes using a scintillation counter (1600TR-Packard). Membranes carrying the RNAs to be detected were pre-hybridized for at least 1 h at 30°C in RNA hybridization buffer. The membranes were then incubated at 30°C over night after addition of at least 1-2x10_6 cpm of radioactively labeled probe per blot. The membranes were washed twice 15 min in 40-50 ml 2x SSC at 30°C. Signals were acquired exposing the membrane to a Phosphoimager screen (Fujifilm). Screens were read out with the FLA-3000 phosphor imager (Fujifilm) and data were analyzed and further processed with the Multigauge V3.0 software (Fujifilm).

5.2.5 Work with proteins

5.2.5.1 Determination of protein concentration of biological samples

Protein concentrations were determined using the Bio-Rad Protein Assay which is based on the method by Bradford (Bradford, 1976). Briefly, 0.5-5 µl of the protein solution to be tested (or appropriate dilutions of it) were mixed with 1 ml protein assay dye after diluting the reagent to the working concentration according to the instructions of the manufacturer. The approximate protein concentrations in µg/µl were calculated by dividing the observed absorbance at 595 nm by the sample volume and multiplying with the factor 23 which had been determined using a BSA standard curve.

5.2.5.2 Methanol-chloroform precipitation of proteins

Protein precipitation was performed using the methanol-chloroform precipitation method (Wessel and Flügge, 1984). The volume of the sample was adjusted to 150 µl with H_2O, followed by the addition of four volumes of methanol (600 µl), one volume of chloroform (150 µl), and three volumes of water (450 µl). After each of these steps the sample was thoroughly mixed by vortexing. After incubation for 5 min at 4°C, the sample was centrifuged for 5 min at 13000 rpm and 4°C. The supernatant was discarded without disturbing the interphase which contains the precipitated proteins. Upon addition of another three volumes of methanol (450

µl) and vortexing, the sample was incubated for 5 min at 4°C before centrifugation for 5 min at 13000 rpm and 4°C. The supernatant was completely removed and the protein pellet dried for 10 min in an Eppendorf SpeedVac Concentrator.

5.2.5.3 Denaturing protein extraction

Yeast cell pellets (1-2 OD_{600}) were resuspended in 1 ml cold water, mixed with 150 µl pre-treatment solution (1.85 M NaOH, 1 M β-mercaptoethanol), and incubated for 15 min at 4°C. Proteins were precipitated with 150 µl 55% (w/v) TCA for 15 min at 4°C and pelleted by centrifugation for 10 min at 13000 rpm and 4°C. The supernatant was discarded and the pellet was resuspended in 25 - 50 µl HU buffer. The pH of the sample was neutralized using NH_3 gas, if necessary. Proteins were solubilised by incubating the sample for 10 min at 65°C for subsequent separation by SDS-PAGE.

5.2.5.4 SDS-Poly acryl amid electrophoresis (SDS-PAGE)

Proteins were separated according to their molecular weight using the vertical discontinuous SDS-polyacrylamide gel electrophoresis method introduced by Laemmli (Laemmli, 1970). Depending on the size of the proteins of interest and the purpose different gel (systems) were used. The discontinuous system used in this work consisted of a lower separating gel composed of 8%, 10% or 12% acrylamide, 375 mM Tris-HCl pH 8.8, and 0.1% (w/v) SDS and an upper “stacking” gel composed of 4% acrylamide, 125 mM Tris-HCl pH 6.8, and 0.1% (w/v) SDS. Gels were run for ~1.5 h at 50 mA and 180 V in 1x electrophoresis buffer. Molecular weights of the different proteins were estimated using protein markers of known molecular weight (see list of consumables 5.1.10). In case the proteins of interest were of rather low molecular weight (10-40 kDa, as ribosomal proteins), a modified gel system with a higher acryl amid concentration (16%) and 6 M urea was used to increase the resolution. If the proteins of interest were in a broad range (~20 – 150 kDa) and/or if the quality of the subsequently stained gel should be increased, pre-poured gels with a 4-12% acryl amid gradient (NuPAGE® 4-12% Bis-Tris gels) were used. Both, sample processing and gel run were performed as described in the manual.

5.2.5.5 Western Blot

Proteins separated by SDS-PAGE (see above) were transferred to a PVDF or to a nitrocellulose membrane using a Trans-Blot SD Semi-Dry Transfer Cell (Bio-Rad). The gel and the PVDF membrane, pre-treated with methanol, were placed in the transfer cell between two piles of three blotting papers soaked with transfer buffer. In case of transfer to a nitrocellulose membrane, gel and membrane were pre-treated with transfer buffer. Transfer was performed for 1 h at 24 V. To control the blotting of the proteins before immunodetection (see below), the total protein content was reversibly stained with Ponceau S by incubating the membrane in Poinceau staining solution for 2 min and subsequent destaining with water until the protein bands were visible.

5.2.5.6 Immuno detection of transferred proteins

To avoid unspecific binding of the antibodies, the membrane was blocked with non-related proteins from bovine milk prior to specific immunodetection of proteins by incubating the membrane in 5% (w/v) milk powder in 1x PBST on a shaker for 30 min - 1 h at RT or overnight at 4°C. The antibodies were diluted to an adequate working concentration (section 5.1.6) in 1% (w/v) milk powder in 1x PBST. Incubations were performed in 50 ml tubes on a turning wheel for 1 h (primary antibodies) or 30 min (secondary antibodies) at RT. After each antibody incubation step, the membrane was washed in 1x PBST for three times 10 min on a shaker. In order to detect the specifically bound antibodies, the membrane was incubated for ~1 min at RT with 1 ml BM Chemiluminescence Blotting Substrate (POD; Roche) which was prepared according to the instructions of the manufacturer. This reagent contains hydrogen peroxide and luminal, which is a substrate for the horseradish peroxidase conjugated to the secondary antibodies. The light, which is emitted during this reaction at the corresponding specific positions on the membrane, was detected with a LAS-3000 chemiluminescence imager using Image Reader LAS-3000 V2.2 followed by quantitative analysis using Multi Gauge V3.0 (Fujifilm). A luminsecent marker (Glow writer) was used to label the positions of lanes and/or bands of the protein marker on the gel.

5.2.5.7 Coomassie staining of proteins

Polyacrylamide gels were normally stained with Coomassie Brilliant Blue R-250 in order to visualize the total protein content. Briefly, the gel was incubated in the Coomassie staining solution for 1 h on a shaker at RT. Destaining was performed by incubating the gel in destaining solution or water 3-4x for 30 min until protein bands showed up significantly over the background staining. Optionally, the gel was dried in a vacuum gel dryer system for 2 h at 80°C or bands were excised for subsequent protein identification using mass spectrometry. In case the amounts of the proteins of interest were limiting, the quality of the staining could be increased by using a commercially available “SimplyBlue™ SafeStain” solution (Invitrogen). In this case, pre-poured gradient gels (NuPAGE® 4-12% Bis-Tris – see 5.2.5.4) were normally used to separate the sample. The detailed procedure of staining and de-staining was performed as written in the manual.

5.2.5.8 Silver staining of proteins

To stain polyacrylamide gels with low protein content, the more sensitive silver staining was preferred over the Coomassie staining. The proteins were fixed in the gel by incubation in fixation-solution (50 % (v/v) methanol, 12 % (v/v) acetic acid, 0.02 % (v/v) formaldehyde) for 1 h or over night (RT). Afterwards the gel was washed in 50 % (v/v) ethanol for 20 min and incubated in 0.8 mM $Na_2S_2O_3$ for 1 min, directly followed by three 20 seconds wash steps with water. Next, the gel was incubated in staining-solution (12 mM $AgNO_3$, 0.03 % (v/v) formaldehyde) for 20 min and washed two times for 20 seconds with water. The stained protein bands became visible upon incubation with developing solution (566 mM Na_2CO_3,

0.02 % (v/v) formaldehyde, 0.016 mM $Na_2S_2O_3$). The development was stopped with 1 % acetic acid.

5.2.6 Affinity purification of RNPs via epitope tagged fusion proteins

5.2.6.1 Affinity purification of (pre-) rRNPs using IgG coupled magnetic beads

TAP-tagged LSU biogenesis factors and associated preribosomal particles were purified from total cellular extracts in one step using rabbit IgG coupled to magnetic beads (basically as described in Ohmayer et al., 2013). A cell pellet corresponding to 1 l yeast culture with OD600 = 0.8-1.2 was resuspended in 1.5 ml of cold A200/300 buffer (20 mM Tris HCl pH 8, either 200 mM or 300mM KCl, 5 mM MgOAc, 2 mM Benzamidine, 1 mM PMSF, and 0.04 U/mL RNasin) per g of cell pellet; 0.8 mL of this cell suspension was added to 1.4 ml glass beads (Ø 0.75–1 mm) and divided into 2-ml reaction tubes. A cell lysate was prepared by vigorous shaking of the cell suspension in an IKA-Vibrax VXR shaker at 4°C for 15 min, followed by 2 min on ice. This procedure was repeated twice. The cell lysate was cleared from cell debris by two centrifugation steps, once for 5 minutes at 14,000 rpm and once for 10 minutes at 14,000 rpm in a table top centrifuge at 4°C. The protein concentration of the cleared lysate was determined using the Bradford assay (see 5.2.5.1). Triton X-100 and Tween 20 were added to the cell lysate to final concentrations of 0.5% (w/v) and 0.1% (w/v), respectively (= buffer A200 +T/T). One percent (v/v) of the lysate were taken for Western and Northern blotting analyses, respectively (“Input” samples). Equal amounts of cell lysate (typically 1 ml with 20–50 mg of total protein) were incubated for 1 h at 4°C with 200 µl of an IgG (rabbit serum, I5006-100MG, Sigma)-coupled magnetic beads slurry (1 mm BcMag, FC-102, Bioclone) equilibrated in MB buffer containing 0.5% Triton X-100 and 0.1% Tween. The beads were washed four times with 1 ml cold buffer A200 +T/T. Twenty percent of the suspension was taken for RNA analyses by Northern blotting. The remaining part of the suspension was washed two times with 1 ml AC buffer (100 mM NH_4OAc pH 7.4, 0.1 mM $MgCl_2$) to remove remaining salt from the sample. Bound proteins were eluted two times with 500 µl of freshly prepared 500 mM NH_4OH solution for 20 min at RT. After both eluate fractions were pooled, 100µl (10%) were taken for SDS-PAGE and/or Western analyses. Both, samples (the 90% and 10% aliquots) were lyophilized overnight, stored at -20°C or immediatelly further processed either for semi quantitative mass spectrometric protein analyses as described below (5.2.7), or dissolved in appropriate buffer to perform SDS PAGE (see 5.2.5.4).

5.2.6.2 Affinity purification of (pre-) rRNPs using anti-FLAG antibody coupled sepharose beads

FLAG tagged rpS26 (Figures 18-20) or one of the 16 FLAG tagged LSU r-proteins (Figures 21, 22, ad 36) were purified from total cellular extracts in one step using anti-FLAG coupled sepharose beads (as described in Ohmayer et al., 2013). The cellular extracts corresponding to 250 ml yeast culture with OD600 = 0.8-1.2 were produced as described above (5.2.6.1) using the same buffers (A200/300 containing 200 or 300 mM KCl as indicated in the Figure legends). Equal amounts of cell lysate (typically 0.5 ml with 20–50 mg of total protein) were

incubated for 1 h at 4°C with 100 µl of anti FLAG-coupled M2 beads (Sigma) equilibrated in buffer A200/300 +T/T (containing 0.5% Triton X-100 and 0.1% Tween). Washing and elution of rpS26-FLAG and associated (pre-) rRNPs for further analyses by semi-quantitative mass spectrometry was performed as described above (5.2.6.1). Total RNA of the (pre-) rRNPs co-purified via the FLAG-tagged LSU r-proteins was extracted by hot acidic phenol-chloroform treatment (5.2.4.1).

5.2.7 Processing of protein samples for quantitative MS

5.2.7.1 Reduction of disulfide bonds and blocking of cystein residues

The whole iTRAQ label procedure was done as described in the manual of the iTRAQ™ labeling kit (Invitrogen) with minor modifications. The lyophilised protein samples were resuspended in 20 µl dissolution buffer (iTRAQ™ labelling kit, Invitrogen) and reduced with 2µl reducing reagent (5 mM Tris-(2-carboxyethyl)phosphine) at 60°C for 1 h. Reduced cysteins residues were blocked with 1µl “blocking reagent” (10 mM methyl-methanethiosulfonate (MMTS)) at room temperature for 10 min. The 1.5 ml micro-reaction tubes were from the Eppendorf company (“safe lock tubes”) to avoid potential contamination of the plastic material.

5.2.7.2 Trypsin digest

Up to four reduced and blocked samples (see above) that were aimed to be compared to each other were incubated with one batch containing 25 µg of Trypsin (sequencing grad – Roche). To this end, the trypsin was thoroughly dissolved with varying amounts of water (20-40µl) to add 10µl of the trypsin solution to each sample. After careful mixing and brief centrifugation the sample was incubated at 37°C for 16-20 h.

5.2.7.3 iTRAQ label procedure

After the trypsin digest, each sample was centrifuged again (13000 rpm, 1 min, RT). The up to four individual iTRAQ reagents (with reporter groups of 114-117 Da) were allowed to achieve RT. The content of each label was mixed with 70µl Ethanol and added to one of the up to four samples and incubated for 1 h at RT. Afterwards, the individually labeled samples that should be compared to each other were fused in a fresh 1.5ml orig. Eppendorf tube. To remove the solvent it was put into a speed-vac evaporator. The sample was stored at -20°C or further processed for the nano-HPLC run as described below.

5.2.7.4 preparation for HPLC

The fused iTRAQ labeled samples were thoroughly resuspended in 0.1% TFA and incubated at 30°C for 30-60 min. To remove undissolved material it was centrifuged in a table top centrifuge for 10 min at 13000 rpm (RT). The supernatant was transferred to an appropriate tube which is compatible with the nano HPLC device.

5.2.7.5 HPLC run

The separation of the iTRAQ labeled tryptic peptides was done on a Ultimate 3000 nano HPLC device from LC Packings (Dionex). Half of the sample (15µl) were injected with a draw speed of 100 nl/sec. Loading occurred with a loading pump flow of 20 µl/min. After loading onto the pre-column (Ø 300µm x 5mm; C18 PepMap100, 5µm particle size, 100Å pore size (P/N 160454) Thermo Scientific) the sample was eluted to the main column (C18-Pep-Mep column (LC-Packings or Thermo Fischer), Ø75µm x 150 mm; 3 µm particle size, 100Å pore size (P/N 164568))) a constant micro pump flow of 0.3-0.33 µl/min (depending on the column pressure which should be in a range of 100-130 bar) was started. A gradient of solution A (0.055% (v/v) TFA) and B (80% Acetronitril (v/v) and 0.05% (v/v) TFA) was run as followed: 0–12 min from 5% solution B to 15% solution B; 12-95 min from 15% solution B to 37% solution B; 95-143 min from 37% solution B to 62% solution B; 143-155 min from 62% solution B to 95% solution B; 155-168 min constantly 95% solution B; 168-173 min from 95% solution B to 5% solution B; 173-180 min constantly 5% solution B. In order to control and follow the performance of the nano HPLC device several parameters were recorded: UV absorbance at 214nm; loading pump pressure, and micro pump pressure. The signal to the spotting device (Probot) to start was given between 35 and 45 min after loading the sample depending on the UV chromatogram. The machine was operated with the chromelion software.

5.2.7.6 Mix with MALDI matrix and automatized spotting on sample plate

To constantly mix the material eluting from the nano HPLC with the MALDI matrix material and to “spot” this mixture on each of the 384 spots of the sample carrier for the mass spectrometer, the “Probot” device (LC packing / Dionex) was used. 5x the volume eluting from the column of Matrix solution (70% (v/v) Acetonitrile, 0.1% (vv) TFA, and 2,5 mg/ml CHCA = α-cyano-4-hydroxy cinnamic acid) was added to the elution via a syringe pump. This mixture was spotted for 20 sec on each of the 384 (381) spots resulting in 127 min total spotting time.
After the run, 0.6 µl of the peptide calibration mix (a 1/20 dilution of the 6 peptide mixture (P/N 4368762 – AB Sciex) in matrix solution (see above)) was spotted on each of the 13 calibration spots distributed over the whole sample plate. The sample plates could be stored in a dry room at 16°C for up to 4 weeks.

5.2.8 Quantitative mass spectrometry procedure and data base search

5.2.8.1 Chosen MS and MS/MS settings

All MS analyses were performed on an Applied Biosystems 4800 Proteomics Analyzer MALDI-TOF/TOF mass spectrometer operated in positive ion reflector mode. The m/z range was between 800-4000 Da (m/z) with a focus mass of 2000 Da (m/z). In the “MS mode” 50 sub-spectra were recorded for each of the 384 spots with 37 shots per sub-spectrum. The laser intensity was adapted before each run in order to achieve an average peak intensity of 10^3 - 10^4. The sample plate was moved before every sub-spectrum in a “random uniform”

manner. Prior to each analysis, an internal calibration to a 6 peptide mix (P/N 4368762 – AB Sciex) was done with the following settings: S/N ratio >20; Flag monoisomeric peak; adduct: H; mass tolerance 0.5 m/z; ≥ 5 of the 6 peptides had to match; max. outlier error: 10ppm; min peak width at full width half maximum (FWHM) 2.9 (bins); local noise window width: 250 m/z. Subsequently performed MS and MS/MS modes were based on this calibration.

After the “MS run” (without fragmentation) of each of the 384 spots, all obtained spectra were subjected to an “interpretation” in which the most appropriate ions were selected for fragmentation in the MS/MS mode. All tryptic peptides derived from trypsin itself were excluded for further fragmentation. The “minimum chromatogram peak width was set to 1 with a fraction to fraction mass tolerance of 200 ppm and a minimum S/N ratio of 10. Precursors of one spot within a resolution of 200 were excluded. For each spot, up to 11 precursors were selected for fragmentation. The strongest precursor ions were first fragmented.

The MS/MS run was done in an “MS-MS-1kV-positive” operating mode. The fragmentation of the precursor ions occurred via collision induced dissociation (CID). The “metastable suppressor” setting was switched “on”. Again, the sample plate was moved before every sub-spectrum. For each selected fragment ion, 50 shots per sub-spectrum added up to a total of 2750 sub-spectra which were added up. The laser intensity for the MS/MS mode was adapted before the run (and was typically 30% higher than the laser intensity chosen for the MS mode).

5.2.8.2 Data base searches and settings for iTRAQ quantification

The NCBInr protein sequence database with the Mascot search engine (Matrix Science) implemented in the GPS Explorer software (V.3.6, Applied Biosystems) was used to solve the identity of the peptides and to quantify the respective ratios of the iTRAQ reporter ions. Prior to the database search, the MS/MS spectra had to be filtered with the following settings: mass range: 50 Da – 20 Da below precursor mass; minimum S/N filter: 5; mass exclusion tolerance: 3 Da; mass exclusion list: 115.5 Da; peak density filter: 50 peaks per 200 Da; max. Number of peaks: 80.

The search was restricted to proteins from *S.cerevisiae.* Three modifications of the tryptic peptides were set as fixed: to N-terminus of each peptide and ε-amino group of each lysine residue iTRAQ was added (+145 Da); to cysteine residues MMTS (Methyl methanethiosulfonate) was added. Oxidation of methionine residues (methioninsulfoxid) was set as variable modification (+16 Da). The maximum number of missed trypsin cleavages was set to 1. Further settings: MS/MS fragment tolerance mass: 0.2 Da (monoisotopic); precursor tolerance: 150 ppm; peptide charges: +1; maximum peptide ranks: 2. The total ion score, given as confidence interval (C.I. score) had to be at least 95%.

For the quantification of the reporter ion peaks a fragment tolerance of 0.1 Da was defined. The correction factors for the iTRAQ reagents which are given in each kit (iTRAQ® Reagent multiplex kit) were taken into account by the GPS explorer software during the calculation. They are normally very constant (typically as shown in table below).

iTRAQ label	% -2 Da	% -1 Da	% +- 0Da	% +1 Da	% +2 Da
114	0	1	92.9	5.9	0.2
115	0	2	92.3	5.6	0.1
116	0	3	92.4	4.5	0.1
117	0.1	4	92.4	3.5	0

5.2.9 Processing, analysis and visualization of the MS raw data

5.2.9.1 Normalization

All obtained average iTRAQ ratios were transformed and expressed in a log2 scale to weight ratios below and above 1 in an equivalent way. The normalization of the log2 transformed iTRAQ ratios occurred via two different ways. In case the chosen bait protein for both affinity purified samples that were compared to each other were the same, the average iTRAQ ratio of this bait protein was set to one (thus after log2 transformation to zero). In case different bait proteins were different (as done in the comparative analyses of “wild type-like particles” – see Figures 19-20) the log2 transformed iTRAQ ratio of the median protein (within the group of proteins of interest – e.g. LSU r-proteins or LSU biogenesis factors) was set to zero. In this case, the normalization was done with the cluster 3.0 software (see below) using the setting “median center arrays”.

5.2.9.2 Hierarchical cluster analyses

Hierarchical cluster analyses to compute the similarity (or difference) in regard to each other of both, the pair wise comparisons themselves or the (log2 transformed and normalized) iTRAQ ratios of the group of proteins of interest was done using the software “cluster 3.0” which was developed for gene expression analyses (mRNA micro arrays) (Eisen et al., 1998). The distance matrices of the data shown in the dendrograms in Figures 19 and 20 were calculated by the “City block distance” method and hierarchical clustering analyses were done with the “centroid linkage” algorithm for both comparison of similarities between the different datasets and of the behavior of proteins in the various experiments.

5.2.9.3 Visualization of MS data

Cluster visualization (tree and heat map) was done with Java Treeview (see http://www.eisenlab.org/eisen/?page_id=42). The heat maps and the corresponding dendrograms were exported with the Java Treeview software to “postscript”. The resulting

postscript files (.ps) were further processed for better visualization using the Adobe illustrator CS3 software.

5.2.10 Other methods

5.2.10.1 Preparation of IgG coupled to magnetic beads

One batch of the magnetic beads (Bioclone BcMag Epoxy-Activated Magnetic Beads No. Fc102 1µm, 300mg, $1,7x10^8$ beads Ø1 µm) was resuspended in 50% Acetone to achieve a concentration of 30 mg/ml (300 mg in 10 ml) and vigorously vortexed. The supernatant was removed after placing the tube in the magnetic separator. The beads were next washed four times in the tube bottle with 10 ml 0.1M NaPO4 pH 8.5 (and vortexed for 30 sec in each wash step). The beads were transferred in 4 ml 0,1M NaPO4, pH 8.5, to a 50 ml falcon tube and gently shook for 10 min at RT. In the mean time the antibody mix (AB mix) was prepared as followed: 100 mg rabbit IgGs (SIGMA I5006-100MG) were resuspended in the plastic bottle with 7 ml water (to achieve a concentration of 14 mg/ml). The AB mix was filled in 1.5ml micro reaction tubes and centrifuged on a table top centrifuge for 10 min at 13000 rpm and 4°C. The supernatants were collected in one falcon tube and 10 ml 0,1M NaPO4, pH 8.5 were added. Next, 6.65 ml 3M Ammoniumsulfat were slowly added under gentle mixing. Final impurities were removed by centrifugation at 2000 rpm for 3 min at RT. The falcon tube with the magnetic beads was washed once again with 20 ml 0,1M NaPO4, pH 8.5 before the AB mix added. This mix was incubated at 25°C in a rotating wheel for 18 -48 h, the coupling reaction occurs during that time. The coupled beads were next washed with several solutions in a 50 ml falcon tube, the washing solution were removed as fast as possible. A first wash step with 20 ml 100mM Glycin HCl, pH 2.5 was followed by a washing step with 20 ml 10 mM Tris pH 8.8. The next washing step with 20 ml freshly prepared Triethylamine solution was followed by 4 wash steps with 20 ml 1x PBS at RT for 5 min on a rotating wheel. Finally the beads were washed twice with 1x PBS supplemented with 0.5% (v/v) Trition X-100 for 5 and 15 minutes, respectively. Before making 1 ml aliquots the beads were carefully resuspended in 16 ml 1x PBS with 0.02% Natriumazid (NaN3) to avoid growth of microorganisms. The aliquots were stored at 4°C and remained in good quality for at least one year.

6 References

Adams, C.C., Jakovljevic, J., Roman, J., Harnpicharnchai, P., and Woolford, J.L., Jr (2002). Saccharomyces cerevisiae nucleolar protein Nop7p is necessary for biogenesis of 60S ribosomal subunits. RNA *8*, 150–165.

Adilakshmi, T., Bellur, D.L., and Woodson, S.A. (2008). Concurrent nucleation of 16S folding and induced fit in 30S ribosome assembly. Nature *455*, 1268–1272.

Agalarov, S.C., Zheleznyakova, E.N., Selivanova, O.M., Zheleznaya, L.A., Matvienko, N.I., Vasiliev, V.D., and Spirin, A.S. (1998). In vitro assembly of a ribonucleoprotein particle corresponding to the platform domain of the 30S ribosomal subunit. Proc. Natl. Acad. Sci. U.S.A. *95*, 999–1003.

Agalarov, S.C., Selivanova, O.M., Zheleznyakova, E.N., Zheleznaya, L.A., Matvienko, N.I., and Spirin, A.S. (1999). Independent in vitro assembly of all three major morphological parts of the 30S ribosomal subunit of Thermus thermophilus. Eur. J. Biochem. *266*, 533–537.

Agashe, V.R., and Hartl, F.U. (2000). Roles of molecular chaperones in cytoplasmic protein folding. Semin. Cell Dev. Biol. *11*, 15–25.

Akanuma, G., Nanamiya, H., Natori, Y., Yano, K., Suzuki, S., Omata, S., Ishizuka, M., Sekine, Y., and Kawamura, F. (2012). Inactivation of Ribosomal Protein Genes in Bacillus subtilis Reveals Importance of Each Ribosomal Protein for Cell Proliferation and Cell Differentiation. J. Bacteriol. *194*, 6282–6291.

Alix, J.-H., and Nierhaus, K.H. (2003). DnaK-facilitated ribosome assembly in Escherichia coli revisited. RNA *9*, 787–793.

Allmang, C., and Tollervey, D. (1998). The role of the 3' external transcribed spacer in yeast pre-rRNA processing. J. Mol. Biol. *278*, 67–78.

Allmang, C., Mitchell, P., Petfalski, E., and Tollervey, D. (2000). Degradation of ribosomal RNA precursors by the exosome. Nucleic Acids Res. *28*, 1684–1691.

Altvater, M., Chang, Y., Melnik, A., Occhipinti, L., Schütz, S., Rothenbusch, U., Picotti, P., and Panse, V.G. (2012). Targeted proteomics reveals compositional dynamics of 60S pre-ribosomes after nuclear export. Mol. Syst. Biol. *8*, 628.

Amberg, D.C., and Cold Spring Harbor Laboratory (2005). Methods in yeast genetics: a Cold Spring Harbor Laboratory course manual (Cold Spring Harbor, N.Y: Cold Spring Harbor Laboratory Press).

Anger, A.M., Armache, J.-P., Berninghausen, O., Habeck, M., Subklewe, M., Wilson, D.N., and Beckmann, R. (2013). Structures of the human and Drosophila 80S ribosome. Nature *497*, 80–85.

Auger-Buendia, M.A., Longuet, M., and Tavitian, A. (1979). Kinetic studies on ribosomal proteins assembly in preribosomal particles and ribosomal subunits of mammalian cells. Biochim. Biophys. Acta *563*, 113–128.

Babiano, R., and de la Cruz, J. (2010). Ribosomal protein L35 is required for 27SB pre-rRNA processing in Saccharomyces cerevisiae. Nucleic Acids Res. *38*, 5177–5192.

Babiano, R., Gamalinda, M., Woolford, J.L., Jr, and de la Cruz, J. (2012). Saccharomyces cerevisiae ribosomal protein L26 is not essential for ribosome assembly and function. Molecular and Cellular Biology.

Babiano, R., Badis, G., Saveanu, C., Namane, A., Doyen, A., Díaz-Quintana, A., Jacquier, A., Fromont-Racine, M., and de la Cruz, J. (2013). Yeast ribosomal protein L7 and its homologue Rlp7 are simultaneously present at distinct sites on pre-60S ribosomal particles. Nucleic Acids Res.

Ball, S. (2011). Diamond Blackfan anemia. Hematology Am Soc Hematol Educ Program *2011*, 487–491.

Ballesta, J.P., and Remacha, M. (1996). The large ribosomal subunit stalk as a regulatory element of the eukaryotic translational machinery. Prog. Nucleic Acid Res. Mol. Biol. *55*, 157–193.

Ban, N., Nissen, P., Hansen, J., Moore, P.B., and Steitz, T.A. (2000). The complete atomic structure of the large ribosomal subunit at 2.4 A resolution. Science *289*, 905–920.

Baronas-Lowell, D.M., and Warner, J.R. (1990). Ribosomal protein L30 is dispensable in the yeast Saccharomyces cerevisiae. Mol. Cell. Biol. *10*, 5235–5243.

Bassler, J., Grandi, P., Gadal, O., Lessmann, T., Petfalski, E., Tollervey, D., Lechner, J., and Hurt, E. (2001). Identification of a 60S preribosomal particle that is closely linked to nuclear export. Mol. Cell *8*, 517–529.

Bassler, J., Kallas, M., Pertschy, B., Ulbrich, C., Thoms, M., and Hurt, E. (2010). The AAA-ATPase Rea1 drives removal of biogenesis factors during multiple stages of 60S ribosome assembly. Mol. Cell *38*, 712–721.

Baßler, J., Klein, I., Schmidt, C., Kallas, M., Thomson, E., Wagner, M.A., Bradatsch, B., Rechberger, G., Strohmaier, H., Hurt, E., et al. (2012). The conserved Bud20 zinc finger protein is a new component of the ribosomal 60S subunit export machinery. Mol. Cell. Biol.

Basu, U., Si, K., Warner, J.R., and Maitra, U. (2001). The Saccharomyces cerevisiae TIF6 gene encoding translation initiation factor 6 is required for 60S ribosomal subunit biogenesis. Mol. Cell. Biol. *21*, 1453–1462.

Baxter-Roshek, J.L., Petrov, A.N., and Dinman, J.D. (2007). Optimization of ribosome structure and function by rRNA base modification. PLoS ONE *2*, e174.

Benelli, D., and Londei, P. (2009). Begin at the beginning: evolution of translational initiation. Res. Microbiol. *160*, 493–501.

Bernstein, K.A., Gallagher, J.E.G., Mitchell, B.M., Granneman, S., and Baserga, S.J. (2004). The small-subunit processome is a ribosome assembly intermediate. Eukaryotic Cell *3*, 1619–1626.

Blattner, C., Jennebach, S., Herzog, F., Mayer, A., Cheung, A.C.M., Witte, G., Lorenzen, K., Hopfner, K.-P., Heck, A.J.R., Aebersold, R., et al. (2011). Molecular basis of Rrn3-regulated RNA polymerase I initiation and cell growth. Genes Dev. *25*, 2093–2105.

Bradatsch, B., Katahira, J., Kowalinski, E., Bange, G., Yao, W., Sekimoto, T., Baumgärtel, V., Boese, G., Bassler, J., Wild, K., et al. (2007). Arx1 functions as an unorthodox nuclear export receptor for the 60S preribosomal subunit. Mol. Cell *27*, 767–779.

Bradatsch, B., Leidig, C., Granneman, S., Gnädig, M., Tollervey, D., Böttcher, B., Beckmann, R., and Hurt, E. (2012). Structure of the pre-60S ribosomal subunit with nuclear export factor Arx1 bound at the exit tunnel. Nat. Struct. Mol. Biol.

Bradford, M.M. (1976). A rapid and sensitive method for the quantitation of microgram quantities of protein utilizing the principle of protein-dye binding. Anal. Biochem. *72*, 248–254.

Brand, R.C., Klootwijk, J., Van Steenbergen, T.J., De Kok, A.J., and Planta, R.J. (1977). Secondary methylation of yeast ribosomal precursor RNA. Eur. J. Biochem. *75*, 311–318.

Briggs, M.W., Burkard, K.T., and Butler, J.S. (1998). Rrp6p, the yeast homologue of the human PM-Scl 100-kDa autoantigen, is essential for efficient 5.8 S rRNA 3' end formation. J. Biol. Chem. *273*, 13255–13263.

Brodersen, D.E., and Nissen, P. (2005). The social life of ribosomal proteins. FEBS J. *272*, 2098–2108.

Bubunenko, M., Korepanov, A., Court, D.L., Jagannathan, I., Dickinson, D., Chaudhuri, B.R., Garber, M.B., and Culver, G.M. (2006). 30S ribosomal subunits can be assembled in vivo without primary binding ribosomal protein S15. RNA *12*, 1229–1239.

Buhler, J.M., Huet, J., Davies, K.E., Sentenac, A., and Fromageot, P. (1980). Immunological studies of yeast nuclear RNA polymerases at the subunit level. J. Biol. Chem. *255*, 9949–9954.

Bunner, A.E., Nord, S., Wikström, P.M., and Williamson, J.R. (2010). The effect of ribosome assembly cofactors on in vitro 30S subunit reconstitution. J. Mol. Biol. *398*, 1–7.

Burger, F., Daugeron, M.C., and Linder, P. (2000). Dbp10p, a putative RNA helicase from Saccharomyces cerevisiae, is required for ribosome biogenesis. Nucleic Acids Res. *28*, 2315–2323.

Burroughs, L., Woolfrey, A., and Shimamura, A. (2009). Shwachman-Diamond Syndrome: A Review of the Clinical Presentation, Molecular Pathogenesis, Diagnosis, and Treatment. Hematology/Oncology Clinics of North America *23*, 233–248.

Bussiere, C., Hashem, Y., Arora, S., Frank, J., and Johnson, A.W. (2012). Integrity of the P-site is probed during maturation of the 60S ribosomal subunit. J. Cell Biol. *197*, 747–759.

Campbell, M.G., and Karbstein, K. (2011). Protein-protein interactions within late pre-40S ribosomes. PLoS ONE *6*, e16194.

Chakraborty, A., Uechi, T., and Kenmochi, N. (2011). Guarding the “translation apparatus”: defective ribosome biogenesis and the p53 signaling pathway. Wiley Interdiscip Rev RNA *2*, 507–522.

Chandramouli, P., Topf, M., Ménétret, J.-F., Eswar, N., Cannone, J.J., Gutell, R.R., Sali, A., and Akey, C.W. (2008). Structure of the mammalian 80S ribosome at 8.7 A resolution. Structure *16*, 535–548.

Charette, M., and Gray, M.W. (2000). Pseudouridine in RNA: what, where, how, and why. IUBMB Life *49*, 341–351.

Chen, S.S., and Williamson, J.R. (2012). Characterization of the Ribosome Biogenesis Landscape in E. coli using Quantitative Mass Spectrometry. J. Mol. Biol.

Chen, S.S., Sperling, E., Silverman, J.M., Davis, J.H., and Williamson, J.R. (2012). Measuring the dynamics of E. coli ribosome biogenesis using pulse-labeling and quantitative mass spectrometry. Mol Biosyst *8*, 3325–3334.

Chooi, W.Y., and Leiby, K.R. (1981). An electron microscopic method for localization of ribosomal proteins during transcription of ribosomal DNA: a method for studying protein assembly. Proc. Natl. Acad. Sci. U.S.A. *78*, 4823–4827.

Chook, Y.M., and Süel, K.E. (2011). Nuclear import by karyopherin-βs: Recognition and inhibition. Biochimica et Biophysica Acta (BBA) - Molecular Cell Research *1813*, 1593–1606.

Chu, S., Archer, R.H., Zengel, J.M., and Lindahl, L. (1994). The RNA of RNase MRP is required for normal processing of ribosomal RNA. Proc. Natl. Acad. Sci. U.S.A. *91*, 659–663.

Clark, C.G., Tague, B.W., Ware, V.C., and Gerbi, S.A. (1984). Xenopus laevis 28S ribosomal RNA: a secondary structure model and its evolutionary and functional implications. Nucleic Acids Res. *12*, 6197–6220.

Clatterbuck Soper, S.F., Dator, R.P., Limbach, P.A., and Woodson, S.A. (2013). In vivo X-ray footprinting of pre-30S ribosomes reveals chaperone-dependent remodeling of late assembly intermediates. Mol. Cell *52*, 506–516.

De la Cruz, J., Kressler, D., Rojo, M., Tollervey, D., and Linder, P. (1998). Spb4p, an essential putative RNA helicase, is required for a late step in the assembly of 60S ribosomal subunits in Saccharomyces cerevisiae. RNA *4*, 1268–1281.

De la Cruz, J., Lacombe, T., Deloche, O., Linder, P., and Kressler, D. (2004). The putative RNA helicase Dbp6p functionally interacts with Rpl3p, Nop8p and the novel trans-acting Factor Rsa3p during biogenesis of 60S ribosomal subunits in Saccharomyces cerevisiae. Genetics *166*, 1687–1699.

De la Cruz, J., Sanz-Martínez, E., and Remacha, M. (2005). The essential WD-repeat protein Rsa4p is required for rRNA processing and intra-nuclear transport of 60S ribosomal subunits. Nucleic Acids Res. *33*, 5728–5739.

DeLabre, M.L., Kessl, J., Karamanou, S., and Trumpower, B.L. (2002). RPL29 codes for a non-essential protein of the 60S ribosomal subunit in Saccharomyces cerevisiae and exhibits synthetic lethality with mutations in genes for proteins required for subunit coupling. Biochim. Biophys. Acta *1574*, 255–261.

Dembowski, J.A., Kuo, B., and Woolford, J.L., Jr (2013a). Has1 regulates consecutive maturation and processing steps for assembly of 60S ribosomal subunits. Nucleic Acids Res.

Dembowski, J.A., Ramesh, M., McManus, C.J., and Woolford, J.L., Jr (2013b). Identification of the binding site of Rlp7 on assembling 60S ribosomal subunits in Saccharomyces cerevisiae. RNA.

Demoinet, E., Jacquier, A., Lutfalla, G., and Fromont-Racine, M. (2007). The Hsp40 chaperone Jjj1 is required for the nucleo-cytoplasmic recycling of preribosomal factors in Saccharomyces cerevisiae. RNA *13*, 1570–1581.

Deutschbauer, A.M., Jaramillo, D.F., Proctor, M., Kumm, J., Hillenmeyer, M.E., Davis, R.W., Nislow, C., and Giaever, G. (2005). Mechanisms of Haploinsufficiency Revealed by Genome-Wide Profiling in Yeast. Genetics *169*, 1915–1925.

Dez, C., Froment, C., Noaillac-Depeyre, J., Monsarrat, B., Caizergues-Ferrer, M., and Henry, Y. (2004). Npa1p, a component of very early pre-60S ribosomal particles, associates with a subset of small nucleolar RNPs required for peptidyl transferase center modification. Mol. Cell. Biol. *24*, 6324–6337.

Dick, F.A., Eisinger, D.P., and Trumpower, B.L. (1997). Exchangeability of Qsr1p, a large ribosomal subunit protein required for subunit joining, suggests a novel translational regulatory mechanism. FEBS Lett. *419*, 1–3.

Dohme, F., and Nierhaus, K.H. (1976). Total reconstitution and assembly of 50 S subunits from Escherichia coli Ribosomes in vitro. J. Mol. Biol. *107*, 585–599.

Dosil, M., and Bustelo, X.R. (2004). Functional characterization of Pwp2, a WD family protein essential for the assembly of the 90 S pre-ribosomal particle. J. Biol. Chem. *279*, 37385–37397.

Dragon, F., Gallagher, J.E.G., Compagnone-Post, P.A., Mitchell, B.M., Porwancher, K.A., Wehner, K.A., Wormsley, S., Settlage, R.E., Shabanowitz, J., Osheim, Y., et al. (2002). A large nucleolar U3 ribonucleoprotein required for 18S ribosomal RNA biogenesis. Nature *417*, 967–970.

Draptchinskaia, N., Gustavsson, P., Andersson, B., Pettersson, M., Willig, T.N., Dianzani, I., Ball, S., Tchernia, G., Klar, J., Matsson, H., et al. (1999). The gene encoding ribosomal protein S19 is mutated in Diamond-Blackfan anaemia. Nat. Genet. *21*, 169–175.

Drouin, G., and de Sá, M.M. (1995). The concerted evolution of 5S ribosomal genes linked to the repeat units of other multigene families. Mol. Biol. Evol. *12*, 481–493.

Dube, P., Wieske, M., Stark, H., Schatz, M., Stahl, J., Zemlin, F., Lutsch, G., and van Heel, M. (1998). The 80S rat liver ribosome at 25 A resolution by electron cryomicroscopy and angular reconstitution. Structure *6*, 389–399.

Dunbar, D.A., Dragon, F., Lee, S.J., and Baserga, S.J. (2000). A nucleolar protein related to ribosomal protein L7 is required for an early step in large ribosomal subunit biogenesis. Proc. Natl. Acad. Sci. U.S.A. *97*, 13027–13032.

Ebersberger, I., Simm, S., Leisegang, M.S., Schmitzberger, P., Mirus, O., Haeseler, A. von, Bohnsack, M.T., and Schleiff, E. (2013). The evolution of the ribosome biogenesis pathway from a yeast perspective. Nucl. Acids Res. gkt1137.

Egebjerg, J., Christiansen, J., and Garrett, R.A. (1991). Attachment sites of primary binding proteins L1, L2 and L23 on 23 S ribosomal RNA of Escherichia coli. J. Mol. Biol. *222*, 251–264.

Eisen, M.B., Spellman, P.T., Brown, P.O., and Botstein, D. (1998). Cluster analysis and display of genome-wide expression patterns. Proc. Natl. Acad. Sci. U.S.A. *95*, 14863–14868.

Engel, C., Sainsbury, S., Cheung, A.C., Kostrewa, D., and Cramer, P. (2013). RNA polymerase I structure and transcription regulation. Nature *502*, 650–655.

Faber, A.W., Van Dijk, M., Raué, H.A., and Vos, J.C. (2002). Ngl2p is a Ccr4p-like RNA nuclease essential for the final step in 3'-end processing of 5.8S rRNA in Saccharomyces cerevisiae. RNA *8*, 1095–1101.

Fang, F., Phillips, S., and Butler, J.S. (2005). Rat1p and Rai1p function with the nuclear exosome in the processing and degradation of rRNA precursors. RNA *11*, 1571–1578.

Fatica, A., Cronshaw, A.D., Dlakić, M., and Tollervey, D. (2002). Ssf1p prevents premature processing of an early pre-60S ribosomal particle. Mol. Cell *9*, 341–351.

Fatica, A., Oeffinger, M., Dlakić, M., and Tollervey, D. (2003a). Nob1p is required for cleavage of the 3' end of 18S rRNA. Mol. Cell. Biol. *23*, 1798–1807.

Fatica, A., Oeffinger, M., Tollervey, D., and Bozzoni, I. (2003b). Cic1p/Nsa3p is required for synthesis and nuclear export of 60S ribosomal subunits. RNA *9*, 1431–1436.

Fedyukina, D.V., and Cavagnero, S. (2011). Protein folding at the exit tunnel. Annu Rev Biophys *40*, 337–359.

Fernandez-Pevida, A., Rodriguez-Galan, O., Diaz-Quintana, A., Kressler, D., and de la Cruz, J. (2012). Yeast ribosomal protein L40 assembles late into pre-60S ribosomes and is required for their cytoplasmic maturation. J. Biol. Chem.

Fernández-Tornero, C., Moreno-Morcillo, M., Rashid, U.J., Taylor, N.M.I., Ruiz, F.M., Gruene, T., Legrand, P., Steuerwald, U., and Müller, C.W. (2013). Crystal structure of the 14-subunit RNA polymerase I. Nature *502*, 644–649.

Ferreira-Cerca, S., Pöll, G., Gleizes, P.-E., Tschochner, H., and Milkereit, P. (2005). Roles of eukaryotic ribosomal proteins in maturation and transport of pre-18S rRNA and ribosome function. Mol. Cell *20*, 263–275.

Ferreira-Cerca, S., Pöll, G., Kühn, H., Neueder, A., Jakob, S., Tschochner, H., and Milkereit, P. (2007). Analysis of the in vivo assembly pathway of eukaryotic 40S ribosomal proteins. Mol. Cell *28*, 446–457.

Finch, A.J., Hilcenko, C., Basse, N., Drynan, L.F., Goyenechea, B., Menne, T.F., Fernández, Á.G., Simpson, P., D'Santos, C.S., Arends, M.J., et al. (2011). Uncoupling of GTP hydrolysis from eIF6 release on the ribosome causes Shwachman-Diamond syndrome. Genes Dev. *25*, 917–929.

Fox, G.E., and Woese, C.R. (1975). 5S RNA secondary structure. Nature *256*, 505–507.

Francisco-Velilla, R., Remacha, M., and Ballesta, J.P.G. (2013). Carboxy terminal modifications of the P0 protein reveal alternative mechanisms of nuclear ribosomal stalk assembly. Nucleic Acids Res. *41*, 8628–8636.

Freed, E.F., Bleichert, F., Dutca, L.M., and Baserga, S.J. (2010). When ribosomes go bad: diseases of ribosome biogenesis. Mol Biosyst *6*, 481–493.

French, S.L., Osheim, Y.N., Cioci, F., Nomura, M., and Beyer, A.L. (2003). In exponentially growing Saccharomyces cerevisiae cells, rRNA synthesis is determined by the summed RNA polymerase I loading rate rather than by the number of active genes. Mol. Cell. Biol. *23*, 1558–1568.

Frey, S., Richter, R.P., and Görlich, D. (2006). FG-rich repeats of nuclear pore proteins form a three-dimensional meshwork with hydrogel-like properties. Science *314*, 815–817.

Fromont-Racine, M., Senger, B., Saveanu, C., and Fasiolo, F. (2003). Ribosome assembly in eukaryotes. Gene *313*, 17–42.

Gadal, O., Strauss, D., Kessl, J., Trumpower, B., Tollervey, D., and Hurt, E. (2001). Nuclear export of 60s ribosomal subunits depends on Xpo1p and requires a nuclear export sequence-containing factor, Nmd3p, that associates with the large subunit protein Rpl10p. Mol. Cell. Biol. *21*, 3405–3415.

Galani, K., Nissan, T.A., Petfalski, E., Tollervey, D., and Hurt, E. (2004). Rea1, a dynein-related nuclear AAA-ATPase, is involved in late rRNA processing and nuclear export of 60 S subunits. J. Biol. Chem. *279*, 55411–55418.

Gallagher, J.E.G., Dunbar, D.A., Granneman, S., Mitchell, B.M., Osheim, Y., Beyer, A.L., and Baserga, S.J. (2004). RNA polymerase I transcription and pre-rRNA processing are linked by specific SSU processome components. Genes Dev. *18*, 2506–2517.

Gamalinda, M., Jakovljevic, J., Babiano, R., Talkish, J., de la Cruz, J., and Woolford, J.L., Jr (2013). Yeast polypeptide exit tunnel ribosomal proteins L17, L35 and L37 are necessary to recruit late-assembling factors required for 27SB pre-rRNA processing. Nucleic Acids Res. *41*, 1965–1983.

Gamalinda, M., Ohmayer, U., Jakovljevic, J., Kumcuoglu, B., Woolford, J., Mbom, B., Lin, L., and Woolford, J.L. (2014). A hierarchical model for assembly of eukaryotic 60S ribosomal subunit domains. Genes Dev. *28*, 198–210.

García-Gómez, J.J., Lebaron, S., Froment, C., Monsarrat, B., Henry, Y., and de la Cruz, J. (2011). Dynamics of the putative RNA helicase Spb4 during ribosome assembly in Saccharomyces cerevisiae. Mol. Cell. Biol. *31*, 4156–4164.

Gartmann, M., Blau, M., Armache, J.-P., Mielke, T., Topf, M., and Beckmann, R. (2010). Mechanism of eIF6-mediated inhibition of ribosomal subunit joining. J. Biol. Chem. *285*, 14848–14851.

Gautier, T., Bergès, T., Tollervey, D., and Hurt, E. (1997). Nucleolar KKE/D repeat proteins Nop56p and Nop58p interact with Nop1p and are required for ribosome biogenesis. Mol. Cell. Biol. *17*, 7088–7098.

Geerlings, T.H., Vos, J.C., and Raué, H.A. (2000). The final step in the formation of 25S rRNA in Saccharomyces cerevisiae is performed by 5'-->3' exonucleases. RNA *6*, 1698–1703.

Gerbi, S.A. (1986). The evolution of eukaryotic ribosomal DNA. BioSystems *19*, 247–258.

Giaever, G., Chu, A.M., Ni, L., Connelly, C., Riles, L., Véronneau, S., Dow, S., Lucau-Danila, A., Anderson, K., André, B., et al. (2002). Functional profiling of the Saccharomyces cerevisiae genome. Nature *418*, 387–391.

Gilbert, W.V. (2011). Functional specialization of ribosomes? Trends Biochem. Sci. *36*, 127–132.

Golomb, L., and Oren, M. (2011). DePICTing p53 activation: a new nucleolar link to cancer. Cancer Cell *20*, 283–284.

Görlich, D., and Kutay, U. (1999). Transport between the cell nucleus and the cytoplasm. Annu. Rev. Cell Dev. Biol. *15*, 607–660.

Granato, D.C., Gonzales, F.A., Luz, J.S., Cassiola, F., Machado-Santelli, G.M., and Oliveira, C.C. (2005). Nop53p, an essential nucleolar protein that interacts with Nop17p and Nip7p, is required for pre-rRNA processing in Saccharomyces cerevisiae. FEBS J. *272*, 4450–4463.

Granato, D.C., Machado-Santelli, G.M., and Oliveira, C.C. (2008). Nop53p interacts with 5.8S rRNA co-transcriptionally, and regulates processing of pre-rRNA by the exosome. FEBS J. *275*, 4164–4178.

Grandi, P., Rybin, V., Bassler, J., Petfalski, E., Strauss, D., Marzioch, M., Schäfer, T., Kuster, B., Tschochner, H., Tollervey, D., et al. (2002). 90S pre-ribosomes include the 35S pre-rRNA, the U3 snoRNP, and 40S subunit processing factors but predominantly lack 60S synthesis factors. Mol. Cell *10*, 105–115.

Granneman, S., and Baserga, S.J. (2005). Crosstalk in gene expression: coupling and co-regulation of rDNA transcription, pre-ribosome assembly and pre-rRNA processing. Curr. Opin. Cell Biol. *17*, 281–286.

Granneman, S., Gallagher, J.E.G., Vogelzangs, J., Horstman, W., van Venrooij, W.J., Baserga, S.J., and Pruijn, G.J.M. (2003). The human Imp3 and Imp4 proteins form a ternary complex with hMpp10, which only interacts with the U3 snoRNA in 60-80S ribonucleoprotein complexes. Nucleic Acids Res. *31*, 1877–1887.

Granneman, S., Kudla, G., Petfalski, E., and Tollervey, D. (2009). Identification of protein binding sites on U3 snoRNA and pre-rRNA by UV cross-linking and high-throughput analysis of cDNAs. Proc. Natl. Acad. Sci. U.S.A. *106*, 9613–9618.

Granneman, S., Petfalski, E., Swiatkowska, A., and Tollervey, D. (2010). Cracking pre-40S ribosomal subunit structure by systematic analyses of RNA-protein cross-linking. EMBO J. *29*, 2026–2036.

Granneman, S., Petfalski, E., and Tollervey, D. (2011). A cluster of ribosome synthesis factors regulate pre-rRNA folding and 5.8S rRNA maturation by the Rat1 exonuclease. EMBO J. *30*, 4006–4019.

Greber, B.J., Boehringer, D., Montellese, C., and Ban, N. (2012). Cryo-EM structures of Arx1 and maturation factors Rei1 and Jjj1 bound to the 60S ribosomal subunit. Nat. Struct. Mol. Biol.

Gregory, L.A., Aguissa-Touré, A.-H., Pinaud, N., Legrand, P., Gleizes, P.-E., and Fribourg, S. (2007). Molecular basis of Diamond–Blackfan anemia: structure and function analysis of RPS19. Nucl. Acids Res. *35*, 5913–5921.

Haeusler, R.A., and Engelke, D.R. (2006). Spatial organization of transcription by RNA polymerase III. Nucleic Acids Res. *34*, 4826–4836.

Harnpicharnchai, P., Jakovljevic, J., Horsey, E., Miles, T., Roman, J., Rout, M., Meagher, D., Imai, B., Guo, Y., Brame, C.J., et al. (2001). Composition and functional characterization of yeast 66S ribosome assembly intermediates. Mol. Cell *8*, 505–515.

Hedges, J., West, M., and Johnson, A.W. (2005). Release of the export adapter, Nmd3p, from the 60S ribosomal subunit requires Rpl10p and the cytoplasmic GTPase Lsg1p. EMBO J. *24*, 567–579.

Held, W.A., Ballou, B., Mizushima, S., and Nomura, M. (1974). Assembly mapping of 30 S ribosomal proteins from Escherichia coli. Further studies. J. Biol. Chem. *249*, 3103–3111.

Henras, A.K., Soudet, J., Gérus, M., Lebaron, S., Caizergues-Ferrer, M., Mougin, A., and Henry, Y. (2008). The post-transcriptional steps of eukaryotic ribosome biogenesis. Cell. Mol. Life Sci. *65*, 2334–2359.

Henry, Y., Wood, H., Morrissey, J.P., Petfalski, E., Kearsey, S., and Tollervey, D. (1994). The 5' end of yeast 5.8S rRNA is generated by exonucleases from an upstream cleavage site. EMBO J. *13*, 2452–2463.

Herold, M., and Nierhaus, K.H. (1987). Incorporation of six additional proteins to complete the assembly map of the 50 S subunit from Escherichia coli ribosomes. J. Biol. Chem. *262*, 8826–8833.

Hierlmeier, T., Merl, J., Sauert, M., Perez-Fernandez, J., Schultz, P., Bruckmann, A., Hamperl, S., Ohmayer, U., Rachel, R., Jacob, A., et al. (2012). Rrp5p, Noc1p and Noc2p form a protein module which is part of early large ribosomal subunit precursors in S. cerevisiae. Nucleic Acids Res.

Hinnebusch, A.G. (2014). The Scanning Mechanism of Eukaryotic Translation Initiation. Annu. Rev. Biochem.

Ho, J.H., and Johnson, A.W. (1999). NMD3 encodes an essential cytoplasmic protein required for stable 60S ribosomal subunits in Saccharomyces cerevisiae. Mol. Cell. Biol. *19*, 2389–2399.

Ho, J.H., Kallstrom, G., and Johnson, A.W. (2000). Nmd3p is a Crm1p-dependent adapter protein for nuclear export of the large ribosomal subunit. J. Cell Biol. *151*, 1057–1066.

Hofer, A., Bussiere, C., and Johnson, A.W. (2007). Mutational analysis of the ribosomal protein Rpl10 from yeast. J. Biol. Chem. *282*, 32630–32639.

Van Hoof, A., Lennertz, P., and Parker, R. (2000). Three conserved members of the RNase D family have unique and overlapping functions in the processing of 5S, 5.8S, U4, U5, RNase MRP and RNase P RNAs in yeast. EMBO J. *19*, 1357–1365.

Horos, R., and von Lindern, M. (2012). Molecular mechanisms of pathology and treatment in Diamond Blackfan Anaemia. Br. J. Haematol. *159*, 514–527.

Horsey, E.W., Jakovljevic, J., Miles, T.D., Harnpicharnchai, P., and Woolford, J.L., Jr (2004). Role of the yeast Rrp1 protein in the dynamics of pre-ribosome maturation. RNA *10*, 813–827.

Houseley, J., and Tollervey, D. (2009). The many pathways of RNA degradation. Cell *136*, 763–776.

Huber, M.D., Dworet, J.H., Shire, K., Frappier, L., and McAlear, M.A. (2000). The budding yeast homolog of the human EBNA1-binding protein 2 (Ebp2p) is an essential nucleolar protein required for pre-rRNA processing. J. Biol. Chem. *275*, 28764–28773.

Hung, N.-J., Lo, K.-Y., Patel, S.S., Helmke, K., and Johnson, A.W. (2008). Arx1 is a nuclear export receptor for the 60S ribosomal subunit in yeast. Mol. Biol. Cell *19*, 735–744.

Jakob, S., Ohmayer, U., Neueder, A., Hierlmeier, T., Perez-Fernandez, J., Hochmuth, E., Deutzmann, R., Griesenbeck, J., Tschochner, H., and Milkereit, P. (2012). Interrelationships between yeast ribosomal protein assembly events and transient ribosome biogenesis factors interactions in early pre-ribosomes. PLoS ONE *7*, e32552.

Jakovljevic, J., de Mayolo, P.A., Miles, T.D., Nguyen, T.M.-L., Léger-Silvestre, I., Gas, N., and Woolford, J.L., Jr (2004). The carboxy-terminal extension of yeast ribosomal protein S14 is necessary for maturation of 43S preribosomes. Mol. Cell *14*, 331–342.

Jakovljevic, J., Ohmayer, U., Gamalinda, M., Talkish, J., Alexander, L., Linnemann, J., Milkereit, P., and Woolford, J.L., Jr (2012). Ribosomal proteins L7 and L8 function in concert with six A_3 assembly factors to propagate assembly of domains I and II of 25S rRNA in yeast 60S ribosomal subunits. RNA *18*, 1805–1822.

Jenner, L., Melnikov, S., de Loubresse, N.G., Ben-Shem, A., Iskakova, M., Urzhumtsev, A., Meskauskas, A., Dinman, J., Yusupova, G., and Yusupov, M. (2012). Crystal structure of the 80S yeast ribosome. Curr. Opin. Struct. Biol.

Jomaa, A., Jain, N., Davis, J.H., Williamson, J.R., Britton, R.A., and Ortega, J. (2013). Functional domains of the 50S subunit mature late in the assembly process. Nucleic Acids Res.

Joseph, N., Krauskopf, E., Vera, M.I., and Michot, B. (1999). Ribosomal internal transcribed spacer 2 (ITS2) exhibits a common core of secondary structure in vertebrates and yeast. Nucleic Acids Res. *27*, 4533–4540.

Kallstrom, G., Hedges, J., and Johnson, A. (2003). The putative GTPases Nog1p and Lsg1p are required for 60S ribosomal subunit biogenesis and are localized to the nucleus and cytoplasm, respectively. Mol. Cell. Biol. *23*, 4344–4355.

Kappel, L., Loibl, M., Zisser, G., Klein, I., Fruhmann, G., Gruber, C., Unterweger, S., Rechberger, G., Pertschy, B., and Bergler, H. (2012). Rlp24 activates the AAA-ATPase Drg1 to initiate cytoplasmic pre-60S maturation. J. Cell Biol. *199*, 771–782.

Karbstein, K. (2011). Inside the 40S ribosome assembly machinery. Current Opinion in Chemical Biology.

Karbstein, K. (2013). Quality control mechanisms during ribosome maturation. Trends Cell Biol. *23*, 242–250.

Kaser, A., Bogengruber, E., Hallegger, M., Doppler, E., Lepperdinger, G., Jantsch, M., Breitenbach, M., and Kreil, G. (2001). Brix from xenopus laevis and brx1p from yeast define a new family of proteins involved in the biogenesis of large ribosomal subunits. Biol. Chem. *382*, 1637–1647.

Kass, S., Tyc, K., Steitz, J.A., and Sollner-Webb, B. (1990). The U3 small nucleolar ribonucleoprotein functions in the first step of preribosomal RNA processing. Cell *60*, 897–908.

Kellis, M., Birren, B.W., and Lander, E.S. (2004). Proof and evolutionary analysis of ancient genome duplication in the yeast Saccharomyces cerevisiae. Nature *428*, 617–624.

Kemmler, S., Occhipinti, L., Veisu, M., and Panse, V.G. (2009). Yvh1 is required for a late maturation step in the 60S biogenesis pathway. J. Cell Biol. *186*, 863–880.

Kim, H., Abeysirigunawarden, S.C., Chen, K., Mayerle, M., Ragunathan, K., Luthey-Schulten, Z., Ha, T., and Woodson, S.A. (2014). Protein-guided RNA dynamics during early ribosome assembly. Nature *506*, 334–338.

King, T.H., Liu, B., McCully, R.R., and Fournier, M.J. (2003). Ribosome structure and activity are altered in cells lacking snoRNPs that form pseudouridines in the peptidyl transferase center. Mol. Cell *11*, 425–435.

Klein, D.J., Moore, P.B., and Steitz, T.A. (2004). The roles of ribosomal proteins in the structure assembly, and evolution of the large ribosomal subunit. J. Mol. Biol. *340*, 141–177.

Klinge, S., Voigts-Hoffmann, F., Leibundgut, M., Arpagaus, S., and Ban, N. (2011). Crystal Structure of the Eukaryotic 60S Ribosomal Subunit in Complex with Initiation Factor 6. Science.

Knop, M., Siegers, K., Pereira, G., Zachariae, W., Winsor, B., Nasmyth, K., and Schiebel, E. (1999). Epitope tagging of yeast genes using a PCR-based strategy: more tags and improved practical routines. Yeast *15*, 963–972.

Komili, S., Farny, N.G., Roth, F.P., and Silver, P.A. (2007). Functional specificity among ribosomal proteins regulates gene expression. Cell *131*, 557–571.

Korepanov, A.P., Korobeinikova, A.V., Shestakov, S.A., Garber, M.B., and Gongadze, G.M. (2012). Protein L5 is crucial for in vivo assembly of the bacterial 50S ribosomal subunit central protuberance. Nucleic Acids Res. *40*, 9153–9159.

Kos, M., and Tollervey, D. (2010). Yeast pre-rRNA processing and modification occur cotranscriptionally. Mol. Cell *37*, 809–820.

Kressler, D., Rojo, M., Linder, P., and Cruz, J. (1999). Spb1p is a putative methyltransferase required for 60S ribosomal subunit biogenesis in Saccharomyces cerevisiae. Nucleic Acids Res. *27*, 4598–4608.

Kressler, D., Roser, D., Pertschy, B., and Hurt, E. (2008). The AAA ATPase Rix7 powers progression of ribosome biogenesis by stripping Nsa1 from pre-60S particles. J. Cell Biol. *181*, 935–944.

Kressler, D., Hurt, E., and Bassler, J. (2010). Driving ribosome assembly. Biochim. Biophys. Acta *1803*, 673–683.

Kressler, D., Hurt, E., Bergler, H., and Baßler, J. (2012a). The power of AAA-ATPases on the road of pre-60S ribosome maturation - Molecular machines that strip pre-ribosomal particles. Biochimica Et Biophysica Acta *1823*, 92–100.

Kressler, D., Bange, G., Ogawa, Y., Stjepanovic, G., Bradatsch, B., Pratte, D., Amlacher, S., Strauß, D., Yoneda, Y., Katahira, J., et al. (2012b). Synchronizing nuclear import of ribosomal proteins with ribosome assembly. Science *338*, 666–671.

Krogan, N.J., Peng, W.-T., Cagney, G., Robinson, M.D., Haw, R., Zhong, G., Guo, X., Zhang, X., Canadien, V., Richards, D.P., et al. (2004). High-definition macromolecular composition of yeast RNA-processing complexes. Mol. Cell *13*, 225–239.

Krüger, T., Zentgraf, H., and Scheer, U. (2007). Intranucleolar sites of ribosome biogenesis defined by the localization of early binding ribosomal proteins. J. Cell Biol. *177*, 573–578.

Kruiswijk, T., and Planta, R.J. (1974). Analysis of the protein composition of yeast ribosomal subunits by two-dimensional polyacrylamide gel electrophoresis. Mol Biol Rep *1*, 409–415.

Kruiswijk, T., Planta, R.J., and Krop, J.M. (1978). The course of the assembly of ribosomal subunits in yeast. Biochim. Biophys. Acta *517*, 378–389.

Kühn, H., Hierlmeier, T., Merl, J., Jakob, S., Aguissa-Touré, A.-H., Milkereit, P., and Tschochner, H. (2009). The Noc-domain containing C-terminus of Noc4p mediates both formation of the Noc4p-Nop14p submodule and its incorporation into the SSU processome. PLoS ONE *4*, e8370.

LaCava, J., Houseley, J., Saveanu, C., Petfalski, E., Thompson, E., Jacquier, A., and Tollervey, D. (2005). RNA degradation by the exosome is promoted by a nuclear polyadenylation complex. Cell *121*, 713–724.

Laemmli, U.K. (1970). Cleavage of structural proteins during the assembly of the head of bacteriophage T4. Nature *227*, 680–685.

Lafontaine, D.L., and Tollervey, D. (1999). Nop58p is a common component of the box C+D snoRNPs that is required for snoRNA stability. RNA *5*, 455–467.

Lafontaine, D., Delcour, J., Glasser, A.L., Desgrès, J., and Vandenhaute, J. (1994). The DIM1 gene responsible for the conserved m6(2)Am6(2)A dimethylation in the 3'-terminal loop of 18 S rRNA is essential in yeast. J. Mol. Biol. *241*, 492–497.

Lake, J.A. (1976). Ribosome structure determined by electron microscopy of Escherichia coli small subunits, large subunits and monomeric ribosomes. J. Mol. Biol. *105*, 131–139.

Lamanna, A.C., and Karbstein, K. (2009). Nob1 binds the single-stranded cleavage site D at the 3'-end of 18S rRNA with its PIN domain. Proc. Natl. Acad. Sci. U.S.A. *106*, 14259–14264.

Lamanna, A.C., and Karbstein, K. (2011). An RNA conformational switch regulates pre-18S rRNA cleavage. J. Mol. Biol. *405*, 3–17.

Lastick, S.M. (1980). The assembly of ribosomes in HeLa cell nucleoli. Eur. J. Biochem. *113*, 175–182.

Lastick, S.M., and McConkey, E.H. (1976). Exchange and stability of HeLa ribosomal proteins in vivo. J. Biol. Chem. *251*, 2867–2875.

Lavergne, J.P., Marzouki, A., Reboud, J.P., and Reboud, A.M. (1988). Reconstitution of the active rat liver 60 S ribosomal subunit from different preparations of core particles and split proteins. FEBS Lett. *236*, 345–351.

Lebaron, S., Schneider, C., van Nues, R.W., Swiatkowska, A., Walsh, D., Böttcher, B., Granneman, S., Watkins, N.J., and Tollervey, D. (2012). Proofreading of pre-40S ribosome maturation by a translation initiation factor and 60S subunits. Nat Struct Mol Biol *19*, 744–753.

Lebaron, S., Segerstolpe, A., French, S.L., Dudnakova, T., de Lima Alves, F., Granneman, S., Rappsilber, J., Beyer, A.L., Wieslander, L., and Tollervey, D. (2013). Rrp5 Binding at Multiple Sites Coordinates Pre-rRNA Processing and Assembly. Mol. Cell.

Lebreton, A., Saveanu, C., Decourty, L., Rain, J.-C., Jacquier, A., and Fromont-Racine, M. (2006a). A functional network involved in the recycling of nucleocytoplasmic pre-60S factors. J. Cell Biol. *173*, 349–360.

Lebreton, A., Saveanu, C., Decourty, L., Jacquier, A., and Fromont-Racine, M. (2006b). Nsa2 is an unstable, conserved factor required for the maturation of 27 SB pre-rRNAs. J. Biol. Chem. *281*, 27099–27108.

Lebreton, A., Rousselle, J.-C., Lenormand, P., Namane, A., Jacquier, A., Fromont-Racine, M., and Saveanu, C. (2008). 60S ribosomal subunit assembly dynamics defined by semi-quantitative mass spectrometry of purified complexes. Nucleic Acids Res. *36*, 4988–4999.

Lecompte, O., Ripp, R., Thierry, J.-C., Moras, D., and Poch, O. (2002). Comparative analysis of ribosomal proteins in complete genomes: an example of reductive evolution at the domain scale. Nucleic Acids Res. *30*, 5382–5390.

Lee, S.J., and Baserga, S.J. (1999). Imp3p and Imp4p, two specific components of the U3 small nucleolar ribonucleoprotein that are essential for pre-18S rRNA processing. Mol. Cell. Biol. *19*, 5441–5452.

Léger-Silvestre, I., Trumtel, S., Noaillac-Depeyre, J., and Gas, N. (1999). Functional compartmentalization of the nucleus in the budding yeast Saccharomyces cerevisiae. Chromosoma *108*, 103–113.

Léger-Silvestre, I., Milkereit, P., Ferreira-Cerca, S., Saveanu, C., Rousselle, J.-C., Choesmel, V., Guinefoleau, C., Gas, N., and Gleizes, P.-E. (2004). The ribosomal protein Rps15p is required for nuclear exit of the 40S subunit precursors in yeast. EMBO J. *23*, 2336–2347.

Léger-Silvestre, I., Caffrey, J.M., Dawaliby, R., Alvarez-Arias, D.A., Gas, N., Bertolone, S.J., Gleizes, P.-E., and Ellis, S.R. (2005). Specific Role for Yeast Homologs of the Diamond Blackfan Anemia-associated Rps19 Protein in Ribosome Synthesis. J. Biol. Chem. *280*, 38177–38185.

Leidig, C., Thoms, M., Holdermann, I., Bradatsch, B., Berninghausen, O., Bange, G., Sinning, I., Hurt, E., and Beckmann, R. (2014). 60S ribosome biogenesis requires rotation of the 5S ribonucleoprotein particle. Nat Commun *5*, 3491.

Li, H.D., Zagorski, J., and Fournier, M.J. (1990). Depletion of U14 small nuclear RNA (snR128) disrupts production of 18S rRNA in Saccharomyces cerevisiae. Mol. Cell. Biol. *10*, 1145–1152.

Li, N., Chen, Y., Guo, Q., Zhang, Y., Yuan, Y., Ma, C., Deng, H., Lei, J., and Gao, N. (2013). Cryo-EM structures of the late-stage assembly intermediates of the bacterial 50S ribosomal subunit. Nucleic Acids Res. *41*, 7073–7083.

Li, Z., Lee, I., Moradi, E., Hung, N.-J., Johnson, A.W., and Marcotte, E.M. (2009). Rational extension of the ribosome biogenesis pathway using network-guided genetics. PLoS Biol. *7*, e1000213.

Liang, X., Liu, Q., and Fournier, M.J. (2007). rRNA modifications in an intersubunit bridge of the ribosome strongly affect both ribosome biogenesis and activity. Mol. Cell *28*, 965–977.

Liang, X.-H., Liu, Q., and Fournier, M.J. (2009). Loss of rRNA modifications in the decoding center of the ribosome impairs translation and strongly delays pre-rRNA processing. RNA *15*, 1716–1728.

Lindahl, L., Archer, R.H., and Zengel, J.M. (1992). A new rRNA processing mutant of Saccharomyces cerevisiae. Nucleic Acids Res. *20*, 295–301.

Lo, K.-Y., Li, Z., Wang, F., Marcotte, E.M., and Johnson, A.W. (2009). Ribosome stalk assembly requires the dual-specificity phosphatase Yvh1 for the exchange of Mrt4 with P0. J. Cell Biol. *186*, 849–862.

Lo, K.-Y., Li, Z., Bussiere, C., Bresson, S., Marcotte, E.M., and Johnson, A.W. (2010). Defining the pathway of cytoplasmic maturation of the 60S ribosomal subunit. Mol. Cell *39*, 196–208.

Long, E.O., and Dawid, I.B. (1980). Repeated genes in eukaryotes. Annu. Rev. Biochem. *49*, 727–764.

Lukowiak, A.A., Granneman, S., Mattox, S.A., Speckmann, W.A., Jones, K., Pluk, H., Venrooij, W.J., Terns, R.M., and Terns, M.P. (2000). Interaction of the U3-55k protein with U3 snoRNA is mediated by the box B/C motif of U3 and the WD repeats of U3-55k. Nucleic Acids Res. *28*, 3462–3471.

Lygerou, Z., Allmang, C., Tollervey, D., and Séraphin, B. (1996). Accurate processing of a eukaryotic precursor ribosomal RNA by ribonuclease MRP in vitro. Science *272*, 268–270.

Mager, W.H., Planta, R.J., Ballesta, J.G., Lee, J.C., Mizuta, K., Suzuki, K., Warner, J.R., and Woolford, J. (1997). A new nomenclature for the cytoplasmic ribosomal proteins of Saccharomyces cerevisiae. Nucleic Acids Res. *25*, 4872–4875.

Maki, J.A., Schnobrich, D.J., and Culver, G.M. (2002). The DnaK chaperone system facilitates 30S ribosomal subunit assembly. Mol. Cell *10*, 129–138.

Maki, J.A., Southworth, D.R., and Culver, G.M. (2003). Demonstration of the role of the DnaK chaperone system in assembly of 30S ribosomal subunits using a purified in vitro system. RNA *9*, 1418–1421.

Mangiarotti, G., and Chiaberge, S. (1997). Reconstitution of functional eukaryotic ribosomes from Dictyostelium discoideum ribosomal proteins and RNA. J. Biol. Chem. *272*, 19682–19687.

Marquardt, O., Roth, H.E., Wystup, G., and Nierhaus, K.H. (1979). Binding of Escherichia coli ribosomal proteins to 23S RNA under reconstitution conditions for the 50S subunit. Nucleic Acids Res. *6*, 3641–3650.

Matsuo, Y., Granneman, S., Thoms, M., Manikas, R.-G., Tollervey, D., and Hurt, E. (2013). Coupled GTPase and remodelling ATPase activities form a checkpoint for ribosome export. Nature.

Mayerle, M., and Woodson, S.A. (2013). Specific contacts between protein S4 and ribosomal RNA are required at multiple stages of ribosome assembly. RNA *19*, 574–585.

Mayerle, M., Bellur, D.L., and Woodson, S.A. (2011). Slow formation of stable complexes during coincubation of minimal rRNA and ribosomal protein S4. J. Mol. Biol. *412*, 453–465.

McConkey, E.H., Bielka, H., Gordon, J., Lastick, S.M., Lin, A., Ogata, K., Reboud, J.P., Traugh, J.A., Traut, R.R., Warner, J.R., et al. (1979). Proposed uniform nomenclature for mammalian ribosomal proteins. Mol. Gen. Genet. *169*, 1–6.

Menne, T.F., Goyenechea, B., Sánchez-Puig, N., Wong, C.C., Tonkin, L.M., Ancliff, P.J., Brost, R.L., Costanzo, M., Boone, C., and Warren, A.J. (2007). The Shwachman-Bodian-Diamond syndrome protein mediates translational activation of ribosomes in yeast. Nat Genet *39*, 486–495.

Merl, J., Jakob, S., Ridinger, K., Hierlmeier, T., Deutzmann, R., Milkereit, P., and Tschochner, H. (2010). Analysis of ribosome biogenesis factor-modules in yeast cells depleted from pre-ribosomes. Nucleic Acids Res. *38*, 3068–3080.

Meyer, A.E., Hung, N.-J., Yang, P., Johnson, A.W., and Craig, E.A. (2007). The specialized cytosolic J-protein, Jjj1, functions in 60S ribosomal subunit biogenesis. Proc. Natl. Acad. Sci. U.S.A. *104*, 1558–1563.

Meyer, A.E., Hoover, L.A., and Craig, E.A. (2010). The cytosolic J-protein, Jjj1, and Rei1 function in the removal of the pre-60 S subunit factor Arx1. J. Biol. Chem. *285*, 961–968.

Miles, T.D., Jakovljevic, J., Horsey, E.W., Harnpicharnchai, P., Tang, L., and Woolford, J.L., Jr (2005). Ytm1, Nop7, and Erb1 form a complex necessary for maturation of yeast 66S preribosomes. Mol. Cell. Biol. *25*, 10419–10432.

Milkereit, P., Gadal, O., Podtelejnikov, A., Trumtel, S., Gas, N., Petfalski, E., Tollervey, D., Mann, M., Hurt, E., and Tschochner, H. (2001). Maturation and intranuclear transport of pre-ribosomes requires Noc proteins. Cell *105*, 499–509.

Milkereit, P., Strauss, D., Bassler, J., Gadal, O., Kühn, H., Schütz, S., Gas, N., Lechner, J., Hurt, E., and Tschochner, H. (2003). A Noc complex specifically involved in the formation and nuclear export of ribosomal 40 S subunits. J. Biol. Chem. *278*, 4072–4081.

Miller, O.L., Jr, and Beatty, B.R. (1969). Visualization of nucleolar genes. Science *164*, 955–957.

Mitchell, P., Petfalski, E., and Tollervey, D. (1996). The 3' end of yeast 5.8S rRNA is generated by an exonuclease processing mechanism. Genes Dev. *10*, 502–513.

Mitsui, K., Nakagawa, T., and Tsurugi, K. (1988). On the size and the role of a free cytosolic pool of acidic ribosomal proteins in yeast Saccharomyces cerevisiae. J. Biochem. *104*, 908–911.

Mizushima, S., and Nomura, M. (1970). Assembly mapping of 30S ribosomal proteins from E. coli. Nature *226*, 1214.

Montanaro, L., Treré, D., and Derenzini, M. (2008). Nucleolus, ribosomes, and cancer. Am. J. Pathol. *173*, 301–310.

Moore, P.B., and Steitz, T.A. (2011). The roles of RNA in the synthesis of protein. Cold Spring Harb Perspect Biol *3*, a003780.

Moore, J.B., Farrar, J.E., Arceci, R.J., Liu, J.M., and Ellis, S.R. (2010). Distinct ribosome maturation defects in yeast models of Diamond-Blackfan anemia and Shwachman-Diamond syndrome. Haematologica *95*, 57–64.

Morgan, D.G., Ménétret, J.F., Radermacher, M., Neuhof, A., Akey, I.V., Rapoport, T.A., and Akey, C.W. (2000). A comparison of the yeast and rabbit 80 S ribosome reveals the topology of the nascent chain exit tunnel, inter-subunit bridges and mammalian rRNA expansion segments. J. Mol. Biol. *301*, 301–321.

Morita, D., Miyoshi, K., Matsui, Y., Toh-E, A., Shinkawa, H., Miyakawa, T., and Mizuta, K. (2002). Rpf2p, an evolutionarily conserved protein, interacts with ribosomal protein L11 and is essential for the processing of 27 SB Pre-rRNA to 25 S rRNA and the 60 S ribosomal subunit assembly in Saccharomyces cerevisiae. J. Biol. Chem. *277*, 28780–28786.

Morrissey, J.P., and Tollervey, D. (1993). Yeast snR30 is a small nucleolar RNA required for 18S rRNA synthesis. Mol. Cell. Biol. *13*, 2469–2477.

Moss, T., Langlois, F., Gagnon-Kugler, T., and Stefanovsky, V. (2007). A housekeeper with power of attorney: the rRNA genes in ribosome biogenesis. Cell. Mol. Life Sci. *64*, 29–49.

Németh, A., Perez-Fernandez, J., Merkl, P., Hamperl, S., Gerber, J., Griesenbeck, J., and Tschochner, H. (2013). RNA polymerase I termination: Where is the end? Biochim. Biophys. Acta *1829*, 306–317.

Nierhaus, K.H., and Dohme, F. (1974). Total reconstitution of functionally active 50S ribosomal subunits from Escherichia coli. Proc. Natl. Acad. Sci. U.S.A. *71*, 4713–4717.

Nierhaus, K.H., and Wilson, D.N. (2004). Protein synthesis and ribosome structure: translating the genome (Weinheim).

Nierhaus, K.H., Bordasch, K., and Homann, H.E. (1973). Ribosomal proteins. 43. In vivo assembly of Escherichia coli ribosomal proteins. J. Mol. Biol. *74*, 587–597.

Nissan, T.A., Bassler, J., Petfalski, E., Tollervey, D., and Hurt, E. (2002). 60S pre-ribosome formation viewed from assembly in the nucleolus until export to the cytoplasm. EMBO J. *21*, 5539–5547.

Nissan, T.A., Galani, K., Maco, B., Tollervey, D., Aebi, U., and Hurt, E. (2004). A pre-ribosome with a tadpole-like structure functions in ATP-dependent maturation of 60S subunits. Mol. Cell *15*, 295–301.

Nissen, P., Hansen, J., Ban, N., Moore, P.B., and Steitz, T.A. (2000). The structural basis of ribosome activity in peptide bond synthesis. Science *289*, 920–930.

Noller, H.F., Kop, J., Wheaton, V., Brosius, J., Gutell, R.R., Kopylov, A.M., Dohme, F., Herr, W., Stahl, D.A., Gupta, R., et al. (1981). Secondary structure model for 23S ribosomal RNA. Nucleic Acids Res. *9*, 6167–6189.

Van Nues, R.W., Venema, J., Rientjes, J.M., Dirks-Mulder, A., and Raué, H.A. (1995). Processing of eukaryotic pre-rRNA: the role of the transcribed spacers. Biochem. Cell Biol. *73*, 789–801.

Van Nues, R.W., Venema, J., Planta, R.J., and Raué, H.A. (1997). Variable region V1 of Saccharomyces cerevisiae 18S rRNA participates in biogenesis and function of the small ribosomal subunit. Chromosoma *105*, 523–531.

Oeffinger, M., Leung, A., Lamond, A., Tollervey, D., and Lueng, A. (2002). Yeast Pescadillo is required for multiple activities during 60S ribosomal subunit synthesis. RNA *8*, 626–636.

Oeffinger, M., Zenklusen, D., Ferguson, A., Wei, K.E., El Hage, A., Tollervey, D., Chait, B.T., Singer, R.H., and Rout, M.P. (2009). Rrp17p is a eukaryotic exonuclease required for 5' end processing of Pre-60S ribosomal RNA. Mol. Cell *36*, 768–781.

Ogle, J.M., Brodersen, D.E., Clemons, W.M., Jr, Tarry, M.J., Carter, A.P., and Ramakrishnan, V. (2001). Recognition of cognate transfer RNA by the 30S ribosomal subunit. Science *292*, 897–902.

Ohmayer, U., Perez-Fernandez, J., Hierlmeier, T., Pöll, G., Williams, L., Griesenbeck, J., Tschochner, H., and Milkereit, P. (2012). Local tertiary structure probing of ribonucleoprotein particles by nuclease fusion proteins. PLoS ONE *7*, e42449.

Ohmayer, U., Gamalinda, M., Sauert, M., Ossowski, J., Pöll, G., Linnemann, J., Hierlmeier, T., Perez-Fernandez, J., Kumcuoglu, B., Leger-Silvestre, I., et al. (2013). Studies on the assembly characteristics of large subunit ribosomal proteins in S. cerevisae. PLoS ONE *8*, e68412.

Osheim, Y.N., French, S.L., Keck, K.M., Champion, E.A., Spasov, K., Dragon, F., Baserga, S.J., and Beyer, A.L. (2004). Pre-18S ribosomal RNA is structurally compacted into the SSU processome prior to being cleaved from nascent transcripts in Saccharomyces cerevisiae. Mol. Cell *16*, 943–954.

Peculis, B.A., and Greer, C.L. (1998). The structure of the ITS2-proximal stem is required for pre-rRNA processing in yeast. RNA *4*, 1610–1622.

Peisker, K., Braun, D., Wölfle, T., Hentschel, J., Fünfschilling, U., Fischer, G., Sickmann, A., and Rospert, S. (2008). Ribosome-associated complex binds to ribosomes in close proximity of Rpl31 at the exit of the polypeptide tunnel in yeast. Mol. Biol. Cell *19*, 5279–5288.

Pérez-Fernández, J., Román, A., De Las Rivas, J., Bustelo, X.R., and Dosil, M. (2007). The 90S preribosome is a multimodular structure that is assembled through a hierarchical mechanism. Mol. Cell. Biol. *27*, 5414–5429.

Pérez-Fernández, J., Martín-Marcos, P., and Dosil, M. (2011). Elucidation of the assembly events required for the recruitment of Utp20, Imp4 and Bms1 onto nascent pre-ribosomes. Nucleic Acids Res. *39*, 8105–8121.

Pertschy, B., Saveanu, C., Zisser, G., Lebreton, A., Tengg, M., Jacquier, A., Liebminger, E., Nobis, B., Kappel, L., van der Klei, I., et al. (2007). Cytoplasmic recycling of 60S preribosomal factors depends on the AAA protein Drg1. Mol. Cell. Biol. *27*, 6581–6592.

Pestov, D.G., Stockelman, M.G., Strezoska, Z., and Lau, L.F. (2001). ERB1, the yeast homolog of mammalian Bop1, is an essential gene required for maturation of the 25S and 5.8S ribosomal RNAs. Nucleic Acids Res. *29*, 3621–3630.

Petes, T.D. (1979). Yeast ribosomal DNA genes are located on chromosome XII. Proc. Natl. Acad. Sci. U.S.A. *76*, 410–414.

Philippsen, P., Thomas, M., Kramer, R.A., and Davis, R.W. (1978). Unique arrangement of coding sequences for 5 S, 5.8 S, 18 S and 25 S ribosomal RNA in Saccharomyces cerevisiae as determined by R-loop and hybridization analysis. J. Mol. Biol. *123*, 387–404.

Planta, R.J., and Mager, W.H. (1998). The list of cytoplasmic ribosomal proteins of Saccharomyces cerevisiae. Yeast *14*, 471–477.

Pöll, G., Braun, T., Jakovljevic, J., Neueder, A., Jakob, S., Woolford, J.L., Jr, Tschochner, H., and Milkereit, P. (2009). rRNA maturation in yeast cells depleted of large ribosomal subunit proteins. PLoS ONE *4*, e8249.

Powers, T., Daubresse, G., and Noller, H.F. (1993). Dynamics of in vitro assembly of 16 S rRNA into 30 S ribosomal subunits. J. Mol. Biol. *232*, 362–374.

Puig, O., Caspary, F., Rigaut, G., Rutz, B., Bouveret, E., Bragado-Nilsson, E., Wilm, M., and Séraphin, B. (2001). The tandem affinity purification (TAP) method: a general procedure of protein complex purification. Methods *24*, 218–229.

Rachfall, N., Schmitt, K., Bandau, S., Smolinski, N., Ehrenreich, A., Valerius, O., and Braus, G.H. (2013). RACK1/Asc1p, a ribosomal node in cellular signaling. Mol. Cell Proteomics *12*, 87–105.

Reboud, A.M., Buisson, M., Amoros, M.J., and Reboud, J.P. (1972). Partial in vitro reconstitution of active 40S ribosomal subunits from rat liver. Biochem. Biophys. Res. Commun. *46*, 2012–2018.

Remacha, M., Jimenez-Diaz, A., Bermejo, B., Rodriguez-Gabriel, M.A., Guarinos, E., and Ballesta, J.P. (1995). Ribosomal acidic phosphoproteins P1 and P2 are not required for cell viability but regulate the pattern of protein expression in Saccharomyces cerevisiae. Mol. Cell. Biol. *15*, 4754–4762.

Retèl, J., van den Bos, R.C., and Planta, R.J. (1969). Characteristics of the methylation in vivo of ribosomal RNA in yeast. Biochim. Biophys. Acta *195*, 370–380.

Rich, B.E., and Steitz, J.A. (1987). Human acidic ribosomal phosphoproteins P0, P1, and P2: analysis of cDNA clones, in vitro synthesis, and assembly. Mol. Cell. Biol. *7*, 4065–4074.

Ridgeway, W.K., Millar, D.P., and Williamson, J.R. (2012). Quantitation of ten 30S ribosomal assembly intermediates using fluorescence triple correlation spectroscopy. Proc. Natl. Acad. Sci. U.S.A. *109*, 13614–13619.

Rodnina, M.V. (2013). The ribosome as a versatile catalyst: reactions at the peptidyl transferase center. Curr. Opin. Struct. Biol. *23*, 595–602.

Rodnina, M.V., and Wintermeyer, W. (2009). Recent mechanistic insights into eukaryotic ribosomes. Curr. Opin. Cell Biol. *21*, 435–443.

Rodríguez-Galán, O., García-Gómez, J.J., and de la Cruz, J. (2013). Yeast and human RNA helicases involved in ribosome biogenesis: current status and perspectives. Biochim. Biophys. Acta *1829*, 775–790.

Rodríguez-Mateos, M., García-Gómez, J.J., Francisco-Velilla, R., Remacha, M., de la Cruz, J., and Ballesta, J.P.G. (2009a). Role and dynamics of the ribosomal protein P0 and its related trans-acting factor Mrt4 during ribosome assembly in Saccharomyces cerevisiae. Nucleic Acids Res. *37*, 7519–7532.

Rodríguez-Mateos, M., Abia, D., García-Gómez, J.J., Morreale, A., de la Cruz, J., Santos, C., Remacha, M., and Ballesta, J.P.G. (2009b). The amino terminal domain from Mrt4 protein can functionally replace the RNA binding domain of the ribosomal P0 protein. Nucleic Acids Res. *37*, 3514–3521.

Röhl, R., Roth, H.E., and Nierhaus, K.H. (1982). Inter-protein dependences during assembly of the 50S subunit from Escherichia coli ribosomes. Hoppe-Seyler's Z. Physiol. Chem. *363*, 143–157.

Rosado, I.V., Dez, C., Lebaron, S., Caizergues-Ferrer, M., Henry, Y., and de la Cruz, J. (2007a). Characterization of Saccharomyces cerevisiae Npa2p (Urb2p) reveals a low-molecular-mass complex containing Dbp6p, Npa1p (Urb1p), Nop8p, and Rsa3p involved in early steps of 60S ribosomal subunit biogenesis. Mol. Cell. Biol. *27*, 1207–1221.

Rosado, I.V., Kressler, D., and de la Cruz, J. (2007b). Functional analysis of Saccharomyces cerevisiae ribosomal protein Rpl3p in ribosome synthesis. Nucleic Acids Res. *35*, 4203–4213.

Ross, P.L., Huang, Y.N., Marchese, J.N., Williamson, B., Parker, K., Hattan, S., Khainovski, N., Pillai, S., Dey, S., Daniels, S., et al. (2004). Multiplexed protein quantitation in Saccharomyces cerevisiae using amine-reactive isobaric tagging reagents. Mol. Cell Proteomics *3*, 1154–1169.

Roth, H.E., and Nierhaus, K.H. (1980). Assembly map of the 50-S subunit from Escherichia coli ribosomes, covering the proteins present in the first reconstitution intermediate particle. Eur. J. Biochem. *103*, 95–98.

Rout, M.P., Blobel, G., and Aitchison, J.D. (1997). A Distinct Nuclear Import Pathway Used by Ribosomal Proteins. Cell *89*, 715–725.

Ruggero, D., and Pandolfi, P.P. (2003). Does the ribosome translate cancer? Nat. Rev. Cancer *3*, 179–192.

Saenz-Robles, M.T., Remacha, M., Vilella, M.D., Zinker, S., and Ballesta, J.P. (1990). The acidic ribosomal proteins as regulators of the eukaryotic ribosomal activity. Biochim. Biophys. Acta *1050*, 51–55.

Sahasranaman, A., Dembowski, J., Strahler, J., Andrews, P., Maddock, J., and Woolford, J.L., Jr (2011). Assembly of Saccharomyces cerevisiae 60S ribosomal subunits: role of factors required for 27S pre-rRNA processing. EMBO J. *30*, 4020–4032.

Samaha, R.R., O'Brien, B., O'Brien, T.W., and Noller, H.F. (1994). Independent in vitro assembly of a ribonucleoprotein particle containing the 3' domain of 16S rRNA. Proc. Natl. Acad. Sci. U.S.A. *91*, 7884–7888.

Samanta, M.P., and Liang, S. (2003). Predicting protein functions from redundancies in large-scale protein interaction networks. Proc. Natl. Acad. Sci. U.S.A. *100*, 12579–12583.

Sasaki, M., Kawahara, K., Nishio, M., Mimori, K., Kogo, R., Hamada, K., Itoh, B., Wang, J., Komatsu, Y., Yang, Y.R., et al. (2011). Regulation of the MDM2-P53 pathway and tumor growth by PICT1 via nucleolar RPL11. Nat. Med. *17*, 944–951.

Saveanu, C., Bienvenu, D., Namane, A., Gleizes, P.E., Gas, N., Jacquier, A., and Fromont-Racine, M. (2001). Nog2p, a putative GTPase associated with pre-60S subunits and required for late 60S maturation steps. EMBO J. *20*, 6475–6484.

Saveanu, C., Namane, A., Gleizes, P.-E., Lebreton, A., Rousselle, J.-C., Noaillac-Depeyre, J., Gas, N., Jacquier, A., and Fromont-Racine, M. (2003). Sequential protein association with nascent 60S ribosomal particles. Mol. Cell. Biol. *23*, 4449–4460.

Saveanu, C., Rousselle, J.-C., Lenormand, P., Namane, A., Jacquier, A., and Fromont-Racine, M. (2007). The p21-activated protein kinase inhibitor Skb15 and its budding yeast homologue are 60S ribosome assembly factors. Mol. Cell. Biol. *27*, 2897–2909.

Savino, R., and Gerbi, S.A. (1990). In vivo disruption of Xenopus U3 snRNA affects ribosomal RNA processing. EMBO J. *9*, 2299–2308.

Schäfer, T., Strauss, D., Petfalski, E., Tollervey, D., and Hurt, E. (2003). The path from nucleolar 90S to cytoplasmic 40S pre-ribosomes. EMBO J. *22*, 1370–1380.

Schäfer, T., Maco, B., Petfalski, E., Tollervey, D., Böttcher, B., Aebi, U., and Hurt, E. (2006). Hrr25-dependent phosphorylation state regulates organization of the pre-40S subunit. Nature *441*, 651–655.

Schluenzen, F., Tocilj, A., Zarivach, R., Harms, J., Gluehmann, M., Janell, D., Bashan, A., Bartels, H., Agmon, I., Franceschi, F., et al. (2000). Structure of functionally activated small ribosomal subunit at 3.3 angstroms resolution. Cell *102*, 615–623.

Schmeing, T.M., Voorhees, R.M., Kelley, A.C., and Ramakrishnan, V. (2011). How mutations in tRNA distant from the anticodon affect the fidelity of decoding. Nat. Struct. Mol. Biol. *18*, 432–436.

Schmitt, M.E., and Clayton, D.A. (1993). Nuclear RNase MRP is required for correct processing of pre-5.8S rRNA in Saccharomyces cerevisiae. Mol. Cell. Biol. *13*, 7935–7941.

Schmitt, M.E., Brown, T.A., and Trumpower, B.L. (1990). A rapid and simple method for preparation of RNA from Saccharomyces cerevisiae. Nucleic Acids Res. *18*, 3091–3092.

Schuwirth, B.S., Borovinskaya, M.A., Hau, C.W., Zhang, W., Vila-Sanjurjo, A., Holton, J.M., and Cate, J.H.D. (2005). Structures of the bacterial ribosome at 3.5 A resolution. Science *310*, 827–834.

Seiser, R.M., Sundberg, A.E., Wollam, B.J., Zobel-Thropp, P., Baldwin, K., Spector, M.D., and Lycan, D.E. (2006). Ltv1 is required for efficient nuclear export of the ribosomal small subunit in Saccharomyces cerevisiae. Genetics *174*, 679–691.

Senapin, S., Clark-Walker, G.D., Chen, X.J., Séraphin, B., and Daugeron, M.-C. (2003). RRP20, a component of the 90S preribosome, is required for pre-18S rRNA processing in Saccharomyces cerevisiae. Nucleic Acids Res. *31*, 2524–2533.

Senger, B., Lafontaine, D.L., Graindorge, J.S., Gadal, O., Camasses, A., Sanni, A., Garnier, J.M., Breitenbach, M., Hurt, E., and Fasiolo, F. (2001). The nucle(ol)ar Tif6p and Efl1p are required for a late cytoplasmic step of ribosome synthesis. Mol. Cell *8*, 1363–1373.

Sengupta, J., Bussiere, C., Pallesen, J., West, M., Johnson, A.W., and Frank, J. (2010). Characterization of the nuclear export adaptor protein Nmd3 in association with the 60S ribosomal subunit. J. Cell Biol. *189*, 1079–1086.

Ben-Shem, A., Garreau de Loubresse, N., Melnikov, S., Jenner, L., Yusupova, G., and Yusupov, M. (2011). The Structure of the Eukaryotic Ribosome at 3.0 Å Resolution. Science.

Shimoji, K., Jakovljevic, J., Tsuchihashi, K., Umeki, Y., Wan, K., Kawasaki, S., Talkish, J., Woolford, J.L., Jr, and Mizuta, K. (2012). Ebp2 and Brx1 function cooperatively in 60S ribosomal subunit assembly in Saccharomyces cerevisiae. Nucleic Acids Res. *40*, 4574–4588.

Sievers, A., Beringer, M., Rodnina, M.V., and Wolfenden, R. (2004). The ribosome as an entropy trap. PNAS *101*, 7897–7901.

Sloan, K.E., Bohnsack, M.T., and Watkins, N.J. (2013). The 5S RNP couples p53 homeostasis to ribosome biogenesis and nucleolar stress. Cell Rep *5*, 237–247.

Sondalle, S.B., and Baserga, S.J. (2014). Human diseases of the SSU processome. Biochim. Biophys. Acta *1842*, 758–764.

Sonenberg, N., and Hinnebusch, A.G. (2009). Regulation of translation initiation in eukaryotes: mechanisms and biological targets. Cell *136*, 731–745.

Spahn, C.M., Beckmann, R., Eswar, N., Penczek, P.A., Sali, A., Blobel, G., and Frank, J. (2001). Structure of the 80S ribosome from Saccharomyces cerevisiae--tRNA-ribosome and subunit-subunit interactions. Cell *107*, 373–386.

Spillmann, S., Dohme, F., and Nierhaus, K.H. (1977). Assembly in vitro of the 50 S subunit from Escherichia coli ribosomes: proteins essential for the first heat-dependent conformational change. J. Mol. Biol. *115*, 513–523.

Stage-Zimmermann, T., Schmidt, U., and Silver, P.A. (2000). Factors affecting nuclear export of the 60S ribosomal subunit in vivo. Mol. Biol. Cell *11*, 3777–3789.

Steffen, K.K., McCormick, M.A., Pham, K.M., MacKay, V.L., Delaney, J.R., Murakami, C.J., Kaeberlein, M., and Kennedy, B.K. (2012). Ribosome deficiency protects against ER stress in Saccharomyces cerevisiae. Genetics *191*, 107–118.

Steitz, T.A. (2008). A structural understanding of the dynamic ribosome machine. Nat. Rev. Mol. Cell Biol. *9*, 242–253.

Stern, S., Powers, T., Changchien, L.M., and Noller, H.F. (1989). RNA-protein interactions in 30S ribosomal subunits: folding and function of 16S rRNA. Science *244*, 783–790.

Stöffler, G., and Stöffler-Meilicke, M. (1984). Immunoelectron microscopy of ribosomes. Annu. Rev. Biophys. Bioeng. *13*, 303–330.

Strunk, B.S., and Karbstein, K. (2009). Powering through ribosome assembly. RNA *15*, 2083–2104.

Strunk, B.S., Loucks, C.R., Su, M., Vashisth, H., Cheng, S., Schilling, J., Brooks, C.L., 3rd, Karbstein, K., and Skiniotis, G. (2011). Ribosome assembly factors prevent premature translation initiation by 40S assembly intermediates. Science *333*, 1449–1453.

Strunk, B.S., Novak, M.N., Young, C.L., and Karbstein, K. (2012). A Translation-Like Cycle Is a Quality Control Checkpoint for Maturing 40S Ribosome Subunits. Cell *150*, 111–121.

Suzuki, A., Kogo, R., Kawahara, K., Sasaki, M., Nishio, M., Maehama, T., Sasaki, T., Mimori, K., and Mori, M. (2012). A New PICTure of nucleolar stress. Cancer Science.

Sweeney, R., Chen, L., and Yao, M.C. (1994). An rRNA variable region has an evolutionarily conserved essential role despite sequence divergence. Mol. Cell. Biol. *14*, 4203–4215.

Sydorskyy, Y., Dilworth, D.J., Halloran, B., Yi, E.C., Makhnevych, T., Wozniak, R.W., and Aitchison, J.D. (2005). Nop53p is a novel nucleolar 60S ribosomal subunit biogenesis protein. Biochem. J. *388*, 819–826.

Tafforeau, L., Zorbas, C., Langhendries, J.-L., Mullineux, S.-T., Stamatopoulou, V., Mullier, R., Wacheul, L., and Lafontaine, D.L.J. (2013). The Complexity of Human Ribosome Biogenesis Revealed by Systematic Nucleolar Screening of Pre-rRNA Processing Factors. Mol. Cell *51*, 539–551.

Talkington, M.W.T., Siuzdak, G., and Williamson, J.R. (2005). An assembly landscape for the 30S ribosomal subunit. Nature *438*, 628–632.

Talkish, J., Zhang, J., Jakovljevic, J., Horsey, E.W., and Woolford, J.L., Jr (2012). Hierarchical recruitment into nascent ribosomes of assembly factors required for 27SB pre-rRNA processing in Saccharomyces cerevisiae. Nucleic Acids Research.

Talkish, J., Campbell, I.W., Sahasranaman, A., Jakovljevic, J., and Woolford, J.L., Jr (2014). Ribosome assembly factors Pwp1 and Nop12 are important for folding of 5.8S rRNA during ribosome biogenesis in Saccharomyces cerevisiae. Mol. Cell. Biol.

Thiry, M., and Lafontaine, D.L.J. (2005). Birth of a nucleolus: the evolution of nucleolar compartments. Trends Cell Biol. *15*, 194–199.

Thomas, F., and Kutay, U. (2003). Biogenesis and nuclear export of ribosomal subunits in higher eukaryotes depend on the CRM1 export pathway. J. Cell. Sci. *116*, 2409–2419.

Thompson, J., Kim, D.F., O'Connor, M., Lieberman, K.R., Bayfield, M.A., Gregory, S.T., Green, R., Noller, H.F., and Dahlberg, A.E. (2001). Analysis of mutations at residues A2451 and G2447 of 23S rRNA in the peptidyltransferase active site of the 50S ribosomal subunit. Proc. Natl. Acad. Sci. U.S.A. *98*, 9002–9007.

Thomson, E., and Tollervey, D. (2005). Nop53p is required for late 60S ribosome subunit maturation and nuclear export in yeast. RNA *11*, 1215–1224.

Thomson, E., and Tollervey, D. (2010). The final step in 5.8S rRNA processing is cytoplasmic in Saccharomyces cerevisiae. Mol. Cell. Biol. *30*, 976–984.

Thomson, E., Ferreira-Cerca, S., and Hurt, E. (2013). Eukaryotic ribosome biogenesis at a glance. J. Cell. Sci. *126*, 4815–4821.

Trapman, J., Retèl, J., and Planta, R.J. (1975). Ribosomal precursor particles from yeast. Exp. Cell Res. *90*, 95–104.

Traub, P., and Nomura, M. (1968). Structure and function of E. coli ribosomes. V. Reconstitution of functionally active 30S ribosomal particles from RNA and proteins. Proc. Natl. Acad. Sci. U.S.A. *59*, 777–784.

Traub, P., and Nomura, M. (1969). Structure and function of Escherichia coli ribosomes. VI. Mechanism of assembly of 30 s ribosomes studied in vitro. J. Mol. Biol. *40*, 391–413.

Tschochner, H., and Hurt, E. (2003). Pre-ribosomes on the road from the nucleolus to the cytoplasm. Trends Cell Biol. *13*, 255–263.

Tsujii, R., Miyoshi, K., Tsuno, A., Matsui, Y., Toh-e, A., Miyakawa, T., and Mizuta, K. (2000). Ebp2p, yeast homologue of a human protein that interacts with Epstein-Barr virus nuclear antigen 1, is required for pre-rRNA processing and ribosomal subunit assembly. Genes Cells *5*, 543–553.

Tsurugi, K., and Ogata, K. (1985). Evidence for the exchangeability of acidic ribosomal proteins on cytoplasmic ribosomes in regenerating rat liver. J. Biochem. *98*, 1427–1431.

Udem, S.A., and Warner, J.R. (1972). Ribosomal RNA synthesis in Saccharomyces cerevisiae. J. Mol. Biol. *65*, 227–242.

Udem, S.A., and Warner, J.R. (1973). The cytoplasmic maturation of a ribosomal precursor ribonucleic acid in yeast. J. Biol. Chem. *248*, 1412–1416.

Ulbrich, C., Diepholz, M., Bassler, J., Kressler, D., Pertschy, B., Galani, K., Böttcher, B., and Hurt, E. (2009). Mechanochemical removal of ribosome biogenesis factors from nascent 60S ribosomal subunits. Cell *138*, 911–922.

Valenzuela, D.M., Chaudhuri, A., and Maitra, U. (1982). Eukaryotic ribosomal subunit anti-association activity of calf liver is contained in a single polypeptide chain protein of Mr = 25,500 (eukaryotic initiation factor 6). J. Biol. Chem. *257*, 7712–7719.

Vanácová, S., Wolf, J., Martin, G., Blank, D., Dettwiler, S., Friedlein, A., Langen, H., Keith, G., and Keller, W. (2005). A new yeast poly(A) polymerase complex involved in RNA quality control. PLoS Biol. *3*, e189.

Vanrobays, E., Gelugne, J.-P., Gleizes, P.-E., and Caizergues-Ferrer, M. (2003). Late cytoplasmic maturation of the small ribosomal subunit requires RIO proteins in Saccharomyces cerevisiae. Mol. Cell. Biol. *23*, 2083–2095.

Vanrobays, E., Gélugne, J.-P., Caizergues-Ferrer, M., and Lafontaine, D.L.J. (2004). Dim2p, a KH-domain protein required for small ribosomal subunit synthesis. RNA *10*, 645–656.

Venema, J., and Tollervey, D. (1995). Processing of pre-ribosomal RNA in Saccharomyces cerevisiae. Yeast *11*, 1629–1650.

Venema, J., and Tollervey, D. (1996). RRP5 is required for formation of both 18S and 5.8S rRNA in yeast. EMBO J. *15*, 5701–5714.

Venema, J., Vos, H.R., Faber, A.W., van Venrooij, W.J., and Raué, H.A. (2000). Yeast Rrp9p is an evolutionarily conserved U3 snoRNP protein essential for early pre-rRNA processing cleavages and requires box C for its association. RNA *6*, 1660–1671.

Vinokurova, L.V., Dubtsova, E.A., Yashina, N.I., Shulyatyev, I.S., and Osipenko, Y.V. (2014). [Shwachman-Diamond syndrome]. Ter. Arkh. *86*, 72–75.

Voorhees, R.M., and Ramakrishnan, V. (2013). Structural basis of the translational elongation cycle. Annu. Rev. Biochem. *82*, 203–236.

Voorhees, R.M., Weixlbaumer, A., Loakes, D., Kelley, A.C., and Ramakrishnan, V. (2009). Insights into substrate stabilization from snapshots of the peptidyl transferase center of the intact 70S ribosome. Nat. Struct. Mol. Biol. *16*, 528–533.

Vos, H.R., Bax, R., Faber, A.W., Vos, J.C., and Raué, H.A. (2004). U3 snoRNP and Rrp5p associate independently with Saccharomyces cerevisiae 35S pre-rRNA, but Rrp5p is essential for association of Rok1p. Nucleic Acids Res. *32*, 5827–5833.

Wang, R., and Brattain, M.G. (2007). The maximal size of protein to diffuse through the nuclear pore is larger than 60kDa. FEBS Lett. *581*, 3164–3170.

Warner, J.R. (1971). The assembly of ribosomes in yeast. J. Biol. Chem. *246*, 447–454.

Warner, J.R. (1999). The economics of ribosome biosynthesis in yeast. Trends Biochem. Sci. *24*, 437–440.

Watkins, N.J., and Bohnsack, M.T. (2012). The box C/D and H/ACA snoRNPs: key players in the modification, processing and the dynamic folding of ribosomal RNA. Wiley Interdiscip Rev RNA *3*, 397–414.

Weinger, J.S., Parnell, K.M., Dorner, S., Green, R., and Strobel, S.A. (2004). Substrate-assisted catalysis of peptide bond formation by the ribosome. Nat Struct Mol Biol *11*, 1101–1106.

Weitzmann, C.J., Cunningham, P.R., Nurse, K., and Ofengand, J. (1993). Chemical evidence for domain assembly of the Escherichia coli 30S ribosome. FASEB J. *7*, 177–180.

Wery, M., Ruidant, S., Schillewaert, S., Leporé, N., and Lafontaine, D.L.J. (2009). The nuclear poly(A) polymerase and Exosome cofactor Trf5 is recruited cotranscriptionally to nucleolar surveillance. RNA *15*, 406–419.

Wessel, D., and Flügge, U.I. (1984). A method for the quantitative recovery of protein in dilute solution in the presence of detergents and lipids. Anal. Biochem. *138*, 141–143.

West, M., Hedges, J.B., Chen, A., and Johnson, A.W. (2005). Defining the order in which Nmd3p and Rpl10p load onto nascent 60S ribosomal subunits. Mol. Cell. Biol. *25*, 3802–3813.

White, J., Li, Z., Sardana, R., Bujnicki, J.M., Marcotte, E.M., and Johnson, A.W. (2008). Bud23 methylates G1575 of 18S rRNA and is required for efficient nuclear export of pre-40S subunits. Mol. Cell. Biol. *28*, 3151–3161.

Wilson, D.N., and Doudna Cate, J.H. (2012). The structure and function of the eukaryotic ribosome. Cold Spring Harb Perspect Biol *4*.

Wimberly, B.T., Brodersen, D.E., Clemons, W.M., Jr, Morgan-Warren, R.J., Carter, A.P., Vonrhein, C., Hartsch, T., and Ramakrishnan, V. (2000). Structure of the 30S ribosomal subunit. Nature *407*, 327–339.

Woese, C.R., Magrum, L.J., Gupta, R., Siegel, R.B., Stahl, D.A., Kop, J., Crawford, N., Brosius, J., Gutell, R., Hogan, J.J., et al. (1980). Secondary structure model for bacterial 16S ribosomal RNA: phylogenetic, enzymatic and chemical evidence. Nucleic Acids Res. *8*, 2275–2293.

Wolfe, K.H., and Shields, D.C. (1997). Molecular evidence for an ancient duplication of the entire yeast genome. Nature *387*, 708–713.

Woodson, S.A. (2011). RNA folding pathways and the self-assembly of ribosomes. Acc. Chem. Res. *44*, 1312–1319.

Woolford, J.L., Jr, and Baserga, S.J. (2013). Ribosome Biogenesis in the Yeast Saccharomyces cerevisiae. Genetics *195*, 643–681.

Wu, K., Wu, P., and Aris, J.P. (2001). Nucleolar protein Nop12p participates in synthesis of 25S rRNA in Saccharomyces cerevisiae. Nucleic Acids Res. *29*, 2938–2949.

Wurm, J.P., Meyer, B., Bahr, U., Held, M., Frolow, O., Kötter, P., Engels, J.W., Heckel, A., Karas, M., Entian, K.-D., et al. (2010). The ribosome assembly factor Nep1 responsible for Bowen-Conradi syndrome is a pseudouridine-N1-specific methyltransferase. Nucleic Acids Res. *38*, 2387–2398.

Xue, S., and Barna, M. (2012). Specialized ribosomes: a new frontier in gene regulation and organismal biology. Nat. Rev. Mol. Cell Biol. *13*, 355–369.

Yao, W., Roser, D., Köhler, A., Bradatsch, B., Bassler, J., and Hurt, E. (2007). Nuclear export of ribosomal 60S subunits by the general mRNA export receptor Mex67-Mtr2. Mol. Cell *26*, 51–62.

Yao, W., Lutzmann, M., and Hurt, E. (2008). A versatile interaction platform on the Mex67-Mtr2 receptor creates an overlap between mRNA and ribosome export. EMBO J. *27*, 6–16.

Yao, Y., Demoinet, E., Saveanu, C., Lenormand, P., Jacquier, A., and Fromont-Racine, M. (2010). Ecm1 is a new pre-ribosomal factor involved in pre-60S particle export. RNA *16*, 1007–1017.

Yeh, L.C., and Lee, J.C. (1990). Structural analysis of the internal transcribed spacer 2 of the precursor ribosomal RNA from Saccharomyces cerevisiae. J. Mol. Biol. *211*, 699–712.

Yeh, L.C., Thweatt, R., and Lee, J.C. (1990). Internal transcribed spacer 1 of the yeast precursor ribosomal RNA. Higher order structure and common structural motifs. Biochemistry *29*, 5911–5918.

Yusupov, M.M., Yusupova, G.Z., Baucom, A., Lieberman, K., Earnest, T.N., Cate, J.H., and Noller, H.F. (2001). Crystal structure of the ribosome at 5.5 A resolution. Science *292*, 883–896.

Zaher, H.S., Shaw, J.J., Strobel, S.A., and Green, R. (2011). The 2′-OH group of the peptidyl-tRNA stabilizes an active conformation of the ribosomal PTC. The EMBO Journal *30*, 2445–2453.

Zhang, J., Harnpicharnchai, P., Jakovljevic, J., Tang, L., Guo, Y., Oeffinger, M., Rout, M.P., Hiley, S.L., Hughes, T., and Woolford, J.L., Jr (2007). Assembly factors Rpf2 and Rrs1 recruit 5S rRNA and ribosomal proteins rpL5 and rpL11 into nascent ribosomes. Genes Dev. *21*, 2580–2592.

Zinker, S. (1980). P5/P5' the acidic ribosomal phosphoproteins from Saccharomyces cerevisiae. Biochim. Biophys. Acta *606*, 76–82.

Zinker, S., and Warner, J.R. (1976). The ribosomal proteins of Saccharomyces cerevisiae. Phosphorylated and exchangeable proteins. J. Biol. Chem. *251*, 1799–1807.

7 Abbreviations

Å	*Ångström* (1/10 nano meter)
aa	amino acid
AmpR	resistance marker for ampicillin
APS	ammonium persulfate
ATP	adenosine triphosphate
bp	base pair(s)
CID	collision induced dissociation
cpm	counts per minute
cryo-EM	cryo-electron microscopy
Da	Dalton
DNA	desoxyribonucleic acid
dNTP	2-desoxyribonucleotide 5' triphosphate
EDTA	ethylene diamine tetra acetate
EGTA	ethylene glycol tetraacetic acid
EM	electron microscopy
EtBr	Ethidiumbromide
ETS	external transcribed spacer
FRET	fluorescence resonance energy transfer
FWHM	full width at half maximun
g	gram(s)
GentR	resistance marker for gentamycin,
GFP	green fluorescent protein
h	hour(s)
HA	hemagglutinin
IP	immunoprecipitation (also used for “affinity purified fraction”)
iTRAQ	isobaric tag for relative and absolute quantitation
ITS 1/2	internal transcribed spacer 1/2
k	kilo
kb	kilo base pair(s)
l	liter(s)
LB	lysogeny broth
LSU	large ribosomal subunit
M	molar (mol/l)
MALDI	matrix-assisted laser desorption/ionisation
mg	milligram(s)
min	minute(s)
ml	milliliter(s)
mm	millimeter(s)
mRNA	messenger RNA
MS	mass spectrometry
MS/MS	tandem mass spectrometry
MW	molecular weight
NB	Northern blotting
nm	nanometer(s)
nt	nucleotide(s)
OD	optical density (absorption at 600nm)
PAGE	poly acryl amide gel electrophoresis
Pmol	picomol
ProtA	Protein A
PCR	polymerase chain reaction
PEG	poly ethylene glycol
pGAL	GAL1/10 promoter
pH	negative decadic logarithm of [H+]
Pol-I	RNA polymerase I
Pol-II	RNA polymerase II
Pol-III	RNA polymerase III
ppm	parts per million
pre-	precursor
rDNA	ribosomal DNA
RNA	ribonucleic acid
RNP	ribonucleoprotein complex
rpm	rotations per minute

r-protein	ribosomal protein
rpL	ribosomal protein of the large subunit
rpS	ribosomal protein of the small subunit
rRNA	ribosomal RNA
RT	room temperature
s	second(s)
s	sedimentation coefficient
S	Svedberg Units
SCD	synthetic complete medium containing glucose
SCG	synthetic complete medium containing galactose
SDS	sodium dodecyl sulfate
S/N	signal to noise ratio
snoRNA	small nucleolar ribonucleic acid
snoRNP	small nucleolar ribonucleoprotein
SSU	small ribosomal subunit
TAP tag	tandem affinity purification tag
Taq	Thermus aquaticus
TCA	tri-chloro acetic acid
TFA	tri-fluoro acetic acid
TEMED	tetramethylethylenediamine
TOF	time of flight
Tris	tris(hydroxy methyl) amino methane
ts	temperature sensitive
U	unit(s)
WB	Western blotting
wt	wild type
YPD	full medium containing glucose
YPG	full medium containing galactose
µ	micro

8 Table of Figures

9 Publications

2014 Michael Gamalinda*, Uli Ohmayer*, Jelena Jakovljevic, et al.
A hierarchical model for assembly of eukaryotic 60S ribosomal subunit domains.
Genes Dev 28: 198-210

2013 Uli Ohmayer, Michael Gamalinda, Martina Sauert, et al.
Studies on the Assembly Characteristics of Large Subunit Ribosomal Proteins in *S. cerevisae.*
PLoS ONE 8: e68412

2013 Thomas Hierlmeier, Juliane Merl, Martina Sauert et al.
Rrp5p, Noc1p and Noc2p form a protein module which is part of early large ribosomal subunit precursors in *S. cerevisiae.*
Nucleic Acids Res. 2013, 41: 1191–1210

2012 Jelena Jakovljevic, Uli Ohmayer, Michael Gamalinda, et al.
Ribosomal proteins L7 and L8 function in concert with six A3 assembly factors to propagate assembly of domains I and II of 25S rRNA in yeast 60S ribosomal subunits.
RNA 18: 1805–1822.

2012 Uli Ohmayer*, Jorge Perez-Fernandez*, Thomas Hierlmeier*, et al.
Local tertiary structure probing of ribonucleoprotein particles by nuclease fusion proteins.
PLoS ONE 7: e42449

2012 Steffen Jakob, Uli Ohmayer, Andreas Neueder et al.
Interrelationships between Yeast Ribosomal Protein Assembly Events and Transient Ribosome Biogenesis Factors Interactions in Early Pre-Ribosomes.
PLoS ONE 7: e32552.

* these authors contributed equally to the publication

10 Acknowledgements / Danksagung

Zuletzt möchte ich mich bei allen Personen bedanken, die zum Gelingen dieser Arbeit beigetragen haben.

Insbesondere natürlich bei meinem Betreuer Dr. Philipp Milkereit für die interessante Themenstellung dieser Arbeit bei deren Ausführung ich eine Menge lernen konnte. Danke für die hervorragende Unterstützung in allen Belangen, angefangen bei der Planung und Durchführung der Experimente sowie der Auswertung, Interpretation und Veröffentlichung der Ergebnisse! Selbiges gilt für meinen Doktorvater Prof. Dr. Herbert Tschochner, der mich stets unterstützt hat und mir z.B. die Teilnahme an mehreren hochinteressanten internationalen Konferenzen ermöglichte.

Außerdem gilt mein Dank PD Dr. Joachim Griesenbeck, Dr. Jorge Pérez Fernández und Dr. Sebastien Ferreira-Cerca für die vielen hilfreichen Diskussionen und Vorschläge. Prof. Dr. Alexander Buchberger von der Uni Würzburg möchte ich für seine Bereitschaft, mich als externer Mentor während der Doktorarbeit zu begleiten, ebenfalls herzlich danken.

Vielen Dank auch an alle anderen aktuellen und ehemaligen Mitglieder unserer „Ribosomenbiogenese“ - Subgruppe, die immer mit Rat und Tat zur Seite standen. Insbesondere möchte ich Dr. Thomas Hierlmeier, Dr. Steffen Jakob, Dr. Andreas Neueder und Dr. Juliane Merl für die tatkräftige Unterstützung danken. Auch Gisela Pöll (die gute Seele des Labors), Julius Ossowski, Martina Sauert, Christian Müller, Shuang Li, Kristin Hergert und Jan Linnemann möchte ich herzlich danken.

Außerdem möchte ich mich bei Michael Gamalinda, Jelena Jakovljevic und der gesamten Gruppe von John Woolford in Pittsburgh, Pennsylvania für die langjährige Kollaboration danken. Selbiges gilt für Prof. Dr. Helmut Bergler und seiner Gruppe in Graz, Österreich und Álvaro Gil und die Gruppe von Mercedes Tamame in Salamanca, Spanien.

Allen anderen Mitgliedern des „House of the Ribosome“ danke ich für die angenehme Atmosphäre und die vielen schönen Feierlichkeiten in und außerhalb des Labors.

Besonderer Dank gilt meiner Familie, die mir stets moralisch und natürlich finanziell zur Seite stand um mir durch die Finanzierung des Studiums den Weg zur Promotion zu ebnen. Meinen Freunden und ganz besonders meiner Freundin Kathrin danke ich für die (viel wichtigere) Zeit außerhalb des Labors.